

UNIVERSITÀ DEGLI STUDI DI MILANO

SCUOLA DI DOTTORATO  
*Scuola di Dottorato Terra, Ambiente e Biodiversità*

DIPARTIMENTO  
*Scienze della Terra "A. Desio"*

*Dottorato di Ricerca in Scienze Naturalistiche e Ambientali  
(XXVI ciclo)*

**Modellazione distribuita del bilancio energetico e  
dell'ablazione di un ghiacciaio alpino:  
il Ghiacciaio dei Forni**

---

**Modelling the distributed energy budget and the  
melting amount of an Alpine glacier:  
the case study of Forni Glacier (Italy)**

S.F.D. GE004 - Macroarea 04/A3

**Antonella Senese**  
Matricola R08993

**TUTORE:**  
prof. Claudio Smiraglia

**CO-TUTORE:**  
prof. Maurizio Maugeri  
PhD Guglielmina Diolaiuti  
PhD Andrea Zerboni

**COORDINATORE DEL DOTTORATO:**  
prof. Nicola Saino

A.A. 2012/2013



*Un ghiacciaio è come un fiume vorticoso e spumante, agghiacciato anche talvolta nell'atto che precipitava formando una cascata.*

Abate Stoppani, da "Il Bel Paese"





**Contents**

<b>Abstract</b> .....	1
<b>Riassunto</b> .....	3
<b>Chapter 1</b> .....	5
Introduction.....	6
1. Aims.....	6
2. Introduction to mass balance models.....	7
3. Introduction to energy balance models.....	8
4. Introduction to numerical models.....	9
5. The Forni Glacier.....	10
6. Thesis organization.....	12
References.....	14
<b>Chapter 2</b> .....	17
Energy and mass balance of Forni Glacier (Stelvio National Park, Italian Alps) from a 4-year meteorological data record.....	18
Abstract.....	18
1. Introduction.....	19
2. The AWS1 Forni.....	23
3. Methods .....	26
3.1 Solid precipitation.....	26
3.2 Radiation.....	27
3.3 Turbulent fluxes.....	27
3.4 Surface energy and mass balance .....	28
4. Results.....	30
4.1. Meteorology.....	30
4.2. Energy balance.....	33
4.3. Mass balance.....	35
5. Discussions .....	38
6. Conclusions.....	42
References.....	45
<b>Chapter 3</b> .....	50
Surface energy budget and melt amount for the years 2009 and 2010 at the Forni Glacier (Italian Alps, Lombardy).....	51
Abstract.....	51
1. Microclimate of glacier: from the first pioneer investigations to the actual Alpine measurements.....	52
2. The Italian AWS network and the AWS1 Forni.....	53
3. Methods .....	56
4. Results.....	58
5. Conclusions.....	66
References.....	68
<b>Chapter 4</b> .....	74
Air temperature thresholds to evaluate snow melting at the surface of Alpine glaciers by degree-day models: the case study of Forni Glacier (Italy).....	75
Abstract.....	75

## Contents

---

1. Introduction and study aims.....	77
2. Data and methods.....	79
3. Results.....	82
4. Discussions and conclusions.....	88
References.....	91
<b>Chapter 5</b> .....	93
An enhanced T-index model including solar and infrared radiation to evaluate distributed ice melt at the Forni Glacier tongue (Italian Alps).....	94
Abstract.....	94
1. Introduction and aims .....	95
2. Methods .....	98
2.1. Air temperature .....	98
2.2. Net solar radiation.....	99
2.3. Net infrared radiation.....	103
2.4. Ablation computation .....	107
3. Results and discussion .....	109
3.1 Incoming solar radiation .....	109
3.2 Infrared radiation .....	111
3.3 Ablation computation .....	112
4. Conclusions.....	115
References.....	117
<b>Chapter 6</b> .....	120
A pilot study to evaluate sparse supraglacial debris and dust and their influence on ice albedo of Alpine glaciers: the case study of the Forni Glacier (Italy).....	121
Abstract.....	121
1. Introduction.....	122
2. Study area .....	123
3. Methods .....	124
3.1 Debris cover quantification.....	125
3.2 Albedo.....	127
3.3 Sedimentological analyses and debris coverage rate evaluation .....	129
4. Results.....	130
4.1. Debris coverage ratio ( $d$ ) and ice albedo ( $\alpha$ ).....	130
4.2. Debris features and debris coverage rate ( $C_r$ ).....	134
5. Discussion.....	138
6. Conclusions.....	142
References.....	145
<b>Chapter 7</b> .....	150
Computation of turbulent fluxes distributed over the glacier surface. The case study of the Forni Glacier (Italian Alps) .....	151
Abstract.....	151
1. Introduction.....	152
2. Methods .....	155
3. Results and discussions.....	160
4. Conclusions.....	164
References.....	168
<b>Chapter 8</b> .....	170

## Contents

---

Ablation computation at the debris-covered area of Forni Glacier: an approach based on computation of debris thermal resistivity .....	171
Abstract.....	171
1. Introduction.....	172
2. Methods .....	175
3. Results.....	177
4. Discussion and conclusion.....	180
References.....	182
<b>Chapter 9</b> .....	185
Conclusions.....	186
References.....	200
<b>Acknowledgements</b> .....	203
<b>Ringraziamenti</b> .....	204
<b>Curriculum vitae</b> .....	206
<b>List of publications</b> .....	207

## **Abstract**

This research deals with the estimation of the distributed snow and ice ablation amounts at an alpine glacier surface with a diurnal or sub-diurnal temporal resolution. Several methods were applied from the easiest one which depends only on the air temperature to the most exhaustive ones based on the energy budget. For this reason we applied and tested some models to estimate and distribute the meteorological parameters and the energy fluxes. For each analysed variable, the modelled values were compared to the ones measured at the surface of the Forni Glacier (Italian Alps) in order to investigate the reliability of the chosen approach. All the computations were aimed at obtaining the distribution of the factors driving the glacier energy budget on a digital elevation model (DEM) 20 x 20 m grid spaced which describes the surface of an Alpine debris free glacier (the Forni Glacier, Italian Alps).

In this way i) the spatial and temporal distribution of air temperature and vapour pressure conditions were evaluated; ii) the spatial distribution of topographic shading and of potential and global solar radiation for selected time intervals was predicted; iii) the distributed incoming infrared radiation was modelled; iv) the distributed turbulent fluxes were assessed; v) the spatial and temporal variations of the energy balance components were investigated; vi) the melt amount over the debris-covered areas was quantified as well; and vii) the short-term energy balance variations of a whole glacierized area can be easily computed.

Firstly the point energy and mass balance was modelled from measured (from a supraglacial automatic weather station set up on the tongue of the Forni Glacier, AWS1 Forni) and estimated values. Since the physical processes were assessed at the AWS1 Forni site, the distribution of the melting processes over the Forni Glacier surface was considered. In particular initially a simple degree-day model was applied with respect to the snow ablation focussing on the suitability of the chosen temperature threshold which witnesses melting conditions. In fact, melt does not necessarily occur at daily average air temperatures higher than 273.15 K, since it is determined by the surface energy budget which in turn is only indirectly affected by air temperature.



## Abstract

---

Several enhanced T-index models including solar radiation were considered as well. A new enhanced T-index model including infrared radiation was developed to evaluate distributed ice melt and compared with the other T-index methods. Different approaches were further tested to distribute the input meteorological and energy data driving the enhanced T-index methods (i.e. air temperature, solar and infrared radiation), which should allow a wider application of this approach upon glaciers not equipped with AWS, or without a net radiometer, necessary to directly measure infrared flux.

Moreover, the parameters affecting temporal and spatial albedo variability were considered: sparse and fine debris and dust, and rainfalls. In particular a method to investigate the characteristics of sparse and fine debris coverage at the glacier melting surface and its relation to ice albedo was proposed. In fact despite the abundant literature dealing with dust and black carbon deposition on glacier accumulation areas, few studies that describe the distribution and properties of fine and discontinuous debris and black carbon at the melting surface of glaciers are available. A protocol to i) sample fine and sparse supraglacial debris and dust, ii) quantify its surface coverage, iii) describe its composition and sedimentological properties, iv) measure ice albedo, and v) identify the relationship between albedo and fine debris coverage, was developed.

The distribution of the turbulent fluxes was also investigated. The main focuses were the distribution of the vapour pressure and the assessment of the katabatic and the background turbulent exchange coefficients.

Finally the melting conditions and rate were also assessed over the glacier debris-covered area, which in the case of the Forni Glacier corresponds to the medial moraines. In this case a simple approach was applied based on the fact that the conductive heat flux depends on the temperature gradient from debris surface to ice.

## Riassunto

Scopo di questo lavoro è stata la modellazione distribuita della fusione della neve e/o del ghiaccio sulla superficie di un ghiacciaio alpino (il Ghiacciaio dei Forni, Italia). A questo scopo sono stati applicati diversi metodi partendo dal più semplice (che dipende solo dalla temperatura dell'aria) a quelli più sofisticati (basati sul bilancio energetico). Sono stati applicati e testati, quindi, alcuni modelli per stimare e spazializzare i parametri meteorologici e i flussi energetici. Per ogni variabile analizzata, sono stati confrontati i valori modellizzati con quelli effettivamente misurati: in questo modo è stato possibile investigare l'affidabilità degli approcci scelti. Tutte le elaborazioni per la distribuzione dei parametri in ingresso che permettono la quantificazione del bilancio energetico superficiale sono state applicate a tutte le celle di un modello di elevazione digitale (DEM) con maglia 20 m x 20 m che descrive la superficie del Ghiacciaio dei Forni (Alpi Italiane).

In questo modo è stato possibile i) valutare le condizioni distribuite spazialmente e temporalmente di temperatura dell'aria e di pressione di vapore; ii) predire in determinati intervalli di tempo la distribuzione spaziale sia dell'ombreggiamento dovuto alla topografia circostante che della radiazione solare potenziale e globale; iii) modellare la radiazione infrarossa in arrivo dall'atmosfera; iv) definire i flussi turbolenti distribuiti; v) investigare le variazioni sia spaziali che temporali dei componenti del bilancio energetico; vi) quantificare i tassi di fusione anche nelle porzioni coperte da detrito; e vii) predisporre tutti i dati input necessari per calcolare le variazioni distribuite ad alta risoluzione temporale del bilancio energetico di tutta un'area glacializzata.

Il primo passaggio è consistito nel definire a livello puntuale il modello di bilancio energetico e, quindi, di massa a partire sia da dati misurati (attraverso una stazione meteorologica automatica supragliaciale installata sulla lingua del Ghiacciaio dei Forni, AWS1 Forni) sia da valori stimati. Una volta che sono stati ben definiti a livello puntuale i processi fisici coinvolti nella fusione, si è passati alla distribuzione degli stessi. Si è partiti dal modello di ablazione più semplice (*T-index* o *degree-day*) focalizzando lo studio sulla scelta della soglia di temperatura media giornaliera dell'aria che testimonia la presenza di fusione. Infatti tali condizioni possono verificarsi anche

con temperature medie giornaliere inferiori a 273.15 K, in quanto è il bilancio energetico che governa i processi di fusione.

Successivamente sono stati testati diversi modelli di *T-index* che includono anche la componente radiativa (e non solo la temperatura dell'aria). In particolare è stato introdotto un nuovo approccio che considera anche la radiazione infrarossa netta. Inoltre sono stati applicati alcuni metodi per distribuire gli input meteorologici a questi modelli di *T-index*. In questo modo si è cercata una maggiore e più ampia applicazione di questi approcci anche su quei ghiacciai che non dispongono di stazioni meteorologiche o in particolare di un radiometro netto, necessario per le misure dirette della radiazione infrarossa.

Inoltre sono stati considerati i parametri che possono influenzare la variabilità dell'albedo superficiale: il detrito fine e sparso e l'acqua meteorica. In particolare si è proposto un metodo per investigare le caratteristiche del detrito fine e sparso che ricopre la superficie della lingua d'ablazione e le sue relazioni con l'albedo del ghiaccio. Infatti nonostante l'abbondante letteratura riguardante la deposizione delle polveri e del *black carbon* nelle zone di accumulo dei ghiacciai, sono disponibili pochi studi che descrivono questi fenomeni sulla superficie d'ablazione. Quindi è stato sviluppato un protocollo per i) campionare il detrito fine e sparso supraglaciaie; ii) quantificare la sua copertura superficiale; iii) descrivere la sua composizione e le sue proprietà sedimentologiche; iv) misurare l'albedo; e v) identificare le relazioni tra l'albedo e la copertura detritica fine.

Si è passati poi ad analizzare la distribuzione dei flussi turbolenti. Lo scopo principale è stato quello di distribuire la pressione di vapore e di definire i coefficienti di scambio turbolento sia catabatico che di *back-ground*.

Infine sono state investigate le condizioni di fusione e il tasso di ablazione anche nelle porzioni del ghiacciaio coperte da detrito (ovvero le morene mediane nel caso del Ghiacciaio dei Forni). A questo scopo è stato applicato un modello semplice basato sul fatto che il flusso di calore conduttivo dipende dal gradiente di temperatura fra la superficie e il ghiaccio.

# Chapter 1

## Introduction

### 1. Aims

This research deals with the estimation of the distributed snow and ice ablation amounts at an alpine glacier surface with a diurnal or sub-diurnal temporal resolution. Several methods were applied from the easiest one which depends only on the air temperature (Braithwaite, 1995) to the most exhaustive ones based on the energy budget (e.g. Brun et al., 1989; Blöschl et al., 1991; Arnold et al., 1996; Klok and Oerlemans, 2002). For this reason we applied and tested some models to estimate and distribute the meteorological parameters and the energy fluxes. For each analysed variable, the modelled values were compared to the measured ones in order to investigate the reliability of the chosen approach. All the computations were performed for each grid point of a digital elevation model (DEM) over the surface of an Alpine debris free glacier (the Forni Glacier, Italian Alps).

The objectives of this study were:

- ✓ to compute short-term energy balance variations of a whole glacierized area;
- ✓ to investigate the spatial and temporal variations of the energy balance components;
- ✓ to evaluate the air temperature and vapour pressure conditions;
- ✓ to predict the spatial distribution of topographic shading and of potential and global solar radiation for selected time intervals;
- ✓ to model the incoming infrared radiation;
- ✓ to assess the turbulent fluxes;
- ✓ to quantify the melt amount also over the glacier debris-covered areas.

### 2. Introduction to mass balance models

Distributed glacier mass balance models are affected by three main problems associated with such large-area applications: i) the required meteorological input data; ii) the spatial extrapolation or interpolation of these data in complex topography; and iii) model validation. Several studies have calibrated and validated the model results with measured runoff (e.g. Escher-Vetter, 1985; Hock and Holmgren, 2005) or the point-specific results at ablation stakes (e.g. Arnold et al., 1996; Brock et al., 2000; Klok and Oerlemans, 2002; Reijmer and Hock, 2008). However, studies that compare the model results with measured mass balances as obtained in the field by traditional methods over an entire balance year are more rare (e.g. Gerbaux et al., 2005; Schuler et al., 2005; Machguth et al., 2006).

A direct comparison of measured and modelled mass balance is difficult, as the interpolation techniques could be completely different. Field measurements might be interpolated to the entire glacier surface by a polynomial regression or kriging techniques (e.g. Hock and Jensen, 1999), whereas a model calculates mass balance for individual grid points from a digital elevation model (DEM) and zonal averaging (e.g. Machguth et al., 2006). Moreover, the processes considered during the careful interpretation of the field data using local knowledge are not the same as those used by a model that accounts for topographic effects such as shading from a DEM (e.g. Klok and Oerlemans, 2002). A comparison with model results could reveal that the values measured at point locations are not representative of the mass balance of an elevation band (Arnold et al., 2006). Compared with mass-balance profiles derived from a regression, the results from distributed models have a higher variability with elevation, and might thus yield different mass-balance gradients (Machguth et al., 2006). As a result of the rapidly changing glacier geometries in the last two decades (see for example the disintegration of the Careser Glacier, Italy reported by Carturan and Seppi, 2007), formerly established regressions for mass-balance determination might be less valid today. Moreover, in the last two decades, many glaciers in the Alps have been completely free of snow during or at the end of the ablation period, and some have even lost all firn reserves. The related changes in albedo have considerable influence on the melt rates and could substantially modify mass-balance profiles, with increasing ablation towards higher elevations (Paul et al., 2005).

Such new conditions might be better captured by a distributed model than by the currently applied extrapolation of measurements, as melt of snow and ice could be modelled very accurately (e.g. Hock, 2005). However, processes related to accumulation (e.g. wind redistribution of snow) are still less well understood and are subject to ongoing research (Bernhardt et al., 2009). Accordingly, accumulation is only roughly parameterized in current models, or is used as a tuning factor to fit measurements at specific sites (e.g. Klok and Oerlemans, 2002). Nevertheless, as annual balance for glaciers in the Alps is determined largely by the summer balance, a good agreement between measured and modelled mass balance was obtained in most of these studies.

### 3. Introduction to energy balance models

A physically based approach to compute ice and snow melt involves the assessment of the energy fluxes to and from the surface. At a surface temperature of  $0^{\circ}\text{C}$ , any surplus of energy at the surface-air interface is assumed to be used immediately for melting. The energy balance in terms of its components is expressed as (see for example Hock, 2005):

$$Q_N + Q_H + Q_L + Q_G + Q_R + Q_M = 0 \quad (1)$$

where  $Q_N$  is the net radiation,  $Q_H$  is the sensible heat flux,  $Q_L$  is the latent heat flux ( $Q_H$  and  $Q_L$  are referred to as turbulent heat fluxes),  $Q_G$  is the ground heat flux (i.e. the change in heat of a vertical column from the surface to the depth at which vertical heat transfer is negligible),  $Q_R$  is the sensible heat flux supplied by rain and  $Q_M$  is the energy consumed by melt. As commonly defined in glaciology a positive sign indicates an energy gain to the surface, a negative sign an energy loss. Melt rates,  $M$ , are then computed from the available energy from:

$$M = \frac{Q_M}{\rho_w L_f} \quad (2)$$

where  $\rho_w$  denotes the density of water and  $L_f$  the latent heat of fusion.

Energy-balance models fall into two categories:

- point studies assess the energy budget at one location, usually the site of a climate station;
- distributed models involve estimating the budget over an area, usually on a square grid.

Complete energy budget measurements are seldom available or only over short time frame due to the enormous equipment and maintenance requirements. Hence methods of computing the energy budget components from standard meteorological observations have been developed and applied in most studies (among others see Hoinkes, 1955; La Chapelle, 1959; Ambach and Hoinkes, 1963; Föhn, 1973). Despite simplifying assumptions inherent to these methods, they have provided reliable estimates of ablation. The main challenge for distributed studies is the extrapolation of input data and energy budget components to the entire grid. Examples of studies regarding grid-based energy balance are Funk (1985), Escher-Vetter (1985) and Arnold et al. (1996).

#### **4. Introduction to numerical models**

A model is a conceptual or mathematical representation of a phenomenon, usually conceptualised as a system. It provides an idealised framework for logical reasoning, mathematical or computational evaluation as well as hypothesis testing. Explicit assumptions about or simplifications of the system may be part of model development: how these decisions affect the utility of the model will depend on whether the model serves its intended purpose with satisfactory accuracy. Rykiel (1996) suggests that model ‘validation’ can be separated into evaluations of theory, implementation and data. While some statistical tests can be performed to measure differences between model behaviour and the behaviour of the system, ‘validation’ ultimately depends on whether the model and its behaviour are reasonable in the judgement of knowledgeable people. The value of a model depends on its usefulness for a given purpose and not its sophistication. Simple models can be more useful than models which incorporate many processes, especially when data are limited. Choosing the appropriate point along the continuum of model complexity depends on data availability, modelling (usually computer) resources and the questions under investigation. The data needed to obtain



credible results usually increase with increasing model complexity and with the number of processes that are represented. In mountain environments, lateral variations of surface and subsurface conditions as well as micro-climatology are far greater than in lowland environments.

A model precision is closely linked to measurements, on the other hand valid and meaningful measurements can't be made without a continuous improvement and updating of the models.

## 5. The Forni Glacier

Forni Glacier is the largest Italian valley glacier (11.36 km<sup>2</sup>), situated in Upper Valtellina, Ortles-Cevedale Group (Rhaetian Alps), part of the Stelvio National Park. It's a composite valley glacier, formed by three ice streams, merging into a tongue that extends over 2 km. It is currently 3 km long and has retreated 2.5 km since its Little Ice Age Maximum and 520 meters in the 1981-2003 period. The western basin, the widest one, is limited at the upper part by the watershed connecting San Giacomo Mount (3280 m a.s.l.), Pedranzini Peak (3599 m a.s.l.), Dosegù Peak (3555 m a.s.l.) and San Matteo Mount (3684 m a.s.l.). It has a north-west orientation and it's separated from the central basin by a nunatak called Isola Persa (previously this term was referred to a westerner promontory, that separated a little flow from the main flow; this is clear from a topographic map of Hydrological Office of Po of 1929). From the studies of Desio (1967) the accumulation area was connected to other near glaciers: from the peaks in addition to the glacier flowing along the Forni Valley, there are other three glaciers flowing along Vedretta Cerena and Vedretta Dosegù (from west to east).

The central basin represents the main accumulation area and it's the direct upward extension of Forni Valley. This valley is 1.5 km long, with an orientation south-north and it originates from Orsi Hill (3304 m a.s.l.). The upper boundary is defined by the line linking San Matteo Peak and Peio Peak (3549 m a.s.l.), from which there is the outcrop splitting the central and eastern basins.

The eastern basin is better delimited than the other two, it's composed by a wide cirque enclosed by the ridge from Peio Peak to Vioz Mount (3644 m a.s.l.) and to Palon de la Mare (3704 m a.s.l.). This cirque is divided in three parts by two promontories

## 1. Introduction

---

originating three different flows: on the right there is Vedretta of Palon de la Mare and the other two joining at 3150 m a.s.l. into the downer tongue. Also this basin is connected to other glaciers: Vedrette of Vioz and of Rossa (Desio, 1967).

The three flows of accumulation merge at 2700-2800 m a.s.l. where it begins the proper tongue. From the confluence of these three flows, two medial moraines originate separating the three tongues. The terminus is at 2480 m a.s.l. and it's composed by three lobes from which the melt water come out originating Frodolfo Stream.

Metamorphic rocks, mostly micaschist rich in quartz, muscovite, chlorite and albite (formerly called "Filladi di Bormio Formation"), constitute the dominant lithology (Pozzi, 1969); these rocks emerge from the glacier surface as nunatacks (mainly in the accumulation basins) and as rock outcrops on the glacier tongue. These latter results enlarging and increasing their size and number due to the ongoing glacier retreating and thinning phase (Diolaiuti and Smiraglia, 2010; Diolaiuti et al., 2012).

Forni Glacier, similarly to the largest part of the Alpine glaciers, has been retreating since the end of Little Ice Age (LIA, about 1860, Pelfini, 1988) (Fig. 1). The first measurements devoted to collect data describing Forni Glacier length changes started in 1895 (Diolaiuti and Smiraglia, 2010). Moreover Forni Glacier is also included in the list of glaciers monitored by the Italian Glaciological Committee (CGI) to evaluate changes in length (CGI, 1913-2011); in addition from historic maps and aerial photos, its area coverage has been calculated for the last 150 years. The results show that the Forni Glacier has experienced a marked decrease in length and area: from 17.80 km<sup>2</sup> at the end of the LIA (~1860) to 11.36 km<sup>2</sup> in 2007 (-36.2%). In the same time frame its tongue retreated by about 2 km (Diolaiuti and Smiraglia, 2010).

Records for length variations in the Forni Glacier are among the longest standing in the Italian Alps (from 1833), making Forni a benchmark glacier of primary importance. Fluctuation data for the glacier terminus show a basic retreating trend from 1895 to the present. A more detailed analysis of the terminus data reveals a more complex picture, showing a strong retreat from the end of the LIA up to the seventies, then a small advancing phase up to the second half of the eighties, when glacier decrease again became dominant. More precisely, the cumulative retreat in the period 1895-1970 is 1.55 km equal to a mean yearly value of -20.1 m, the cumulative advance in the time window 1971-1981 is 0.30 km equal to a mean yearly value of +30 m and the most recent cumulative retreat in the period 1982-2011 is 0.80 km equal to a mean yearly value of -27.6 m. Then the retreat rates evaluated for recent decades resulted stronger

than the ones calculated for the 1895-1970 period. Glacier volume and thickness changes were analyzed by Merli et al. (2001) who found a thickness reduction of about 70 m in the period 1929-1998.



*Fig. 1: The Forni Glacier in (from the left) 1890, 1941 and 2007.*

## 6. Thesis organization

As discussed in the previous sections, physical processes that govern the interaction between climate and glaciers are important to be studied, making use of both measurements and physically based models, to understand the response of glaciers to climate change. The research described in this thesis addresses this topic.

- The first step (Chapters 2 and 3) was to investigate the point energy and mass balance from measured (from a supraglacial automatic weather station set up on the tongue of the Forni Glacier, AWS1 Forni) and estimated values.
- Since the physical processes were assessed at the AWS1 Forni site, the distribution of the melting processes over the Forni Glacier surface was considered (Chapters from 4 to 7):
  - Firstly a simple degree-day model was applied with respect to the snow ablation (Chapters 4). In particular the suitability of the chosen temperature threshold witnessing melting conditions was investigated. In fact, melt does not necessarily occur at daily air temperatures higher than 273.15 K, since it is

determined by the surface energy budget which in turn is only indirectly affected by air temperature.

- Secondly several enhanced T-index models including solar radiation were considered (Chapters 5). A new enhanced T-index model including infrared radiation was developed to evaluate distributed ice melt and compared with the other T-index methods. We further tested different approaches to distribute the input meteorological and energy data driving the enhanced T-index methods (i.e. air temperature, solar and infrared radiation), which should allow a wider application of this approach upon glaciers not equipped with AWS, or without a net radiometer, necessary to directly measure infrared flux.
- In spite of the previous analyses which assumed the albedo constant over the glacier surface, in Chapters 6 the parameters affecting temporal and spatial albedo variability were considered: sparse and fine debris and dust and rainfalls. In particular a method to investigate the characteristics of sparse and fine debris coverage at the glacier melting surface and its relation to ice albedo was proposed. In fact despite the abundant literature dealing with dust and black carbon deposition on glacier accumulation areas, few studies that describe the distribution and properties of fine and discontinuous debris and black carbon at the melting surface of glaciers are available. A protocol to i) sample fine and sparse supraglacial debris and dust, ii) quantify its surface coverage, iii) describe its composition and sedimentological properties, iv) measure ice albedo and v) identify the relationship between albedo and fine debris coverage, was developed.
- The distribution of the turbulent fluxes was investigated in Chapter 7. The main focus is the distribution of the vapour pressure, as the air temperature was already analysed in Chapters 5. Moreover the katabatic and the back-ground turbulent exchange coefficients are taken into account.
- Finally the melting conditions and rate were also assessed over the debris-covered area, which in the case of the Forni Glacier corresponds to the medial moraines (Chapters 8). In this case a simple approach was applied based on the fact that the conductive heat flux depends on the temperature gradient from surface debris to ice.

## References

- Ambach W. and Hoinkes H.C. (1963): The heat balance of an Alpine snowfield (Kesselwandferner 3240 m, Oetztal Alps, 1958). Wallingford: IAHS Publication 61, 24–36.
- Arnold N.S., Willis I.C., Sharp M.J., Richards K.S. and Lawson W.J. (1996): A distributed surface energy-balance model for a small valley glacier. I. Development and testing for Haut Glacier d’Arolla, Valais, Switzerland. *J. Glaciol.*, 42(140), 77-89.
- Arnold N.S., Rees W.G., Hodson A.J. and Kohler J. (2006): Topographic controls on the surface energy balance of a high Arctic valley glacier. *J. Geophys. Res.*, 111(F2), F02011. (10.1029/2005JF000426.)
- Bernhardt M., Zängl G., Liston G.E., Strasser U. and Mauser W. (2009): Using wind fields from a high resolution atmospheric model for simulating snow dynamics in mountainous terrain. *Hydrol. Process.*, 23 (7), 1064-1075.
- Blöschl G., Kirnbauer B. and Gutknecht D. (1991): Distributed snowmelt simulations in an Alpine catchment. 1. Model evaluation on the basis of snow cover patterns. *Water Resources Research*, 27, 3171-79.
- Braithwaite R.J. (1995): Positive degree-day factors for ablation on the Greenland ice sheet studied by energy-balance modelling. *Journal of Glaciology*, 41, 153-60.
- Brock B.W., Willis I.C., Sharp M.J. and Arnold N.S. (2000): Modelling seasonal and spatial variations in the surface energy balance of Haut Glacier d’Arolla, Switzerland. *Ann. Glaciol.*, 31, 53-62.
- Brun E., Martin E., Simon V., Gendre C. and Coleou C. (1989): An energy and mass model of snow cover suitable for operational avalanche forecasting. *Journal of Glaciology*, 35, 333–42.
- Carturan L. and Seppi R. (2007): Recent mass balance results and morphological evolution of Careser Glacier (Central Alps). *Geogr. Fis. Din. Quat.*, 30 (1), 33-42.
- Comitato Glaciologico Italiano – CGI (1913-1977): Campagne Glaciologiche, Bollettino del Comitato Glaciologico Italiano. Series 1 and 2, Annual glacier surveys are also available on line at: [www.glaciologia.it](http://www.glaciologia.it)
- Comitato Glaciologico Italiano – CGI (1978-2011): Campagne Glaciologiche, Geografia Fisica e Dinamica Quaternaria. Vol 1-35. Also available on line at: [www.glaciologia.it](http://www.glaciologia.it)

- Desio A. (1967): I Ghiacciai del Gruppo Ortles – Cevedale (Alpi Centrali). Comitato Glaciologico Italiano – CNR, Torino.
- Diolaiuti G. and Smiraglia C. (2010): Changing glaciers in a changing climate: how vanishing geomorphosites have been driving deep changes in mountain landscapes and environments. *Géomorphologie: relief, processus, environnement*, 2, 131-152.
- Diolaiuti G., Bocchiola D., D’Agata C. and Smiraglia C. (2012): Evidence of climate change impact upon glaciers' recession within the Italian Alps: the case of Lombardy glaciers. *Theoretical and Applied Climatology*, 109 (3-4), 429-445. DOI 10.1007/s00704-012-0589-y
- Escher-Vetter H. (1985): Energy balance calculations from five years' meteorological records at Vernagtferner, Oetztal Alps. *Z. Gletscherkd. Glazialgeol.*, 21 (1-2), 397-402.
- Föhn P.M.B. (1973): Short-term snow melt and ablation derived from heat- and mass-balance measurements. *Journal of Glaciology*, 12, 275–289.
- Funk M. (1985): Räumliche Verteilung der Massenbilanz auf dem Rhonegletscher und ihre Beziehung zu Klimaelementen. *Zürcher Geographische Schriften* 24, Department of Geography, ETH Zürich, 183 pp.
- Gerbaux M., Genthon C., Etchevers P., Vincent C. and Dedieu J.P. (2005): Surface mass balance of glaciers in the French Alps: distributed modeling and sensitivity to climate change. *J. Glaciol.*, 51 (175), 561-572.
- Hock R. and Jensen H. (1999): Application of kriging interpolation for glacier mass balance computations. *Geogr. Ann.*, 81A (4), 611-619.
- Hock R. and Holmgren B. (2005): A distributed surface energy balance model for complex topography and its application to Storglaciaren, Sweden. *J. Glaciol.*, 51 (172), 25-36.
- Hock R. (2005): Glacier melt: a review on processes and their modelling. *Progr. Phys. Geogr.*, 29 (3), 362-391.
- Hoinkes H.C. (1955): Measurements of ablation and heat balance on alpine glaciers. *Journal of Glaciology*, 2, 497-501.
- Klok E.J. and Oerlemans J. (2002): Model study of the spatial distribution of the energy and mass balance of Morteratschgletscher, Switzerland. *J. Glaciol.*, 48 (163), 505-518.
- La Chapelle E. (1959): Annual mass and energy exchange on the Blue Glacier. *Journal of Geophysical Research*, 64, 443-49.

- Machguth H., Paul F., Hoelzle M. and Haeberli W. (2006): Distributed glacier mass-balance modelling as an important component of modern multi-level glacier monitoring. *Ann. Glaciol.*, 43, 335-343.
- Merli F., Pavan M., Rossi G., Smiraglia C., Tamburini A. and Ubiali G. (2001): Variazioni di spessore e di volume della lingua del ghiacciaio dei Forni (Alpi Centrali, Gruppo Ortles-Cevedale) nel XX secolo. Risultati e confronti di metodologie. *Suppl. Geografia Fisica e Dinamica Quaternaria*, 5, 121-128.
- Paul F., Machguth H. and Kääb A. (2005): On the impact of glacier albedo under conditions of extreme glacier melt: the summer of 2003 in the Alps. *EARSeL eProc.*, 4(2), 139-149.
- Pelfini M. (1988): Contributo alla conoscenza delle fluttuazioni oloceniche del Ghiacciaio dei Forni. *Natura bresciana*, 24, 237-257.
- Pozzi R. (1969): *Geologia del Parco dello Stelvio*. Istituti di Geologia e Paleontologia dell'Università degli Studi di Milano ed. 22, nuova Serie.
- Reijmer C.H. and Hock R. (2008): Internal accumulation on Storglaciären, Sweden, in a multi-layer snow model coupled to a distributed energy- and mass-balance model. *J. Glaciol.*, 54 (184), 61-72.
- Rykiel E.J. (1996): Testing ecological models: the meaning of validation. *Ecological Modelling*, 90, 229-244.
- Schuler T.V., Hock R., Jackson M., Elvehøy H., Braun M., Brown I. and Hagen J.O. (2005): Distributed mass-balance and climate sensitivity modelling of Engabreen, Norway. *Ann. Glaciol.*, 42, 395-401.

# Chapter 2



## **Energy and mass balance of Forni Glacier (Stelvio National Park, Italian Alps) from a 4-year meteorological data record**

### **Abstract**

Since 26<sup>th</sup> September 2005 an Automatic Weather Station (AWS1 Forni) has been running on the ablation area of the largest Italian valley glacier, Forni, in the Ortles-Cevedale Group. A four year record (from 1<sup>st</sup> October 2005 to 30<sup>th</sup> September 2009) of air temperature, relative humidity, wind speed and direction, incoming and outgoing radiative fluxes, air pressure, liquid precipitation and snow depth is considered. The meteorological data are analyzed to describe glacier surface conditions, to calculate the energy balance and to evaluate the ice ablation amount. Snow accumulation was measured thus permitting the estimation of the glacier point mass balance.

An annual average amount of melt of  $-5.4 \pm 0.021$  m w.e. was calculated and an annual average amount of accumulation of  $+0.7 \pm 0.006$  m w.e. was measured at the AWS site. The annual average amount of mass balance was  $-4.7 \pm 0.023$  m w.e..

Our analyses show that surface conditions during summer and fall seasons are important in regulating glacier albedo and then mass balance. In particular, snow cover presence due to a longer persistence of spring snow, summer snowfalls and earlier fall solid precipitation drives the duration of the ice melt period.

## 1. Introduction

Changes in climatic forcing are directly reflected by the mass budget of snow and ice surfaces (von Hann, 1897; Hock, 2005). Understanding the impact of changing climate conditions on glacier melt is a prerequisite for projections of glacier volume changes which are needed for mountain hydrology studies, to analyze natural hazard frequency and to forecast sea level rise. In recent years, numerical models have been frequently used to study the properties of individual glaciers and ice caps, to understand their fluctuations in history, and to make projections of future behaviour for imposed climate scenarios (e.g. Gregory and Oerlemans, 1998; Oerlemans et al., 1998). The numerical approach embraces both glacier ice-flow and mass balance models. The latter translate meteorological conditions into glacier mass balance. The general experience from numerical studies (Wallinga and van de Wal, 1998; Oerlemans, 2000) confirms that uncertainties in the mass-balance models are strongly reflected in the output. Then, to improve ice flow modelling and glacier projections it is important to refine the calculation of the glacier mass balance. A general problem in testing and calibrating mass-balance models is the scarceness of meteorological data from glaciers.

The glacier surface differs from its surroundings during the ablation season due to the surface characteristics. Low surface temperature and varying albedo conditions characterize the glacier surface, while external mountain slopes areas, with no snow cover during summer, presents lower albedo of rock surfaces, which are warming faster than the glacier surface during the day. The surface energy balance of lateral slopes is higher and influences the nearby glacier surface through increased outgoing longwave radiation flux and air temperature. The differences are minimized during the winter season and in the accumulation area due to snow cover distribution, reflecting more than 50% of the incoming shortwave radiation due to a high albedo. Therefore to calculate the glacier energy balance, direct measurements of energy fluxes at the interface between atmospheric boundary layer and glacier surface are necessary (Greuell and Oerlemans, 1986).

An important question to be answered is how the atmospheric boundary layer overlying a glacier filters the large-scale climatic signal. Especially when the glacier surface is melting and the air is warm, a boundary layer with special properties is present (e.g. Munro, 1989; van den Broeke et al., 1994; Greuell et al., 1997). The structure of the atmospheric boundary layer over the glacier influences the surface energy budget by

## 2. Energy and mass balance of Forni Glacier (Stelvio National Park, Italian Alps) from a 4-year meteorological data record

---

controlling the latent and sensible turbulent heat fluxes. The glacier winds generate turbulence in the stably stratified surface layer and are especially well developed during periods with weak synoptic flow and strong insolation, enhancing the melt rates. In the accumulation zone, where the temperatures are lower and the surface-layer stratification is unstable (except during summer), the atmospheric boundary layer is more sensitive to external forcing, such as the valley wind, transporting moist and warm air from the valley floor. The pronounced mass flux divergence within the lower parts of the atmosphere during the night, caused by the combined effect of the glacier and mountain wind, produces drying and warming of the atmospheric boundary layer air (van den Broeke, 1997). Turbulent cooling of the air by the melting ice surface results in a down-glacier directed flow component.

From these considerations, it is clear that ground measurements of the meteorological parameters on glaciers are very useful. Systematic investigations of the heat budget of a melting glacier did not start until after the Second World War. Pioneering work was done by Capello (1959-1960) and Ambach (1963). A series of other investigations followed (e.g. Björnsson, 1972; Hogg et al., 1982; Ishikawa et al., 1992), and these studies have given basic insight into the nature of the energy budget on glaciers. In the recent decade, glacio-meteorological experiments have been carried out and the components of the surface energy flux were measured simultaneously at a large number of automatic weather stations (AWSs) (Oerlemans and Vugts, 1993; Greuell et al., 1997; Oerlemans et al., 1999). Large data sets have been obtained, providing insight into altitudinal gradients of meteorological quantities and improving glacier melt modelling (Munro and Marosz-Wantuch, 2009). Also on debris-covered glaciers, meteorological data and energy fluxes have been collected by installing seasonal AWSs (Brock et al., 2010). Most of the studies provided supraglacial meteorological data and energy fluxes measurements for shorter periods (one or more ablation seasons). However, longer records of data are needed to calculate the annual energy and mass balance and these can only be obtained from AWSs permanently located at the glacier surface.

Most AWSs are located in the accumulation zone, due to the higher stability, whereas, only a few are present in the glacier ablation area. The main reason is the high melt rates in the ablation area, which compromise the stability of the AWSs at the glacier surface during the ablation season. Dynamic supraglacial morphologies and crevasses characterizing the ablation area, also represent a problem. From 1987 several permanent

## 2. Energy and mass balance of Forni Glacier (Stelvio National Park, Italian Alps) from a 4-year meteorological data record

---

AWSs have been located on the glacier ablation areas. To set up the AWSs, structures (a mast with four legs) able to stay freely on the ice surface and to adjust to the melting surface are used. This allowed the installation of AWSs designed to provide data all year round on the melting zones of the Greenland ice-sheet, of Hardangerjokulen (Norway) and of the Morteratschgletscher (Switzerland) (Oerlemans, 2000; Oerlemans and Klok, 2002; Klok and Oerlemans, 2004). Up to now the longest glacier data series, was obtained from the AWS located on the Morteratschgletscher (Switzerland). Due to the possibility of regular visits and to the favourable atmospheric conditions (little icing) a good quality meteorological data set was obtained during the last 2 decades (Oerlemans, 2001; 2009). The Morteratschgletscher AWS was used as a valuable example for the installation of the first Italian permanent AWS on the ablation area of Forni Glacier, in the Alps (Citterio et al., 2007).

On the Italian Alpine glaciers, a long tradition of field surveying is present: length variation and mass balance measurements started respectively in 1895 at Forni Glacier (Lombardy) and in 1967 at Careser Glacier, (Trentino) (Smiraglia, 2003). Nevertheless continuous monitoring of long-term meteorological data, energy fluxes measured directly at the glacier surface and energy balance studies are still lacking. During the last decades, the Italian AWSs (collecting data during different periods) were located in the glacierized areas on rock exposures, nunataks or buildings (such as mountain huts), thus making the meteorological data representative of high mountain atmospheric conditions but not very useful for analysis of the supraglacial micrometeorology. The first permanent Italian AWS on a glacier ablation area was installed on Forni Glacier on the 26<sup>th</sup> of September 2005. The aim was to collect meteorological data, to measure the energy fluxes at the glacier/atmosphere interface, to calculate energy available for the ice ablation and to measure the snow accumulation. The Forni AWS results are also interesting for comparison with the AWS located on the Morteratsch Glacier managed by Institute for Marine and Atmospheric Research Utrecht (IMAU). Forni and Morteratsch glaciers are situated on the south side and north side respectively of the Alps: both with north aspect and similar geometry settings. The main differences between the two AWSs locations are: the AWS Forni is about 500 m higher than AWS Morteratsch (Oerlemans, 2001), Morteratsch Glacier has a larger area (16 km<sup>2</sup>) than the Forni Glacier (12 km<sup>2</sup>) and the Forni site is dryer (i.e.: smaller precipitation and smaller relative humidity values) (Table 1).

2. Energy and mass balance of Forni Glacier (Stelvio National Park, Italian Alps) from a 4-year meteorological data record

*Tab. 1: Comparison between Forni and Morteratsch Glacier: site characteristics, meteorological and energy balance data. Morteratsch Glacier data are annual mean values of 2000, except the albedo which is the mean value of 1995.*

	<b>Forni Glacier</b>	<b>Morteratsch Glacier</b>
<b>Coordinates</b>	46° 23' 56" N; 10° 35' 25" E	46° 24' 34" N; 9°55' 54" E
<b>Elevation range (m a.s.l.)</b>	2600 - 3670	1900 - 4049
<b>Length (km)</b>	3	7
<b>Area (km<sup>2</sup>)</b>	12	16
<b>AWS elevation (m a.s.l.)</b>	2631	2100
<b>net SW (W m<sup>-2</sup>)</b>	68	67
<b>net Lw (W m<sup>-2</sup>)</b>	-38	-36
<b>SH (W m<sup>-2</sup>)</b>	18	36
<b>LE (W m<sup>-2</sup>)</b>	-5	6
<b>R<sub>s</sub> (W m<sup>-2</sup>)</b>	36	76
<b>SW in (W m<sup>-2</sup>)</b>	151	136
<b>SW out (W m<sup>-2</sup>)</b>	91	72
<b>SW in extra-terrestrial (W m<sup>-2</sup>)</b>	267	292
<b>Air temperature °C</b>	-1.3	2.1
<b>Snow albedo</b>	0.85	0.75
<b>Ice albedo</b>	0.35	0.35

In this chapter a 4-year record of hourly meteorological data (from 1<sup>st</sup> October 2005 to 30<sup>th</sup> September 2009) measured in the ablation area of Forni Glacier, is analyzed with the aims of describing glacier surface conditions, evaluating the surface energy and mass exchanges and the present study analyzes a new data set of meteorological observations obtained over the melting Forni Glacier surface to investigate processes and surface characteristics which are driving the surface energy balance. The focus is energy and mass balance calculation and the sensitivity to the albedo and the conditions in which melting and condensation occurs. The availability of humidity, air pressure and wind velocity data permits a more accurate calculation of turbulent fluxes than other studies (i.e. Oerlemans, 2000; Klok and Oerlemans, 2002). The study represents a further development of the previous paper by Citterio et al. (2007), which dealt with 1 year of meteorological data. The analysis of the interannual variability of the energy and mass balance estimations is performed. Then we compare our results on Forni Glacier to previous studies on different glacier sites (e.g. Morteratsch Glacier, Switzerland; Peyto Glacier, Canada). The influence of surface albedo variability on ice melting is evaluated to analyze and discuss the parameters influencing the surface energy budget of an alpine glacier. Furthermore the energy and mass balance results from our study contribute to the evaluation of the meltwater discharge from Forni Glacier basin, in Stelvio National

## 2. Energy and mass balance of Forni Glacier (Stelvio National Park, Italian Alps) from a 4-year meteorological data record

Park. This is particularly important as Forni meltwater is also utilized for hydropower production.

### 2. The AWS1 Forni

The Automatic Weather Station Forni (AWS1 Forni) is set up on the ablation tongue at the base of the Eastern icefall of Forni Glacier. Forni is the largest Italian valley glacier (surface area of about 12 km<sup>2</sup>), and is situated in the Ortles-Cevedale Group, Stelvio National Park, Lombardy Alps. The glacier is about 3 km long (Fig. 1), has a northward down sloping surface and stretches over an elevation range of 2600 to 3670 m a.s.l.. The WGS84 coordinates of AWS1 Forni are: 46° 23' 56.0" N (46.40° N), 10° 35' 25.2" E (10.60° E), 2631 m a.s.l. (Fig. 1). The AWS location is a good compromise between the need to minimize local topographical effects (almost flat surface and absence of crevasses) and to decrease the probability of snow avalanches during winter in the AWS vicinity. The AWS is positioned on the lower glacier sector, at 800 m from the glacier terminus.

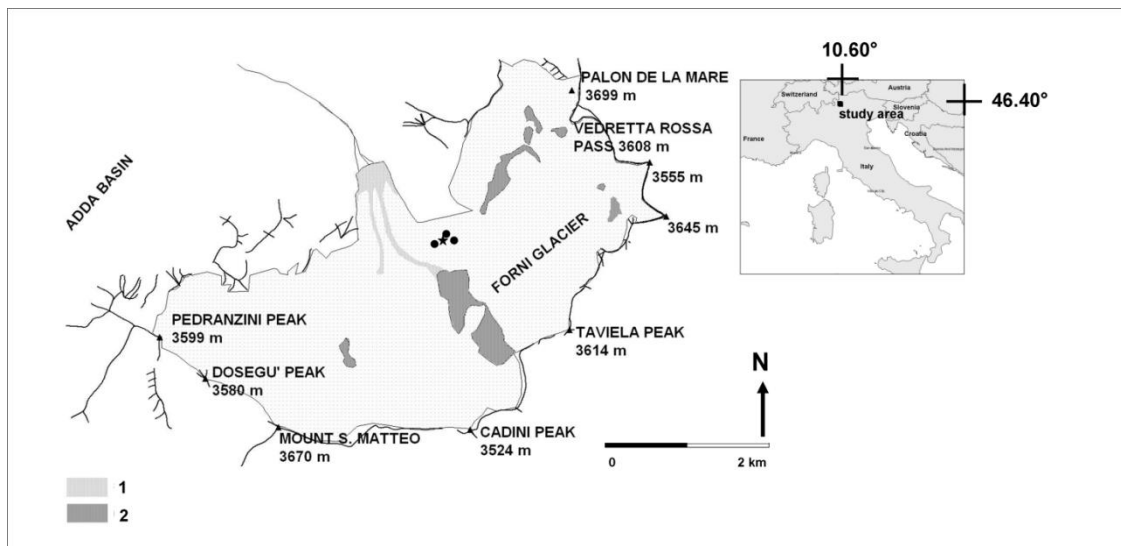


Fig. 1: Location (black star) of the AWS1 Forni and the three ablation stakes (black dots); the AWS and the ablation stakes are located in an area of about 50 m<sup>2</sup>. The light gray areas are used to mark supraglacial debris coverage, the dark gray areas are used to indicate rock exposures and nunataks.

## 2. Energy and mass balance of Forni Glacier (Stelvio National Park, Italian Alps) from a 4-year meteorological data record

---

The AWS was installed on 26<sup>th</sup> of September 2005. In the following years the AWS was checked several times, particularly during the first year, without any problem being observed (Citterio et al., 2007). The AWS is equipped with sensors (Table 2, Fig. 2) for measuring air temperature and humidity (naturally ventilated sensor), wind speed and direction, air pressure, the four components of the radiation budget (longwave in and out, solar in and out). A 1000 cm<sup>2</sup> unheated rain gauge and a Campbell SR-50 sonic ranger are also set up to measure respectively rain and snow depth.

The whole system is supported by a four-leg, 5 m high stainless steel mast standing on the ice surface according to the construction and setting proposed and tested by IMAU (Oerlemans, 2001). The AWS stands freely on the ice, and adjusts to the melting surface during summer. Supraglacial morphologies (bedières) may develop at the AWS location, which can compromise the stability. In this case the AWS needs to be moved on a more stable surface. The height where instruments are placed was chosen in order to permit their activity also during the winter time when snow covers the glacier surface and partially buries the AWS mast.

The sonic ranger is installed on the AWS mast, measuring only the accumulation and not the ice ablation. An important feature of the thermo-hygrometer is the radiation shield with natural ventilation, thus permitting an air flow around the sensor limiting the error due to the radiation overheating. Due to the naturally ventilated sensor our air temperature measurements could be overestimated (up to a few degrees) during high radiation/low wind speed conditions (Georges and Kaser, 2002); on the other hand such conditions seem to be dominating only during limited periods (early spring). The albedo values during snow fall events are overestimated due to snow presence on the upfacing pyranometer. To solve this problem the values affected by the overestimations were filtered and not considered in our analysis. No problems of rime ice accumulation on instruments were observed during the 4 years of data collection, based on the analysis of wind speed and direction data (which are consistent over the entire period).

Power is supplied by two solar panels (40 Watt) and a lead-gel battery; the battery voltage over time is recorded by the datalogger. The battery-only power supply, in the present configuration is estimated in excess of two months, with the solar panels permanently obscured by snow accumulation and accounting for low temperature operation and self discharge. Data points, sampled at 60-second intervals and averaged over a 30-minute time period for most of the sensors (see the fourth column in Table 2), are recorded in the flash memory card, including the basic distribution parameters

## 2. Energy and mass balance of Forni Glacier (Stelvio National Park, Italian Alps) from a 4-year meteorological data record

---

(minimum, mean, maximum and standard deviation values). Wind data are sampled every 5 seconds, and then processed to obtain an hourly data set of information, including minimum, maximum and average speed, dominant wind direction.



*Fig. 2: AWS1 Forni. The instruments are marked with numbers: (1) wind speed and direction, (2) rain gauge, (3) net radiometer CNRI, (4) sonic ranger, (5) thermo-hygrometer, (6) solar panels, and (7) barometer inside the datalogger box (photo by G. Diolaiuti).*



## 2. Energy and mass balance of Forni Glacier (Stelvio National Park, Italian Alps) from a 4-year meteorological data record

*Tab. 2: Sensor specifications installed at the AWS1 Forni.*

Variable	Range	Accuracy	Recording rate	Height	Manufacturer
<b>Data Logger</b>				1.5 m	LSI-Lastem Babuc ABC
<b>Air Temperature</b>	-30 - +70 °C	±0.001°C	30 min.	2.6 m	LSI-Lastem DMA570
<b>Relative Humidity</b>	0 - 100 %	±1%	30 min.	2.6 m	LSI-Lastem DMA570
<b>Air Pressure</b>	400 - 800 hPa or mBar	±10hPa	60 min.	1.5 m (inside the logger box)	LSI-Lastem DQA223
<b>Solar Radiation</b>	0.3 - 3 µm	±5% of the value	30 min.	3.17 m	Kipp and Zonen CNR-1
<b>Infrared Radiation</b>	5 - 50 µm	±5% of the value	30 min.	3.17 m	Kipp and Zonen CNR-1
<b>Snow level</b>	0 - 1000 cm	±2 cm	60 min.	3.17 m	Sonic Ranger Campbell SR50
<b>Liquid precipitation</b>	0 - 1000 mm	±1mm	30 min.	1.5 m	LSI-Lastem DQA035
<b>Wind Speed</b>	0 - 50 m s <sup>-1</sup>	±1%	60 min.	5 m	LSI-Lastem DNA022
<b>Wind Direction</b>	0° - 360°	±1°	60 min.	5 m	LSI-Lastem DNA022

## 3. Methods

AWS1 Forni has been running continuously since its installation with only one interruption between the 5<sup>th</sup> and the 11<sup>th</sup> of October 2008. In this study we analyze and compare 4 hydrological years (for the hydrological year we consider the period from 1<sup>st</sup> October to 30<sup>th</sup> September of the next year). All the annual values are averaged on the hydrological year basis.

### 3.1 Solid precipitation

Snowfall measurements provide important information for evaluating glacier accumulation and thus mass balance. Forni Glacier is one of the sites frequently monitored by Centro Nivometeorologico di Bormio of the Lombardy Regional Agency for Environmental Protection (ARPA Lombardia), therefore is possible to compare the collected snow pit data to the data record from the sonic ranger of AWS1 Forni. Comparison of the two data sets confirms the reliability of the data acquired by the sonic ranger over one year of data (Citterio et al., 2007). In our analysis we use a 140 kg

## 2. Energy and mass balance of Forni Glacier (Stelvio National Park, Italian Alps) from a 4-year meteorological data record

---

$\text{m}^{-3}$  fresh snow density and to distinguish snowfall from liquid precipitation, a  $+1.5^\circ\text{C}$  temperature threshold value (Hock, 1999; Klok and Oerlemans, 2002; Huss et al., 2009; Paul et al., 2009).

### 3.2 Radiation

To calculate the surface energy balance, the hourly radiation data were analyzed. At the glacier surface, solar radiation is the most important energy balance component driving ice and snow melt. Therefore the albedo (from here  $\alpha$ ) is an important and noteworthy parameter of glacier surface to be analyzed in terms of temporal variability.

Firstly we filtered the incoming and outgoing shortwave radiation data ( $SW_{in}$  and  $SW_{out}$ , respectively) in order to remove erroneous values (e.g.: after a snow fall event, values showing  $SW_{out}$  exceeding  $SW_{in}$  due to the presence of fresh snow on the top pyranometer); then the following relation was applied:

$$\alpha = \frac{SW_{out}}{SW_{in}} \quad (1)$$

The incoming and outgoing longwave radiation ( $LW_{in}$  and  $LW_{out}$ , respectively), were measured by the CNR1 pyrgeometers. The acquired data represent the flux at each sensor surface, and the values have been converted to the ground and atmospheric (upward and downward) directional flux by Stephan-Boltzmann's law.

### 3.3 Turbulent fluxes

Because measurements are available for one level only, no attempt was made to use sophisticated schemes for the calculation of the turbulent heat fluxes. Instead the well-known bulk aerodynamic formulas were used according to the methods introduced by Oerlemans (2000):

$$SH = \rho_a \cdot c_p \cdot C_h \cdot V_{2m} \cdot (T_{2m} - T_S) \quad (2)$$

## 2. Energy and mass balance of Forni Glacier (Stelvio National Park, Italian Alps) from a 4-year meteorological data record

---

$$LE = 0.622 \cdot \rho_a \cdot L_V \cdot C_h V_{2m} \cdot \frac{(e_{2m} - e_S)}{p} \quad (3)$$

where  $\rho_a$  is air density ( $0.87 \text{ kg m}^{-3}$ ),  $c_p$  is the specific heat of dry air ( $1.006 \text{ kJ kg}^{-1} \text{ }^\circ\text{C}^{-1}$ ),  $C_h$  is the turbulent exchange coefficient ( $0.00127 \pm 0.00030$ ; from Oerlemans, 2000),  $V_{2m}$  is wind speed value at 2 m,  $T_{2m}$  is air temperature value at 2 m,  $T_S$  is the surface temperature,  $L_V$  is the latent heat of vaporization (Harrison, 1963),  $e_{2m}$  is vapor pressure value at 2 m,  $e_S$  is vapor pressure value at the surface (calculated using the Wexler formula; Wexler, 1976) and  $p$  is air pressure value at sensor level. The  $T_S$  is calculated by using the Stephan-Boltzmann law:  $T_S = 4 \sqrt{(LW_{out} \cdot \sigma^{-1} \cdot \varepsilon^{-1})}$ , where  $\sigma$  is the Stephan-Boltzmann constant,  $5.67 \cdot 10^{-8} \text{ W m}^{-2} \text{ K}^{-4}$  and  $\varepsilon$  is the emissivity of the snow/ice surface, assumed to be equal to the unity. Wind speed and air temperature and humidity are measured at 5 m and 2.6 m respectively, then they are calculated at 2 m (following the method introduced by Oerlemans, 2000). The  $C_h$  is assumed to be constant, because no information on how the roughness lengths change during the year is available (Oerlemans and Klok, 2002). An overestimation of the turbulent fluxes calculations may occur in spring due to overestimation of air temperature under low wind/high global radiation conditions.

The outgoing longwave flux at the glacier surface cannot exceed the flux for a melting surface, which is about  $316 \text{ W m}^{-2}$ . However, since the sensor is installed at a height of about 3.17 m, we can assume a contribution from the air layer between the surface and the sensor. The measured flux can therefore be slightly larger than  $316 \text{ W m}^{-2}$  (Oerlemans, 2009): in these cases the surface temperature is set to  $0^\circ\text{C}$  (Oesch et al., 2002; Pellicciotti et al., 2008; Rupper and Roe, 2008; Mölg and Hardy, 2004; Oke, 1987).

### 3.4 Surface energy and mass balance

To calculate the glacier energy and mass balance components, we applied the following methods by considering the hourly meteorological values.

The energy balance at the glacier surface ( $R_S$ ) determines the net energy available for heating and melting.  $R_S$  was calculated as:

## 2. Energy and mass balance of Forni Glacier (Stelvio National Park, Italian Alps) from a 4-year meteorological data record

---

$$R_S = SW_{net} + LW_{net} + SH + LE \quad (4)$$

All the fluxes ( $\text{W m}^{-2}$ ) were defined positive when directed towards the surface. The conductive heat flux at the surface was neglected since no temperature sensors were located in the snowpack and in the ice surface layer. During the ablation season (i.e.: from June to October), when melting occurs and surface ice temperature is  $\sim 0^\circ\text{C}$ , at the glacier surface all the energy is used to melt the ice. Consequently the conductive heat flux at the surface is equal to zero thus permitting to calculate  $R_S$  without considering it. Differently, when the glacier surface is not at the melting point (i.e.: from October to June) and  $R_S$  is lower than  $0 \text{ W m}^{-2}$ , the surface cools and the conductive heat flux value is not equal to zero and has to be evaluated. In our study, neglecting the conductive heat flux at the surface, is resulting in a slight overestimation of ice melting.

The glacier annual mass balance is the sum of accumulation and ablation (i.e.: mass gain and loss, respectively) over a one year long period. On Forni Glacier the main ablation process is the surface melting which occurs from late spring to early fall. Then we focused on the ice and snow melting ( $M$ ) calculation from the glacier energy balance. The negative  $M$  value was added to the snow accumulation ( $P_{solid}$ ) positive value thus giving the specific annual mass balance ( $B$ ) at the location of the AWS1 Forni.

The ablation amount ( $M$ ) was obtained from:

$$M = - \frac{R_S}{L_m} \quad (5)$$

where  $M$  is the rate of change of mass ( $\text{kg m}^{-2}$  or  $\text{mm w.e.}$ ),  $L_m$  is the latent heat of melting ( $3.34 \times 10^5 \text{ J kg}^{-1}$ ). It is assumed that melting occurs as soon as the surface temperature is at  $0^\circ\text{C}$  and  $R_S$  is positive.

The accumulation amount was calculated considering daily fresh snow values recorded by the sonic ranger. To convert accumulated fresh snow into water equivalent a density of  $140 \text{ kg m}^{-3}$  was used to obtain the solid precipitation value ( $P_{solid}$ ).

Finally the mass balance ( $B$ ) was calculated as:

$$B = \int_0^T (M + P_{solid}) dt \quad (6)$$

## 2. Energy and mass balance of Forni Glacier (Stelvio National Park, Italian Alps) from a 4-year meteorological data record

---

where  $t$  is the time during the 4-year period we analyzed (from 0 to  $T$ , that is from 00:00 am of 1<sup>st</sup> October 2005 to 11:00 pm of 30<sup>th</sup> September 2009). The calculation is made also on an annual basis (from 1<sup>st</sup> October to 30<sup>th</sup> September of the next year).

## 4. Results

### 4.1. Meteorology

The data collected by the AWS1 Forni are summarized in Figure 3. Daily average values of wind speed, air temperature, global radiation and clear-sky global radiation, albedo, snow depth and accumulated fresh snow are shown. In general, wind speed values were low (Fig. 3a): a 4-year mean value of  $4.99 \text{ m s}^{-1}$  was found; nevertheless daily maxima up to  $17 \text{ m s}^{-1}$  were registered (e.g.:  $17.03 \text{ m s}^{-1}$  on 06/09/2007) and maximum hourly values exceed  $25 \text{ m s}^{-1}$  (e.g.:  $25.11 \text{ m s}^{-1}$  on 27/01/08 at 10:00 am). By analyzing the hourly data the low wind speed values (lower than  $1.5 \text{ m s}^{-1}$ ) or calm state ( $0 \text{ m s}^{-1}$ ) are accounting for 9% over the entire period (1% of calm state) on Forni Glacier thus minimizing the air temperature overestimations.

Daily mean values of air temperature are shown in Figure 3b. From the analysis of all the daily mean temperature data, an annual diagram was obtained with an expected annual cycle (maxima occurring in the summer and minima during winter). Over the 4-year period an average air temperature of  $-1.3^\circ\text{C}$  was found and the annual range was typically  $7.4^\circ\text{C}$ . Regarding the extreme mean daily values, the AWS measured  $-22.9^\circ\text{C}$  in winter (29/12/2005) and  $+11.1^\circ\text{C}$  in the summer time (25/06/2008).

The Figure 3c shows global radiation trend. An interesting feature is the increase in the daily variability in spring, which is due to the increasing potential incoming shortwave radiation. This increases the contrast between clear days (high values) and cloudy days (low values). This feature, observed also on Morteratschgletscher, seems to be enhance by the disappearance of snow cover on the sides of the glacier valley, reducing the effect of multiple reflection over the glacier surface (Oerlemans, 2000). A mean global radiation of  $151 \text{ W m}^{-2}$  was measured. A comparison with the annual mean extra-terrestrial irradiance, calculated for the same latitude and elevation and equal to  $267 \text{ W m}^{-2}$ , makes clear that shading and clouds strongly decrease the amount of solar energy at

## 2. Energy and mass balance of Forni Glacier (Stelvio National Park, Italian Alps) from a 4-year meteorological data record

---

the glacier surface. The reduction is of ca. 44% excluding the processes of scattering and absorption of the clear atmosphere.

The mean 4-year albedo value (Fig. 3d) is 0.65. During the accumulation season, the 4 year mean annual albedo value was 0.85 while during the ablation season, the mean annual value was 0.35. This shows a marked seasonal cycle related to the different surface reflectivity between ice and snow (Table 3). In fact, a snow fall implies higher albedo, increasing outgoing radiation and less energy available for melting.

The last two panels of Figure 3 (Figs. 3e and 3f) present the snow data. In the panel e, snow depth (m) is measured at the sonic ranger. A large annual variability is seen. To underline the correlation between snow depth and accumulated fresh snow, in the last panel the yearly fresh snow accumulation (with a density of  $140 \text{ kg m}^{-3}$ ) is represented. Comparing these two parameters, higher values of snow depth are related to the higher amounts of fresh snow (e.g.: in 2009).

2. Energy and mass balance of Forni Glacier (Stelvio National Park, Italian Alps) from a 4-year meteorological data record

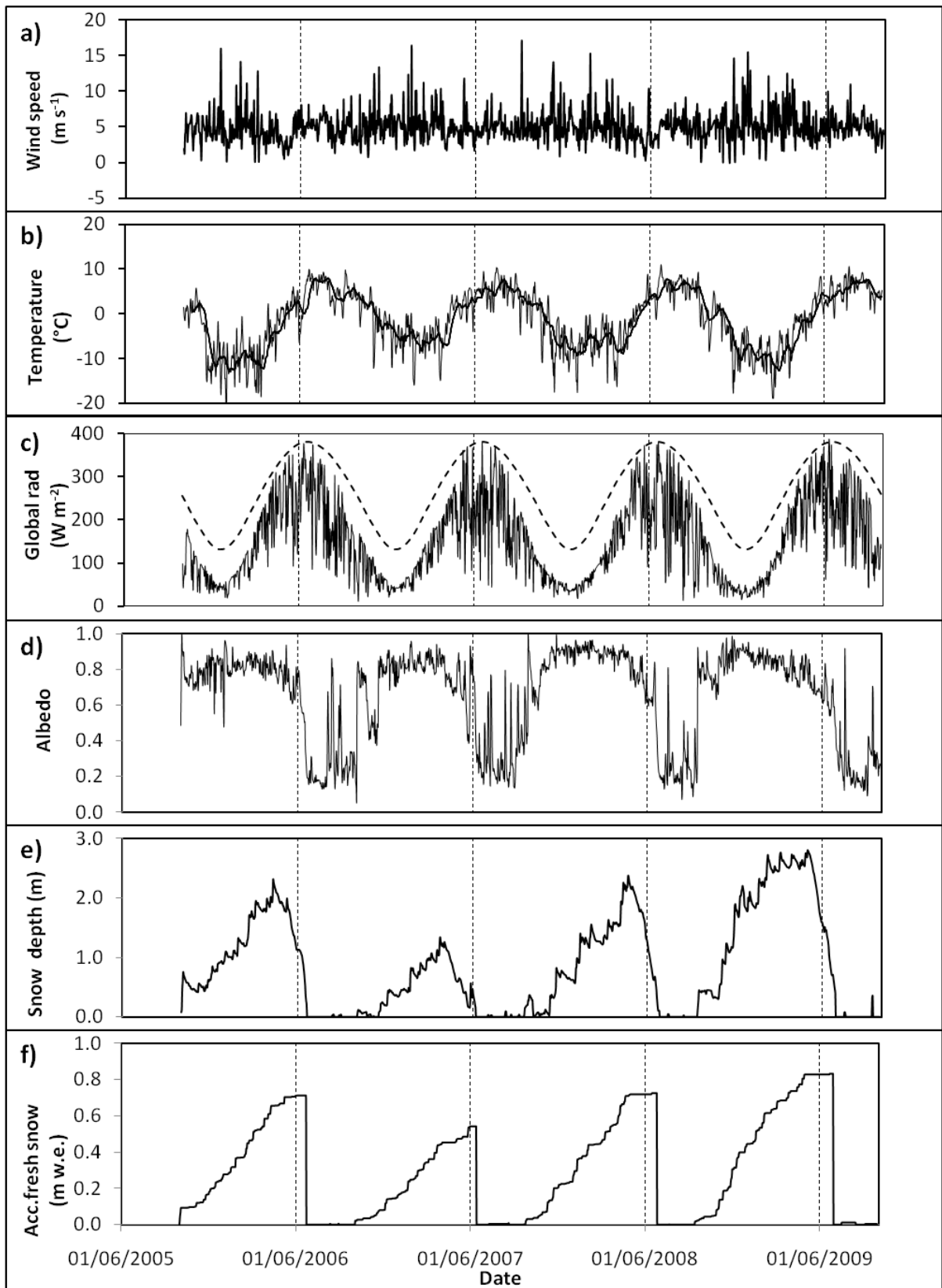


Fig. 3: Daily mean values of (a) wind speed; (b) air temperature; (c) global radiation (solid curve) and clear-sky global radiation (dashed curve); (d) albedo; (e) snow depth (m); and (f) accumulated fresh snow (m w.e.) for the entire period, from 1<sup>st</sup> October 2005 to 30<sup>th</sup> September 2009. The dates shown are dd/mm/yyyy.

## 4.2. Energy balance

The components of the glacier surface energy balance are summarized in Figure 4. Daily mean values are characterized by similar trends of the annual cycle over the analysis period (from 1<sup>st</sup> October 2005 to 30<sup>th</sup> September 2009): all the maximum values occur during summer, and all minimum during winter except the values of net longwave radiation. In particular, the net shortwave radiation shows maxima during the summer (ranging from 250 W m<sup>-2</sup> to 300 W m<sup>-2</sup>) and the minima during winter (with values nearby 0 W m<sup>-2</sup>); net longwave data vary between slightly positive values (close to 0 W m<sup>-2</sup>) and negative values (up to -100 W m<sup>-2</sup>, realistic values due to the 0° C glacier surface). Daily *LW* average values are rarely positive and usually slightly positive values occur only during warm and not too cloudy summer days. The sensible heat flux is generally positive and exceeds the latent heat flux. The latent heat flux is generally positive during the ablation season, during the rest of the year is negative, due to low humidity in combination with a minimal temperature difference between the surface and the air (Oerlemans, 2000). A similar trend is found for the net energy ( $R_S$ ) diagram with maxima of ca. 300 W m<sup>-2</sup> and minima of ca. -100 W m<sup>-2</sup>. The negative values characterize the winter periods, when ice melting is absent. The increase in net energy is very steep in late spring/early summer due to the transition from a snow covered to a bare ice surface. The transition from bare ice to snow cover in October/November has a more gradual, because then the incoming shortwave radiation flux is reduced. Analyzing the annual mean values of all parameters, the year 2007/2008 is characterized by a lower *SWnet* and  $R_S$ ; instead the year 2008/2009 is dominated by a higher *SWnet*, *LWnet* and *LE*. The highest  $R_S$  is calculated in 2005/2006 with intermediate values of *SWnet*, *LWnet* and *LE*.

Filtering surface temperature ( $T_S$ ), net energy ( $R_S$ ) and latent heat flux (*LE*) data, the hours characterized by melting (i.e.: when  $T_S=0^\circ\text{C}$  and  $R_S>0\text{ W m}^{-2}$ ) and condensation (when  $T_S=0^\circ\text{C}$  and  $LE>0\text{ W m}^{-2}$ ) are found (Fig. 5). Considering only these hours which accounts for about 31% for melting and about 24% for condensation, *SWnet*, *LWnet*, *SH*, *LE* and  $R_S$  are averaged. By analyzing these mean values, the net shortwave prove to be the parameter with the highest energy flux during both melting and condensation conditions (with values of 176 W m<sup>-2</sup> and 123 W m<sup>-2</sup>, respectively). Moreover, some differences are found: during melting,  $R_S$  is higher than during condensation; during melting the net longwave reaches values of -24 W m<sup>-2</sup>, instead during condensation -20



2. Energy and mass balance of Forni Glacier (Stelvio National Park, Italian Alps) from a 4-year meteorological data record

$\text{W m}^{-2}$ . The latent heat flux value is higher during condensation ( $12 \text{ W m}^{-2}$ ) than during melting ( $4 \text{ W m}^{-2}$ ). Sensible heat flux value is similar in both situations (ca.  $30 \text{ W m}^{-2}$ ).

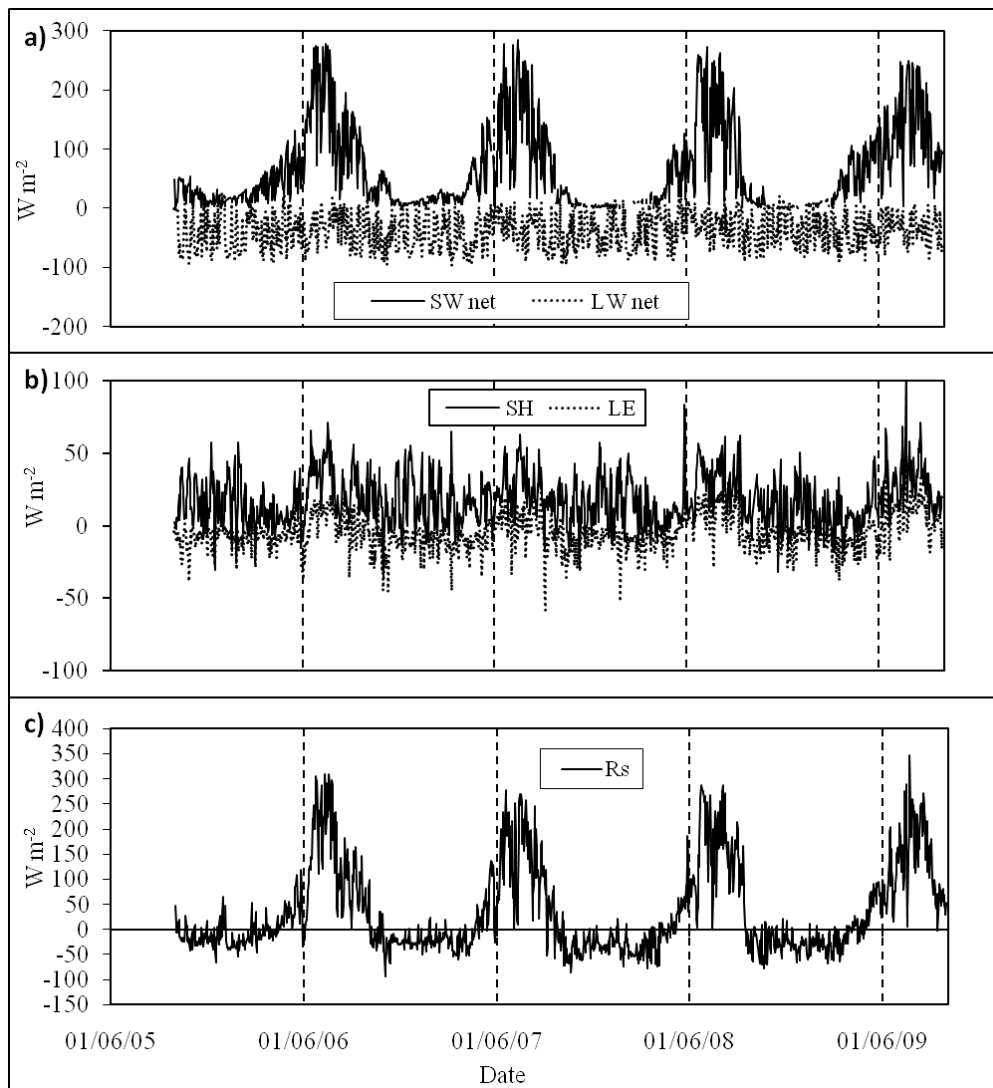


Fig. 4: Components of the surface energy balance, showing daily mean values: (a) net shortwave and longwave radiation, (b) turbulent fluxes of sensible and latent heat, and (c) net energy available for ice/snow melting (please note the differences in vertical scales). The dates shown are dd/mm/yy.

## 2. Energy and mass balance of Forni Glacier (Stelvio National Park, Italian Alps) from a 4-year meteorological data record

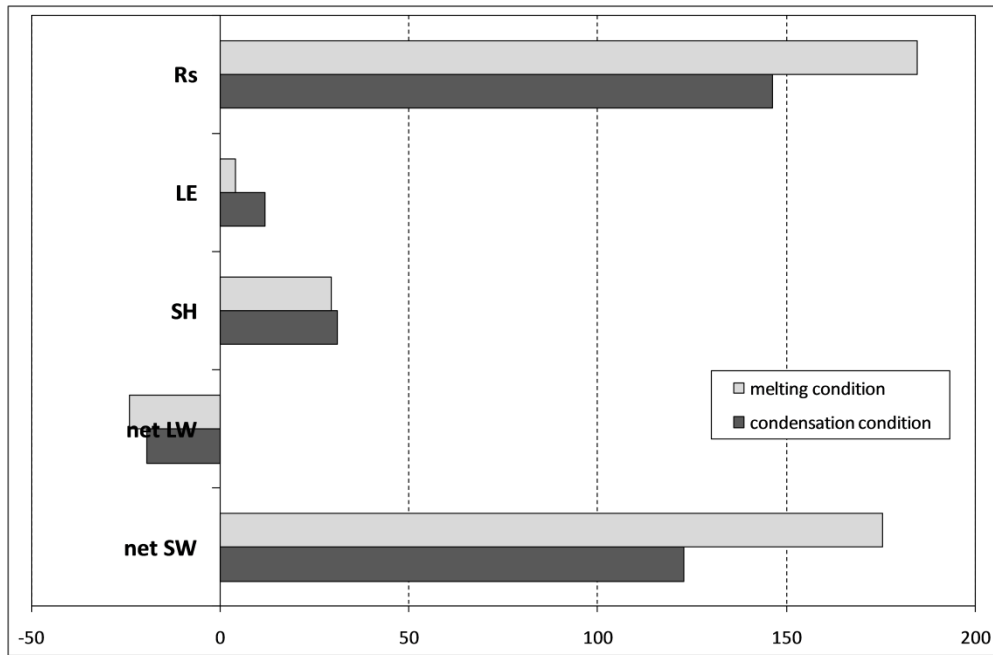


Fig. 5: Components of the surface energy flux (from hourly mean values), averaged over time, when melting (i.e. about 31% of the time) (light gray) and condensation (i.e. about 24% of the time) (dark gray) conditions occurred. The units of measure for the x-axis are  $W m^{-2}$ .

### 4.3. Mass balance

The solid precipitations curve (Fig. 3f) is characterized by a step wise increase during the winter period and quite stable conditions during the summer period when only a few snowfalls occur. In fact when the ablation processes dominate, the air temperature is warmer and solar radiation influence is higher. The total accumulation during the 4 years was +2.8 m w.e.. The maximum value is registered during 2008/2009 (Table 3), characterized by heavier snow falls ( $+0.8 \pm 0.007$  m w.e.). An intermediate total yearly value of  $+0.7 \pm 0.006$  m w.e. is measured during 2005/2006 and 2007/2008, whereas 2006/2007 is characterized by the minimum value ( $+0.6 \pm 0.005$  m w.e.).

Figure 6 shows the cumulative ablation and mass balance curves over the entire period. The melt is calculated from the complete energy balance and considering only melting hours. A total melt value of  $-21.6$  kg  $m^{-2}$  or m w.e. was calculated. The annual values are presented in Table 3. The highest loses occur during 2005/2006 and 2008/2009, instead less ablation characterize the 2007/2008.

## 2. Energy and mass balance of Forni Glacier (Stelvio National Park, Italian Alps) from a 4-year meteorological data record

Analyzing daily values of mass balance (Fig. 7), we can observe how the mass losses prevail over gains. The accumulation does not exceed +0.05 m w.e./day and the ablation values reach up -0.09 m w.e./day. Moreover, the cycle of surface mass balance is shown: during winter the melting is absent, instead it dominates during ablation season (June-October). This cycle is evident also analyzing the cumulative curve (Fig. 6); in fact, during winter the mass balance curve is characterized by a slow increase followed by a fast and strong decrease during the summer period. Summing the solid precipitation ( $P_{solid}$ ) with the ablation ( $M$ ) the cumulative mass balance value ( $B$ ) over the 4-year study period resulted -18.8 m (w.e.). Similar net mass balance values (-4.8 or -4.9 m w.e) were found in all years except 2007/2008 (-4.2 m w.e.).

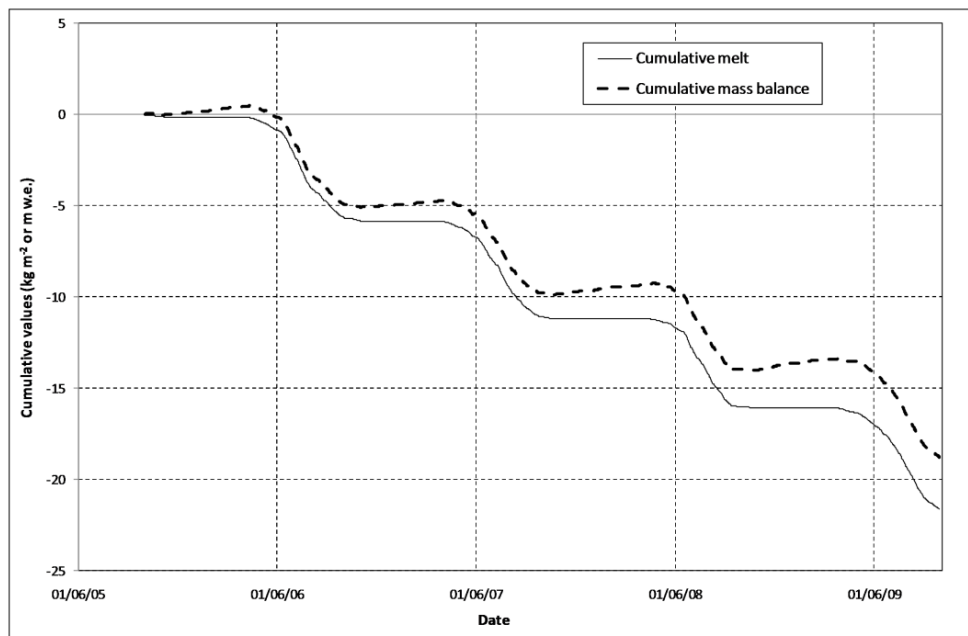


Fig. 6: Cumulative melt (solid curve) and cumulative mass balance (dashed curve) calculated over the 4-year period. Values were obtained from hourly data analysis. The dates shown are dd/mm/yy.

2. Energy and mass balance of Forni Glacier (Stelvio National Park, Italian Alps) from a 4-year meteorological data record

*Tab. 3: Comparison of cumulative melting, solid precipitation, mass balance, net shortwave radiation, and mean energy balance, air temperature and albedo annual values (from 1<sup>st</sup> October of the year  $x$  to 30<sup>th</sup> September of the year  $x+1$ ) and meteorological seasons (meteorological fall from 1<sup>st</sup> September to 30<sup>th</sup> November; meteorological winter from 1<sup>st</sup> December to 28<sup>th</sup>/29<sup>th</sup> February; meteorological spring from 1<sup>st</sup> March to 31<sup>st</sup> May; meteorological summer from 1<sup>st</sup> June to 31<sup>st</sup> August).*

Hydrological year	Cumulative melting (m w.e.)	Cumulative solid precipitation (m w.e.)	Cumulative mass balance (m w.e.)	Mean albedo	Mean energy balance (W m <sup>-2</sup> )	Cumulative net shortwave radiation (MJ)	Mean air temperature (°C)
<b>2005/2006</b>	-5.6±0.021	+0.7±0.006	-4.9±0.023		42	2244	-2.1
<b>fall</b>				0.77	-16	128	-2.6
<b>winter</b>				0.82	-19	105	-10.4
<b>spring</b>				0.78	16	439	-3.1
<b>summer</b>				0.34	153	1270	5.1
<b>2006/2007</b>	-5.5± 0.020	+0.6±0.005	-4.9±0.021		35	2228	-0.2
<b>fall</b>				0.51	18	470	1.5
<b>winter</b>				0.82	-21	101	-5.7
<b>spring</b>				0.76	13	499	-1.1
<b>summer</b>				0.33	150	1208	5.6
<b>2007/2008</b>	-5.0±0.021	+0.7±0.006	-4.2±0.023		33	1886	-1.3
<b>fall</b>				0.70	-12	395	-1.4
<b>winter</b>				0.90	-31	51	-6.8
<b>spring</b>				0.84	7	334	-3.0
<b>summer</b>				0.34	162	1240	5.9
<b>2008/2009</b>	-5.6±0.020	+0.8±0.007	-4.8±0.023		40	2180	-1.5
<b>fall</b>				0.71	0	226	-1.2
<b>winter</b>				0.87	-27	77	-9.6
<b>spring</b>				0.78	16	543	-2.0
<b>summer</b>				0.37	156	1238	5.9

## 2. Energy and mass balance of Forni Glacier (Stelvio National Park, Italian Alps) from a 4-year meteorological data record

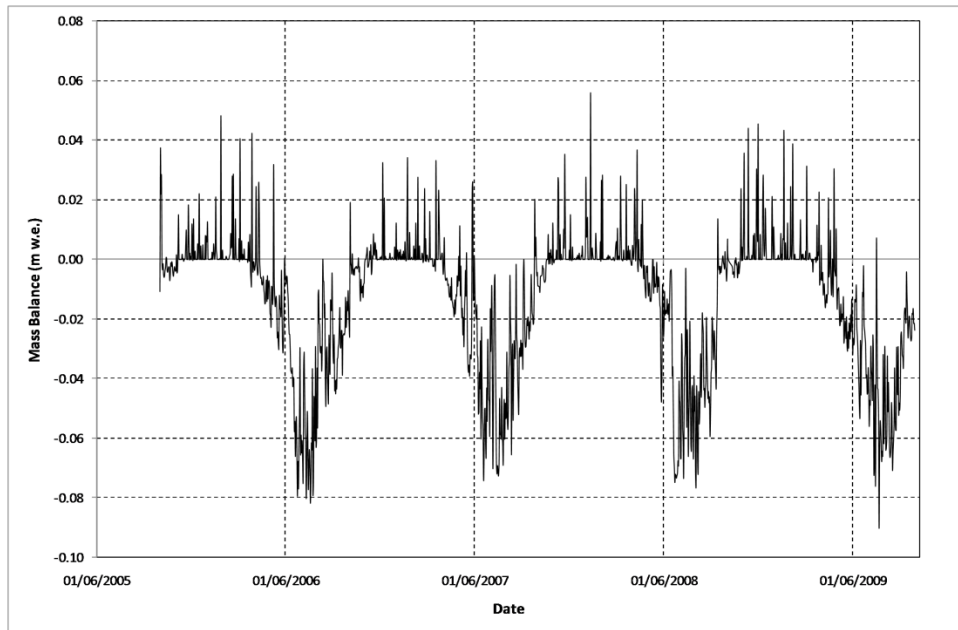


Fig. 7: Point glacier mass balance calculated over the 4-year period: the daily total values obtained from hourly data analysis are shown. The dates shown are dd/mm/yyyy.

## 5. Discussions

To assess the glacier ablation calculations from the energy fluxes, we compare the calculated ablation data to the measured values. The comparison is performed for a short but meaningful time frame during the summer season 2009 when some ablation stakes were located near the AWS1 Forni. On 24<sup>th</sup> July 2009 three ablation stakes were installed (according to the method introduced by Kaser et al., 2003). Measured ablation data from 24<sup>th</sup> July to 30<sup>th</sup> August 2009 are available for comparison with the values derived from the surface energy balance. The ablation amount at the stake locations was measured on 16<sup>th</sup> August 2009 and at the end of the period (on 30<sup>th</sup> August 2009). Two values for each stake can be compared to the calculated ice melting values (Table 4) and an ice density of  $917 \text{ kg m}^{-3}$  is used to convert observed mass balances in meter water equivalent. The comparison period we chose (from 24<sup>th</sup> July to 30<sup>th</sup> August 2009) has relatively low wind speed and no, or few, periods of negative air temperature (Fig. 3 a and b). Thus, it is not representative of the full range of conditions that may occur during the ablation season even if on the Forni Glacier summer days frequently show no negative air temperatures (Table 3) and the AWS site is characterized by low wind conditions. Nevertheless our results demonstrate that the simple empirical calculation of

## 2. Energy and mass balance of Forni Glacier (Stelvio National Park, Italian Alps) from a 4-year meteorological data record

the turbulent fluxes is valid and the heat conduction into snow/ice has little effect on total available melt energy.

Average measured melting is found to be -1.97 m w.e., compared to the -2.03 m w.e of ice melting obtained from the energy balance calculation. In spite of the slight overestimation of melt from the energy balance, the two data sets are fairly well in agreement. In view of general errors involved in the measurements of ice ablation and radiation budget, the difference between calculated and observed values is rather small. In particular, the measured change of the glacier surface is a point measurement and not an accurate estimate of the mass loss in an area of 10 m x 10 m. Differences of several tens of centimeters easily develop during the ablation season between point measurements and nearby areas (Müller and Keeler, 1969). This is evident if ablation data collected from the three ablation stakes are compared and differences up to 20 cm can be found.

*Tab. 4: Measured and modeled ice melting (m w.e.) data at AWS1 Forni, using three ablation stakes (74, s1 and s2), in an area (100 m<sup>2</sup>) around the AWS site (Fig. 1). An ice density of 917 kg m<sup>-3</sup> is used to calculate melting (w. e.).*

Data sources	Time frame		
	from 24-07-09 to 16-08-09	from 16-08-09 to 30-08-09	from 24-07-09 to 30-08-09
Stake 74	-1.20	-0.71	-1.91
Stake s1	-1.27	-0.71	-1.98
Stake s2	-1.41	-0.61	-2.02
<b>Average measured ice melting (w. e.)</b>	-1.29	-0.68	-1.97
<b>Calculated ice melting (w. e.)</b>	-1.32	-0.71	-2.03

The availability of outgoing longwave radiation data permitted to accurately calculate the surface temperature and consequently the turbulent fluxes and surface energy balance. If no temperature sensor is installed at the glacier surface,  $T_S$  can be calculated from the outgoing longwave radiation flux, surface energy flux (e.g. Klok and Oerlemans, 2002) or air temperature (e.g. Oerlemans, 2000). Setting up surface temperature as function of air temperature is incorrect, in particular when the surface energy balance is negative and measured air temperatures are positive, and also when air temperatures are  $< 0^\circ\text{C}$  and  $R_S$  is positive. These inconsistencies have impacts on the outgoing longwave flux as well as the turbulent heat fluxes (Anslow et al., 2008).

## 2. Energy and mass balance of Forni Glacier (Stelvio National Park, Italian Alps) from a 4-year meteorological data record

---

Consequently different methods impact the energy budget calculations. In our study on Forni Glacier, the turbulent heat fluxes are calculated from the LWout data differently from Oerlemans (2000) on Morteratsch glacier, where the *LW* sensor was not available and  $T_S$  is calculated from the air temperature. Furthermore in the present analysis, humidity, wind velocity and air temperature are measured at  $> 2$  m at the AWS and then calculated at 2 m thus permitting to estimate *LE* with more precision. In Klok and Oerlemans (2002) the turbulent fluxes calculations are different due to the absence of the wind sensor. The pattern of our energy balance values (Fig. 4) is in agreement with results from Klok and Oerlemans (2002) on Morteratsch Glacier rather than in Oerlemans (2000).

In Table 1 is shown a comparison between Forni and Morteratsch Glaciers, in particular the differences in AWS location and energy balance results are reported. We refer to Oerlemans (2007) for the characteristics of the site. The Morteratsch data refer to annual mean values surveyed in 2000, except albedo (1995). Radiation and albedo values are similar, instead greater differences are found between the turbulent fluxes: in particular *SH* and *LE* values on Forni result lower than on Morteratsch. The climatic setting of the two glaciers is the same, with Forni being a bit sunnier, then differences in air temperature and hence turbulent fluxes are simply due to the higher elevation of the AWS1 Forni.

In Table 3 we summarize the annual and seasonal values of the most important parameters to identifying the factors driving the 4 year-glacier mass balance.

The mass balance values result more negative ( $-4.9 \pm 0.022$  m w.e.) during hydrological years 2005/2006 and 2006/2007 characterized by a high melting values. During 2005/2006, the high mean energy balance and cumulative net shortwave radiation may have played an important role. Instead 2006/2007 displays a fall season showing a positive mean energy balance, which seems affecting the trend of solid precipitation. In fact this year is characterized by the lowest snow accumulation ( $+0.6 \pm 0.005$  m w.e.). Differently, during 2007/2008, the cumulative mass balance is less negative ( $-4.2 \pm 0.023$  m w.e.) due to the lowest cumulative melt. This year is also characterized by the lowest mean energy balance and the lowest cumulative net shortwave radiation, and the snow accumulation corresponds to the 4 year mean value ( $+0.7 \pm 0.006$  m w.e.). During 2008/2009 the mass balance is lower than during 2005/2006 probably due to a slightly higher snow amount even if the cumulative melting presents the same value.

## 2. Energy and mass balance of Forni Glacier (Stelvio National Park, Italian Alps) from a 4-year meteorological data record

---

Concerning the annual and seasonal air temperature mean values (Table 3), a clear connection with the mass balance is not found. In fact, both the lowest mean air temperature values in 2005/2006 and the warmest ones in 2006/2007 correspond to a high cumulative melt. Instead from our results the mass balance and melting amount appear more influenced by surface energy balance and surface conditions. Generally the albedo is very important in controlling magnitude and rates of snow and ice ablation. At the Forni AWS the mean summer albedo does not show strong changes during the analysed period. The fall albedo displays a unique very low value in 2006/2007 (0.51) corresponding to a positive mean energy balance ( $18 \text{ W m}^{-2}$ ) and to a more negative cumulative melting. Also spring albedo shows a single year (2007/2008) with a higher value (0.84) instead all the other values are varying between 0.76 and 0.78. The lowest melt occurs in the year with the highest spring albedo differently higher melt amounts are found in periods with lower spring albedo.

The presence of fresh snow at the glacier surface reduces the adsorbed energy available for melting and also regulates the duration of ice ablation season by delaying its start and/or anticipating the end. By analyzing the albedo and the snow cover trend (Fig. 3 last three panels) during the summer/fall seasons, we find for each year the time frames characterized by ice albedo (i.e. from ca. 0.15 to ca. 0.4). Then the following ice ablation periods are found: 93 days in 2005/2006, 93 days in 2006/2007, 80 days in 2007/2008 and 90 days in 2008/2009. These results are in agreement with the mass balance budget, in fact the summer/fall with the shortest period featuring ice albedo corresponds to the less negative melt and mass balance values (2007/2008). Longer time frames with glacier ice exposed to melt processes are found when stronger negative mass balance occur (e.g. 2005/2006, 2006/2007).

Then from our analysis surface conditions are crucial in determining the net energy available for ice melting thus underling the important role played by summer and fall solid precipitation which change glacier reflectivity even if in some cases only for short time frames. When the ice ablation season is characterized by frequent snowfall it corresponds to a minor adsorption of energy and then in a minor melt. Particularly important in determining the time length of ice melt season are the duration of spring snow cover (whenever longer it may postpone the start of ice melting) and the occurrence of earlier fall solid precipitation; the latter may anticipate the end of the ablation season. In fact, in 2007/2008 when the less negative melt is found, the end of the ablation season is marked by snowfall occurred on the 14<sup>th</sup> of September.



## 2. Energy and mass balance of Forni Glacier (Stelvio National Park, Italian Alps) from a 4-year meteorological data record

---

Differently during the other hydrological years, characterized by higher melt amount, the ablation season extends up to the end of September.

Summarizing the main factors driving the Forni Glacier mass balance are: snowfall events (especially during the ablation season), snow cover persistence and albedo. A higher net cumulative shortwave radiation increases snow and ice melting, and consequently causes a lower albedo. Moreover, an albedo decrease could be also due to the debris presence at the snow and ice surface (Flanner et al., 2009; Nakawo and Young, 1982; Mihalcea et al., 2006). In the case of Forni Glacier, a continuous debris cover is present only along the well developed medial moraines (Smiraglia, 1989), which are hundreds of meters distant from the AWS, thus making debris cover influence negligible at the AWS location. On the other hand, atmospheric soot (dust and black carbon) could also be responsible for decreasing the surface reflectivity of snow and then reducing its persistence. Dust and black carbon could be present at the glacier surface due to different causes including both natural sources and anthropogenic ones. The latter are linked to diesel combustion and deforestation. The natural sources can be from bacterial decomposition of organic matter (Takeuchi et al., 2001; Takeuchi, 2002; Fujita, 2007), fine sediments from moraines, from Sahara (Sodemann et al., 2006), from fires and from volcano eruptions. Up to now no data are available for Italian glaciers describing atmospheric soot presence and then its role in driving surface albedo. On the Forni Glacier a pilot experiment is presently ongoing to collect snow samples for evaluating dust and black carbon presence (personal communication from P. Bonasoni, 2011). This could give us important information for describing glacier reflectivity evolution and then to project future glacier melt under climate and atmospheric change scenarios.

## 6. Conclusions

The results obtained from AWS1 Forni during the four-year period of data acquisition prove to be consistent with results from other AWSs located on the melting surface of other glaciers (i.e. the AWSs on Morteratschgletscher, see Oerlemans, 2000; Klok and Oerlemans, 2002).

The AWS1 Forni delivers a unique dataset on meteorological conditions on a glacier snout in the Italian Alps. The dataset (4 mass balance years) allows the study of the

## 2. Energy and mass balance of Forni Glacier (Stelvio National Park, Italian Alps) from a 4-year meteorological data record

---

seasonal variation of surface energy fluxes. In particular, the complete surface energy balance was calculated at the AWS location, where radiative fluxes are known and non-radiative contributing factors (sensible and latent heat) can be calculated. Also the hourly-scale analysis allows the calculation of surface ablation.

The complete energy balance analysis confirms that the parameter most influencing the surface net energy available for melting ice/snow ( $R_S$ ) is the net shortwave radiation ( $SW_{net}$ ), during melting ( $T_S=0^\circ\text{C}$  and  $R_S>0 \text{ W m}^{-2}$ ) and condensation ( $T_S=0^\circ\text{C}$  and  $LE>0 \text{ W m}^{-2}$ ) conditions. For a mean  $R_S$  value of  $185 \text{ W m}^{-2}$  (during melting) and  $146 \text{ W m}^{-2}$  (during condensation), mean  $SW_{net}$  is  $176 \text{ W m}^{-2}$  and  $123 \text{ W m}^{-2}$ , respectively; instead  $SH$  is ca.  $30 \text{ W m}^{-2}$  for both conditions, and  $LE$  was  $4 \text{ W m}^{-2}$  and  $12 \text{ W m}^{-2}$ , respectively. Therefore, non-radiative fluxes have less influence on ablation (during melting  $SH$  is ca. 16% and  $LE$  is ca. 2% of the  $R_S$  amount, and during condensation  $SH$  is ca. 21% and  $LE$  is ca. 8% ).

These results are also supported by the comparison between field-measured and calculated ablation values during summer 2009, which shows only small differences mainly due to the ice surface ablation variability. Moreover our results demonstrate that the simple empirical calculation of the turbulent fluxes is valid and the heat conduction into snow/ice has little effect on total available melt energy.

During the 4-year analysis, the total ice ablation calculated from the complete energy balance is  $-21.7 \text{ kg m}^{-2}$  or m w.e., and the mass accumulation is  $+2.8 \text{ m w.e.}$ , thus giving a mass balance of  $-18.8 \text{ m w.e.}$  The maximum melt is registered during 2005/2006 and 2008/2009 with an amount of  $-5.6 \pm 0.020 \text{ m w.e.}$ , instead the minimum during 2007/2008 ( $-5.0 \pm 0.021 \text{ m w.e.}$ ). 2008/2009 is characterized by the highest accumulation ( $+0.8 \pm 0.007 \text{ m w.e.}$ ) and 2006/2007 by the smallest one ( $+0.6 \pm 0.005 \text{ m w.e.}$ ). The most negative mass balance is observed during 2005/2006 and 2006/2007 ( $-4.9 \pm 0.023$  and  $-4.9 \pm 0.021$ , respectively), whereas the less negative ones occurs during 2007/2008 ( $-4.2 \pm 0.023 \text{ m w.e.}$ ).

Our findings suggest that the surface conditions, especially the role played by the solid precipitation during summer and fall seasons, are important in determining the net energy available for ice melting. Particularly important are the permanence of spring snow cover (whenever longer it may postpone the start of ice melting) and the occurrence of earlier solid precipitation during the fall season.

Glacier energy budget is also controlled by surface albedo. Its seasonal changes are driven by snowfalls and dust deposition. On this latter, the current literature (Flanner et

## 2. Energy and mass balance of Forni Glacier (Stelvio National Park, Italian Alps) from a 4-year meteorological data record

---

al., 2009) suggests to consider the possibility that atmospheric soot (dust and black carbon) is playing a role in driving the spring decrease of snow albedo also on the Alpine glaciers' surfaces. Therefore the next step of our research will be to analyze with further details the glacier surface over a one-year period, also sampling snow and ice to find any correlations between surface reflectivity and atmospheric soot presence. Moreover we like to extend the computation of the glacier surface energy balance to the entire glacier basin.

## References

- Ambach W. (1963): Untersuchungen zum Energieumsatz in der Ablationzone des Grönländischen Inlandeises. *Meddelelser om Grønland*, 174, 4-311.
- Anslow F., Hostetler S., Bidlake W.R. and Clark P.U. (2008): Distributed energy balance modeling of South Cascade Glacier, Washington and assessment of model uncertainty. *Journal Geophysical Research*, 113, F02019, doi: 10.1029/2007JF000850.
- Björnsson H. (1972): Bæsigisarjökull, North Iceland. Results of glaciological investigations 1967-1968. Part II. The energy balance. *Jökull*, 22, 44-59.
- Brock B.W., Mihalcea C., Kirkbride M., Diolaiuti G., Cutler M. and Smiraglia C. (2010): Meteorology and Surface Energy Fluxes In the 2005-2007 Ablation Seasons at Miage Debris-Covered Glacier, Mont Blanc Massif, Italian Alps. *Journal of Geophysical Research*, 115, D09106, doi:10.1029/2009JD013224.
- Capello C.F. (1959-1960): Ricerche di microclimatologia sulla superficie glaciale del Miage. *Bollettino del Comitato Glaciologico Italiano*, 9 (II serie, parte prima), 95-154.
- Citterio M., Diolaiuti G., Smiraglia C., Verza G. and Meraldi E. (2007): Initial results from the Automatic Weather Station (AWS) on the ablation tongue of Forni Glacier (Upper Valtellina, Italy). *Geografia Fisica e Dinamica Quaternaria*, 30: 141-151.
- Flanner M.G., Zender C.S., Hess P.G., Mahowald N.M., Painter T.H. Ramanathan V. and Rasch P.J. (2009): Springtime warming and reduced snow cover from carbonaceous particles. *Atmospheric Chemistry and Physics*, 9, 2481-2497.
- Fujita K. (2007): Effect of dust event timing on glacier runoff: sensitivity analysis for a Tibetan glacier. *Hydrological Processes*, 21 (21), 2892-2896.
- Georges C. and Kaser G. (2002): Ventilated and unventilated air temperature measurements for glacier-climate studies on a tropical high mountain site. *Journal of Geophysical Research*, 107 (D24), 4775, doi: 10.1029/2002JD002503
- Gregory J.M. and Oerlemans J. (1998): Simulated future sea-level rise due to glacier melt based on regionally and seasonally resolved temperature changes. *Nature*, 391 (6666), 474-476.
- Greuell W., Knap W. and Smeets P. (1997): Elevational changes in meteorological variables along a mid-latitude glacier during summer. *Journal of Geophysical Research*, 102 (D22), 25941-25954.

2. Energy and mass balance of Forni Glacier (Stelvio National Park, Italian Alps) from a 4-year meteorological data record

---

- Greuell W. and Oerlemans J. (1986): Sensitivity studies with a mass balance model including temperature profile calculations inside the glacier. *Zeitschrift für Gletscherkunde und Glazialgeologie*, 22 (2), 101-124.
- Harrison L.P. (1963): Fundamentals concepts and definitions relating to humidity. In Wexler A. (Editor) *Humidity and moisture*. Reinhold Publishing Co., N.Y, 3.
- Hock R. (1999): A distributed temperature-index ice- and snowmelt model including potential direct solar radiation. *Journal of Glaciology*, 45 (149), 101-111.
- Hock R. (2005): Glacier melt: a review on processes and their modelling. *Progress in Physical Geography*, 29 (3), 362-391.
- Hogg I.G.G., Paren J.G. and Timmis R.J. (1982): Summer heat and ice balances on Hodges Glacier, South Georgia, Falkland Islands Dependencies. *Journal of Glaciology*, 28 (99), 221-228.
- Huss M., Funk M. and Ohmura A. (2009): Strong Alpine glacier melt in the 1940s due to enhanced solar radiation. *Geophysical Research letters*, 36, L23501.
- Ishikawa N., Owens I.F. and Sturman A.P. (1992): Heat balance studies characteristics during fine periods on the lower parts of the Franz Josef Glacier, South Westland, New Zealand. *International Journal of Climatology*, 12, 397-410.
- Kaser G., Fountain A. and Jansson P. (2003): A manual for monitoring the mass balance of mountain glaciers. IHP, Technical Documents in Hydrology, 59. UNESCO, Paris.
- Klok E.J. and Oerlemans J. (2002): Model study of the spatial distribution of the energy and mass balance of Morteratschgletscher, Switzerland. *Journal of Glaciology*, 48 (163), 505-518.
- Klok E.J. and Oerlemans J. (2004): Modelled climate sensitivity of the mass balance of Morteratschgletscher and its dependence on albedo parameterization. *International Journal of Climatology*, 24, 231-245.
- Mihalcea C., Mayer C., Diolaiuti G., Lambrecht A., Smiraglia C. and Tartari G. (2006): Ice ablation and meteorological conditions on the debris-covered area of Baltoro glacier, Karakoram, Pakistan. *Annals of Glaciology*, 43, 292-300.
- Mölg T. and Hardy D.R. (2004): Ablation and associated energy balance of a horizontal glacier surface on Kilimanjaro. *Journal of Geophysical Research*, 109, D16104, doi:10.1029/2003JD004338.
- Müller F. and Keeler C. M. (1969): Errors in short-term ablation measurements on melting ice surface. *Journal of Glaciology*, 8 (52), 91-105.

2. Energy and mass balance of Forni Glacier (Stelvio National Park, Italian Alps) from a 4-year meteorological data record

---

- Munro D.S. (1989): Surface roughness and bulk heat transfer on a glacier: comparison with eddy correlation. *Journal of Glaciology*, 8 (121), 343-348.
- Munro D.S. and Marosz-Wantuch M. (2009): Modeling Ablation on Place Glacier, British Columbia, from Glacier and Off-glacier Data Sets. *Arctic, Antarctic, and Alpine Research*, 41 (2), 246-256.
- Nakawo M. and Young G.J. (1982): Estimate of glacier ablation under a debris layer from surface temperature and meteorological variables. *Journal of Glaciology*, 28 (98), 29-34.
- Oerlemans J. (2000): Analysis of a 3 years meteorological record from the ablation zone of Morteratschgletscher, Switzerland: energy and mass balance. *Journal of Glaciology*, 46 (155), 571-579.
- Oerlemans J. (2001): *Glaciers and Climate Change*. Balkema, Lisse. 115 pp.
- Oerlemans J. (2007): Estimating response times of Vadret da Morteratsch, Vadret da Palü, Briksdalsbreen and Nigardsbreen from their length records. *Journal of Glaciology*, 53 (182), 357-362.
- Oerlemans J. (2009): Retreating alpine glaciers: increased melt rates due to accumulation of dust (Vadret da Morteratsch, Switzerland). *Journal of Glaciology*, 55 (192), 729-736.
- Oerlemans J. & Vugts H.F. (1993): A meteorological experiment in the melting zone of the Greenland ice sheet. *Bulletin of the American Meteorological Society*, 74 (3), 355-365.
- Oerlemans J., Anderson B., Hubbard A., Huybrechts P., Jóhannesson T., Knap W.H., Schmeits M., Stroeven A.P., van de Wal R.S.W., Wallinga J. and Zuo Z. (1998): Modelling the response of glaciers to climate warming. *Climate Dynamics*, 14 (4), 267-274.
- Oerlemans J., Björnsson H., Kuhn M., Obleitner F., Palsson F., Smeets P., Vugts H.F. and De Wolde J. (1999): Glacio-meteorological investigations on Vatnajökull, Iceland, summer 1996. *Boundary-Layer Meteorology*, 92, 3-26.
- Oerlemans J. and Klok E.J. (2002): Energy balance of a glacier surface: analysis of automatic weather station data from the Morteratschgletscher, Switzerland. *Arctic, Antarctic, and Alpine Research*, 34 (4), 477-485.
- Oesch D., Wunderle S. and Hauser A. (2002): Snow surface temperature from AVHRR as a proxy for snowmelt in the Alps. *Proceedings of EARSeL-LISSIG-Workshop Observing our Cryosphere from Space*, Bern, March 11-13, 2002.

2. Energy and mass balance of Forni Glacier (Stelvio National Park, Italian Alps) from a 4-year meteorological data record

---

- Oke T.R. (1987): *Boundary Layer Climates*. 2nd edition, Routledge, London. 443 pp.
- Paul F., Escher-Vetter H. and Machguth H. (2009): Comparison of mass balances for Vernagtferner, Oetzal Alps, as obtained from direct measurements and distributed modeling. *Annals of Glaciology*, 50, 169-177.
- Pellicciotti F., Helbing J., Rivera A., Favier V., Corripio J., Araos J., Sicart J.E. and Carenzo M. (2008): A study of the energy balance and melt regime on Juncal Norte Glacier, semi-arid Andes of central Chile, using melt models of different complexity. *Hydrological Processes*, 22, 3980-3997.
- Rupper S. and Roe G. (2008): Glacier Changes and Regional Climate: A Mass and Energy Balance Approach. *Journal of Climate*, 21, 5384-5401.
- Smiraglia C. (1989): The medial moraines of Ghiacciaio dei Forni, Valtellina, Italy: morphology and sedimentology. *Journal of Glaciology*, 35 (119), 81-84.
- Smiraglia C. (2003): Le ricerche di glaciologia e di morfologia glaciale in Italia. Evoluzione recente e ipotesi di tendenza. In Biancotti A. and Motta M. (eds.), *Risposta dei processi geomorfologici alle variazioni ambientali. Atti del Convegno Conclusivo Programma MURST 1997, Bologna 10-11 February 2000*, Brigati, Genova, 397-408.
- Sodemann H., Palmer A.S., Schwierz C., Schwikowski M. and Wernli H. (2006): The transport history of two Saharan dust events archived in an Alpine ice core. *Atmospheric Chemistry and Physics*, 6 (3), 667-688.
- Takeuchi N. (2002): Optical characteristics of cryoconite (surface dust) on glaciers: the relationship between light absorbency and the property of organic matter contained in the cryoconite. *Annals of Glaciology*, 34, 409-414.
- Takeuchi N., Kohshima S., Shiraiwa T. and Kubota K. (2001): Characteristics of cryoconite (surface dust on glaciers) and surface albedo of Patagonia glacier, Tyndall Glacier, Southern Patagonia Icefield. *Bulletin of Glaciological Research*, 18, 65-69.
- van den Broeke M.R., Dwyer P.G. and Henneken E.A.C. (1994): Heat, momentum and moisture budgets of the katabatic layer over the melting zone of West Greenland ice sheet in summer. *Boundary-Layer Meteorology*, 71 (4), 393-413.
- van den Broeke M.R. (1997): Structure and diurnal variation of the atmospheric boundary layer over a mid-latitude glacier in summer. *Boundary-Layer Meteorology*, 83, 183-205.
- von Hann J. (1897): *Handbuch der Klimatologie*. J. Engelhorn, Stuttgart, Germany.

2. Energy and mass balance of Forni Glacier (Stelvio National Park, Italian Alps) from a  
4-year meteorological data record

---

Wallinga J. and van de Wal R.S.W. (1998): Sensitivity of Rhonegletscher, Switzerland, to climate change: experiments with a one-dimensional flowline model. *Journal of Glaciology*, 44 (147), 383–393.

Wexler A. (1976): Vapor pressure formulation for water in the range 0° to 100°C-A Revision. *Journal of Research of the National Bureau of Standards*, 80A, 775.



# Chapter 3

## **Surface energy budget and melt amount for the years 2009 and 2010 at the Forni Glacier (Italian Alps, Lombardy)**

### **Abstract**

This paper reports the surface energy budget and the melt amount evaluated at one location at the Forni Glacier (Italian Alps, Lombardy) during the years 2009 and 2010. The analysis was supported by high resolution meteorology and energy data collected by an Automatic Weather Station (named AWS1 Forni) which has been running at the glacier surface (2669 m, ellipsoidal elevation) since 26<sup>th</sup> September 2005. The AWS is also equipped with a sonic ranger to measure snow depth and its variability. It resulted that in the years 2009 and 2010 the glacier melt at about 2700 m of altitude was equal to -11.32 m w.e.; these results were confirmed by comparisons with field ablation data collected nearby the AWS during the summer season 2009 and 2010.

## **1. Microclimate of glacier: from the first pioneer investigations to the actual Alpine measurements**

In spite of the oldest series of direct mass balance measurements in the world was from the Claridenfirn in Switzerland (Vincent et al., 2004) where observations have been carried out since 1914, the first studies performed to describe and analyse glacier microclimate started later, only after the second world war. At the end of the forties Ahlmann (1948) studied processes and mechanisms involved in the strong glacier reduction he observed around the North Atlantic Ocean. Moreover in the same period, a comprehensive study of water, ice and energy budgets was started on several glaciers in Oetztal, Austria, and greatly expanded during the International Hydrological Decade in the 1950s (Hoinkes and Untersteiner, 1952; Hoinkes, 1955), during which several long-term mass balance series were initiated (Hoinkes and Steinacker, 1975; Reinwarth and Escher-Vetter, 1999).

Actual systematic investigations of the meteorological parameters on melting glaciers were performed only from the 1960s (Capello, 1959-1960; Ambach, 1963; Björnsson, 1972; Wendler and Weller, 1974; Munro and Davies, 1978; Hogg et al., 1982; Munro, 1989; Ohata et al., 1989; Ishikawa et al., 1992). These studies provided supraglacial meteorological data and energy fluxes measurements only for short periods (one or more ablation seasons) and only on accumulation basins: Hintereisferner, Austria (Van de Wal et al., 1991), West-Greenland (Oerlemans and Vugts, 1993), Pasterze, Austria (Greuell et al., 1997), Vatnajökull, Iceland (Oerlemans et al., 1999). The data obtained in these experiments have made clear that longer series of measurements from ablation zones are also needed. Especially on larger glaciers, melting on the lower parts is not restricted to the summer season. A better calibration of mass balance models could be achieved if data over longer time periods would be available. Thus from 1987 longer dataset are recorded on the melting zones of the Greenland ice-sheet, of Hardangerjokulen (Norway) and of Morteratschgletscher (Switzerland) (Oerlemans, 2000; Oerlemans and Klok, 2002; Klok and Oerlemans, 2004). Up to now the longest glacier data series is obtained from the Automatic Weather Station (from here AWS) located on the Morteratschgletscher; due to the possibility of regular visits and to the favourable atmospheric conditions (little icing) a good quality meteorological data set is obtained during the last 2 decades (Oerlemans, 2001; 2009).

### 3. Surface energy budget and melt amount for the years 2009 and 2010 at the Forni Glacier (Italian Alps, Lombardy)

---

On short period melting areas also of debris covered glaciers were analysed through AWS for evaluating energy fluxes and supraglacial meteorology features (see the experiment on the Miage debris covered glacier, Mont Blanc, Italian Alps, further details in Brock et al., 2010).

After the recognizing of AWS importance, these stations have been deployed over a wide variety of glaciated surfaces (e.g. continental ice sheets, valley glaciers, sea ice and icebergs) and have a variety of applications, including climate variability assessment, in support of operational weather forecasting, model validation and in avalanche information support. AWS applications share a common challenge of obtaining continuous and reliable measurements both unattended and often in extreme environments. AWSs have facilitated growth in the branch of glacio-meteorology.

The collection of meteorological data recorded by permanent AWSs, in fact, is essential for measuring energy fluxes at the glacier-atmosphere interface and snow accumulation, for calculating the energy available for snow/ice melt, for the validation of mass balance models, meteorological models (regional/mesoscale) and satellite products, for constructing parameterizations for energy balance models (Oerlemans and Vugts, 1993; Greuell et al., 1997; Oerlemans et al., 1999; Oerlemans, 2000; Klok and Oerlemans, 2002; Oerlemans and Klok, 2002; De Ruyter de Wildt et al., 2003; Klok and Oerlemans, 2004; Senese et al., 2012).

The meteorological parameters are also fundamental to characterize glacier surface and sky conditions. For example albedo and cloudiness are the most important parameters that determine the amount of solar radiation adsorbed at the surface (apart from geometric effects like shading): at the glacier surface the solar radiation mainly drives ice and snow melt. From the incoming radiation the cloud conditions can normally be inferred qualitatively: days with overcast conditions are marked by lower values of incoming solar radiation and higher ones of incoming longwave radiation. In fact, clouds and water vapour make the atmospheric emissivity larger. On the contrary glacier outgoing longwave radiation shows less pronounced variations.

## 2. The Italian AWS network and the AWS1 Forni

During the last decades, in Italy some AWSs (collecting data during different periods) were located in the glacierized areas on rock exposures, nunataks or buildings (such as

### 3. Surface energy budget and melt amount for the years 2009 and 2010 at the Forni Glacier (Italian Alps, Lombardy)

---

mountain huts), thus making the meteorological data representative of high mountain atmospheric conditions but not very useful for analysis of the supraglacial micrometeorology.

On the Italian Alps, glacier meteorological experimentation through permanent AWSs started on 26<sup>th</sup> September 2005 with the AWS installed at the Forni Glacier surface (Upper Valtellina, Lombardy Alps) (Citterio et al., 2007, Diolaiuti et al., 2009; Senese et al., 2010; 2012). Then by the Glaciology Group of the University of Milan in summer 2007 a second AWS was set up at the melting surface of the Dosdè Glacier (Piazzì Campo Group, at a high of 2850 m a.s.l., Lombardy Alps) and in winter 2007 a third AWS was installed at the accumulation basin of the Giant Glacier (Mont Blanc Group, at a high of 3430 m a.s.l.) (Fig. 1). All these AWSs (i.e.: Forni, Dosdè and Giant) have been developed in the framework of the SHARE (Stations at High Altitudes for Research on the Environment) project managed by the EvK2CNR Committee (Diolaiuti et al., 2009). Afterwards, other AWSs were installed by other research groups on different Italian glaciers (among the others on the Vedretta della Mare, Trentino). The dataset recorded on Forni Glacier represents the longest one from an Italian AWS.

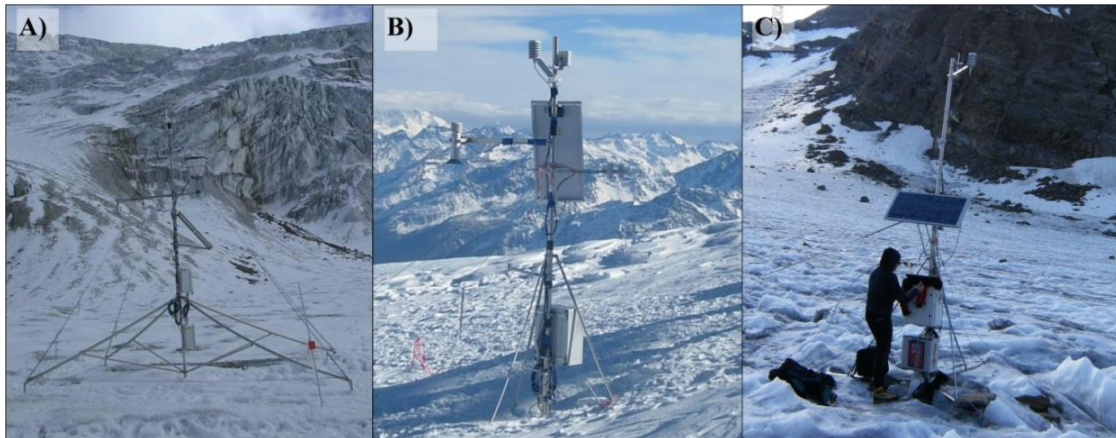


*Fig. 1: The Italian AWS Network. From the left: AWS on Forni (A), on Giant (B) and on Dosdè (C) Glaciers.*

Forni is the largest Italian valley glacier (ca. 12 km<sup>2</sup> of surface area in the Ortles-Cevedale group, Stelvio National Park). The glacier has a northward down-sloping surface and an elevation range between 2600 and 3670 m a.s.l. The AWS here located (named AWS1 Forni) has been set up on the ablation tongue at the WGS84 coordinates 46° 23' 56.0" N, 10° 35' 25.2" E, 2669 m (ellipsoidal elevation) at the base of the

### 3. Surface energy budget and melt amount for the years 2009 and 2010 at the Forni Glacier (Italian Alps, Lombardy)

Eastern icefall (see Tab. 1). The AWS location is a good compromise between the needs for minimizing local topography effects and lowering the probability of avalanches destroying the AWS. The station is located on the lower glacier sector, about 800 m far from the glacier front. Moreover the AWS1 Forni is presently supported by the SHARE Stelvio project (SHARE STELVIO). The station is also part of the CEOP-GEWEX network.

*Tab. 1: Site characteristics, meteorological and energy balance data of the Forni Glacier (data are averaged by annual mean values from 2006 to 2010). In the last two columns the meteorological and energy balance data refer to the year 2009 and 2010.*

<b>Coordinates</b>	46° 23' 56" N; 10° 35' 25" E		
<b>Elevation range (m a.s.l.)</b>	2600 - 3670		
<b>Length (km)</b>	4.7		
<b>Area (km<sup>2</sup>)</b>	12		
<b>AWS elevation (m a.s.l.)</b>	2631		
	<b>Annual mean (2006-2010)</b>	<b>2009</b>	<b>2010</b>
<b>SW<sub>net</sub> (W m<sup>-2</sup>)</b>	67	68	66
<b>LW<sub>net</sub> (W m<sup>-2</sup>)</b>	-36	-36	-31
<b>SH (W m<sup>-2</sup>)</b>	17	16	15
<b>LE (W m<sup>-2</sup>)</b>	-4	-3	-1
<b>R<sub>s</sub> (W m<sup>-2</sup>)</b>	38	43	47
<b>SW<sub>in</sub> (W m<sup>-2</sup>)</b>	154	160	163
<b>SW<sub>out</sub> (W m<sup>-2</sup>)</b>	93	92	102
<b>SW<sub>in extra</sub> (W m<sup>-2</sup>)</b>	267	267	267
<b>Air temperature (°C)</b>	-1.4	-1.6	-2.1
<b>Snow albedo</b>	0.77	0.76	0.78
<b>Ice albedo</b>	0.23	0.24	0.23
<b>Wind speed (m s<sup>-1</sup>)</b>	4.9	5.0	4.5

On the AWS1 Forni are installed sensors (all consistent with World Meteorological Organization, WMO) measuring the main meteorological parameters (for sensor specifications see Table 2). The whole system is supported by a four-leg, 5 m high stainless steel mast standing on the ice surface according to the construction and setting proposed and tested by IMAU (Oerlemans, 2001). The AWS stands freely on the ice, and adjusts to the melting surface during summer.

In this contribution we focus on meteorological data collected in the years 2009 and 2010 by the AWS1 at Forni Glacier surface (further details on previous data available on Citterio et al., 2007; Diolaiuti et al., 2009; Senese et al., 2010; 2012).

3. Surface energy budget and melt amount for the years 2009 and 2010 at the Forni Glacier (Italian Alps, Lombardy)

*Tab. 2: Sensor specifications installed at the AWS1 Forni.*

Variable	Range	Accuracy	Recording rate	Sensor	Manufacturer
Air Temperature	-30 - +70 °C	±0.001°C	30 min.	Naturally ventilated	LSI-Lastem DMA570
Relative Humidity	0 - 100 %	±1%	30 min.	thermohygrometer	
Air Pressure	400 - 800 hPa or mBar	±10hPa	60 min.	Barometer	LSI-Lastem DQA223
Solar Radiation	0.3 - 3 μm	±5% of the value	30 min.	Net radiometer	Kipp&Zonen CNR-1
Infrared Radiation	5 - 50 μm	±5% of the value	30 min.		
Snow level	0 - 1000 cm	±2 cm	60 min.	Sonic Ranger	Campbell SR50
Liquid precipitation	0 - 1000 mm	±1mm	30 min.	Unheated pluviometer	LSI-Lastem DQA035
Wind Speed	0 - 50 m s <sup>-1</sup>	±1%	60 min.	Anemometer	LSI-Lastem DNA022
Wind Direction	0° - 360°	±1°	60 min.	Anemoscopic	LSI-Lastem DNA022

### 3. Methods

AWS1 Forni has been running continuously since its installation with only one interruption between 5<sup>th</sup> and 11<sup>th</sup> October 2008. In this study we analyze the energy budget and the melting amount over 2 years. Moreover we also spent some attention on the main glacier meteorological features derived from the AWS data analysis.

To calculate the surface energy balance, the hourly radiation data were analyzed. At the glacier surface, solar radiation is the most important energy balance component driving ice and snow melt. Therefore the albedo (from here  $\alpha$ ) is an important and noteworthy parameter of glacier surface to be analyzed in terms of temporal variability.

The definition of albedo is based on the concept of irradiance, i.e. the total energy flux incoming in through a hemisphere. The reflection of solar radiation by the glacier surface is the outgoing of a complicated scattering process in the upper layer of the glacier. In fact, albedo is related to thickness and the age of the snowpack, and it depends in a complicated way on crystal structure, surface morphology, dust and soot concentrations, moraine material, the presence of liquid water in veins and at the surface, solar elevation, cloudiness, etc. (e.g. Wiscombe and Warren, 1980a; 1980b;

### 3. Surface energy budget and melt amount for the years 2009 and 2010 at the Forni Glacier (Italian Alps, Lombardy)

---

Takeuchi, 2002; Brock, 2004). In addition the spatial and temporal variation of the albedo is large. This is clear looking at satellite images of sufficiently high resolution that have the advantage to cover the entire glacier area but they are actual and valid only for their acquisition time, moreover the glacier areas in the shade cannot be used to derive the albedo value (see Klok et al., 2003). Another limit of satellite images is that the total amount of reflected radiation cannot be directly measured by satellite, then a mathematical model of the Bi-directional Reflectance Distribution Function (BRDF, see also Nicodemus, 1965) has to be used to translate a sample set of satellite reflectance measurements into estimates of directional-hemispherical reflectance and bi-hemispherical reflectance. (e.g. Strahler et al., 1999). The land surface of the Earth, in fact, exhibits anisotropy in the spatial and angular distribution of scattered radiation due to the presence of topography and landscape objects on the land surface.

To know with a high degree of time resolution the albedo value and its variation on the melting area of a valley glacier the most suitable way is a net radiometer measuring the four radiative components like the sensor installed on our AWS; for calculating albedo the two short wave components (incoming and reflected) should be analysed.

To calculate albedo, firstly the incoming and outgoing shortwave radiation data ( $SW_{in}$  and  $SW_{out}$ , respectively, and measured by the CNR1 pyranometers) are filtered in order to remove erroneous values (e.g.: during snowfall, snowflakes sticks on the upward looking sensor whereas the downward looking sensor remains free of snow, consequently  $SW_{out}$  values exceed  $SW_{in}$ ); then the following relation is applied:

$$\alpha = \frac{SW_{out}}{SW_{in}} \quad (1)$$

The incoming and outgoing longwave radiation ( $LW_{in}$  and  $LW_{out}$ , respectively), are measured by the CNR1 pyrgeometers. The acquired data represent the flux at each sensor surface, and the values have been converted to the ground and atmospheric (upward and downward) directional flux by Stephan-Boltzmann's law also considering the temperature of the CNR1 sensor (measured by the instrument and stored by the AWS data logger).

For the calculation of the turbulent heat fluxes, the bulk aerodynamic formulas are used according to the methods introduced by Oerlemans (2000) and also described by Senese et al. (2012).



### 3. Surface energy budget and melt amount for the years 2009 and 2010 at the Forni Glacier (Italian Alps, Lombardy)

---

The surface energy flux ( $R_S$ ) at the glacier-air interface determining the net energy available for heating and melting of snow/ice, is calculated by the sum between radiative and turbulent fluxes:

$$R_S = SW_{net} + LW_{net} + SH + LE \quad (2)$$

where  $SW_{net}$  and  $LW_{net}$  correspond to the net radiation (shortwave and longwave respectively),  $SH$  and  $LE$  to the sensible and latent heat fluxes.

We calculated the glacier mass lost only for the hours characterized by both positive net energy ( $R_S$ ) and glacier surface temperature (this latter derived from outgoing  $LW$  values):

$$M = - \frac{R_S}{L_m} \quad (3)$$

where  $L_m$  corresponds to the latent heat of melting ( $3.34 \times 10^5 \text{ J kg}^{-1}$ ). Field measurements by ablation stakes installed nearby the AWS were performed during summer 2009 (from 24<sup>th</sup> July to 30<sup>th</sup> August 2009) and 2010 (from 28<sup>th</sup> July to 25<sup>th</sup> August 2010) to validate the melting computation.

## 4. Results

The wind regime in the near surface glacier layer can be better understood with scatter plots of wind speed, wind direction and air temperature (hourly values) (e.g. Oerlemans and Grisogono, 2002).

Analysing wind direction data (Fig. 2), it appears that the wind blows steadily from SE, hence down the glacier, that is along the glacier fall line.

### 3. Surface energy budget and melt amount for the years 2009 and 2010 at the Forni Glacier (Italian Alps, Lombardy)

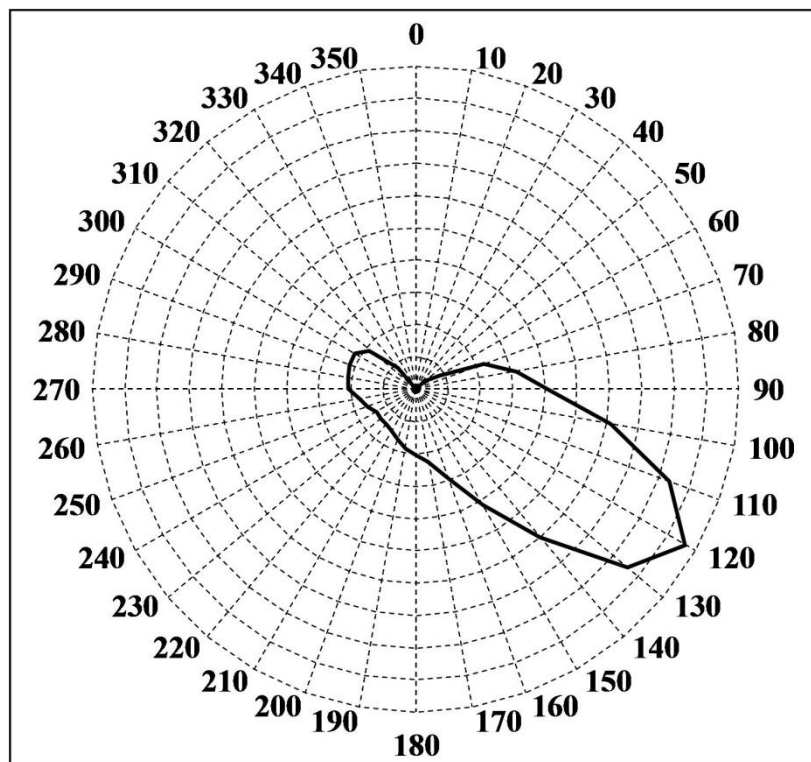


Fig. 2: The frequency of dominant wind direction of provenance observed at the Forni AWS (dashed circular grid spaced by 1% probability of occurrence).

Even if no measurements at different elevations above the surface are available, the direction data show a similar behaviour than the one found by Smeets et al. (1998) on other glaciers where katabatic-type flows are described. In fact this situation characterizes several melting glacier surfaces during a large part of the summer and high latitude areas in wintertime, like Antarctica, where the boundary layer does not show a clear daily cycle. In this period of the year, temperature and vapour pressure at the surface have no a marked daily cycle. Moreover the katabatic-type flows are described as boundary layer flows, in which surface friction and the turbulent sensible heat flux are important components of momentum and the heat budget (Oerlemans, 2005). The cooling of air over a melting and sloping glacier surface generates a downward katabatic-type flow (Oerlemans, 2010). Therefore the forcing of a glacier boundary layer from below is fairly constant and variations in its structure will be related to what happens higher up (Hoinkes, 1954). Katabatic term, in fact, refers to winds that flow down the topographic gradient or out of a valley due to surface cooling that gives this air a greater density than the free atmospheric air. This cooling of slope surfaces, which is due primarily to a net negative surface radiative balance, produces a

### 3. Surface energy budget and melt amount for the years 2009 and 2010 at the Forni Glacier (Italian Alps, Lombardy)

---

temperature difference between the air adjacent to the slope and the ambient air away from the slope. Winds then accelerate from the slope toward the ambient air, where gravity forces the dense flow to follow the sloping surface. Katabatic winds have been observed over sloping terrain of different scales all over the world, including Antarctica (Mawson, 1915; Ball, 1956; 1957; Rees, 1991; Bromwich and Parish, 1998; Renfrew and Anderson, 2002), Greenland (Loewe, 1935; Broeke et al., 1994; Heinemann, 2002), Europe (Tollner, 1931; Ekhardt, 1934; Defant, 1951; Smeets et al., 1998; Oerlemans et al., 1999), North America (Tower, 1903; Buettner and Thyer, 1965; Horst and Doran, 1986; Clements et al., 1989; Doran et al., 2002; Moni et al., 2002; Haiden and Whiteman, 2005; Princevac et al., 2005), and the Mediterranean (Martinez et al., 2006). In wind direction vs wind speed (Fig. 3a), the more frequent wind directions (cluster around a provenance from ca.  $120^\circ$ ) occur with a speed of a few meters per second; these features of direction and speed are characteristics of the katabatic regime (Oerlemans, 2010). However wind directions of ca.  $70^\circ$  and ca.  $170^\circ$  also take place frequently. The faster winds reach speeds of about  $20 \text{ m s}^{-1}$  with a direction of  $40^\circ$ - $80^\circ$  and  $250^\circ$ - $290^\circ$ , always during wintertime. The wind speed shows a daily cycle more clear than the direction values. The annual mean speed results in agreement with values of previous years (Tab. 1): a mean value of  $5 \text{ m s}^{-1}$  (in 2009) and  $4.5 \text{ m s}^{-1}$  (in 2010), both similar to  $4.9 \text{ m s}^{-1}$  averaged from 2006 to 2010.

Analysing wind speed and air temperature ( $T_a$ ) hourly data (Fig. 3b), a positive trend between air temperature and wind speed is found and the increase is clearly nonlinear. In fact higher wind speeds become more frequent for higher temperatures when  $T_a$  is above melting point. Considering the speeds higher than  $5 \text{ m s}^{-1}$ , the 46% occurs with positive temperatures, increasing the speed threshold to  $10 \text{ m s}^{-1}$  the percentage decreases until the 25%.

### 3. Surface energy budget and melt amount for the years 2009 and 2010 at the Forni Glacier (Italian Alps, Lombardy)

---

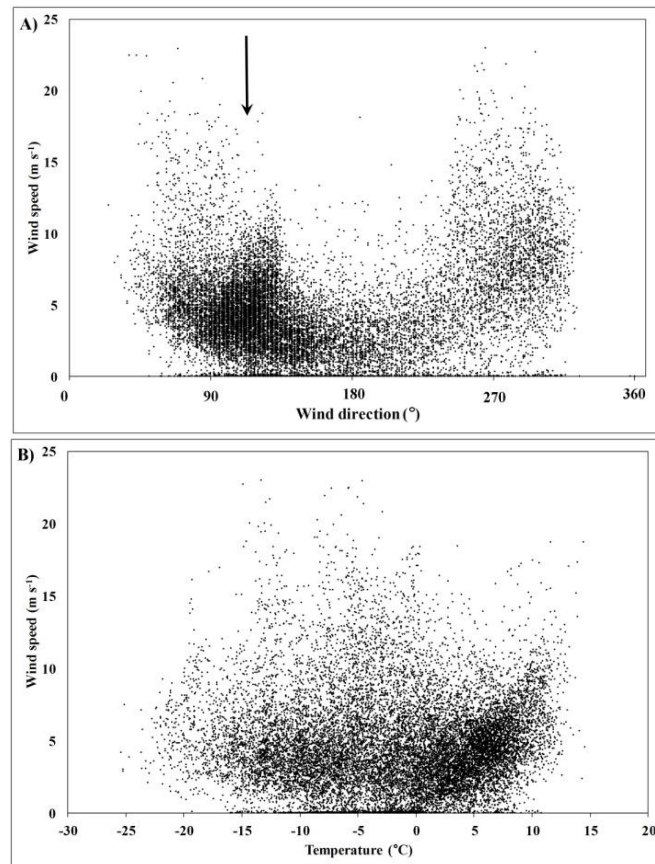


*Fig. 3: Scatter plots showing relations between wind direction (a) and air temperature (b) vs wind speed. Two years (2009 and 2010) of measurements are shown and every dot represents a hourly average value (so every plot contains 17133 points). The arrow indicates the direction of the local fall line of the glacier.*

Analysing the hourly albedo values (Fig. 4), the duration of ice ablation period is calculated for both the years: it results from 29<sup>th</sup> June 2009 to 10<sup>th</sup> October 2009 (104 days) and from 29<sup>th</sup> June 2010 to 24<sup>th</sup> September 2010 (88 days). The switch from winter to summer conditions is very clear: the presence or absence of snow is the most important factor in determining albedo variations on the time scale of days and longer (Senese et al., 2012). Then it's possible to detect the summer snowfall events by steep increases of albedo values (e.g. from 0.2 to 0.8). During 2009 ablation season 2 snowfalls result from our data (totally covering 5 days featuring snow albedo values) and during 2010 ablation season 5 snow fall events are found (covering 16 days). The snow presence affects the melting rate increasing the outgoing shortwave radiation and consequently decreasing the absorbed energy.

### 3. Surface energy budget and melt amount for the years 2009 and 2010 at the Forni Glacier (Italian Alps, Lombardy)

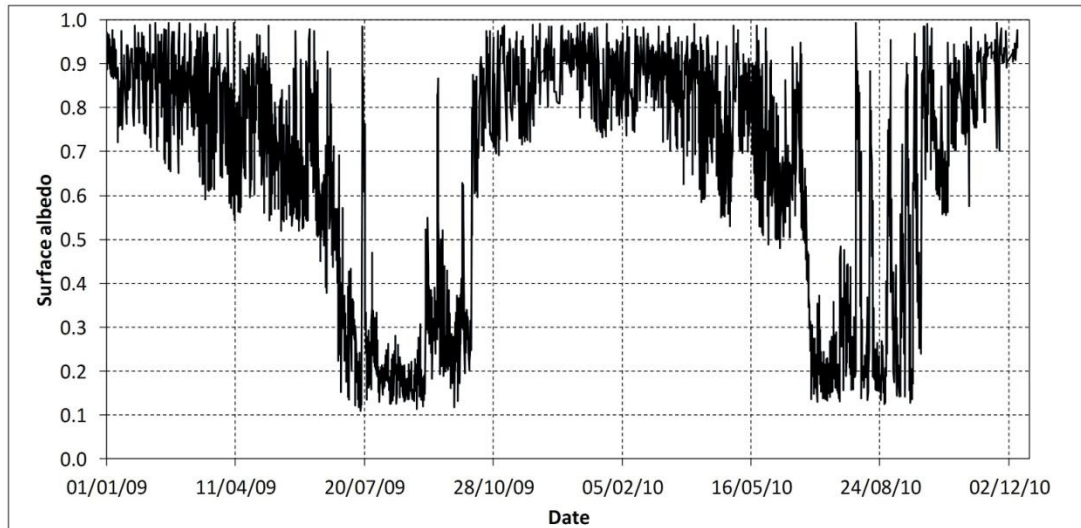


Fig. 4: Hourly albedo values during 2009 and 2010.

Figure 5 shows scatter plot of incoming ( $SW_{in}$ ) versus reflected ( $SW_{out}$ ) solar radiation for two-year periods as hourly measured by AWS1 Forni. There is a clear grouping in the diagram and characteristic albedos for snow/firn and ice are emerging (with a mean value of 0.76 during 2009 and 0.78 during 2010 regarding snow, and 0.24 and 0.23 in 2009 and 2010, respectively, for the ice). These mean values are comparable to the mean values averaged from 2006 to 2010 (Tab. 1). This picture also shows that the snow albedo tends to decrease for larger values of the incoming radiation. This mainly concerns data points from late spring/early summer, when incoming radiation is large, air temperatures are high and snowfall rarely occurs. The snow structure has now been transformed into large grains and there is normally some accumulation of dust on the surface (Oerlemans, 2010).

### 3. Surface energy budget and melt amount for the years 2009 and 2010 at the Forni Glacier (Italian Alps, Lombardy)

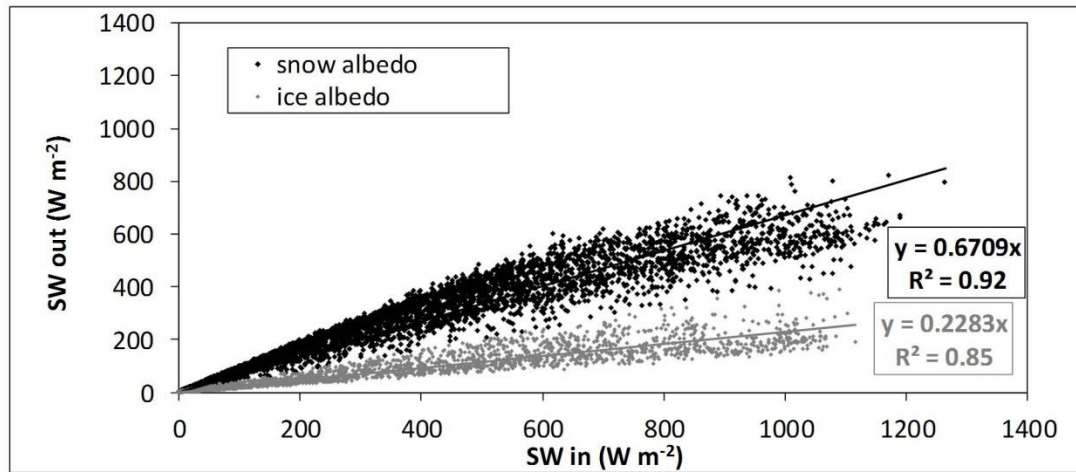


Fig. 5: Hourly albedo values characterizing exposed ice and snow covered surface, during 2009 and 2010.

All the four components of energy balance (Fig. 6) are characterized by similar trends of the annual cycle over the presented period (from January 2009 to December 2010). All the hourly maximum values occur during summer, and all hourly minimum during winter except the values of net longwave radiation ( $LW_{net}$ ). In particular, hourly  $LW_{net}$  data (Fig. 6a) vary between slightly positive values (close to  $0 \text{ W m}^{-2}$ , typical of cloudy days) and negative values (up to  $-100 \text{ W m}^{-2}$ , realistic values due to the  $0^\circ\text{C}$  glacier surface): the large fluctuations from day to day are mainly related to cloudiness, especially in wintertime.

The net shortwave radiation (Fig. 6a) is asymmetric with respect to the summer solstice. It decreases more gradually in fall than in spring. During the transition from snow to ice, the lowering of the albedo occurs when the flux of  $SW_{in}$  is large, determining a very steep increase in the net solar radiation.

During the ablation season the latent heat flux (Fig. 6b) is generally positive, during the rest of the year the negative values are due to low humidity in combination with a minimal temperature difference between the surface and the air (Oerlemans, 2000). The negative net energy values ( $R_s$ ) (Fig. 6c) characterize the winter periods and night-time, when snow/ice melting is absent.

These results are in agreement with finding during the other years (from 2006 to 2010) (Tab. 1). In fact the annual mean values averaged between these 5 years result as  $67 \text{ W m}^{-2}$  regarding the  $SW_{net}$  (in particular  $68 \text{ W m}^{-2}$  during 2009 and  $66 \text{ W m}^{-2}$  during 2010),  $-36 \text{ W m}^{-2}$  regarding the  $LW_{net}$  (in particular  $-36 \text{ W m}^{-2}$  during 2009 and  $-31 \text{ W m}^{-2}$

### 3. Surface energy budget and melt amount for the years 2009 and 2010 at the Forni Glacier (Italian Alps, Lombardy)

during 2010),  $17 \text{ W m}^{-2}$  and  $-4 \text{ W m}^{-2}$  of  $SH$  and  $LE$ , respectively ( $16 \text{ W m}^{-2}$  and  $-3 \text{ W m}^{-2}$  during 2009 and  $15 \text{ W m}^{-2}$  and  $-1 \text{ W m}^{-2}$  during 2010), finally a  $R_s$  value of  $38 \text{ W m}^{-2}$  ( $43 \text{ W m}^{-2}$  and  $47 \text{ W m}^{-2}$  in 2009 and 2010, respectively).

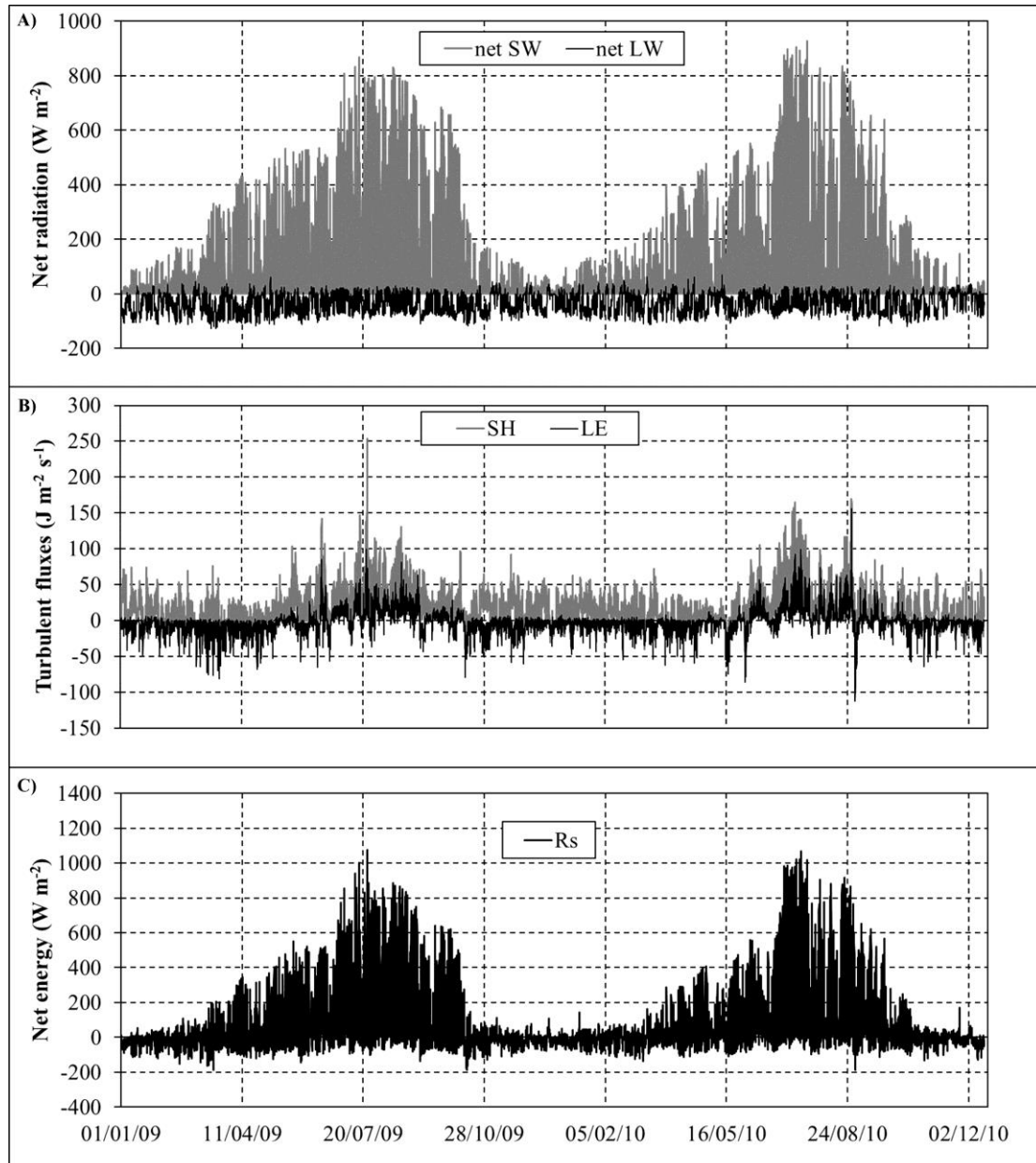


Fig. 6: Daily values of net shortwave ( $SW_{net}$ ) and longwave ( $LW_{net}$ ) radiation (a), turbulent fluxes of sensible ( $SH$ ) and latent ( $LE$ ) heat (b) and surface net energy available for heating and melting of snow/ice (c) from January 2009 to December 2010.

### 3. Surface energy budget and melt amount for the years 2009 and 2010 at the Forni Glacier (Italian Alps, Lombardy)

Considering only the hours characterized by positive net energy ( $R_S$ ) and melting surface temperature, the total calculated mass loss during summer 2009 and 2010 is  $-11.32 \text{ kg m}^{-2}$  (or m w.e.) (Fig. 7).

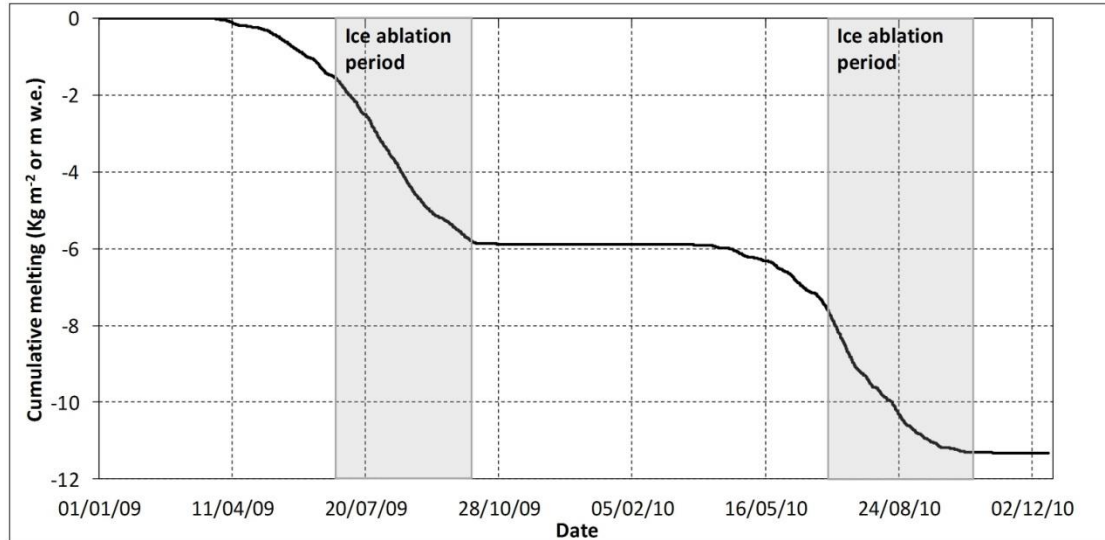


Fig. 7: Cumulative melt calculated over the 2-year period. Values are obtained from hourly data analysis. The period characterized by ice ablation are marked in light grey.

To validate the melting computation, these results are compared to field measurements during summer 2009 (from 24<sup>th</sup> July to 30<sup>th</sup> August 2009) and 2010 (from 28<sup>th</sup> July to 25<sup>th</sup> August 2010). The melting value measured by the ablation stakes installed nearby the AWS (-1.91 m w.e. during 2009 and -1.02 m w.e. during 2010) results in agreement with the calculated one (-1.97 m w.e. during 2009 and -1.07 m w.e. during 2010), thus the applied model is correct (Fig. 8).



### 3. Surface energy budget and melt amount for the years 2009 and 2010 at the Forni Glacier (Italian Alps, Lombardy)

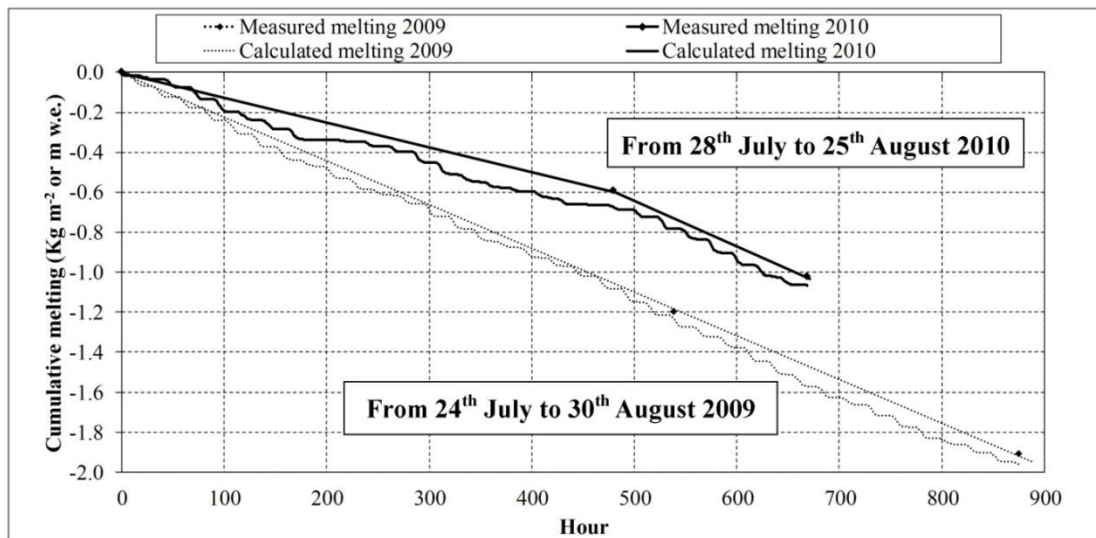


Fig. 8: Comparison between field measurements during summer 2009 (from 24<sup>th</sup> July to 30<sup>th</sup> August 2009) and 2010 (from 28<sup>th</sup> July to 25<sup>th</sup> August 2010) and calculated melt values in the same periods.

## 5. Conclusions

The data collected by permanent AWS permit to quantify the complete energy balance and the melt amount with a high time resolution, also including the turbulent fluxes that affect the glacial ablation for the 20%-30% (Senese et al., 2012), and to describe the surface albedo variability. Moreover sky and surface conditions can be deduced from measured meteorological parameters.

During 2009 and 2010 the results obtained from AWS1 Forni prove to be consistent with results from other 3 years of data acquisition (i.e. Citterio et al, 2007; Senese et al., 2010; 2012).

The wind blows steadily down the glacier from SE that is along the fall line. The wind regime is characterized by a provenance from ca.  $120^\circ$  and a speed of a few meters per second, generally featured katabatic-type flows. Moreover higher wind speeds are found not directly correlated with a particular range of temperature.

Analysing albedo data, the ice ablation periods result long of 104 days (2009) and 88 days (2010). During 2009 ablation season 2 snowfalls are observed (totally covering 5 days featuring snow albedo values) and during 2010 ablation season 5 snow fall events are detected (the snow persisted at the glacier surface for 16 days in total). Moreover the snow albedo (with a mean value of 0.77 between the 2 years) tends to decrease for

### 3. Surface energy budget and melt amount for the years 2009 and 2010 at the Forni Glacier (Italian Alps, Lombardy)

---

larger values of the incoming radiation. The characteristic albedo for ice is found equal to 0.24 (in 2009) and 0.23 (in 2010).

Regarding energy balance, the solar radiation ( $SW_{net}$ ), the turbulent fluxes ( $SH$  and  $LE$ ) and the net energy ( $R_s$ ) are characterized by similar trends with maximum during summer and minimum during winter. Instead the net longwave radiation ( $LW_{net}$ ) results varying between slightly positive values and values up to  $-100 \text{ W m}^{-2}$ .

During 2009-2010 the total calculated mass loss results  $-11.32 \text{ kg m}^{-2}$  (or m w.e.). The comparison of the measured and modelled ice ablation shows differences of less than 0.06 m w.e. and therefore indicates that the model applied is correct.

Consequently the AWSs installed on glaciers are essential for calibrating and validating the glacier energy balance models, to characterize quantitatively the glacier boundary layer conditions, to describe wind regime. On the Italian Alps, the first permanent supraglacial meteorological experimentation is represented by the AWS1 Forni which has been running since September 2005 thus giving the longest dataset from an Italian glacier. In addition other two permanent AWSs are set up in 2007 (on Dosedè and on Giant Glacier). This Italian AWS network obtained the award from international scientific community and concerned to three important network (SHARE, SHARE ITALY and CEOP).

The next research steps will be to install a second AWS on the Forni Glacier to survey the micrometeorology and the energy fluxes in the accumulation basin (at about 3000 m asl) and to extend the computation of the energy budget over the whole glacier surface thus distributing glacier melt. Last but not least our results show that glacier energy budget is also controlled by surface albedo. Its seasonal changes are driven by snowfalls, snow metamorphosis, surface wetness and dust deposition. On this latter, the current literature (Flanner et al., 2009) suggests the possibility that atmospheric soot (dust and black carbon) is playing a role in driving the spring decrease of snow albedo also on Alpine glaciers' surfaces (in addition to the high air temperatures and increased incoming radiation). Therefore another next step of our research will be to analyze with further details the glacier surface over a one-year period, also sampling snow and ice to find any correlations between surface reflectivity and atmospheric soot presence.

## References

- Ambach W. (1963): Untersuchungen zum Energieumsatz in der Ablationzone des Grönländischen Inlandeises. *Meddelelser om Grønland*, 174, 4-311.
- Ahlmann W.H. (1948): Glaciological research on the North Atlantic coasts. Research Series 1, London: Royal Geographical Society, 66 pp.
- Ball F.K. (1956): The theory of strong katabatic winds. *Australian Journal of Physics*, 9, 373-386.
- Ball F.K. (1957): The katabatic wind of Adelie Land and King George V Land. *Tellus*, 9, 201-208.
- Bromwich D.H. and Parish T.R. (1998): Meteorology of the Antarctic. In: Karoly D.J. & Vincent D.G. (eds) *Meteorology of the southern hemisphere: meteorological monographs*, Vol. 27, Issue 49. Boston, MA: American Meteorological Society, 175-200.
- Broeke M.R., Van Den Duynkerke P.G. and Henneken E.A.C. (1994): Heat, momentum and moisture budgets of the katabatic layer over the melting zone of the West Greenland ice sheet in summer. *Boundary Layer Meteorology* 71, 393-413.
- Buettner K.J.K. and Thyer N. (1965): Valley winds in the Mount Rainier area. *Archiv für Meteorologie Geophysik und Bioklimatologie*, Series B 14 (H. 2), 125-147.
- Björnsson H. (1972): Bæsigisarfjökull, North Iceland. Results of glaciological investigations 1967-1968. Part II. The energy balance. *Jökull*, 22, 44-59.
- Brock B.W. (2004): An analysis of short-term albedo variations at Haut Glacier d'Arolla, Switzerland. *Geografiska Annaler*, A86, 53-65.
- Brock B., Mihalcea C., Kirkbride M., Diolaiuti G., Cutler M. and Smiraglia C. (2010): Meteorology and surface energy fluxes in the 2005-2007 ablation seasons at Miage debris-covered glacier, Mont Blanc Massif, Italian Alps. *Journal of Geophysical Research*, doi:10.1029/2009JD013224.
- Capello C.F. (1959-1960): Ricerche di microclimatologia sulla superficie glaciale del Miage. *Bollettino del Comitato Glaciologico Italiano*, 9 (II serie, parte prima), 95-154.
- Citterio M., Diolaiuti G., Smiraglia C., Verza G. and Meraldi E. (2007): Initial results from the Automatic Weather Station (AWS) on the ablation tongue of Forni Glacier (Upper Valtellina, Italy). *Geografia Fisica e Dinamica Quaternaria*, 30, 141-151.

3. Surface energy budget and melt amount for the years 2009 and 2010 at the Forni Glacier (Italian Alps, Lombardy)

---

- Clements W.E., Archuleta J.A. and Hoard D.E. (1989): Mean structure of the nocturnal drainage flow in a deep valley. *Journal of Applied Meteorology*, 28, 457-462.
- De Ruyter De Wildt M., Oerlemans J. and Bjornsson H. (2003): A calibrated mass balance model for Vatnajokull, Iceland. *Jokull*, 52 (161), 1-20.
- Defant F. (1951): Local winds. In: Malone, T. F. (ed.) *Compendium of meteorology*. Boston, MA: American Meteorological Society, 655-672.
- Diolaiuti G., Smiraglia C., Verza G.P., Chillemi R. and Meraldi E. (2009): La rete micro-meteorologica glaciale lombarda: un contributo alla conoscenza dei ghiacciai alpini e delle loro variazioni recenti. In: Smiraglia C., Morandi G. & G. Diolaiuti (Eds.), *Clima e Ghiacciai. La crisi delle risorse glaciali in Lombardia, Regione Lombardia*, 69-92.
- Doran J.C., Fast J.D. and Horel J. (2002): The VTMX 2000 campaign. *Bulletin of American Meteorological Society*, 83, 1233-1247.
- Ekhart E. (1934): Neuere untersuchungen zur aerologie der talwinde. *Beitrage zur Physik der freien Atmosphere*, 21, 245-268.
- Flanner M.G., Zender C.S., Hess P.G., Mahowald N.M., Painter T.H., Ramanathan V. and Rasch P.J. (2009): Springtime warming and reduced snow cover from carbonaceous particles. *Atmospheric Chemistry and Physics*, 9, 2481-2497.
- Greuell J.W., Knap W. and Smeets P. (1997): Elevational changes in meteorological variables along a midlatitude glacier during summer. *Journal of Geophysical Research*, 102 (D22), 25941-25954.
- Haiden T. and Whiteman C.D. (2005): Katabatic flow mechanisms on a low-angle slope. *Journal of Applied Meteorology and Climatology*, 44, 113-126.
- Heinemann G. (2002): Aircraft-based measurements of turbulence structure in the katabatic flow over Greenland. *Boundary Layer Meteorology*, 103, 49-81.
- Hogg I.G.G., Paren J.G. and Timmis R.J. (1982): Summer heat and ice balances on Hodges Glacier, South Georgia, Falkland Islands Dependencies. *Journal of Glaciology*, 28 (99), 221-228.
- Hoinkes H. (1954): Beiträge zur Kenntnis des Gletscherwindes. *Archives for Meteorology, Geophysics, And Bioclimatology*, B6, 36-53.
- Hoinkes H.C. and Untersteiner N. (1952): Wärmeumsatz und Ablation auf Alpengletschern I. Vernagtferner (Oetztaler Alpen), August 1950. *Geografiska Annaler*, 34 (1-2), 99-158.
- Hoinkes H.C. (1955): Measurements of ablation and heat balance on alpine glaciers.

3. Surface energy budget and melt amount for the years 2009 and 2010 at the Forni Glacier (Italian Alps, Lombardy)

---

Journal of Glaciology, 2, 497-501.

- Hoinkes H.C. and Steinacker H. (1975): Hydrometeorological implications of the mass balance of Hintereisferner, 1952–53 to 1968-69. In Proceedings of the Snow and Ice Symposium, Moscow 1971, Wallingford: IAHS Publication 104, 144-49.
- Horst T.W. and Doran J.C. (1986): Nocturnal drainage flow on simple slopes. *Boundary Layer Meteorology*, 3, 263-286.
- Ishikawa N., Owens I.F. and Sturman A.P. (1992): Heat balance studies characteristics during fine periods on the lower parts of the Franz Josef Glacier, South Westland, New Zealand. *International Journal of Climatology*, 12, 397-410.
- Klok E.J. and Oerlemans J. (2002): Model study of the spatial distribution of the energy and mass balance of Morteratschgletscher, Switzerland. *Journal of Glaciology*, 48 (163), 505-518.
- Klok E.J., Greuell J.W. and Oerlemans J. (2003): Temporal and spatial variation of the surface albedo of the Morteratschgletscher, Switzerland, as derived from 12 Landsat images. *Journal of Glaciology*, 49 (167), 491-502.
- Klok E.J. and Oerlemans J. (2004): Modelled climate sensitivity of the mass balance of Morteratschgletscher and its dependence on albedo parameterization. *International Journal of Climatology*, 24, 231-245.
- Loewe F. (1935): Das klima des grönländischen inlandeises. *Handbuch der Klimatologie*, 2, 67-101.
- Martinez D., Cuxart J. and Jimenez M.A. (2006): Katabatic wind over gentle slope on the Majoarca island. 17th Symposium on Boundary Layers and Turbulence, 22-27. May, San Diego, CA.
- Mawson, D. (1915): *Home of the Blizzard*. London: Heineman.
- Moni P., Fernando H.J.S., Princevac M., Chan W.C., Kowalewski T.A. and Pardyjak E.R. (2002): Observations of flow and turbulence in the nocturnal boundary layer over a slope. *Journal of the Atmospheric Sciences*, 59, 2513-2534.
- Munro D.S. (1989): Surface roughness and bulk heat transfer on a glacier: comparison with eddy correlation. *Journal of Glaciology*, 35, 343–348.
- Munro D S. and Davies J.A. (1978): On fitting the log-linear model to wind speed and temperature profiles over a melting glacier. *Boundary-Layer Meteorology*, 15, 423-437.
- Nicodemus F. (1965): Directional reflectance and emissivity of an opaque surface. *Applied Optics*, 4 (7), 767-775.

### 3. Surface energy budget and melt amount for the years 2009 and 2010 at the Forni Glacier (Italian Alps, Lombardy)

---

- Oerlemans J. (2000): Analysis of a 3 years meteorological record from the ablation zone of Morteratschgletscher, Switzerland: energy and mass balance. *Journal of Glaciology*, 46 (155), 571-579.
- Oerlemans J. (2001): *Glaciers and Climate Change*. Balkema, Lisse. 115 pp.
- Oerlemans J. (2005): The microclimate of glaciers. Lecture notes from Karthaus summer school 2005, Utrecht University.
- Oerlemans J. (2009): Retreating alpine glaciers: increased melt rates due to accumulation of dust (Vadret da Morteratsch, Switzerland). *Journal of Glaciology*, 55(192), 729-736.
- Oerlemans J. (2010): *The Microclimate of Valley Glaciers*. Institute for Marine and Atmospheric Research Utrecht, Utrecht University, The Netherlands, pp. 138.
- Oerlemans J. and Vugts H.F. (1993): A meteorological experiment in the melting zone of the Greenland ice sheet. *Bulletin of the American Meteorological Society*, 74, 355-365.
- Oerlemans J., Björnsson H., Kuhn M., Obleitner F., Palsson F., Smeets P. Vugts H.F. and De Wolde J. (1999): Glacio-meteorological investigations on Vatnajökull, Iceland, summer 1996. *Boundary-Layer Meteorology*, 92, 3-26.
- Oerlemans J. and Grisogono B. (2002): Glacier winds and parameterisation of the related surface heat fluxes. *Tellus*, 54A, 440-452.
- Oerlemans J. and Klok E.J. (2002): Energy balance of a glacier surface: analysis of automatic weather station data from the Morteratschgletscher, Switzerland. *Arctic, Antarctic, and Alpine Research*, 34 (4), 477-485.
- Ohata T., Zhongyuan B. and Lingfu D. (1989): Heat balance study on Glacier No. 1 at head of Urumqi River, Tianshan Mountains, China. *Journal of Glaciology and Geocryology*, 11, 298-310.
- Princevac M., Fernando H.J.S. and Whiteman C.D. (2005): Turbulent entrainment into nocturnal gravity-driven flow. *Journal of Fluid Mechanics*, 533, 259-268.
- Rees J.M. (1991): On the characteristics of eddies in the stable atmospheric boundary layer. *Boundary Layer Meteorology*, 55, 325-343.
- Reinwarth O. and Escher-Vetter H. (1999): Mass balance of Vernagtferner, Austria, from 1964/65 to 1996/97: results for three sections and the entire glacier. *Geografiska Annaler*, 81A, 743-51.
- Renfrew I.A. and Anderson P.S. (2002): The surface climatology of an ordinary katabatic wind regime in coastal Antarctica. *Tellus*, 54A, 463-484.

3. Surface energy budget and melt amount for the years 2009 and 2010 at the Forni Glacier (Italian Alps, Lombardy)

---

- Senese A., Diolaiuti G., Mihalcea C. and Smiraglia C. (2010): Evoluzione meteorologica sulla lingua di ablazione del Ghiacciaio dei Forni, gruppo Ortles-Cevedale (Parco Nazionale dello Stelvio, Lombardia) nel periodo 2006-2008. *Bollettino Della Società Geografica Italiana*, XIII, 3(4), 845-864.
- Senese A., Diolaiuti D., Mihalcea C. and Smiraglia C. (2012): Energy and mass balance of Forni Glacier (Stelvio National Park, Italian Alps) from a 4-year meteorological data record. *Arctic, Antarctic, Alpine Research*, 44 (1), 122-134.
- SHARE Stelvio:  
<http://www.evkl2cnr.org/cms/en/share/pilot-projects/ABC/Nepal?filter0=stelvio>
- Smeets C.J.P.P., Duyankerke P.G. and Vugts H.F. (1998): Turbulence characteristics of the stable boundary layer over a mid-latitude glacier. Part I: a combination of katabatic and large-scale forcing. *Boundary Layer Meteorology*, 87, 117-145.
- Strahler A.H., Muller, J-P., Lucht W., Schaaf C.L.B., Tsang T., Gao F., Li X., Lewis P. and Barnsley M. J. (1999): MODIS BRDF/Albedo Product: Algorithm Theoretical Basis Document. Version 5.0, 53 pp. April 1999.
- Tacheuchi N. (2002): Optical characteristics of cryoconite (surface dust) on glacier: the relationship between light absorbency and the property of organic matter contained in the cryoconite. *Annals of Glaciology*, 34, 409-414.
- Tollner H. (1931): Gletscherwinde in den ostalpen. *Meteorologische Zeitschrift*, 48, 414-421.
- Tower W.S. (1903): Mountain and valley breezes. *Monthly Weather Review*, 31, 528-529.
- Van De Wal R.S.W., Oerlemans J. and Van Der Hage J.C. (1991): A study of ablation variations on the tongue of Hintereisferner, Austria. *Journal of Glaciology*, 38, 319-324.
- Vincent C., Kappenberger G., Valla F., Bauder A., Funk M. and Le Meur E. (2004): Ice ablation as evidence of climate change in the Alps over the 20th century. *Journal of Geophysical Research*, 109, D10104, doi:10.1029/2003JD003857.
- Wendler G. and Weller G. (1974): Heat-balance study on Mc-Call Glacier, Brooks Range, Alaska: a contribution to the International Hydrological decade. *Journal of Glaciology*, 13, 13-26.
- Wiscombe W.J. and Warren S.G. (1980a): A model for spectral albedo of snow. I. Pure snow. *Journal of the Atmospheric Sciences*, 37, 2712-2733.
- Wiscombe W.J. and Warren S.G. (1980b): A model for spectral albedo of snow. II.

3. Surface energy budget and melt amount for the years 2009 and 2010 at the Forni  
Glacier (Italian Alps, Lombardy)

---

Snow Containing Atmospheric Aerosols. *Journal of the Atmospheric Sciences*, 37,  
2734-2745.



# Chapter 4

## **Air temperature thresholds to evaluate snow melting at the surface of Alpine glaciers by degree-day models: the case study of Forni Glacier (Italy)**

### **Abstract**

Glacier melt occurs whenever the surface temperature is null (273.15 K) and the net energy budget is positive. These conditions can be assessed by analysing meteorological and energy data acquired by a supraglacial Automatic Weather Station (AWS). In the case this latter is not present at the glacier surface the assessment of actual melting conditions and the evaluation of the melt amount is difficult and simple methods based on degree-day (also named Temperature index) models are generally applied. These models require the choice of a correct temperature threshold. In fact, melt does not necessarily occur at air temperatures higher than 273.15 K, since it is determined by the surface energy budget which in turn is only indirectly affected by air temperature.

This is particularly the case of the late spring period when ablation processes start at the glacier surface thus progressively reducing snow thickness. In this paper, to detect the most indicative air temperature threshold witnessing melt conditions in the April-June period, we have analysed air temperature data recorded from 2006 to 2012 by a supraglacial AWS set up at 2631 m a.s.l. on the ablation tongue of the Forni Glacier (Italian Alps), and by a weather station located outside the studied glacier (at Bormio, a village at 1225 m asl). Moreover we have evaluated the glacier energy budget and the Snow Water Equivalent (SWE) values during this time-frame. Then the ablation amount was estimated both from the surface energy balance (from supraglacial AWS data) and from degree days method (in this latter case applying the mean tropospheric lapse rate to temperature data acquired outside the studied glacier and changing the air temperature threshold) and the results were compared. We found that the mean tropospheric lapse rate permits a good and reliable reconstruction of air temperature data at the glacier surface and the major uncertainty in the computation of snow melt from degree days models is driven by the choice of an appropriate air temperature

4. Air temperature thresholds to evaluate snow melting at the surface of Alpine glaciers  
by degree-day models: the case study of Forni Glacier (Italy)

---

threshold. From our study using a 5.0 K lower threshold value (with respect to the largely applied 273.15 K) avoids most of the sampling problem in the application of the positive degree-day models and permits the most reliable reconstruction of glacier melt.

## 1. Introduction and study aims

Melting processes at glaciers occur when surface temperature is equal to 273.15 K and the surface energy budget is positive (e.g. Hock 2005; Senese et al. 2012a). It is however very difficult assessing these conditions, in particular whenever a supraglacial Automatic Weather Station (AWS) is not located and running at the glacier surface; thus simple models are generally adopted which assume empirical relationships between air temperature and snow or ice melting rates (i.e. Degree Days or T-index models e.g. Braithwaite 1985; Cazorzi and Dalla Fontana 1996; Hock 1999; Pellicciotti et al. 2005). The degree days amount during the ablation period have naturally to be calculated for any point of the glacier surface. The estimation of distributed degree days amount from air temperature data acquired by meteorological stations located outside a glacier is not always simple and the use of an appropriate lapse rate is very important especially if the used meteorological station features a strong elevation difference with respect to the studied glacier. Unfortunately this condition often occurs as meteorological stations are mainly located close to urbanized areas which are at bottom of mountain valleys and only a small number of glaciers are equipped with AWSs. The availability of a supraglacial AWS is also very useful in order to assess presence and persistence of snow cover. These information are particularly useful in the case of late spring/early summer time (April-June) at the glacier ablation zone in order to establish in detail if snow is at the melting point and how long this phenomenon occurs.

A further very important issue in the application of degree days models is the air temperature threshold adopted for melting conditions: generally a daily average value of 273.15 K is used (Braithwaite 1985; Hock 2003; Bocchiola et al. 2010). This assumption neglects the fact that melting does not necessarily occur only when daily average temperature exceeds 273.15 K, and there can be days featuring a negative average temperature value but experiencing a fraction of the time (from a few to several hours) with positive air temperature (thus driving melt). Moreover the surface energy balance can be positive also with negative air temperature (Kuhn 1987). Then the choice of an appropriate air temperature threshold is fundamental to detect the actual melting days and to evaluate the melt amount.

Within this context the aim of this paper is to investigate the relationship between degree days amount and melting processes considering a 7-year period of measures on the Forni Glacier which is the largest Italian valley glacier (Fig. 1). It is widely debris-

#### 4. Air temperature thresholds to evaluate snow melting at the surface of Alpine glaciers by degree-day models: the case study of Forni Glacier (Italy)

free, even if darkening phenomena are shown (Diolaiuti and Smiraglia 2010; Diolaiuti et al. 2012). The measures were performed both by means of a supraglacial AWS (named AWS1 Forni, see Citterio et al. 2007; Senese et al. 2012a; 2012b) and by field surveys (i.e. snow pits and ablation stakes). The goal of the research is to contribute better understanding the use of degree days models focusing on the air temperature threshold. Moreover we aim at evaluating the performances that can be achieved using meteorological stations located outside the glacier to reconstruct supraglacial air temperature conditions.

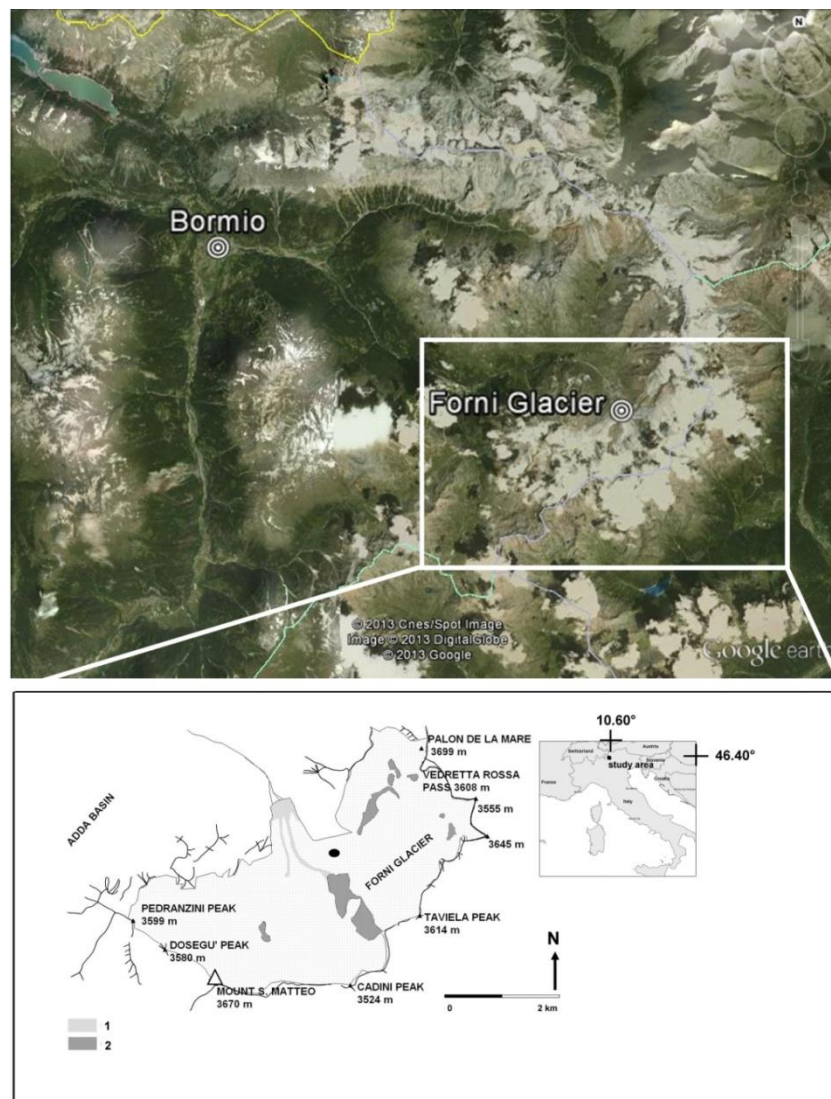


Fig. 1: On the top the location of Bormio (a village at 1225 m a.s.l.) and Forni Glacier (Google Earth © raster base) and in the lower picture the location of the AWS1 Forni (black dot, WGS84 coordinates: 46°23'56.0" N and 10°35'25.2" E, geodetic elevation: 2631 m a.s.l.). In the map the light grey areas (1) are used to mark supraglacial debris coverage and the dark grey zones (2) indicate rock exposures and nunataks.

## 2. Data and methods

The analyses presented in this paper are based on data collected in the 2005-2012 period:

- i) daily average air temperature records ( $T_{AWS}$ ) collected by a supraglacial AWS, the AWS1 Forni at 2631 m a.s.l., and by a meteorological station located at Bormio, a village at 1225 m a.s.l. and about 20 km far from the glacier terminus (Fig. 1); the air temperature data acquired by this second weather station were shifted to the AWS1 Forni elevation by applying the mean tropospheric lapse rate ( $-6.5 \text{ K km}^{-1}$ , the resulting temperature values are indicated  $T_B$  from here).
- ii) Hourly air temperature, relative humidity, wind speed, air pressure, solar and infrared radiation (both incoming and outgoing) data collected by the AWS1 Forni.
- iii) Snow pits annually performed nearby the AWS1 Forni.

The AWS1 Forni (Fig. 1) was set up on the glacier melting tongue on 26<sup>th</sup> September 2005. It was developed in the framework of the SHARE (Stations at High Altitude for Research on the Environment) program and data are quality checked and validated according to the SHARE protocol and available to all the scientific community upon request. This dataset is quite uninterrupted (from 26/09/2005 up to now) with very few gaps (3.05% of the total period). In this study the time frame from 1<sup>st</sup> October 2005 to 31<sup>st</sup> December 2012 is analysed. The Bormio meteorological station is managed by the Lombardy Regional Agency for Environmental Protection (ARPA Lombardia), which takes care data validation and disseminates the data through a dedicated web site. The snow pit data have been provided by personnel from the Centro Nivometeorologico di Bormio of ARPA Lombardia according to the AINEVA protocol. The pits were annually dug at the end of the accumulation period (April-May), only in 2007 no surveys were performed.

The snow and ice melting is assessed from surface energy budget (Melt from Energy Budget,  $M_{EB}$ , calculated from AWS1 Forni data). The net energy ( $R_S$ ) available for heating the surface and melting snow and/or ice is calculated following Senese et al. (2012a). Then whenever the surface temperature is at 273.15 K and  $R_S$  is positive, the ablation amount ( $M_{EB}$ ,  $\text{kg m}^{-2}$  or mm w.e.) is quantified. The obtained results are considered reliable and indicative of the glacier actual melt since in a previous paper (Senese et al., 2012a) the melt amount derived from energy budget computations has been compared to the melt amount measured on the field at a selection of ablation

#### 4. Air temperature thresholds to evaluate snow melting at the surface of Alpine glaciers by degree-day models: the case study of Forni Glacier (Italy)

---

stakes located nearby the AWS1 Forni. These two dataset resulted strongly correlated (less than 3% of difference between modelled cumulative melt and measured cumulative one) thus supporting the application of energy budget computation to assess the actual melt amount. Besides to  $M_{EB}$  we calculated also other two mass loss amounts: i) Melt occurred with 3 driving Conditions ( $M_{3C}$ ) which corresponds to the snow ablation during days featuring positive energy balance, surface temperature of 273.15 K, and albedo  $> 0.4$ ; ii) Melt evaluated only considering the Positive Energy Budget ( $M_{PEB}$ ) which is estimated neglecting glacier surface temperature and conditions.

The snow melting is assessed also by a degree-day model ( $M_{T-INDEX}$ ) following Braithwaite (1985):

$$M_{T-INDEX} = \begin{cases} \sum T \cdot DDF, & T > T_t \\ 0, & T \leq T_t \end{cases} \quad (1)$$

where  $T_t$  corresponds to the air temperature threshold (K) adopted by the model and  $DDF$  to the degree-day factor ( $\text{mm K}^{-1} \text{d}^{-1}$ ). The applied temperature data were  $T_B$ .

The snow Degree-Day Factor ( $sDDF$ ) was found considering the degree days amount and the Snow Water Equivalent ( $SWE$ ) values estimated from snow pits performed nearby the AWS1 Forni. The presence of snow or bare ice was deducted from albedo data (from AWS1 Forni) and then the length of the snow coverage period. In fact, the  $SWE$  was considered completely melted when the albedo becomes lower than 0.4. Finally the  $sDDF$  was calculated as:

$$sDDF = \frac{SWE}{DD_{glacier}} \quad (2)$$

where  $DD_{glacier}$  is the sum of Degree Days (from  $T_B$  data) in the time frame between a snow pit survey and the occurrence of ice albedo. Moreover we also considered different air temperature thresholds.

We chose Bormio temperature record since this village is less affected by thermal inversion than other stations located nearby and inserted in the ARPA Lombardia meteorological network. By comparing  $T_B$  data with data actually measured by the AWS1 Forni (Fig. 2) a high correlation value results as well ( $r = 0.91$ ), with a root mean square error of the modelled temperature slightly over 3 K. Moreover the slope

#### 4. Air temperature thresholds to evaluate snow melting at the surface of Alpine glaciers by degree-day models: the case study of Forni Glacier (Italy)

coefficient of the linear regression between measured and modelled temperatures at the AWS1 Forni site turns out to be very close to 1 (see Fig. 2).

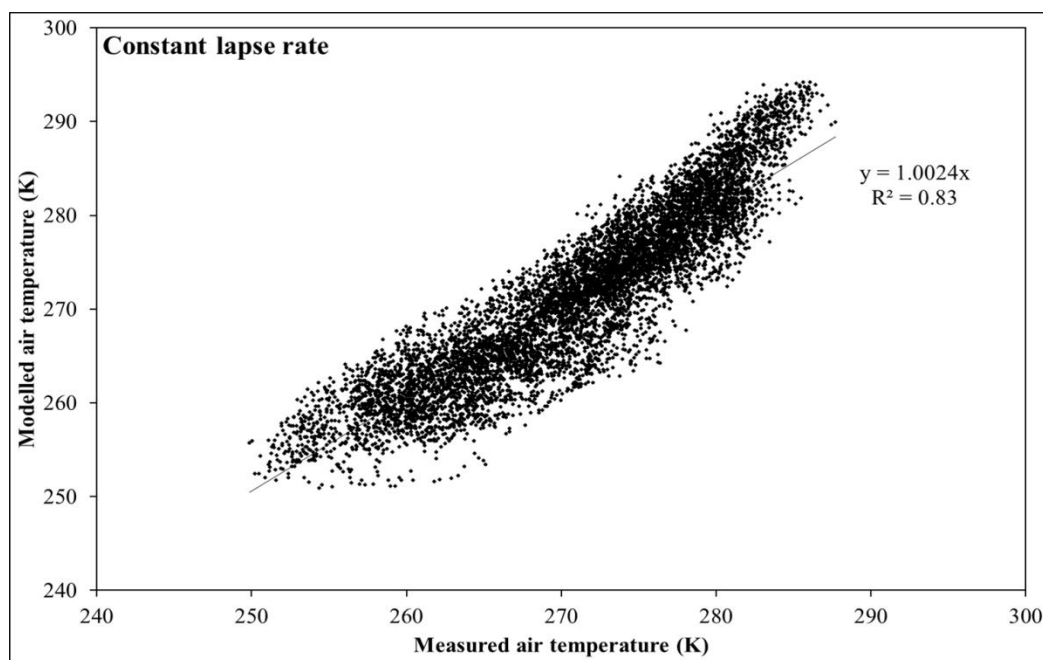


Fig. 2: Hourly temperatures recorded by the AWS1 Forni ( $T_{AWS}$ ) during 2010 ( $x$  axis) vs the modelled ones ( $T_B$ ,  $Y$  axis) derived from Bormio data shifted to the AWS1 Forni elevation through the application of the mean tropospheric lapse rate.

In order to detect the most suitable daily temperature threshold ( $T_t$ ) to adopt in the T-index model for quantifying glacier melting in the April-June period, we considered hourly  $M_{EB}$  values (obtained from AWS1 Forni data) and studied how long ablation occurred in each day (number of hours per day). Then we sorted these data according to temporal length classes (0, 4, 6, 12 and 24 melting hours per day). For each class we calculated the mean, maximum and minimum values of daily average air temperature from  $T_{AWS}$  and  $T_B$  data. These temperature data represent possible thresholds to be applied to calculate degree days driving snow melt. We performed several attempts of running the T-index model by applying the different temperature threshold values and the obtained melt amounts ( $M_{T-INDEX}$ ) were compared with the ones from energy budget computation ( $M_{EB}$ ) thus permitting to select the most suitable and performing threshold values.



### 3. Results

#### 3.1 Melting from energy balance

Melting at the AWS1 Forni site estimated from the energy balance is shown in Figure 4.  $M_{EB}$  was obtained considering only hours characterized by null (273.15 K) surface temperature and positive energy budget. The time window of our analysis is scheduled according to the hydrological year (i.e. at Mid-latitudes from 1<sup>st</sup> October of the year  $x$  to 30<sup>th</sup> September of the year  $x+1$ ). It results a total  $M_{EB}$  of -37.5 m w.e. over a 7-year period.

Supraglacial albedo data permit to detect snow cover presence (albedo > 0.4) during days featuring both positive energy balance and surface temperature of 273.15 K. The occurrence of these three criteria (ranging from 69 to 108 days per year) allows calculation of  $M_{3C}$  (light grey bars in Fig. 3) which is found not negligible with a melt amount from 17.6% to 29.2% of the total annual value. In general the ice melting period (dark grey bars in Fig. 3) results longer (with an average value of 100 days per hydrological year) than the  $M_{3C}$  time frame (89 days per year mean value) with the unique exception of the hydrological year 2009/2010 (88 and 101 days for ice and snow respectively).

#### 4. Air temperature thresholds to evaluate snow melting at the surface of Alpine glaciers by degree-day models: the case study of Forni Glacier (Italy)

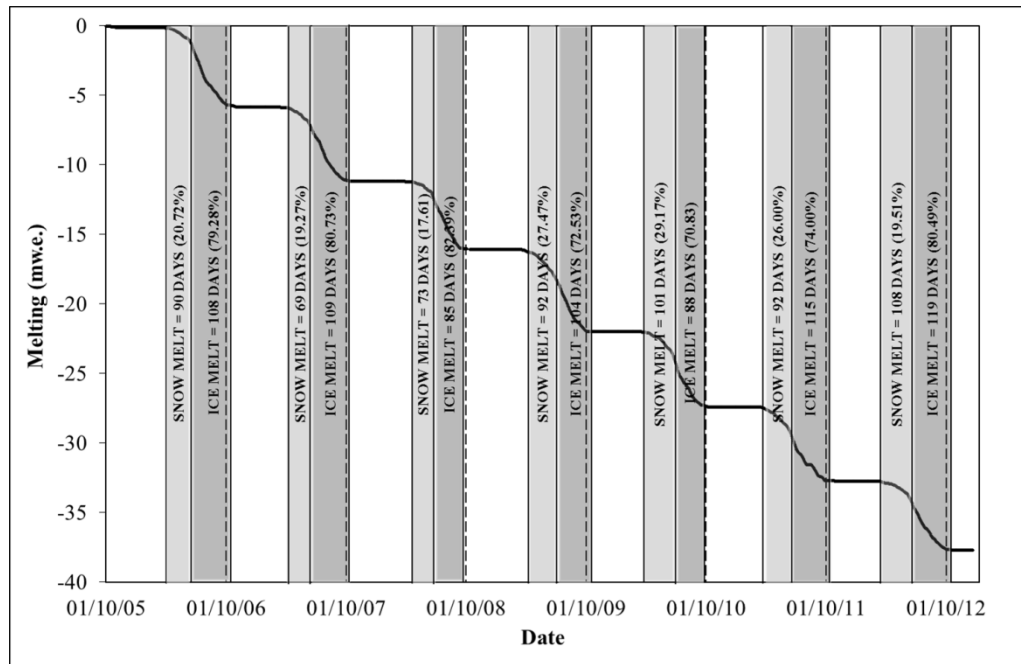


Fig. 3: Cumulative melting amount ( $M_{EB}$ ) over the 7-year period from October 2005 to December 2012. The dotted lines mark the beginning of the hydrological year (1<sup>st</sup> October). In some cases ablation continues also in a few days of October and albedo values remain lower than 0.4. In light grey the time frames with snow melting ( $M_{3C}$ ) and in dark grey the ice melting periods are shown.

In order to assess the importance of the condition concerning glacier surface temperature, we also performed a test calculating ablation ( $M_{PEB}$ ) only from positive energy balance data during April-June period (91 days long) and not considering glacier surface temperature. The results were compared with  $M_{EB}$  values (Table 1). Totally a  $M_{EB}$  for the April-June period over the time window 2006-2012 of -12.72 m w.e. is calculated. This value differs from the  $M_{PEB}$  which results equal to -13.43 m w.e.

The quite wide range of variability of our results suggests further analyses. In fact, the April-June  $M_{EB}$  corresponds to ca. 1/3<sup>rd</sup> of the total  $M_{EB}$  (Table 1). Focusing on this period we found the most intense ablation occurred in 2011 (-2.26 m w.e. contributing for 43.5% with respect to the total  $M_{EB}$  for that year) and the minimum was found in 2008 (-1.55 m w.e., 31.0% of the annual value).

4. Air temperature thresholds to evaluate snow melting at the surface of Alpine glaciers by degree-day models: the case study of Forni Glacier (Italy)

*Tab. 1: For each hydrological year the following data are shown: cumulative annual  $M_{EB}$  value (2<sup>nd</sup> column), cumulative  $M_{EB}$  during April-June (3<sup>rd</sup> column), cumulative  $M_{3C}$  during the snow melting period (5<sup>th</sup> column), cumulative  $M_{PEB}$  during April June (7<sup>th</sup> column) and percentages with respect to the annual  $M_{EB}$  value (4<sup>th</sup>, 6<sup>th</sup> and 8<sup>th</sup> column respectively). All melting amounts are in m w.e.*

Hydrological year	Annual $M_{EB}$	Apr-Jun $M_{EB}$	Apr-Jun $M_{EB}$ % with respect to the annual $M_{EB}$	$M_{3C}$	$M_{3C}$ % with respect to the annual $M_{EB}$	Apr-Jun $M_{PEB}$	Apr-Jun $M_{PEB}$ % with respect to the annual $M_{EB}$
2005/2006	-5.6	-1.91	34.1%	-1.15	20.5%	-1.98	35.4%
2006/2007	-5.5	-2.08	37.7%	-1.00	18.2%	-2.11	38.4%
2007/2008	-5.0	-1.55	31.0%	-0.84	16.8%	-1.85	36.9%
2008/2009	-5.6	-1.68	29.9%	-1.61	28.8%	-1.73	30.9%
2009/2010	-5.6	-1.62	29.0%	-1.54	27.5%	-1.74	31.1%
2010/2011	-5.2	-2.26	43.5%	-1.37	26.4%	-2.33	44.8%
2011/2012	-5.0	-1.63	32.5%	-0.96	19.2%	-1.69	33.9%
<b>TOT</b>	<b>-37.5</b>	<b>-12.72</b>	<b>33.9%</b>	<b>-8.47</b>	<b>22.6%</b>	<b>-13.43</b>	<b>35.8%</b>
<b>MEAN</b>	<b>-5.4</b>	<b>-1.82</b>	<b>33.9%</b>	<b>-1.21</b>	<b>22.57%</b>	<b>-1.92</b>	<b>35.8%</b>

### 3.2 Daily air temperature thresholds witnessing glacier melting in the April-June period

To choose the most suitable daily air temperature threshold ( $T_i$ ) to detect melting days in the April-June period and to evaluate the corresponding melting amount by T-index model we analysed  $T_{AWS}$  and  $T_B$  data (see Tab. 2).

Days without melting (0  $M_{EB}$  hours per day, 3<sup>rd</sup> column in Tab. 2) resulted occurring over 4.9% of the total time frame (April-June over a 7 year long period). On the other hand, days featuring continuous and uninterrupted melting (24  $M_{EB}$  hours per day, 8<sup>th</sup> column in Tab. 2) cover 3.3% of the total time. The cumulative melt occurred over these 21 days is equal to -0.77 m w.e. and it represents only the 6.0% of the total loss. These days are characterized by daily air temperature at AWS1 Forni always positive with a daily mean value of 278.6 K, the maximum of daily average data equal to 282.1 K and the minimum of daily average values of 275.5 K.  $T_B$  data over the same time frames are characterized by a mean daily average of 279.8 K, a maximum of daily average of 284.6 K and a minimum daily temperature of 274.7 K.

#### 4. Air temperature thresholds to evaluate snow melting at the surface of Alpine glaciers by degree-day models: the case study of Forni Glacier (Italy)

---

Days with at least 12  $M_{EB}$  hours (7<sup>th</sup> column in Tab. 2) occurred on the 47.3% of the total analysed time and they represent the 73.3% of the whole ablation (cumulative  $M_{EB}$ : -9.30 m w.e.).

Days with at least 6  $M_{EB}$  hours (6<sup>th</sup> column in Tab. 2) occurred on the 83.8% of the total analysed time and they represent the 97.7% of the whole ablation (cumulative  $M_{EB}$ : -12.43 m w.e.).

Then the largest part of the melt resulted occurring on days with at least 6  $M_{EB}$  hours thus suggesting to consider temperature data calculated for this class as suitable  $T_t$ . In particular the minimum value of the average daily temperature calculated with at least 6  $M_{EB}$  hours per day (268.6 K and 268.1 K considering the  $T_{AWS}$  and  $T_B$  data, respectively) were applied to detect the actual melting days. The first thresholds was applied to  $T_{AWS}$  data and permitted to select 586 melting days describing the 99.4% (-12.64 m w.e.) of the total  $M_{EB}$ . Considering  $T_B$  data, the threshold of 268.1 K permitted to detect 601 melting days giving a cumulative  $M_{EB}$  of -12.66 m w.e. equal to 99.5% of the total.

From our results it is also clear that the use of the 273.15 K as temperature threshold drives an underestimation of ablation. In fact, this value applied to the AWS1 Forni temperature data allows to detect 421 melting days (66.1% with respect to the total time frame) equal to a cumulative  $M_{EB}$  of -11.39 m w.e. (89.5 % with respect to the total melt). The same threshold applied to the  $T_B$  data allowed to select 481 melting days giving a  $M_{EB}$  of -12.00 m w.e. (94.3% with respect to the total value).

In both cases the application of 273.15 K threshold does not represent the most suitable and exhaustive solution and an underestimation up to 10% of the total  $M_{EB}$  in the April-June period can occur.

#### 4. Air temperature thresholds to evaluate snow melting at the surface of Alpine glaciers by degree-day models: the case study of Forni Glacier (Italy)

*Tab. 2: Number of days and daily temperature values (mean, maximum and minimum of the average data) in the April-June period considering different temporal length classes of  $M_{EB}$  hours. The air temperature data are recorded by AWS1 Forni ( $T_{AWS}$ ) and from Bormio meteorological station. These latter data are shifted to the glacier elevation by applying the mean tropospheric lapse rate ( $T_B$ ).*

Hours per day	$M_{EB}$ hours						
	All	0	< 4	≥ 4	≥ 6	≥ 12	24
Number of days	637	31	32	574	534	301	21
% with respect to the total studied period	100.0%	4.9%	5.0%	90.1%	83.8%	47.3%	3.3%
Cumulative $M_{EB}$ (m w.e.)	-12.72	0.00	-0.07	-12.65	-12.43	-9.30	-0.77
Mean average Daily $T_{AWS}$ (K)	274.7	266.0	268.8	275.6	275.9	277.8	278.6
Max of average Daily $T_{AWS}$ (K)	284.3	269.1	275.0	284.3	284.3	284.3	282.1
Min of average Daily $T_{AWS}$ (K)	262.5	262.5	265.8	266.0	268.6	272.0	275.5
Mean average Daily $T_B$ (K)	276.4	267.7	270.2	277.2	277.6	279.4	279.8
Max of average Daily $T_B$ (K)	286.9	275.7	276.9	286.9	286.9	286.9	284.6
Min of average Daily $T_B$ (K)	264.1	264.1	266.8	267.5	268.1	268.9	274.7

### 3.3 Melt calculation from T-index model

Besides the calculation of snow and ice melting by means of the energy balance, the snow daily melting rate at the AWS1 Forni site was also calculated by applying the T-index model ( $M_{T-INDEX}$ ).  $T_B$  data represent the input values to calculate the degree days sum driving snow ablation. We focused on melting in the April-June period from 2006 to 2012.

Different temperature thresholds ( $T_t$ ) estimated from  $T_B$  data were used: the most common and applied value (273.15 K), the minimum of daily average temperature calculated for days featuring at least 6  $M_{EB}$  hours (268.1 K) and the minimum daily average temperature calculated for days featuring 24  $M_{EB}$  hours (274.7 K). By comparing the cumulative  $M_{T-INDEX}$  curves (Fig. 4) a similar trend is evident but the total amount of melting over the 7 year long period results quite different depending on the applied  $T_t$  value: from -6.81 m w.e. (threshold 274.7 K) to -8.23 m w.e. (threshold 268.1 K).

The cumulative  $M_{EB}$  in the same period results -8.23 m w.e. thus underlying that the temperature threshold that better explains magnitude and variability of snow melting corresponds to the minimum of daily average temperature calculated for days featuring at least 6  $M_{EB}$  hours (268.1 K).

#### 4. Air temperature thresholds to evaluate snow melting at the surface of Alpine glaciers by degree-day models: the case study of Forni Glacier (Italy)

With the 268.1 K threshold the snow degree-day factors (see equation 2) results lower than the other two. However the snow  $DDF$  values we found are in agreement with findings in other studies (see Table 3): Hock (2003) reported a snow  $DDF$  ranging from  $2.5 \text{ mm d}^{-1} \text{ K}^{-1}$  (Clyde, 1931) to  $11.6 \text{ mm d}^{-1} \text{ K}^{-1}$  (Kayastha et al., 2000).

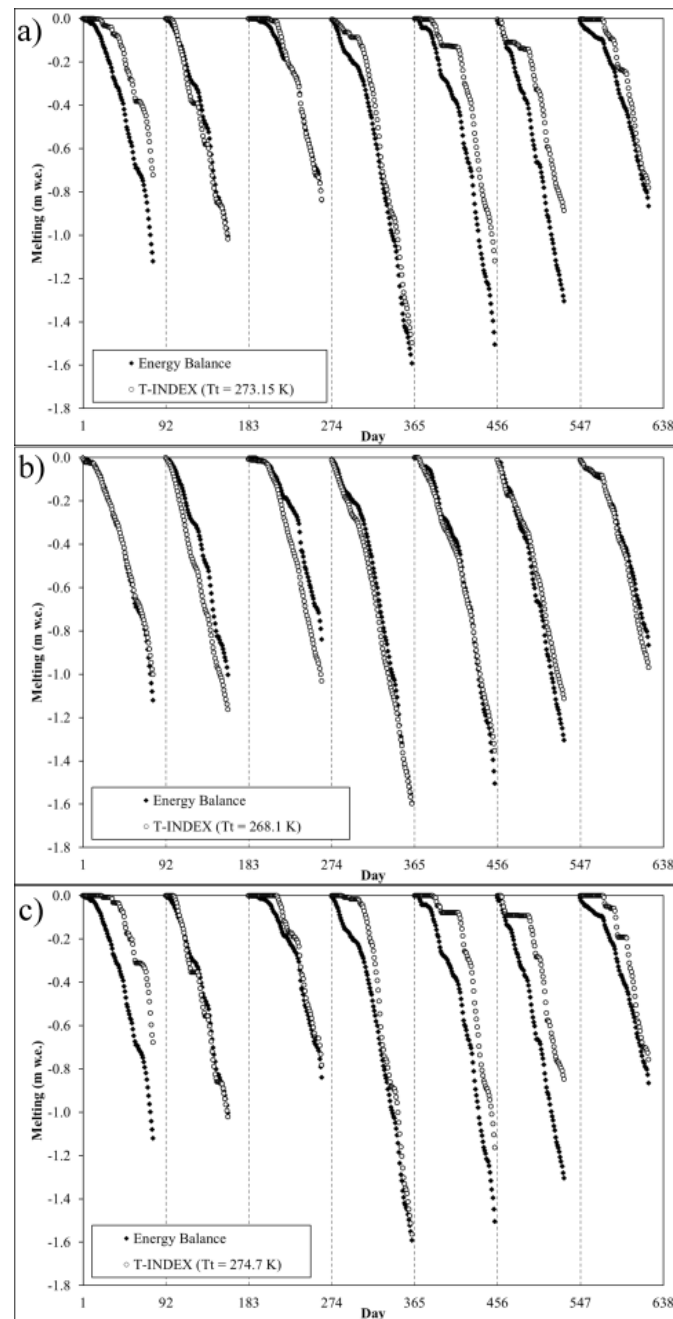


Fig. 4: From April to June 2006-2012 snow melting rate are shown. With black dots are shown the results from the energy balance ( $M_{EB}$ ). White dots represent the results from  $T$ -index model ( $M_{T-INDEX}$ ) by applying different temperature thresholds to  $T_B$  data: 273.15 K (panel a), 268.1 K (panel b) and 274.7 K (panel c). The x-axis indicates the progressive number of the record concerning only April-June data.

#### 4. Air temperature thresholds to evaluate snow melting at the surface of Alpine glaciers by degree-day models: the case study of Forni Glacier (Italy)

*Tab. 3: Mean degree-day factors for snow melting from the literature and from our results.*

	<b>Snow DDF (mm d<sup>-1</sup> K<sup>-1</sup>)</b>
De Quervain (1979)	4.2
Van de Wal (1992)	2.8
Hock (1999)	3.2
Hock (2003)	5.1
Braithwaite (2008)	3.5 1) Winter balance
Braithwaite (2008)	4.6 2) Winter balance plus precipitation
Braithwaite (2008)	4.1 1) and 2) combined
Our results:	
$T_t = 273.15$	3.9
$T_t = 268.1$	2.0
$T_t = 273.7$	5.8

#### 4. Discussions and conclusions

In this study by applying a point energy balance model (following Senese et al., 2012a) at the AWS1 Forni site on the glacier ablation tongue we found that a not negligible annual snow melt ( $M_{3C}$ ) occurs. In the 7-year period 2005-2012 it ranges from 17.6% to 29.2% of the total (ice and snow) annual ablation (total  $M_{EB}$ : -37.5 m w.e.), which was estimated through energy budget computations by considering both positive energy budget and surface temperature above 273.15 K.

Our data also indicate that during April-June at the AWS1 Forni site all the snow coverage disappears due to melting processes; in fact, from 2006 to 2012 the  $M_{3C}$  over the April-June time frame is found -8.47 m w.e. corresponding to the 66.59% of the April-June  $M_{EB}$ . This latter results equal to -12.72 m w.e., representing about 1/3<sup>rd</sup> of the total  $M_{EB}$  calculated over the 7 hydrological years. Moreover we also computed the April-June mass loss without considering the glacier surface temperature and conditions; this ablation, named  $M_{PEB}$ , results equal to -13.43 m w.e. thus underlining an overestimation (+5.6% with respect to the  $M_{EB}$  over the same period). Then the knowledge of glacier surface temperature results really important to assess with a good accuracy the melt amount. On the other hand these information are available only on a small number of glaciers where supraglacial AWS have been running thus suggesting to look for different strategies to assess the snow melt amount. The most diffuse and simple method is the T-index approach based on data acquired outside the studied glacier. Then in our study to compute the degree days amount the input data were air

#### 4. Air temperature thresholds to evaluate snow melting at the surface of Alpine glaciers by degree-day models: the case study of Forni Glacier (Italy)

---

temperature values measured at Bormio (1225 m a.s.l.) and shifted to the AWS1 Forni site elevation (2631 m a.s.l.) applying the mean tropospheric lapse rate ( $-6.5 \text{ K km}^{-1}$ ). To validate this reconstruction we made a comparison among modelled air temperature values ( $T_B$ ) with air temperature actually measured at the AWS1 Forni ( $T_{AWS}$ ). It resulted a strong agreement between the two records of data ( $r = 0.91$ ) suggesting that it is possible to perform a reasonable reconstruction of supraglacial daily average air temperature starting from meteorological data acquired down valley also using a mean tropospheric vertical gradient as lapse rate. Nevertheless this result could depend on the small distance between Bormio and Forni Glacier. But on other glaciers the assessment of a local daily vertical gradient could be needed to reconstruct supraglacial air temperature and degree days amount from data acquired by weather stations located far and farer from the glacier site.

Our analysis indicates that the major uncertainty in computing the degree days amount at the glacier surface and then in assessing snow melt is given by the choice of an appropriate air temperature threshold ( $T_t$ ): a not negligible variability of the cumulative degree days values resulted applying different  $T_t$ . In fact ablation does not occur only with air temperature higher than 273.15 K since it is determined by the surface energy balance and this latter is only indirectly affected by air temperature (Kuhn 1987). Then, to assess the most suitable temperature threshold, we firstly analysed hourly  $M_{EB}$  values (obtained from AWS1 Forni data) in the April-June period to detect if ablation occurs and how long this phenomenon takes (number of hours per day). Then we sorted these data according to temporal length classes (0, 4, 6, 12 and 24 melting hours per day). For each class we calculated the mean, maximum and minimum values of daily average air temperature from  $T_{AWS}$  and  $T_B$  data. Moreover we also evaluated the cumulative  $M_{EB}$  for each temporal length class to evaluate its weight with respect to the total ablation. The largest part of the melting (97.7% of the whole ablation) resulted occurring on days featuring at least 6  $M_{EB}$  hours thus suggesting to consider the minimum average daily temperature value calculated for this class as a suitable temperature threshold (268.6 K and 268.1 K considering the  $T_{AWS}$  and  $T_B$  data respectively). These data were applied to detect the actual melting days. The first threshold was applied to air temperature data from AWS1 Forni and permitted to select 586 melting days describing the 99.4% (-12.64 m w.e.) of the total  $M_{EB}$ . Considering  $T_B$  data, the threshold of 268.1 K permitted to detect 601 melting days giving a cumulative  $M_{EB}$  of -12.66 m w.e. equal to 99.5% of the total.



#### 4. Air temperature thresholds to evaluate snow melting at the surface of Alpine glaciers by degree-day models: the case study of Forni Glacier (Italy)

---

Then we ran a simple T-index model using as input data  $T_B$  and varying the temperature threshold (273.15 K, 268.1 K and 274.7 K). The cumulative  $M_{T-INDEX}$  curves we obtained (Fig. 4) show a similar trend but the total amount of snow melting over the 7 year long period results quite different. The cumulative  $M_{EB}$  in the same period results -8.23 m w.e. and this values is also obtained applying as threshold 268.11 K to  $T_B$  data. These results suggest to use as  $T_t$  the minimum of daily average temperature calculated for days featuring at least 6  $M_{EB}$  hours. This value permits to better explain magnitude and variability of snow melting (Fig. 4).

As regards the threshold 273.15 K, which has been largely used in the literature dealing with degree-day model (e.g. Braithwaite, 1985; Hock, 2003), our tests indicate that it drives an underestimation of snow melt (-11.5% with respect to the  $M_{EB}$  value). Moreover in the case the main purpose should be only the detection of the melting days and not the assessing of the melt amount, the application of the 273.15 K threshold drives an underestimation as well. With this threshold 481 melting days are detected against 601 melting days selected by applying the 268.1 K threshold to  $T_B$  data.

Summarizing it results that applying a different temperature threshold used to assess the cumulative degree days amount considerably affect the magnitude of the estimated melt amount. In fact a 5.0 K lower  $T_t$  value (with respect to the largely applied 273.15 K) avoids most of the sampling problem in the application of the positive T-index models and permits the most reliable reconstruction of snow melt. Moreover our air temperature threshold analysis on an Alpine glacier results in agreement with findings by van den Broeke et al. (2010) in Greenland ice sheet. They found an about 5 K lower threshold value by observing the cumulative distribution of daily average temperature for days with melt at three AWSs. From their study this value resulted to allow also an appropriate calculation of snow and ice degree-day factors. In fact applying the common 273.15 K threshold they obtained non-sense factors values. Then probably the choice of a 268 K value as air temperature threshold for computing degree days amount could be generalized and applied not only on Greenland glaciers but also on Mid latitude and Alpine ones like the Forni Glacier.

## References

AINEVA: [www.aineva.it](http://www.aineva.it)

ARPA Lombardia: <http://www2.arpalombardia.it/siti/arpalombardia/meteo/richesta-dati-misurati/Pagine/RichiestaDatiMisurati.aspx>

Bocchiola D., Mihalcea C., Diolaiuti G., Mosconi B., Smiraglia C. and Rosso R. (2010): Flow prediction in high altitude ungauged catchments: a case study in the Italian Alps (Pantano Basin, Adamello Group), *Advances in Water Resources*, 33, 1224-1234.

Braithwaite R.J. (1985): Calculation of degree-days for glacier-climate research. *Zeitschrift fuer Gletscherkunde und Glazialgeologie*, 20/1984, 1-8.

Braithwaite R.J. (2008): Temperature and precipitation climate at the equilibrium-line altitude of glaciers expressed by the degree-day factor for melting snow. *Journal of Glaciology*, 54 (186), 437-444.

Cazorzi F. and Dalla Fontana G. (1996): Snowmelt modelling by combining air temperature and a distributed radiation index. *J. Hydrol.*, 181(1-4), 169-187.

Citterio M., Diolaiuti G., Smiraglia C., Verza G. and Meraldi E. (2007): Initial results from the automatic weather station (AWS) on the ablation tongue of Forni Glacier (Upper Valtellina, Italy). *Geografia Fisica e Dinamica Quaternaria*, 30, 141-151.

Clyde G.D. (1931): Snow-melting characteristics. *Utah Agricultural Experiment Station Bull.*, 231, 1-23.

De Quervain M. (1979): Schneedeckenablation und Gradtage im Versuchsfeld Weissfluhjoch. *Mitteilung VAW/ETH Zurich*, 41, 215-232.

Diolaiuti G. and Smiraglia C. (2010): Changing glaciers in a changing climate: how vanishing geomorphosites have been driving deep changes in mountain landscapes and environments. *Géomorphologie: relief, processus, environnement*, 2, 131-152.

Diolaiuti G., Bocchiola D., D'Agata C. and Smiraglia C. (2012): Evidence of climate change impact upon glaciers' recession within the Italian Alps: the case of Lombardy glaciers. *Theoretical and Applied Climatology*, 109 (3-4), 429-445. DOI 10.1007/s00704-012-0589-y.

Hock R (1999): A distributed temperature-index ice- and snowmelt model including potential direct solar radiation. *J. Glaciol.*, 45 (149), 101-111.

Hock R. (2003): Temperature index melt modelling in mountain areas. *Journal of Hydrology*, 282 (1-4), 104-15.

4. Air temperature thresholds to evaluate snow melting at the surface of Alpine glaciers by degree-day models: the case study of Forni Glacier (Italy)

---

- Hock R. (2005): Glacier melt: a review of processes and their modeling. *Progress in Physical Geography*, 29 (3), 362-391.
- Kayastha R.B., Ageta Y. and Nakawo M. (2000): Positive degree-day factors for ablation on glaciers in the Nepalese Himalayas: case study on glacier AX010 in Shoron Himal, Nepal. *Bull. Glaciol. Res.*, 17, 1-10.
- Kuhn M. (1987): Micro-meteorological conditions for snow melt. *J. Glaciol.*, 33 (113), 263-272.
- Pellicciotti F., Brock B.W., Strasser U., Burlando P., Funk M. and Corripio J.G. (2005): An enhanced temperature-index glacier melt model including shortwave radiation balance: development and testing for Haut Glacier d'Arolla, Switzerland. *J. Glaciol.*, 51 (175), 573-587.
- SHARE: <http://www.evkc2cnr.org/cms/en/share/monitoring-stations>
- Senese A., Diolaiuti G., Mihalcea C. and Smiraglia C. (2012a): Energy and mass balance of Forni Glacier (Stelvio National Park, Italian Alps) from a 4-year meteorological data record. *Arctic, Antarctic, and Alpine Research*, 44 (1), 122-134.
- Senese A., Diolaiuti G., Verza G.P. and Smiraglia C. (2012b): Surface energy budget and melt amount for the years 2009 and 2010 at the Forni Glacier (Italian Alps, Lombardy). *Geografia Fisica e Dinamica Quaternaria*, 35 (1), 69-77.
- Van de Wal R. (1992): Ice and climate. PhD Thesis, Utrecht University, 144 pp.
- van den Broeke M., Bus C., Ettema J. and Smeets P. (2010): Temperature thresholds for degree-day modeling of Greenland ice sheet melt rates. *Geophysical Research Letters*, 37, L18501.

# Chapter 5

## **An enhanced T-index model including solar and infrared radiation to evaluate distributed ice melt at the Forni Glacier tongue (Italian Alps)**

### **Abstract**

We developed a new enhanced T-index model including infrared radiation to evaluate distributed ice melt. We apply the method for simulating ice melting over the ablation tongue of the Forni Glacier (Italian Alps), where we installed and ran a supraglacial Automatic Weather Station (AWS) ever since September 2005. We benchmarked the performance of the model against other T-index methods, from simple degree-day to enhanced models including incoming shortwave fluxes. We further tested different methods to distribute the input meteorological and energy data driving the enhanced T-index approaches, which should allow a wider application of our approach upon glaciers not equipped with AWS, or without a net radiometer, necessary to directly measure infrared flux.

First, we developed a local lapse rate to depict the yearly variability of the vertical temperature gradient, so assessing the actual thermal conditions at different elevations. We then distributed the incoming solar radiation by taking into account glacier topography and shading. Eventually, the longwave flux was modelled considering cloud cover, and air temperature. Then, our enhanced T-index model was run using as input data the modelled temperature, and energy fluxes, and the results therein were compared against those obtained using observed data.

The results display that i) the application of a local temperature lapse rate provides a better distribution of temperature at the glacier surface; ii) our approach provides acceptable depiction of the distributed solar radiation input and of the incoming infrared radiation; iii) including the longwave input within the enhanced T-index model provides more accurate calculation of ablation, suggesting that the proposed approach may deliver improved ablation estimates when be used upon other Alpine debris free glaciers.

## 1. Introduction and aims

A large variety of ice melt models was developed lately, ranging from physically based energy-balance models (e.g. Brun et al., 1989; Bloschl et al., 1991; Arnold et al., 1996), to empirical methods driven by one or more meteorological variables, mainly by air temperature (e.g. Braithwaite, 1995). Although melt rates are fully described through the surface energy budget, glacier melt models based on the computation of the energy fluxes are not always applicable in mountain and Alpine areas, due to lack of input data. In fact, in high-mountain regions automatic weather stations (AWSs) measuring radiation fluxes are available in few locations, and often placed outside glaciers. Hence, temperature-index (T-index, also named degree-day) based models are widely used for computing snow and ice melt, given that air temperatures are generally available (Braithwaite, 1995). Moreover in the last decades several authors have developed enhanced T-index models, driven not only by air temperature (i.e.: positive degree days), but by shortwave radiation (Cazorzi and Della Fontana, 1996; Pellicciotti et al., 2005). Such approaches generally allow to depict snow and ice melt accurately, and to distribute it spatially whenever a digital elevation model (DEM) of the glacier is available. The main limit of such enhanced models is the need of solar radiation data, possibly measured at the glacier surface. Then, some approaches have been developed to model radiative input on glaciers where no AWSs are located. Regarding the incoming solar flux, the approach proposed by Iqbal (1983) offers an extra-accuracy over more conventional approaches as reviewed by Gueymard (1993). With respect to the incoming longwave radiation a review of models is given by Ellingston et al. (1991). Longwave radiation is usually estimated from empirical relationships with air temperature and vapor pressure (Plüss and Ohmura, 1997; Oerlemans, 2000; Klok and Oerlemans, 2002; Hock, 2005), based on standard meteorological measurements (Kondratyev, 1969).

In this context, simple methods to model energy fluxes (both shortwave and longwave) at the glacier surface starting from easily available meteorological variables (like air temperature) are desirable. Also, improvements of enhanced T-index models to describe magnitude and rates of ice and snow melt are needed. This chapter presents the results of some tests we performed to model distributed air temperature, and energy fluxes, and to evaluate ice melt at the Forni Glacier surface (Italian Alps). More precisely, our main aims were as follows:

## 5. An enhanced T-index model including solar and infrared radiation to evaluate distributed ice melt at the Forni Glacier tongue (Italian Alps)

---

- i. to develop a simple model of distributed glacier melt starting from input data largely available, such as air temperature and radiative fluxes, thus assuring model exportability;
- ii. to develop and test simple and replicable methods for modelling air temperature, input radiative (both long- and short-wave) fluxes, and for distributing them over the whole glacier surface.

A further aim is to evaluate at what extent the models need local data acquired by a supraglacial AWS, and whether they can be applied if meteorological data are measured only outside the glacier.

Then, to reach the above reported goals we applied different T-index models, from an easiest one only considering temperature (Braithwaite, 1995), to most recent and complex ones, which also consider solar radiation (e.g. Pellicciotti et al., 2005). An attempt was also made here, to provide improvement of these approaches by considering net longwave radiation as an input. A suitable site to develop our approach based upon field observations is given by the Forni Glacier (Stelvio National Park, Italian Alps), the largest Italian valley glacier (11.36 km<sup>2</sup> in area), where since September 2005 an automatic weather station (AWS1 Forni, WGS84 coordinates 46°23'56.0" N and 10°35'25.2" E, at 2631 m a.s.l.) was continuously run (Citterio et al., 2007; Senese et al; 2012a;2012b), thus assuring a long sequence of meteorological and energy data.

To run the already available T-index models (Braithwaite, 1995, Cazorzi and Della Fontana, 1997; Pellicciotti et al., 2005), and to develop a new one also considering longwave fluxes, we distributed the solar and infrared fluxes, and the air temperatures upon the whole Forni Glacier surface. We then compared the obtained distributed meteorological values against a selection of field measured data. Finally, the modelled ice ablation was compared against melt rates measured in the field during June-August 2011.

5. An enhanced T-index model including solar and infrared radiation to evaluate distributed ice melt at the Forni Glacier tongue (Italian Alps)

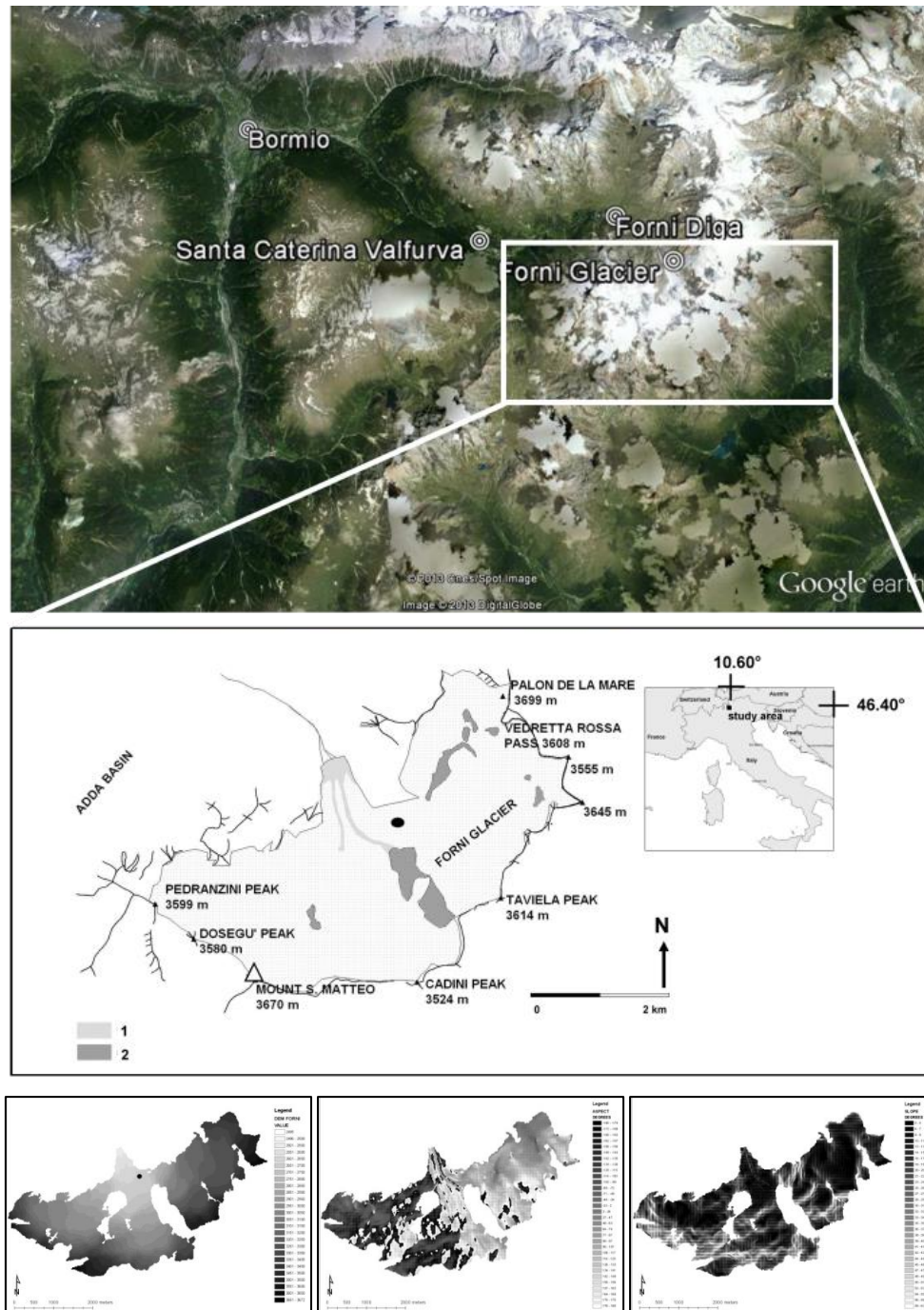


Fig. 1: On the top the location of Bormio, S. Caterina Valfurva, Forni Diga and Forni Glacier (Google Earth © raster base) and in the lower picture the location of the AWS1 Forni (black dot). In the map the light grey areas (1) are used to mark supraglacial debris coverage and the dark grey zones (2) indicate rock exposures and nunataks. At the bottom three maps of the Forni Glacier showing a) elevation, b) aspect, and c) slope.



## 2. Methods

### 2.1. Air temperature

The input data of the distributed air temperature model here are hourly temperatures measured at the AWS1 Forni, and then shifted at each elevation on the glacier. To assess the most suitable lapse rates, we processed 4 years of data (from 1<sup>st</sup> January 2006 to 31<sup>st</sup> December 2009) from Bormio (1225 m a.s.l.), S. Caterina Valfurva (1730 m a.s.l.) and Forni Diga (2180 m a.s.l.) weather stations (villages nearby the Forni Glacier, Fig. 1). We started calculating for each year 3 hourly series of lapse rates. The following couples of weather stations were considered: i) Bormio and AWS1 Forni, ii) S. Caterina Valfurva and AWS1 Forni and iii) Forni Diga and AWS1 Forni, thus obtaining 12 years of hourly data records. To avoid thermal inversion affecting too much the data, only the warmest hours of the day (from 12 am to 4 pm) have been considered in the calculation of the daily average lapse rates. Then, these 12 years of daily records were averaged, to obtain the annual daily lapse rate variability. Data at Bormio, S. Caterina Valfurva, and Forni Diga stations were kindly provided by the Lombardy Regional Agency for Environmental Protection (ARPA Lombardia), which we kindly acknowledge. To smooth this record, a regression model was used as well (Fig. 2). More precisely, we used a relationship function between lapse rate ( $\lambda$ ) and time ( $day$ ), following a truncated Fourier series at the second order:

$$\lambda = -7.88 + 1.27 \cos\left(\frac{day \cdot 2\pi}{365}\right) + 0.45 \sin\left(\frac{day \cdot 2\pi}{365}\right) - 0.16 \cos\left(2 \frac{day \cdot 2\pi}{365}\right) - 0.73 \sin\left(2 \frac{day \cdot 2\pi}{365}\right) \quad (1)$$

where  $day$  corresponds to the Julian date ( $1 = 1^{\text{st}}$  January,  $365 = 31^{\text{st}}$  December). Leap years are neglected and the introduced errors are considered negligible (Hock and Tijm-Reijmer, 2011).

## 5. An enhanced T-index model including solar and infrared radiation to evaluate distributed ice melt at the Forni Glacier tongue (Italian Alps)

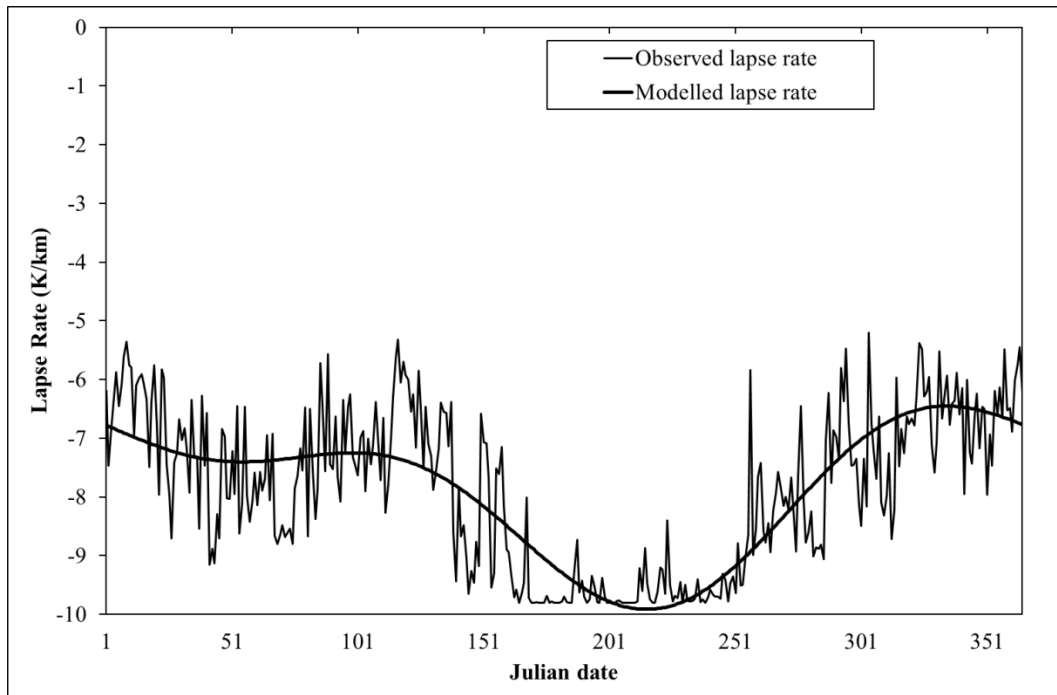


Fig. 2: Daily averaged lapse rate considering only the hottest hours per day (from 12 am to 4 pm, “observed” in the legend) and the smoothed daily values obtained by a truncated Fourier series at the second order (“modeled” in the legend).

### 2.2. Net solar radiation

To model the distributed incoming solar radiation at the Forni Glacier surface, we considered subsequently i) a flat and ideal surface (i.e. we calculated radiation taking into account only the astronomical and geographical factors, neglecting atmospheric absorption and orography, Iqbal, 1983; Allen et al., 2006; Wang et al., 2006), ii) a sloped surface (i.e. we considered slope and aspect too, Garner and Ohmura, 1968; Duffie and Beckman, 1980; Hunter and Goodchild, 1997; Allen et al., 2006), iii) a sloped surface in a complex orographic system (i.e. we evaluated the shading too), and iv) a complex surface (from iii) in an actual atmosphere (i.e. we considered also meteorological conditions, and the multireflection from the surrounding surfaces through the clearness index, Gueymard, 2001; Hock and Noetzli, 1997). We describe here the algorithms we applied to distribute the global radiation.

i) The approach proposed by Iqbal (1983) was considered to estimate the daily exo-atmospheric solar radiation ( $SW_0$ ) received by a flat surface :

5. An enhanced T-index model including solar and infrared radiation to evaluate distributed ice melt at the Forni Glacier tongue (Italian Alps)

---

$$SW_0 = I_0 \cdot E_0 \cdot \int_{w_{sr}}^{w_{ss}} \cos(\theta) \cdot dh \quad (2)$$

where  $I_0$  corresponds to the average solar irradiance at the mean Earth-Sun distance ( $1367 \text{ W m}^{-2}$ ),  $E_0$  is the eccentricity factor (i.e. the correction due to the elliptical orbit of the Earth depending on the day of the year; Spencer, 1971) and  $\theta$  is the angle between the normal to the surface and the solar beam (Oke, 1987),  $w_{sr}$  and  $w_{ss}$  are the sunrise and sunset hour angles, respectively (Allen et al., 2006):

$$w_{ss} = \cos^{-1}(-\tan \Phi \cdot \tan \delta) \quad (3)$$

$$w_{sr} = -w_{ss} = -\cos^{-1}(-\tan \Phi \cdot \tan \delta) \quad (4)$$

where  $\Phi$  is the latitude and  $\delta$  is the solar declination.  $w_{sr}$  and  $w_{ss}$  have opposite values because hour angle is the angular displacement of the sun, east or west of the local meridian. This is due to rotation of the Earth on its axis at  $15^\circ$  per hour: morning ( $w_{sr}$ ) is assumed as negative and afternoon ( $w_{ss}$ ) as positive. At solar noon the hour angle is null. Finally, simplifying the approach proposed by Wang et al. (2006), the daily exo-atmospheric solar radiation received by a flat surface is:

$$SW_0 = 2 \cdot I_0 \cdot E_0 \cdot [(\sin \delta \cdot \sin \Phi) \cdot w_{ss} + (\cos \delta \cdot \cos \Phi) \cdot \sin w_{ss}] \quad (5)$$

ii) For an inclined surface, the angle between the normal to the surface and the solar beam was calculated following Garner and Ohmura (1968) and Duffie and Beckman (1980)

$$SW_0 = I_0 \cdot E_0 \cdot [(\sin \delta \cdot \sin \Phi \cdot \cos S) \cdot (w_{ss} - w_{sr}) - (\sin \delta \cdot \cos \Phi \cdot \cos S \cdot \cos A) \cdot (w_{ss} - w_{sr}) + (\cos \delta \cdot \cos \Phi \cdot \cos S) \cdot (\sin w_{ss} - \sin w_{sr}) + (\cos \delta \cdot \sin \Phi \cdot \sin S \cdot \cos A) \cdot (\sin w_{ss} - \sin w_{sr}) - (\cos \delta \cdot \sin A \cdot \sin S) \cdot (\cos w_{ss} - \cos w_{sr})] \quad (6)$$

where  $S$  is the slope angle and  $A$  is the aspect angle, both calculated following Hunter and Goodchild (1997). The slope ranges from  $0^\circ$  (i.e. horizontal) to  $90^\circ$  (i.e. vertical). The aspect is related to the South, then  $0^\circ$  represents South,  $90^\circ$  East,  $-90^\circ$  West, and  $\pm 180^\circ$  North. To calculate  $w_{sr}$  and  $w_{ss}$  for an inclined surface we applied the method

5. An enhanced T-index model including solar and infrared radiation to evaluate distributed ice melt at the Forni Glacier tongue (Italian Alps)

---

proposed by Allen et al. (2006). Also the auto-shading was estimated following the approach reported by Allen et al. (2006).

iii) To assess whether a grid point is affected by shading (i.e. the orography intercepts the hypothetical line linking this grid point to the Sun), we considered both Sun elevation angle ( $\gamma_{Sun}$ ) and the angle between the mountain peak and the grid point ( $\gamma_{peak-point}$ ):

$$\gamma_{Sun} = \arcsin[\cos(\omega) \cdot \cos(\delta) \cdot \cos(\phi) + \sin(\phi) \cdot \sin(\delta)] \quad (7)$$

and

$$\gamma_{peak-point} = \tanh^{-1} \left( \frac{h_{peak} - h_{point}}{distance\ peak-point} \right) \quad (8)$$

where  $h_{peak}$  and  $h_{point}$  are the mountain peak and grid point elevations, respectively. Then whenever  $\gamma_{Sun} < \gamma_{peak-point}$  the grid point results affected by shading.

iv) To take into account the atmospheric absorption we consider the clearness index ( $K_T$ ) which is the ratio between the global radiation actually received by a surface ( $SW_T$ ), and the exo-atmospheric radiation (i.e. clear sky input without aerosols and zero surface albedo) received by the same surface ( $SW_0$ ) (Gueymard, 2001):

$$K_T = \frac{SW_T}{SW_0} \quad (9)$$

Then

$$SW_T = K_T \cdot SW_0 \quad (10)$$

$K_T$  was calculated for the grid point where the AWS1 Forni is located and the value was considered representative for the whole glacier surface. The incoming solar radiation was measured by a net radiometer (CNR1, Kipp&Zonen) installed at the AWS1 Forni whereas the exo-atmospheric radiation was estimated according to equation 6 as the meteorological station features the same slope of the glacier surface.

5. An enhanced T-index model including solar and infrared radiation to evaluate distributed ice melt at the Forni Glacier tongue (Italian Alps)

---

Four cases were distinguished for the calculation of the incoming solar radiation of any grid point of the glacier ( $SW_{T-point}$ ) depending on whether or not the AWS and the grid point featured shading due to surrounding topography (Hock and Noetzl, 1997):

A) Both AWS and grid point are unshaded:

$$SW_{T-point} = K_T \cdot SW_{0-point} \quad (11)$$

B) Grid point is in the sun and AWS in the shade:

$$SW_{T-point} = K_T^* \cdot SW_{0-point} \quad (12)$$

where  $K_T^*$  is the last value of  $K_T$  measured at the station in sunny conditions.

C) Both AWS and grid point are shaded:

$$SW_{T-point} = SW_{T-AWS} \quad (13)$$

D) Grid point is shaded and AWS is unshaded:

$$SW_{T-point} = 0.15 \cdot SW_{T-AWS} \quad (14)$$

where the 0.15 coefficient was used following Hock and Noetzli (1997). To evaluate the accuracy of the modeled solar data ( $SW_{T-point}$ ), we compared the calculated values against shortwave radiation data measured on the field. In fact, during summer 2011 and 2012 (30<sup>th</sup> June 2011, 4<sup>th</sup> July and 9<sup>th</sup> September 2012) we carried out field surveys at the Forni Glacier tongue by a portable radiometer (CNR1, Kipp&Zonen) collecting a total sample of 18 radiation measurements (Azzoni et al., submitted).

In high-mountain regions the temporal variability of cloudiness is very high, thus influencing  $K_T$  whenever this latter is evaluated with a high time resolution (every 5 minutes or higher). This phenomenon could affect partially our computations, since we derive  $K_T$  from AWS1 Forni data, continuously monitoring radiation at thirty minutes interval, while our portable net radiometer acquired data every 5 minutes in 2011, and every minute in 2012. In order to minimize such discrepancy we calculated  $K_T$  considering, together with the solar average values at the AWS1 Forni, the minimum and the maximum of the recorded data. Then, all the obtained modeled solar values

## 5. An enhanced T-index model including solar and infrared radiation to evaluate distributed ice melt at the Forni Glacier tongue (Italian Alps)

---

(deriving from different  $K_T$ ) were compared against the measured ones, using cumulative radiation data over the same periods. Eventually, to evaluate the net solar flux at each grid point ( $SW_{net-point}$ ) we considered the hourly albedo ( $\alpha_{AWS}$ ), estimated from outgoing/incoming shortwave radiation measured at the AWS1 Forni, and suitable to be applied to the whole glacier tongue:

$$SW_{net-point} = SW_{T-point} \cdot (1 - \alpha_{AWS}) \quad (15)$$

### 2.3. Net infrared radiation

In the available literature concerning estimation of distributed ice melt using energy budget, both the incoming and the outgoing infrared radiation are taken constant in space. Several authors suggest to use of a unique hourly or daily value, over the whole glacier surface (e.g. Hock and Noetzli, 1997). However, incoming energy flux in any given point on the glacier depends upon topographic reflection, and upon spatial cloud-cover variations. To investigate the suitability of a spatially constant value to describe at each time step the infrared radiation over the whole glacier surface, we performed field measurements of incoming long wave radiation (i.e.  $LW_{in}$ ) at different sites spread over the Forni Glacier tongue. The surveys were carried out with a portable radiometer (CNR1, Kipp&Zonen) during 2011 and 2012 ablation seasons. Then we compared these field measurements with the values recorded by the AWS1 Forni, where a net radiometer was installed (CNR1, Kipp&Zonen) (Fig. 3).

5. An enhanced T-index model including solar and infrared radiation to evaluate distributed ice melt at the Forni Glacier tongue (Italian Alps)

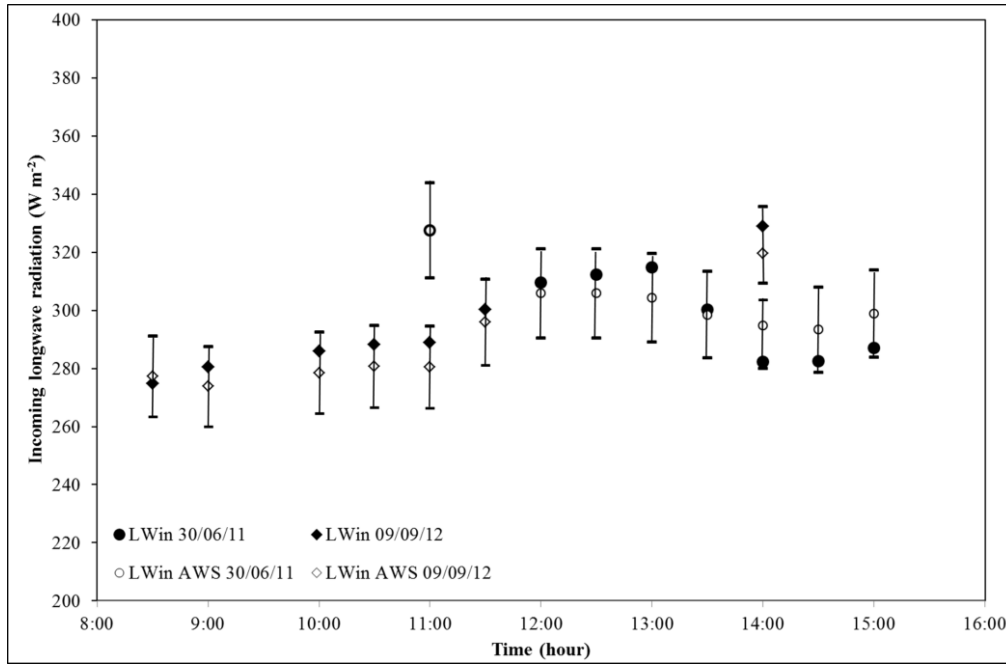


Fig. 3: Comparison of  $LW_{in}$  data acquired at several glacier sites (black series) with  $LW_{in}$  values recorded in the same time frames at the AWSIForni site (white series). On X axis time (hours) is reported, on Y axis  $LW_{in}$  values are indicated ( $Wm^{-2}$ ). The vertical bars show an error range of  $\pm 5\%$  of the measured value (error reported by Kipp&Zonen).

As expected, a fairly regular and synchronous trend is shown both by the spatially distributed, and the AWS longwave measurements. Hence, the assumption of considering quite constant the incoming longwave radiation may be taken as relatively correct (as stated by Hock and Noetzli, 1997). We also considered that mostly supraglacial AWSs are equipped with global solar radiometer, and only in few cases a net radiometer is available, thus limiting the evaluation of the radiative fluxes to the shortwave contribution, and neglecting the longwave one. We then sought for a method to model the incoming longwave flux, applicable also in sites where a net radiometer is not present. The solution we found the most suitable is based upon use of air temperature ( $T_a$ ) and sky emissivity ( $\epsilon$ ) as main input data. The sky emissivity was calculated from cloudiness ( $n$ , assessed from global radiation dataset) and vapor pressure ( $e_a$ , estimated from air temperature and relative humidity values). Hence, in order to model  $LW_{in}$ , a thermo-hygrometer and a global radiometer (both widespread sensors) are necessary. In fact, the incoming infrared component firstly depends upon the cloudiness of the sky. As cloud observations are not available at the Forni Glacier

5. An enhanced T-index model including solar and infrared radiation to evaluate distributed ice melt at the Forni Glacier tongue (Italian Alps)

(and in other sites as well), cloudiness was estimated from the incoming shortwave radiation dataset ( $SW_{AWS}$ ) (Oerlemans, 2000). First, the daily mean global radiation for clear sky was modeled ( $SW_{CS}$ ) by way of a sine-cosine function, adjusted on the measured data and interpolated through the truncated Fourier series at the second order:

$$y = 160.43 - 236.03 \cdot \cos\left(\frac{day \cdot 2\pi}{365}\right) + 27.31 \cdot \sin\left(\frac{day \cdot 2\pi}{365}\right) - 25.14 \cdot \cos\left(2 \frac{day \cdot 2\pi}{365}\right) - 15.11 \cdot \sin\left(2 \frac{day \cdot 2\pi}{365}\right) \quad (16)$$

where  $day$  is the Julian date. To assess the actual clear sky incoming solar radiation without overestimation as due to multiple reflection from snow covered surroundings, we considered the window from May 1<sup>st</sup> to September 30<sup>th</sup> of every year. Then we calculated the daily mean values averaged from 2006 to 2012 (Fig. 4). The 2005 period was excluded by the computation because the AWS1 Forni dataset starts from 1<sup>st</sup> October 2005.

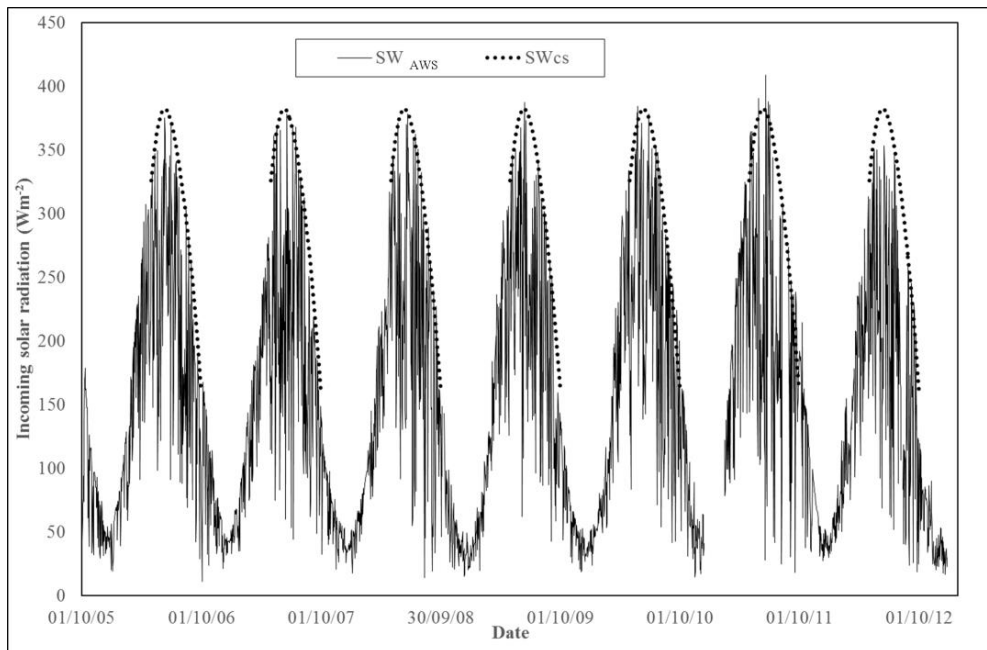


Fig. 4: Clear sky envelope defined for incoming solar radiation (truncated Fourier series at the second factor) and the actual daily mean values from 1<sup>st</sup> October 2005 to 31<sup>st</sup> December 2012.



5. An enhanced T-index model including solar and infrared radiation to evaluate distributed ice melt at the Forni Glacier tongue (Italian Alps)

Then, the atmospheric transmissivity ( $\tau_{cl}$ ) defined by:

$$\tau_{cl} = \frac{SW_{in}^{measured}}{SW_{in}^{clear\ sky}} \quad (17)$$

was found and then the cloudiness ( $n$ ), depending on the altitude, was estimated according to Oerlemans (2001) approach:

$$\tau_{cl} = 1 - (0.41 - 6.5 \cdot 10^{-5} \cdot altitude) n - 0.37 n^2 \quad (18)$$

with altitude is measured in meters a.s.l. Both the atmospheric transmissivity and the cloudiness cannot be higher than 1, then whenever  $\tau_{cl}$  exceeds the unit it was set to 1. The same correction cannot be performed to the values of  $n$  because in eq. 18 if  $n$  is 1  $\tau_{cl}$  is 0.39 (Fig. 5), and modifying  $n$  means altering the sequence of  $\tau_{cl}$  values. To avoid such problem we excluded from our analysis a few values with cloudiness higher than 1.

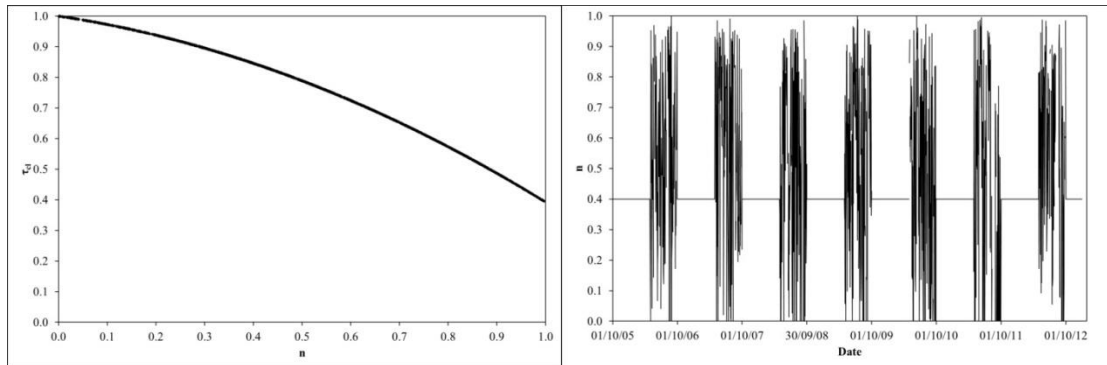


Fig. 5: On the left the relation between the daily mean cloudiness ( $n$ ) and the atmospheric transmissivity ( $\tau_{cl}$ ), used to estimate the cloud amount from the measured incoming shortwave radiation. On the right computed cloudiness ( $n$ ) from the clear sky solar radiation envelope.

Once we estimated cloudiness, we took into account the effect of emissivity for clear ( $\epsilon_{cs}$ ) and overcast ( $\epsilon_{cl}$ ) sky. The latter can be considered constant (0.976 at 2310 m a.s.l.), while the clear-sky emissivity varies according to:

5. An enhanced T-index model including solar and infrared radiation to evaluate distributed ice melt at the Forni Glacier tongue (Italian Alps)

---

$$\varepsilon_{cs} = 0.23 + b \left( \frac{e_a}{T_a} \right)^{1/8} \quad (19)$$

with  $b = 0.475$  (found by Oerlemans, 2001 at 2310 m a.s.l.),  $e_a$  corresponds to the air vapor pressure and  $T_a$  to the air temperature recorded by the AWS1 Forni. Then the total emissivity is:

$$\varepsilon = \varepsilon_{cs}(1 - n^p) + \varepsilon_{cl}n^p \quad (20)$$

with  $p = 2$ . Finally, the incoming longwave radiation was assessed following the Stephan-Boltzmann law:

$$LW_{in} = \varepsilon \cdot \sigma \cdot T_a^4 \quad (21)$$

where  $\sigma$  is  $5.67 \times 10^{-8} \text{ W m}^{-2} \text{ K}^{-4}$ . The method was verified by comparison of the modeled data against the 7-year infrared flux dataset recorded by the AWS1 Forni (from 1<sup>st</sup> October 2005 to 31<sup>st</sup> December 2012). Since a glacier melting surface does not exceed  $0^\circ\text{C}$ , longwave radiation  $LW_{out}$  is generally taken as  $315.6 \text{ W m}^{-2}$  (considering an emissivity  $\varepsilon = 1$ ). However there can be a contribution from the air between the surface and the sensor that could increase the flux from the surface. The net infrared flux  $LW_{net}$  was estimated as:

$$LW_{net} = LW_{in} - LW_{out} \quad (22)$$

## 2.4. Ablation computation

The ice ablation amount ( $M$ , mm per time step) was quantified following different T-index approaches. First, we took into account only air temperature (Braithwaite, 1995):

$$M = \begin{cases} DDF \cdot T_a & T_a > 0^\circ\text{C} \\ 0 & T_a \leq 0^\circ\text{C} \end{cases} \quad (23)$$

5. An enhanced T-index model including solar and infrared radiation to evaluate distributed ice melt at the Forni Glacier tongue (Italian Alps)

where  $DDF$  is the degree days factor ( $\text{mmd}^{-1}\text{°C}^{-1}$ ).  $DDF$  was computed here as the ratio between the measured ablation (mm water equivalent) during a given period, and the sum of the air temperature ( $T_a$ , °C) exceeding a chosen threshold (here, 0°C) in the same period. The analysis was performed here at hourly resolution, so we calculated here a melting factor expressed in  $\text{mm h}^{-1}\text{°C}^{-1}$ .

Then, we considered the solar input, according to Cazorzi and Dalla Fontana (1996):

$$M = \begin{cases} RTMF \cdot (1 - \alpha_{AWS}) \cdot SW_T \cdot T_a & T_a > 0^\circ\text{C} \\ 0 & T_a \leq 0^\circ\text{C} \end{cases} \quad (24)$$

where  $RTMF$  is the Radiative and Temperature melting factor ( $\text{mm h}^{-1}\text{W}^{-1}\text{m}^2\text{°C}^{-1}$ ),  $\alpha$  is the surface albedo,  $SW_T$  is the incoming global radiation ( $\text{W m}^{-2}$ ).

We then adopted the method proposed by Pellicciotti et al. (2005):

$$M = \begin{cases} TMF \cdot T_a + RMF \cdot (1 - \alpha_{AWS}) \cdot SW_T & T_a > 0^\circ\text{C} \\ 0 & T_a \leq 0^\circ\text{C} \end{cases} \quad (25)$$

where  $TMF$  ( $\text{mm h}^{-1}\text{°C}^{-1}$ ) and  $RMF$  ( $\text{mm h}^{-1}\text{W}^{-1}\text{m}^2$ ) are the Temperature and the Radiative melting factors, respectively.  $T_a$  is the air temperature (°C),  $\alpha$  is the surface albedo,  $SW_T$  is the incoming global radiation ( $\text{W m}^{-2}$ ). Once the melting factors were estimated from field ice melt data (collected from 29<sup>th</sup> June to 4<sup>th</sup> August 2011 at the Forni Glacier tongue), they were considered constant in time and space (Hock, 1999).

Given that ablation depends upon the net energy available at the glacier surface, we tested a new approach, by taking into account the net longwave radiation ( $LW_{net}$ ) as well:

$$M = \begin{cases} TMF \cdot T_a + RMF \cdot [(1 - \alpha_{AWS}) \cdot SW_T + LW_{net}] & T_a > 0^\circ\text{C} \\ 0 & T_a \leq 0^\circ\text{C} \end{cases} \quad (26)$$

In Table 1 all the ice melting factors estimated here are shown.

5. An enhanced T-index model including solar and infrared radiation to evaluate distributed ice melt at the Forni Glacier tongue (Italian Alps)

*Tab. 1: All the ice melting factors are shown.*

	DDF (mm d <sup>-1</sup> °C <sup>-1</sup> )	RTMF (m h <sup>-1</sup> W <sup>-1</sup> m <sup>2</sup> °C <sup>-1</sup> )	TMF (mm h <sup>-1</sup> °C <sup>-1</sup> )	RMF (mm h <sup>-1</sup> W <sup>-1</sup> m <sup>2</sup> )
Braithwaite (1995)	6.9 ± 1.1			
Hock (2003)	6.6 – 20.0			
This study	6.9 (d <sup>-1</sup> )			
This study	0.3 (h <sup>-1</sup> )			
Cazorzi and Dalla		0.016 – 0.024		
Fontana (1996) (snow)				
This study (ice)		4.04 x 10 <sup>-7</sup>		
Pellicciotti et al. (2005)			0.05	0.0094
This study			0.024	3.35 x 10 <sup>-6</sup>
This study, also considering $LW_{net}$			0.025	3.34 x 10 <sup>-6</sup>

### 3. Results and discussion

#### 3.1 Incoming solar radiation

Figure 6 shows the distribution of the annual radiation we obtain considering a surface oriented as the Forni Glacier, neglecting the effect of shading and atmospheric absorption (exo-atmospheric surface). The largest value (about 12000 MJ m<sup>-2</sup>) is reached southward with a surface slope of 22.7°, while the smallest one (about 1350 MJ m<sup>-2</sup>) is observed northward with a slope of 62.8°. Auto-shading conditions (estimated according to Allen et al., 2006) occur for slopes higher than 23.3°. Particularly, whenever the slope exceeds 70° auto-shading can occur every day. As expected, the day with the highest solar radiation is the summer solstice (with 41.9 MJ m<sup>-2</sup>, Fig. 6). Generally the northern part of the eastern basin features the most intense solar anywhere in the glacier. Here the slopes are moderate and the main aspect is south and south-west (Fig. 6). As far as the clearness index measured at the AWS1 Forni is concerned, it ranges from 0.1 to 1.3. Taking into account both cloudiness and multi-reflection this is reasonably agrees with the range 0.2-1.2 found by Hock (2005).

5. An enhanced T-index model including solar and infrared radiation to evaluate distributed ice melt at the Forni Glacier tongue (Italian Alps)

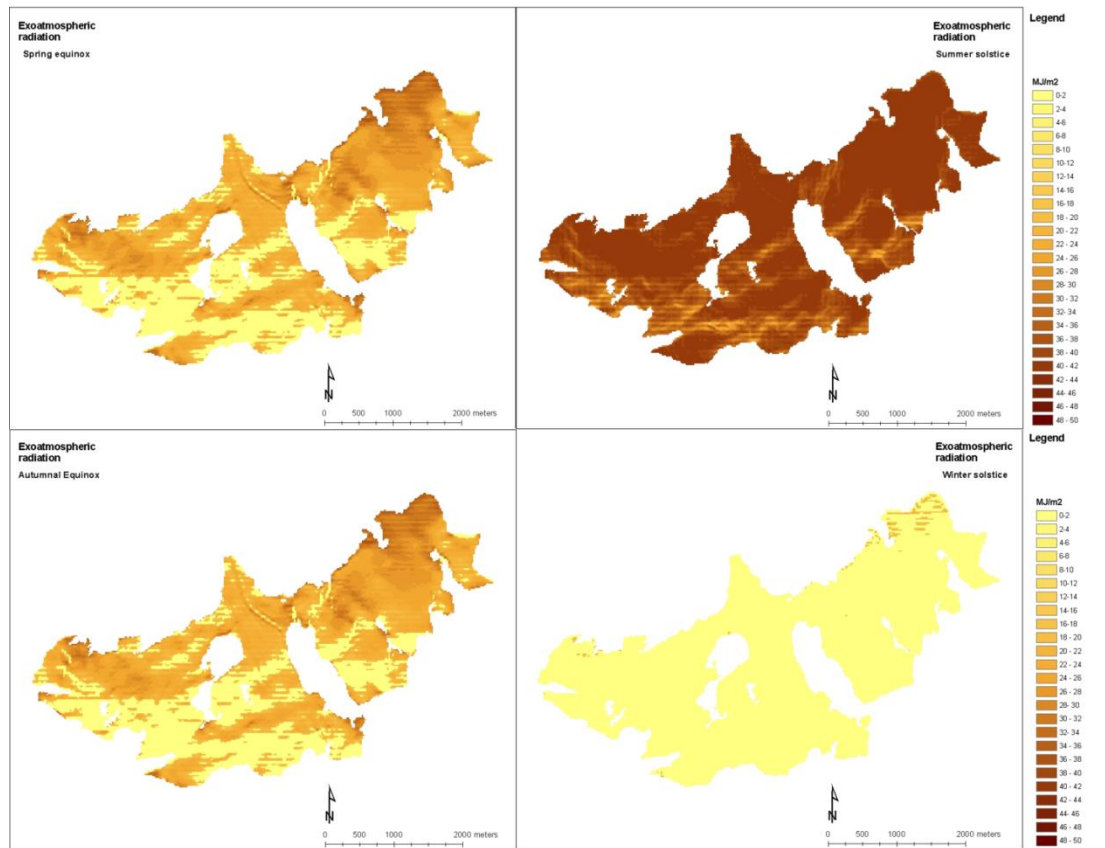


*Fig. 6: Daily radiation for an exo-atmospheric surface oriented as the Forni Glacier during the equinoxes and solstices.*

Validation of our method was performed by comparing the modeled radiation with that measured in 18 sites on the glacier tongue, during summer 2011 and 2012. The model agrees well with observations, with a largest spread of -29.2% to +25.9% against the measured values (mean absolute percentage error 13.4%, Fig. 7).

## 5. An enhanced T-index model including solar and infrared radiation to evaluate distributed ice melt at the Forni Glacier tongue (Italian Alps)

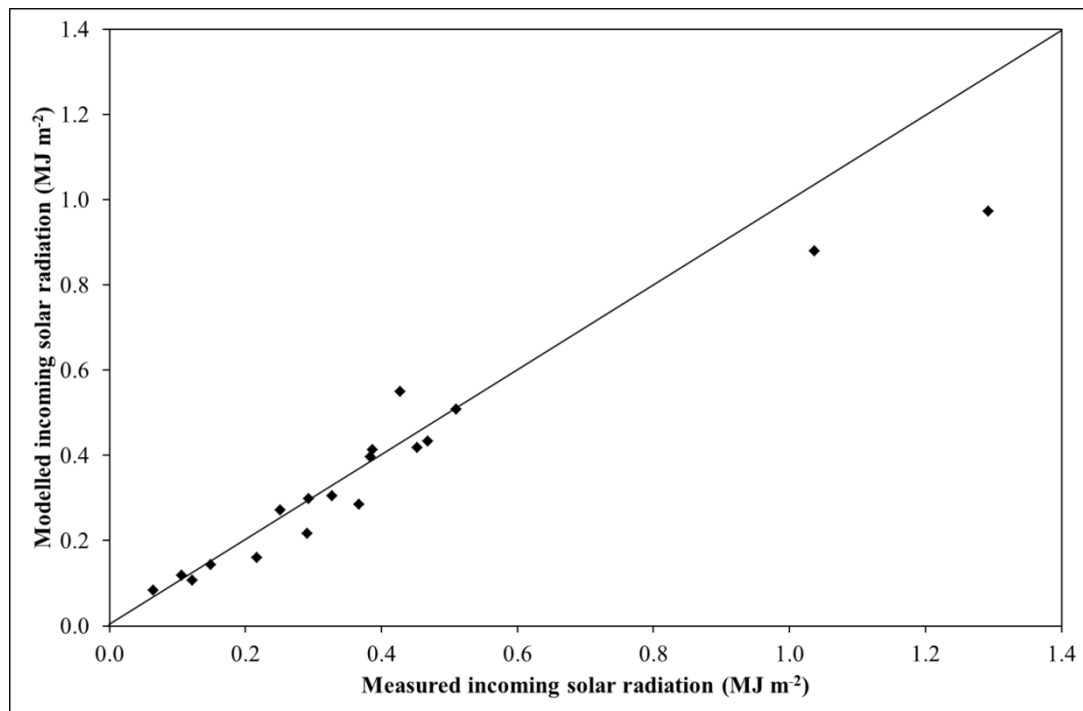


Fig. 7: Measured and modeled incoming solar radiation during summer 2011 and 2012.

### 3.2 Infrared radiation

Given that cloudiness could not be estimated with continuous snow cover on the ground, leading to multi-reflection and potential bias, the infrared model performance was evaluated during May-September for 2006-2012. The average estimated daily incoming radiation was compared against the daily mean values measured at the AWS1 Forni (Fig. 8). A good agreement between the two dataset was found, although there was a significant share of points with incoming infrared radiation underestimated by the model. This can be due by neglecting reflection from the local topography, and by mistakes in cloudiness computation. However, for 14.5% of time underestimation exceeds  $50 \text{ W m}^{-2}$  in absolute value. Because the radiative budget is used to calculate the glacier mass loss, we decided to quantify the error in melting estimates due to underestimation of infrared radiation. If we consider the days featuring an underestimation of  $50 \text{ W m}^{-2}$ , the net longwave radiation results negative whenever the measured cumulated daily net longwave value is lower than  $1 \text{ MJ m}^{-2}$  (i.e. with melt smaller than 3 mm w.e.). Considering the maximum underestimation of  $-90 \text{ W m}^{-2}$  (0.1% of the total period), a cumulated daily net longwave of  $-6 \text{ MJ m}^{-2}$  results instead

5. An enhanced T-index model including solar and infrared radiation to evaluate distributed ice melt at the Forni Glacier tongue (Italian Alps)

in an actual value of  $+1.7 \text{ MJ m}^{-2}$  (or a daily mass loss of about 5 mm w.e.). These results suggest that the effect of underestimation of infrared radiation may be regarded as negligible for the purpose of ice melt assessment.

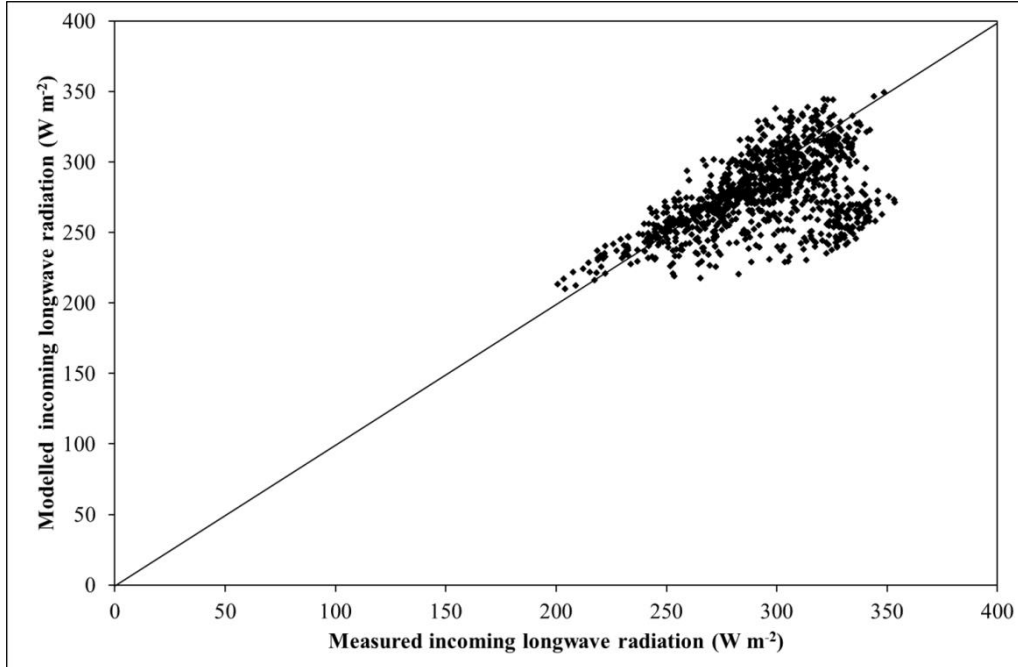


Fig. 8: Modelled and measured daily incoming longwave radiation during May-September time frame from 2005 to 2012.

### 3.3 Ablation computation

In Table 2 the comparison between the measured and modeled cumulated ice ablation values is shown for the different T-index models (equations 23, 24, 25 and 26), from June 29<sup>th</sup> to August 4<sup>th</sup> 2011. The enhanced T-index models using radiation fluxes seem more accurate in describing melt magnitude and rates than the classical degree-day model using solely air temperature. In fact, the degree-day approach shows the highest mean divergence (i.e. 8.91%, in absolute values) from the measured mass loss. Instead, the enhanced T-index method proposed by Pellicciotti et al. (2005) predicts ice melt with a mean difference of 6.84% (absolute). Our enhanced T-index model driven by temperature, solar and infrared radiation has a 6.72% absolute mean error, (see Tab. 3, 10<sup>th</sup> column), thus slightly improving the approach introduced by Pellicciotti et al. (2005). Our model, and the one by Pellicciotti et al. (2005) are most suitable to predict

5. An enhanced T-index model including solar and infrared radiation to evaluate distributed ice melt at the Forni Glacier tongue (Italian Alps)

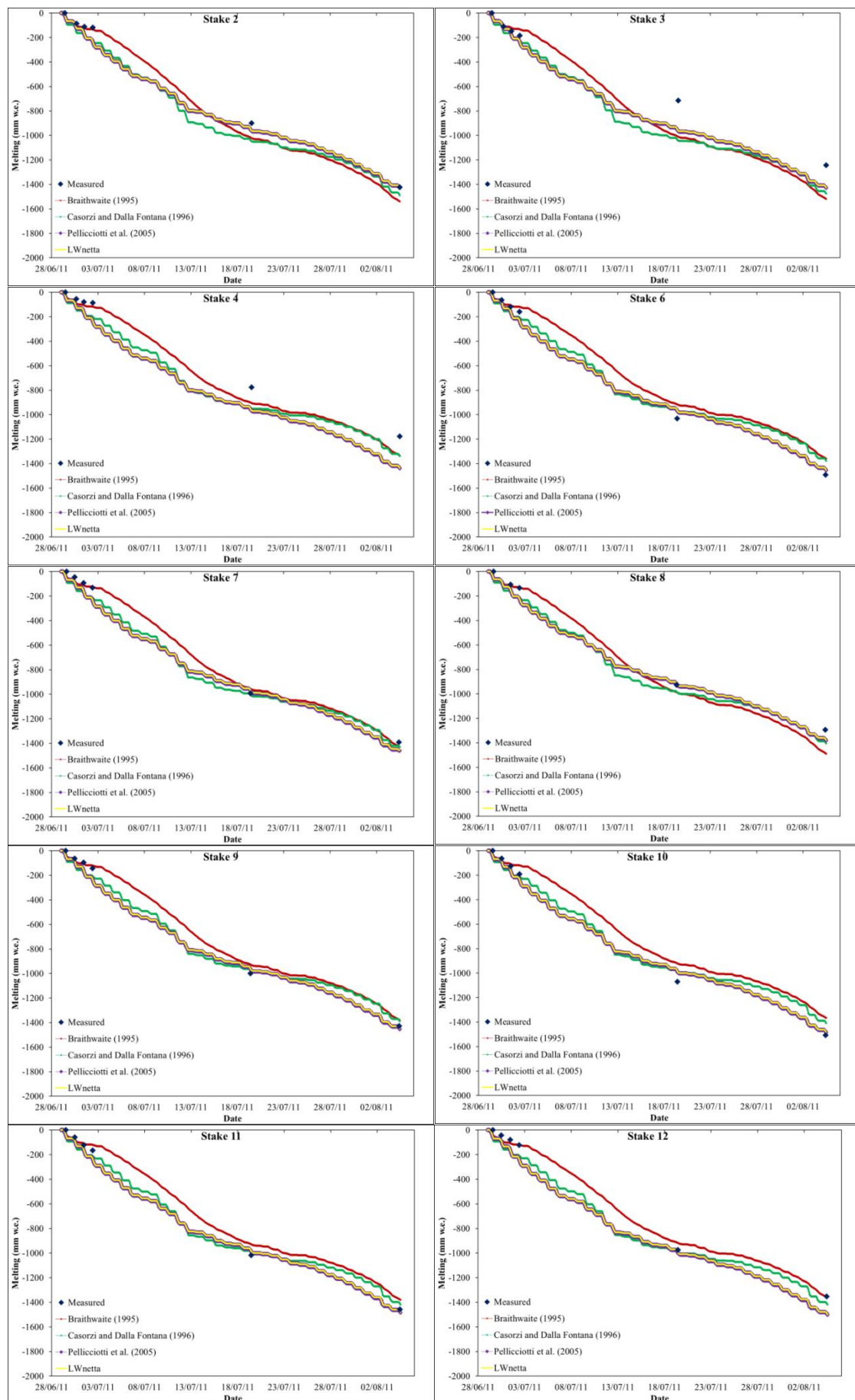
ice melt, and depict well variability over time, thus suggesting that use of radiation indeed improves calculation of ice melt via degree day approach (Fig. 9).

*Tab. 2: The modelled cumulative melt amounts evaluated for each ablation stake site from 29<sup>th</sup> June to 4<sup>th</sup> August 2011 applying different T-index approaches (3<sup>rd</sup>, 5<sup>th</sup>, 7<sup>th</sup> and 9<sup>th</sup> columns) compared to the cumulative measured values (2<sup>nd</sup> column). With  $\Delta M$  are indicated the difference between modelled values and measured data (considering modulus values, 4<sup>th</sup>, 6<sup>th</sup>, 8<sup>th</sup> and 10<sup>th</sup> columns ).*

Stake code	Measured value (mm w.e.)	Modelled following eq. 23 (mm w.e.)	$\Delta M$ (measured-modelled according to eq. 23)	Modelled following eq. 24 (mm w.e.)	$\Delta M$ (measured-modelled according to eq. 24)	Modelled following eq. 25 (mm w.e.)	$\Delta M$ (measured-modelled according to eq. 25)	Modelled according to eq. 26 (mm w.e.)	$\Delta M$ (measured-modelled according to eq. 26)
2	-1424	-1540	+8.18%	-1489	+4.59%	-1432	+0.57%	-1429	+0.37%
3	-1245	-1521	+22.16%	-1477	+18.68%	-1432	+15.00%	-1429	+14.77%
4	-1178	-1335	+13.26%	-1339	+13.68%	-1441	+22.27%	-1438	+22.07%
6	-1492	-1360	-8.85%	-1377	-7.70%	-1457	-2.38%	-1454	-2.55%
7	-1392	-1431	+2.87%	-1429	+2.66%	-1459	+4.88%	-1457	+4.69%
8	-1293	-1489	+15.17%	-1406	+8.72%	-1382	+6.88%	-1379	+6.68%
9	-1428	-1382	-3.26%	-1390	-2.65%	-1455	+1.86%	-1452	+1.68%
10	-1508	-1367	-9.35%	-1409	-6.58%	-1487	-1.42%	-1484	-1.60%
11	-1458	-1382	-5.24%	-1420	-2.61%	-1486	+1.94%	-1484	+1.76%
12	-1353	-1363	+0.75%	-1420	+5.00%	-1505	+11.25%	-1502	+11.05%
<b>AVE</b>			<b>8.91%</b>		<b>7.29%</b>		<b>6.84%</b>		<b>6.72%</b>



## 5. An enhanced T-index model including solar and infrared radiation to evaluate distributed ice melt at the Forni Glacier tongue (Italian Alps)



## 5. An enhanced T-index model including solar and infrared radiation to evaluate distributed ice melt at the Forni Glacier tongue (Italian Alps)

---

*Fig. 9: Melt values modelled by applying the different T-index approaches (equations from 23 to 26) at different sites on the Forni Glacier tongue compared to measured ablation values (from ablation stakes surveyed at the glacier surface from 29<sup>th</sup> June to 4<sup>th</sup> August 2011).*

## 4. Conclusions

In the present study we applied melt models of different complexity to predict ice melting upon the Forni Glacier (Italy). Further, we attempted to improve ice melt prediction by including the net longwave radiation as an input. To apply these algorithms, we distributed the solar and infrared fluxes and the air temperature to the whole glacier surface. The solar radiation distribution was benchmarked against radiation data measured during field campaigns in summer 2011 and 2012. The two datasets are in agreement within -29.2% to +25.9%, with a mean absolute percentage error of 13.4%, thus suggesting to consider suitable the proposed radiation model. A good agreement was further found between the measured (by the AWS1 Forni) and modeled infrared values from 2006 to 2012. In fact, only 14.5% of the samples had underestimation larger than  $50 \text{ W m}^{-2}$ , and the underestimation is always within  $90 \text{ W m}^{-2}$ , which translates in a maximum underestimated daily mass loss of 6 mm w.e. Hence, the infrared model can be considered appropriate and the obtained underestimation possibly negligible. Finally, ice ablation was modeled applying 4 different methods (equations from 23 to 26) during June-August 2011. The radiative approaches here are more suitable than the classical T-index model (Braithwaite, 1995), which features the highest mean divergence (i.e. 8.91%) from the measured mass loss. Our enhanced T-index model, which is driven by temperature, solar and infrared radiation, quantifies with some more accuracy ice melt (6.72% of mean disagreement, see Tab. 3, column 10), slightly improving the approach introduced by Pellicciotti et al. (2005). In summary, our model and the one by Pellicciotti et al. (2005) are the most suitable to predict ice melt and describe ablation variability over time upon the Forni glacier. Thus, it is suggested that upon the Forni Glacier radiation flux may explain part of ice melt variability, and thus one needs to consider all the radiative components to improve the degree-day approach for ice melt assessment (Fig. 9). Eventually, the present study provided some information concerning errors in modeling solar and

5. An enhanced T-index model including solar and infrared radiation to evaluate distributed ice melt at the Forni Glacier tongue (Italian Alps)

---

infrared radiation, useful for quantifying glacier melt rate, and our melt approach displayed that use of both the radiative components may provide some gain in accuracy when estimating ice melting.

## References

- Allen R.G., Trezza R. and Tasumi M. (2006): Analytical integrated functions for daily solar radiation on slopes. *Agricultural and Forest Meteorology*, 139, 55-73.
- Arnold N.S., Willis I.C., Sharp M.J., Richards K.S. and Lawson W.J. (1996): A distributed surface energy-balance model for a small valley glacier. I. Development and testing for Haut Glacier d'Arolla, Valais, Switzerland. *Journal of Glaciology*, 42, 77-89.
- ARPA Lombardia: <http://www2.arpalombardia.it/siti/arpalombardia/meteo/richiesta-dati-misurati/Pagine/RichiestaDatiMisurati.aspx>
- Azzoni R.S., Senese A., Zerboni A., Maugeri M., Smiraglia C. and Diolaiuti G. (submitted): A pilot study to evaluate sparse supraglacial debris and dust and their influence on ice albedo of Alpine glaciers: the case study of the Forni Glacier (Italy).
- Blöschl G., Kirnbauer B. and Gutknecht D. (1991): Distributed snowmelt simulations in an Alpine catchment. 1. Model evaluation on the basis of snow cover patterns. *Water Resources Research*, 27, 3171-79.
- Braithwaite R.J. (1995): Positive degree-day factors for ablation on the Greenland ice sheet studied by energy-balance modelling. *Journal of Glaciology*, 41, 153-60.
- Brun E., Martin E., Simon V., Gendre C. and Coleou C. (1989): An energy and mass model of snow cover suitable for operational avalanche forecasting. *Journal of Glaciology*, 35, 333-342.
- Cazorzi F. and Della Fontana G.D. (1996): Snowmelt modeling by combining air temperature and a distributed radiation index. *Journal of Hydrology*, 181, 169-87.
- Citterio M., Diolaiuti G., Smiraglia C., Verza G. and Meraldi E. (2007): Initial results from the automatic weather station (AWS) on the ablation tongue of Forni Glacier (Upper Valtellina, Italy). *Geografia Fisica e Dinamica Quaternaria*, 30, 141-151.
- Duffie J.A., Beckman W.A. (1980): *Solar Engineering of Thermal Process*, 1st ed. John Wiley and Sons, NY.
- Ellingston R.G., Ellis J. and Fels S. (1991): The intercomparison of radiation codes used in climate models: long-wave results. *Journal of Geophysical Research*, 96, 8929-8953.
- Garner B.J. and Ohmura A., (1968): A method for calculating direct shortwave radiation income of slopes. *J. Appl. Meteorol.*, 7, 796-800.

5. An enhanced T-index model including solar and infrared radiation to evaluate distributed ice melt at the Forni Glacier tongue (Italian Alps)

---

- Gueymard C. (1993): Critical analysis and performance assessment of clear-sky solar-irradiance models using theoretical and measured data. *Solar Energy*, 51(2), 121-38.
- Gueymard C.A. (2001): Parameterized transmittance model for direct beam and circumsolar spectral irradiance. *Solar Energy*, 71 (5), 325-346.
- Hock R. (2003): Temperature index melt modelling in mountain areas. *Journal of Hydrology*, 282 (1-4), 104-15.
- Hock R. (2005): Glacier melt: a review of processes and their modelling, *Progress in Physical Geography*, 29, 362.
- Hock R. and Noetzli C. (1997): Areal melt and discharge modeling of Störglaciären, Sweden. *Annals of glaciology*, 24, 997.
- Hock R. and Tilm-Reijmer C. (2011): A mass-balance, glacier runoff and multi-layer snow model. Program documentation and users manual.
- Hunter G.J. and Goodchild M.F. (1997): Modeling the uncertainty of slope and aspect estimates derived from spatial databases. *Geographical Analysis*, 29 (1), 35-49.
- Iqbal M. (1983): An introduction to solar radiation. Academic Press, Orlando, FL., OSTI ID: 5596615.
- Klok E.J. and Oerlemans J. (2002): Model study of the spatial distribution of the energy and mass balance of Morteratschgletscher, Switzerland. *Journal of Glaciology*, 48, 505-18.
- Kondratyev K.Y. (1969): Radiation in the atmosphere. New York: Academic Press, 912 pp.
- Oerlemans J. (2000): Analysis of a 3 years meteorological record from the ablation zone of Morteratschgletscher, Switzerland: energy and mass balance. *Journal of Glaciology*, 46 (155).
- Oerlemans J. (2001): *Glaciers and Climate Change*, Lisse, Balkema.
- Oke T.R. (1987): *Boundary layer climates*. Second edition. London, Methuen, New York, Routledge Press. 435 pp.
- Pellicciotti F., Brock B., Strasser U., Burlando P., Funk M. and Corripio J. (2005): An enhanced temperature-index glacier melt model including the shortwave radiation balance: development and testing for Haut Glacier d'Arolla, Switzerland. *Journal of Glaciology*, 51 (175), 573-587.
- Plüss C. and Ohmura A. (1997): Longwave radiation on snow-covered mountain surfaces. *Journal of applied meteorology*, 36, 818-824.

5. An enhanced T-index model including solar and infrared radiation to evaluate distributed ice melt at the Forni Glacier tongue (Italian Alps)

---

- Senese A., Diolaiuti G., Mihalcea C. and Smiraglia C. (2012a): Energy and mass balance of Forni Glacier (Stelvio National Park, Italian Alps) from a 4-year meteorological data record. *Arctic, Antarctic, and Alpine Research*, 44 (1), 122-134.
- Senese A, Diolaiuti G, Verza GP and Smiraglia C (2012b): Surface energy budget and melt amount for the years 2009 and 2010 at the Forni Glacier (Italian Alps, Lombardy). *Geografia Fisica e Dinamica Quaternaria*, 35 (1), 69-77.
- Spencer J.W. (1971): Fourier series representation of the position of the sun. *Search*, 2, 172 pp.
- Wang Q., Tenhunen J., Schmidt M., Kolcun O. and Driesler M. (2006): A model to estimate global radiation in complex terrain. *Boundary-Layer Meteorology*, 119, 409-429.

# Chapter 6

## **A pilot study to evaluate sparse supraglacial debris and dust and their influence on ice albedo of Alpine glaciers: the case study of the Forni Glacier (Italy)**

### **Abstract**

We propose a method to investigate the characteristics of sparse and fine debris coverage at the glacier melting surface and its relation to ice albedo. In spite of the abundant literature dealing with dust and black carbon deposition on glacier accumulation areas, few studies that describe the distribution and properties of fine and discontinuous debris and black carbon at the melting surface of glaciers are available. Furthermore, guidelines are needed to standardize field samplings and lab analyses thus permitting comparisons among different glaciers. We developed a protocol to i) sample fine and sparse supraglacial debris and dust, ii) quantify its surface coverage, iii) describe its composition and sedimentological properties, iv) measure ice albedo, and v) identify the relationship between albedo and debris coverage. The procedure was tested at the surface of the Forni Glacier (northern Italy), in summer 2011, 2012 and 2013. Fine debris and dust present marked variability along the glacier tongue and from the beginning to the end of summer, influencing ice albedo pattern and changes. The rainfalls effects on albedo variability are also quantified. Debris and dust analysis indicates generally a local origin (from nesting rockwalls) and the organic content results locally high. Nevertheless the finding of some cenospheres suggests an anthropic contribution to the superficial dust as well.



## 1. Introduction

In recent years, evidence for significant tongue darkening on retreating glaciers have been drawing increasing attention (e.g., Oerlemans et al., 2009; Paul and Kääb, 2005; Paul et al., 2007; Painter et al., 2013). This peculiar surface phenomenon in glaciers in part depends on the exposure of ice surfaces to layers of dust and coarser rock debris (Flanner et al., 2009; Mihalcea et al., 2006; Nakawo and Young, 1982). The consequent effect is a remarkably decreasing of albedo, due to the presence of light absorbing particles (Aoki et al., 2006; Wiscombe and Warren, 1980, 1985) and then an increasing of ice melt magnitude and rate (Nakawo and Rana, 1999).

Supraglacial debris consists of mineral and organic fractions; the latter can consist of black carbon (e.g.: deriving from fossil combustion and fires), organic remains in aerosols and organic particles originating from bacterial decomposition of organic matter (Fujita, 2007; Takeuchi et al., 2001; Takeuchi, 2002), while the mineral fraction may be autochthonous (i.e.: derived from the weathering of rock outcrops and nunataks) or allochthonous. For instance, the deposition of Saharan dust (Sodermann et al., 2006) or volcanic ash (Conway et al., 1996) on glaciers is a well-known phenomenon. Moreover, mineral particles and black carbon can be transported by atmospheric fluxes (Ming et al., 2009; Ramanathan, 2007); a main source for mineral dust is also represented by lateral moraines and debris slopes: in fact, during the summer when warm climatic conditions occur, the dry and unconsolidated materials constituting moraines are easily taken up by wind gusts and deposited tens to hundreds of meters away (Oerlemans et al., 2009).

Some authors have investigated dust deposition on snowpack (e.g.: Qian et al., 2011; Yasunari et al., 2010). A possible snow albedo reduction due to black carbon contamination was revealed by radiation measurements at the snow surface performed at Barrow, Alaska, (Aoki et al., 1998) and in Japanese urban areas (Motoyoshi et al., 2005). In the case of snow and firn a field procedure was developed, followed by further standardized lab-analyses to quantify and describe black carbon presence and features (Yasunari et al., 2010). However, systematic studies to measure the influence of fine sparse debris coverage on glacier ice albedo values are not yet available. For this reason, in this work we discuss a methodology to systematically describe fine supraglacial debris and dust and their influence on ice albedo based on field samplings and lab analyses. We also focus our attention on the development of fine supraglacial debris,

## 6. A pilot study to evaluate sparse supraglacial debris and dust and their influence on ice albedo of Alpine glaciers: the case study of the Forni Glacier (Italy)

---

trying to estimate the evolution of the sedimentological properties and the debris coverage rate during the melting season. Furthermore, we assess the influence of rainfall event on the changes of fine supraglacial debris and consequently on ice albedo.

## 2. Study area

Our experiments were carried out on the ablation tongue of the Forni Glacier (Fig. 1), the widest Italian valley glacier featuring a surface area of 11.36 km<sup>2</sup> (2007 data, Garavaglia et al., 2012). It is located in the Ortles-Cevedale Group, Stelvio National Park, Lombardy Alps. It is widely debris-free, even if darkening phenomena are ongoing (D'Agata et al., 2013) and some authors have recently pointed out that fine and sparse debris is becoming abundant due to the ongoing glacier retreat and thinning phase (Diolaiuti and Smiraglia, 2010, Diolaiuti et al., 2012; Senese et al., 2012a). For this reason, the Forni Glacier can be considered a good laboratory to evaluate fine and sparse debris distribution and seasonal evolution and its influence on ice albedo. The Forni Glacier has a northward down-sloping surface; it is about 3 km long and its altitude ranges from 2600 m to about 3670 m a.s.l. Metamorphic rocks, mostly micaschist rich in quartz, muscovite, chlorite and sericite, constitute the dominant lithology (Montrasio et al., 2008); these rocks emerge from the glacier surface as nunataks (mainly in the accumulation basins) and as rock outcrops (surrounding the glacier tongue). These latter are increasing in size and becoming very frequent due to the ongoing glacier retreat and thinning phase (Diolaiuti and Smiraglia, 2010; Diolaiuti et al., 2012).

Studies on short term changes of the Forni Glacier have been performed through an Automatic Weather Station (named AWS1 Forni) running from 2005 at the glacier melting surface. The AWS1 Forni is already included in the international meteorological network SHARE (Stations at High Altitude for Research on the Environment) managed by EvK2CNR and in the CEOP network (Coordinated Energy and Water Cycle Observation Project), promoted by WCRP (World Climate Research Programme) within the framework of the GEWEX project (Global Energy and Water Cycle Experiment). The AWS1 Forni is located on the ablation tongue (c. 2631 m a.s.l.), about 800 m from the glacier terminus, and it is equipped with sensors for measuring air temperature and humidity, wind speed and direction, atmospheric pressure, liquid precipitation and snow depth, and longwave and shortwave radiations,

## 6. A pilot study to evaluate sparse supraglacial debris and dust and their influence on ice albedo of Alpine glaciers: the case study of the Forni Glacier (Italy)

both incoming and outgoing (Citterio et al., 2007; Diolaiuti et al., 2009; Senese et al., 2010, 2012a, 2012b).

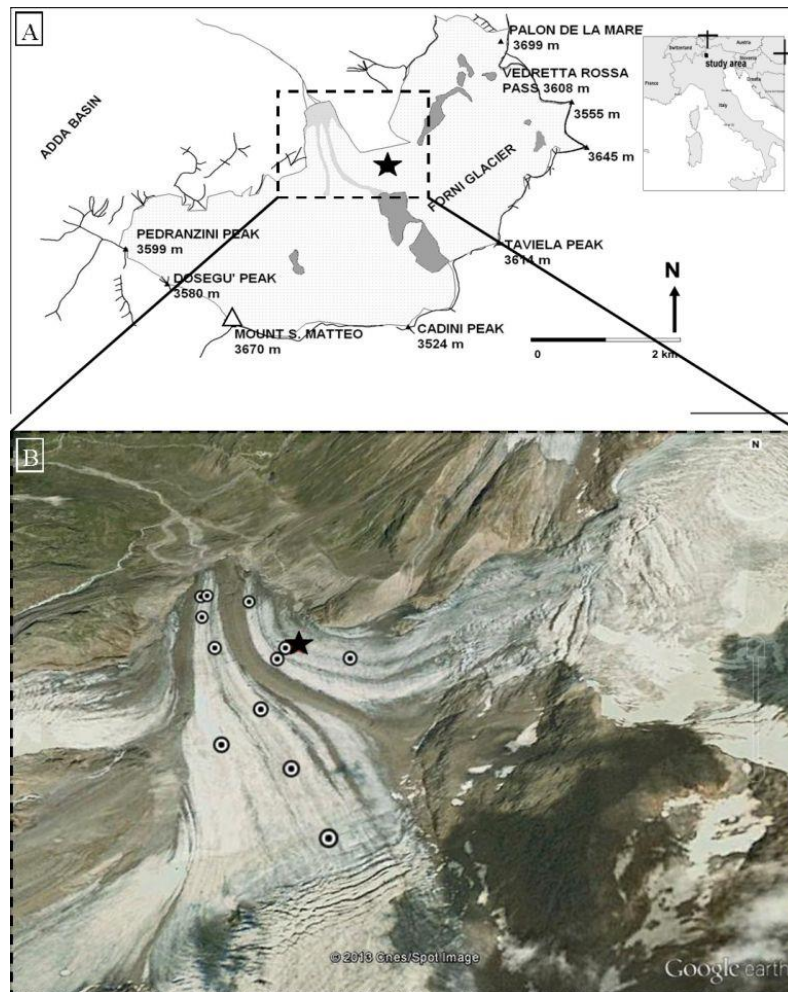


Fig. 1: (A) The position of Forni Glacier in the Italian Alps and of AWSI Forni (black star, in both panels). (B) Enlarged view of the Forni Glacier (image credit: GoogleEarthTM) showing the location of field measurements (black dots).

### 3. Methods

In the time frame 2011-2013 we performed totally 51 field measurements on the debris-free ablation tongue of the Forni Glacier (Fig. 1): both debris quantification (i.e.: spatial distribution) and albedo measures (Fig. 2). Moreover, we sampled the supraglacial debris/dust to assess the debris coverage rate ( $C_r$  from here) and features (totally 13 surveys). The sites for field measurements were chosen considering: i) the homogeneity in debris cover, ii) the presence or absence of fine sparse debris, iii) diverse debris grain

## 6. A pilot study to evaluate sparse supraglacial debris and dust and their influence on ice albedo of Alpine glaciers: the case study of the Forni Glacier (Italy)

size, and iv) different distances from rock slopes and medial moraines, which are the main debris suppliers. The selected sites are representative of the range of surfaces comprising the glacier melting area. Each sampling point belongs to areas featuring similar characteristics, where we selected a parcel of area 1 m x 1 m for debris quantification. The medial moraines were excluded from this work because we focused on fine and sparse debris covered ice and not on actual buried one. Figure 1 shows the study area and the positions of the sites we analysed.

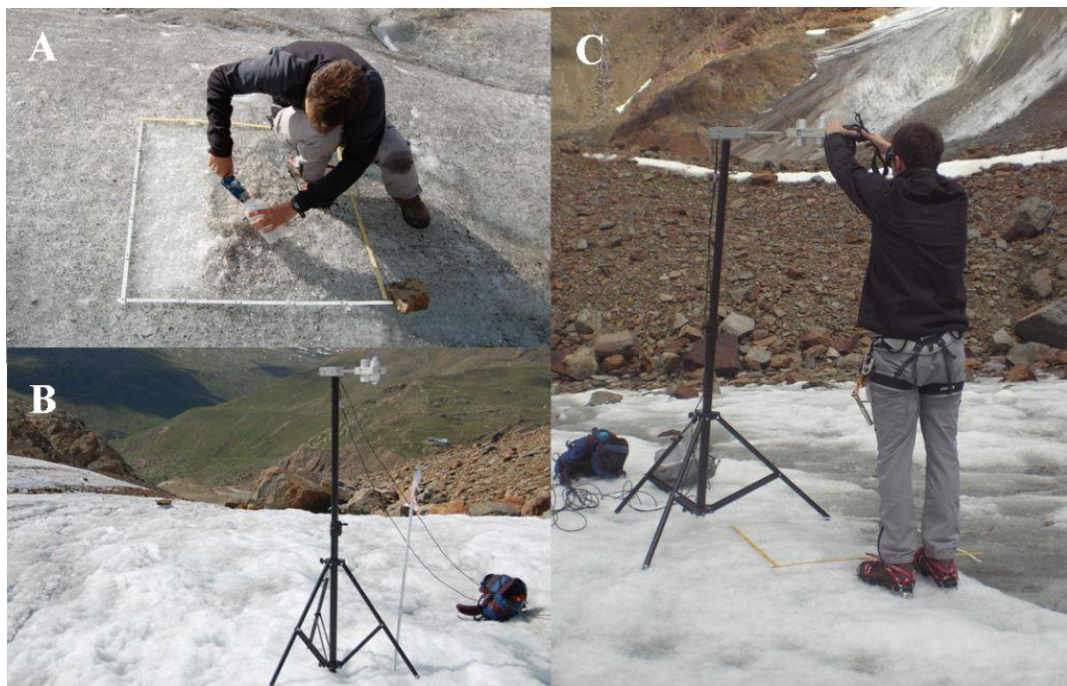


*Fig. 2: Series of pictures illustrating: a) sampling supraglacial debris, b) measuring albedo and c) photographing the parcel of area 1 m x 1 m.*

### 3.1 Debris cover quantification

The quantification of supraglacial sparse and fine debris and dust was performed acquiring high resolution digital images at each analysed site (Fig. 2c) and processing them with image analysis software *ImageJ* following Irvine-Fynn et al. (2010) (Fig. 3). Digital RGB (red-green-blue, in colour composite) photographs of the 1m x 1m parcel were taken using a digital camera (Nikon D40, 6.1 megapixel). From a total of 445 images, we selected one for each measurement site (totally 51): those affected by shadows, deformations, photographic imperfections (e.g. poor exposure, incorrect

## 6. A pilot study to evaluate sparse supraglacial debris and dust and their influence on ice albedo of Alpine glaciers: the case study of the Forni Glacier (Italy)

---

focus) were excluded from the analysis and only images showing clear differences between bare ice and dust/fine debris-covered ice were considered.

The selected images were firstly cropped delimiting the 1 m x 1 m parcel (Fig. 3a). Second, we converted them to 8 bit greyscale in order to highlight the contrast between glacier ice and debris/dust. Third, as a darker grey pixel denotes the presence of debris or shadow (this latter due to surface roughness), we assumed that debris granules could be isolated by thresholding for those pixels with brightness values which fall below a specified GrayScale Threshold level ( $T_{GS}$  from here, Figure 3b).  $T_{GS}$  was specified by a supervised classification in which the threshold was iteratively adjusted until the isolated image pixels best coincide with the debris/dust (Figure 3c). An 8 bit image is composed of 256 grey tones ranging from 0 (black) to 255 (white) and ice surfaces can be isolated by selecting the pixels with brightness values higher than a specified  $T_{GS}$ ; for instance, if the  $T_{GS}$  value is fixed at 100, pixels with a grey tones from 0 to 100 represent debris and pixels with a grey tone from 101 to 255 represent ice. For each image the pixels with a value lower than  $T_{GS}$  were turned into black colour and the other ones into white colour (Figure 3d). Finally the ratio of the surface covered by debris ( $d$  from here) was obtained as:

$$d = \frac{\text{number of black pixels}}{\text{total number of pixels}} \quad (1)$$

In order to investigate the robustness of the method we applied to quantify the ratio of glacier surface covered by debris ( $d$ ) and in particular its sensitivity to changes in the threshold, we performed some tests: i) we varied the chosen  $T_{GS}$  up to  $\pm 10\%$  of its initial value ( $T_{GS+10\%}$  and  $T_{GS-10\%}$ , respectively), and ii) we averaged all the chosen  $T_{GS}$  thus obtaining a unique value ( $T_{GS-AVE}$ ). All these thresholds ( $T_{GS+10\%}$ ,  $T_{GS-10\%}$  and  $T_{GS-AVE}$ ) were applied to each image for re-calculating the ratio of surface covered by debris (i.e.  $d_{+10\%}$ ,  $d_{-10\%}$  and  $d_{AVE}$ , respectively) and the results were compared to the ones derived from the chosen  $T_{GS}$  data.



6. A pilot study to evaluate sparse supraglacial debris and dust and their influence on ice albedo of Alpine glaciers: the case study of the Forni Glacier (Italy)

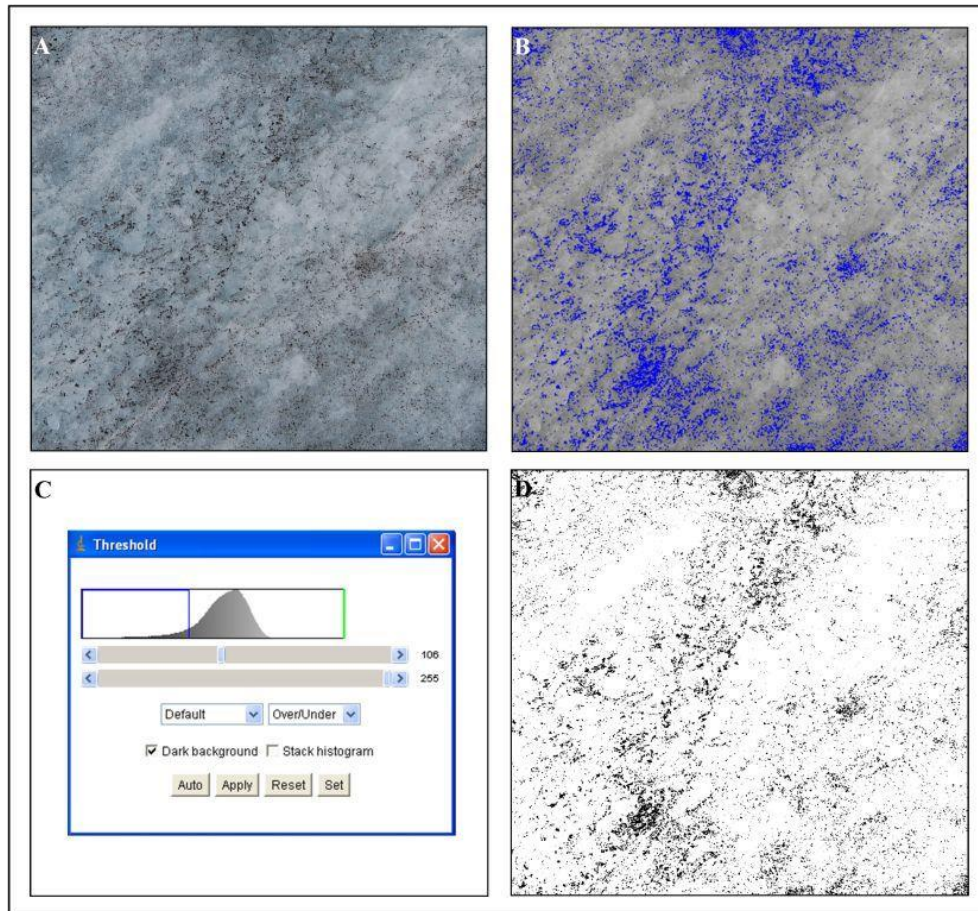


Fig. 3: Example of the procedure followed in image analysis: (a) original cut frame; (b) 8-bit conversion and discrimination between the debris-covered (in blue) and debris-free ice surface; (c) definition of the threshold; (d) calculated debris covered ratio.

### 3.2 Albedo

The albedo ( $\alpha$ ) is defined as the broadband hemispherically averaged reflectance in approximately the spectral range 0.3-2.8  $\mu\text{m}$  (Brock et al., 2000) and depends on solar elevation, cloudiness, presence of liquid water, crystal structure, ice surface conditions and the presence or absence of coverage (rock debris, dust, organic matter, etc.). This parameter can range from 0 (all the  $SW_{in}$  is absorbed by the surface) to 1 (all the  $SW_{in}$  is reflected). It is estimated as the ratio of measured outgoing shortwave to measured incoming shortwave:

$$\alpha = \frac{SW_{out}}{SW_{in}} \quad (2)$$

## 6. A pilot study to evaluate sparse supraglacial debris and dust and their influence on ice albedo of Alpine glaciers: the case study of the Forni Glacier (Italy)

---

For this study the albedo was calculated from radiation data measured using a couple of pyranometers (the ones installed in the net radiometer CNR1, Kipp&Zonen; see Figure 2). The sensor features an accuracy of  $\pm 5\%$  of the measured value. It was equipped with a waterproof box containing a data logger, a 5 Ah battery and a 10 W solar panel on the lateral face. Moreover, a tripod was used to raise the net radiometer for short periods (c. 20-30 min for each measurement) above the ice surface. Tests regarding the influence of the height of the sensor above the surface on albedo values were performed, installing the sensor at various distances from the surface, but no relevant differences in albedo resulted, proper due to the homogeneity of the chosen sites.

The CNR1 net radiometer was chosen for its accuracy and resolution in measuring radiation data, and it is also the same type as the one running at the AWS1 Forni (Citterio et al., 2007; Senese et al., 2012a) thus assuring the comparability among the two datasets. Then the radiation data collected using the portable instrument were crosschecked and analysed against the data acquired by the AWS1 Forni. The radiation measurements were carried out following the guidelines of the World Meteorological Organization (WMO, 2008).

The radiation data were acquired every second, and every minute the minimum, average, maximum and standard deviation values were recorded. Albedo measurements were taken in the central hours of the clear-sky day (i.e. from 11 am to 3 pm, when the solar incidence angles are smaller), thus ensuring the albedo calculations were more accurate and reliable (Brock et al., 2000; Brock, 2004; Oerlemans, 2010). The mean geographic coordinates (WGS84 datum) for each measurement site were recorded by a GPS receiver and the characteristic features of the local ice surface were also noted. Total 51 measurements were carried out from the beginning of the ice ablation period (when snow coverage at the melting tongue disappeared, exposing ice to solar radiation and dust/debris deposition) to the end of the ice melting season (before the occurrence of the first snow fall event covering the glacier ice and preventing dust/debris deposition): 30<sup>th</sup> June and 25<sup>th</sup> August 2011, 4<sup>th</sup> July, 7<sup>th</sup> August and 9<sup>th</sup> September 2012, and 31<sup>st</sup> July and 6<sup>th</sup> September 2013.

Moreover we also analysed the effect of liquid precipitation on glacier albedo variability. In fact the liquid precipitation washes out the finer sediment above glacier ice surface (Oerlemans, 2009) thus changing ice albedo. This water effect was quantified from liquid precipitation temporal length (i.e. number of rainy days) and amount (i.e. mm of rain) and from albedo data measured during 2011-2013 ablation

## 6. A pilot study to evaluate sparse supraglacial debris and dust and their influence on ice albedo of Alpine glaciers: the case study of the Forni Glacier (Italy)

---

seasons by a rain gauge and the net radiometer installed at the AWS1 Forni. We considered an actual rainfall any event occurred whenever the hourly air temperature was over 1.5°C (Senese et al., 2012a) and featuring a hourly liquid precipitation higher than 0.2 mm.

### 3.3 Sedimentological analyses and debris coverage rate evaluation

Several bulk samples of supraglacial sediment were collected from the glacier surface (Fig. 2a) and divided into sub-samples for physical and chemical analyses.

Firstly in 2011 the samples (totally 8) allowed to better characterize the spatial variability of supraglacial debris propriety. Then in 2012 (4<sup>th</sup> July, 7<sup>th</sup> August and 9<sup>th</sup> September) we focused our attention on the temporal evolution of debris features by sampling three sites (identified by ablation stakes) with different conditions of supraglacial debris cover: i) samples 9a, 9b and 9c fine and sparse sediment, ii) samples 10a, 10b and 10c widespread debris cover, and iii) samples 11a, 11b and 11c coarse debris. Finally, in 2012 and 2013 we assessed the debris coverage rate ( $C_r$ ). In the last year the samples were collected 4 times (samples 12a, 12b, 12c, 12d): 11<sup>th</sup> and 31<sup>th</sup> July, 6<sup>th</sup> September and 4<sup>th</sup> October.

Sampling was carried out by scraping the glacier surface with a cleaned chisel, completely removing the surface layer (from 2 to 5 cm deep); the collected material was preserved in appropriate holders. A cold chain (ice boxes) was used to preserve sediment samples at cold temperature conditions (lower than +4°C) during transport to the laboratory, where further analyses were carried out.

For evaluating the debris coverage rate ( $C_r$ ), debris samples were periodically collected from the same sites. First it was necessary to clean the parcel of 1 m x 1 m of area completely removing surface debris (i.e.: scraping at least 2 cm of surface ice). Second, about one month later the sampling of the surface sediments was repeated on the same glacier parcel which was marked on the field to be retrieved. Then in the lab debris samples were dried and weighted. The ratio between the weight of the debris deposited at the ice surface (in grams) and the time frame occurred (days) permitted to evaluate the debris coverage rate ( $C_r$  in g/day):



## 6. A pilot study to evaluate sparse supraglacial debris and dust and their influence on ice albedo of Alpine glaciers: the case study of the Forni Glacier (Italy)

---

$$C_r = \frac{\text{sample weight}}{\text{time frame}} \quad (3)$$

The samples collected in 2011 and 2012 for the spatial and temporal variability were subject to the analytical procedures summarized as follows. Grain-size analyses (Gale and Hoare, 1991) were performed after removing organics using hydrogen peroxide (130 vol) treatment; sediments were wet sieved (diameter from 1000 to 63  $\mu\text{m}$ ), then the finer fraction (63  $\mu\text{m}$ ) was determined by aerometer on the basis of Stokes's law. Humified organic carbon was identified by means of the Walkley and Black (1934) method, using chromic acid to measure the oxidizable organic carbon (titration). Total organic carbon (TOC) was estimated by loss on ignition (LOI; Heiri et al., 2001), with an uncertainty margin of  $\pm 0.1\%$ ; samples were air-dried and organic matter was oxidized at 500-550°C to carbon dioxide and ash, then the weight lost during the reaction was measured by weighing the samples before and after heating.

Additionally, we performed several XRD (X-Ray Diffraction) analyses and SEM (Scanning Electron Microscope) on randomly oriented powder from the bulk debris samples to investigate the mineralogical properties of the fine debris and dust the occurrence of micro features (e.g: pollen, spores, micro fauna, algae, etc..).

## 4. Results

### 4.1. Debris coverage ratio ( $d$ ) and ice albedo ( $\alpha$ )

The image analysis permitted to evaluate 51  $d$  values which were found ranging from a minimum equal to 0.01 to a maximum of 0.63 (Fig. 4). The ice albedo acquired by the net portable radiometer was found varying from 0.06 to 0.32.

6. A pilot study to evaluate sparse supraglacial debris and dust and their influence on ice albedo of Alpine glaciers: the case study of the Forni Glacier (Italy)

---

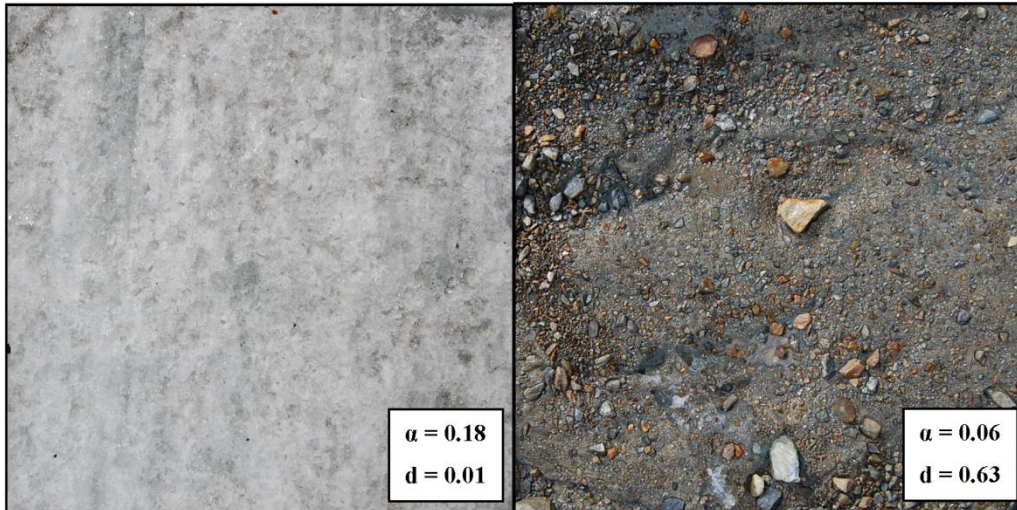


*Fig. 4: Examples of Forni Glacier surfaces: albedo ( $\alpha$ ) and debris cover ratio ( $d$ ) values are shown.*

The two data records resulted highly correlated. The plot showing the natural logarithm of ice albedo (y-axis) vs  $d$  values (x-axis) is reported in Figure 5. The regression line is given by:

$$\ln \alpha = (-2.04 \pm 0.19) \cdot d + (-1.50 \pm 0.04) \quad (4)$$

The correlation is 0.84 (95% coefficient interval ranging from 0.74 to 0.91).

## 6. A pilot study to evaluate sparse supraglacial debris and dust and their influence on ice albedo of Alpine glaciers: the case study of the Forni Glacier (Italy)

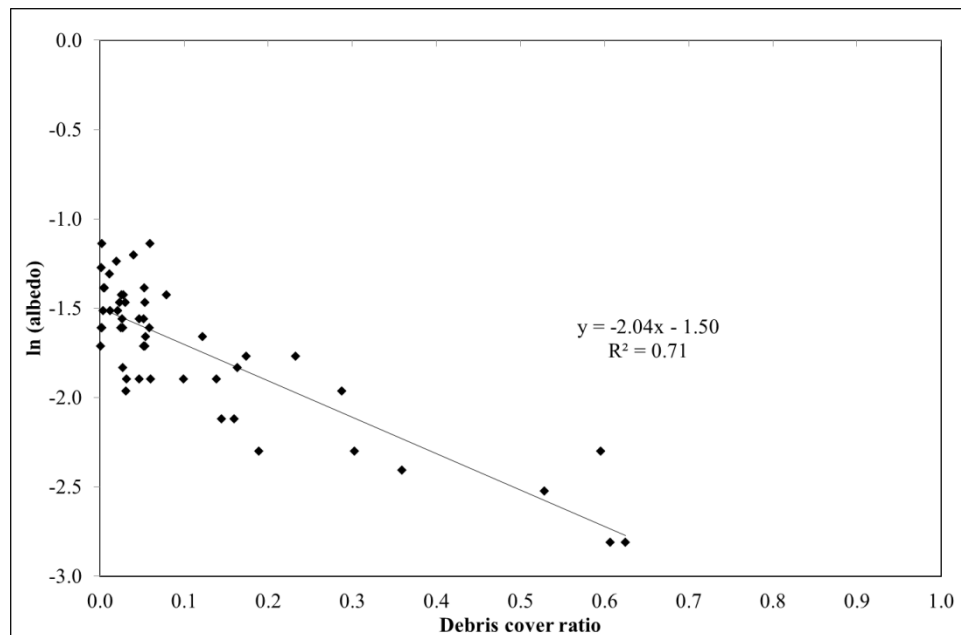


Fig. 5: Albedo natural logarithm values vs debris cover ratio (2011-2013 data).

The most frequent  $d$  value was found lower than 0.10 but our dataset suggests a wide variability of surface features and then the needing for accurate and numerous surveys at the surface of an Alpine glacier devoted to describe  $d$  pattern and then albedo distribution.

To assess the most suitable  $d$  value to differentiate a completely debris-free ice surface from a partially debris-covered one, some attempts were performed. In fact it is almost impossible to find a melting glacier surface completely dust and/or debris free (Oerlemans et al., 2009), thus suggesting that a null  $d$  value (i.e. 0% of debris in a  $1 \text{ m}^2$  parcel) is unrealistic. Then we considered the pictures featuring an albedo value higher than 0.30 and we compared the corresponding  $d$  values. We found that a  $d$  value lower than 0.06 (i.e. 6% of debris coverage over a  $1 \text{ m} \times 1 \text{ m}$  parcel) better witnesses a debris-free surface.

As regards the impact of liquid precipitation on supraglacial fine debris and ice albedo, the Table 1 reports the mean daily albedo values before, during and after a rainfall event. The days before the rainfall featured a mean daily albedo equal to 0.22. Whenever a precipitation occurred the mean daily reflectivity was found as 0.20, due to the water albedo lower than the ice one (i.e. equal to 0.05-0.10, Hartmann, 1994). This phenomenon occurred over 18 events of a total number of 30: 6 featured an albedo increase and 6 steady state albedo conditions. This variable trend can be attributed to the

6. A pilot study to evaluate sparse supraglacial debris and dust and their influence on ice albedo of Alpine glaciers: the case study of the Forni Glacier (Italy)

---

rain amount: in fact a misty rain decreases the surface albedo lower than a heavy liquid precipitation. Once the rain event has washed out the dust, the mean daily albedo resulted 0.26. Generally almost all events (28 over a total number of 30) showed a mean daily albedo increase of +21.2% respect to the value recorded before the rainfall (ranging +3.6% and +62.5% respect to the value recorded before the rainfall). In the case the albedo was higher than 0.30 before the rainfall, the water effect was not so appreciable. In fact this reflectivity value is typical of the bare ice with no debris coverage.

The occurrence of the washing out effect and the consequent reflectivity increase was found to be short lasting. The mean time frame to restore the previous albedo value results equal to 1.8 days (ranging from 1 to 4 days) occurring over 10 events over a total of 30. Whenever the interval between two rainfall was equal to 1 day, the albedo value was higher than the previous rain one (51% of the analysed events).

6. A pilot study to evaluate sparse supraglacial debris and dust and their influence on ice albedo of Alpine glaciers: the case study of the Forni Glacier (Italy)

*Tab. 1: Influence of rainfall on surface albedo ( $\alpha$ ) measured from the AWS1 Forni. In the table are reported the 30 rainy events that occurred in 2011, 2012 and 2013 ablation seasons and the albedo values before, during and after every rainfall.*

Before rainy event		During rainy event		After rainy event		Albedo increasing (%)
Data	$\alpha$	Data	$\alpha$	Data	$\alpha$	
16/06/2011	0.33	17-18/06/2011	0.21	19/06/2011	0.41	24.2
20/06/2011	0.31	21-23/06/2011	0.21	24/06/2011	0.31	0.0
24/06/2011	0.31	25-26/06/2011	0.20	27/06/2011	0.32	3.2
28/06/2011	0.18	29/06/2011	0.18	30/06/2011	0.20	11.1
03/07/2011	0.23	04-08/07/2011	0.20	09/07/2011	0.25	8.7
02/08/2011	0.20	03/08/2011	0.19	04/08/2011	0.24	20.0
31/08/2011	0.25	01/09/2011	0.25	02/09/2011	0.28	12.0
02/09/2011	0.28	03-06/09/2011	0.24	07/09/2011	0.29	3.6
07/09/2011	0.29	08/09/2011	0.22	09/09/2011	0.31	6.9
11/09/2011	0.22	12/09/2011	0.23	13/09/2011	0.25	13.6
19/06/2012	0.20	20-26/06/2012	0.21	27/06/2012	0.22	10.0
01/07/2012	0.17	2-7/07/2012	0.22	08/07/2012	0.19	11.8
08/07/2012	0.19	9-11/07/2012	0.19	12/07/2012	0.23	21.1
12/07/2012	0.23	13-15/07/2012	0.20	16/07/2012	0.29	26.1
19/07/2012	0.20	20-22/07/2012	0.24	22/07/2012	0.27	35.0
23/07/2012	0.21	24-25/07/2012	0.20	26/07/2012	0.22	4.8
26/07/2012	0.22	27-31/07/2012	0.20	01/08/2013	0.23	4.6
02/08/2012	0.20	03-06/08/2012	0.18	07/08/2012	0.24	20.0
24/08/2012	0.16	25-26/08/2012	0.19	27/08/2012	0.26	62.5
23/09/2012	0.22	24-27/09/2012	0.23	28/09/2012	0.32	45.5
28/09/2012	0.32	29/09-02/10/2012	0.24	03/10/2012	0.32	0.0
06/10/2012	0.27	07/10/2012	0.23	08/10/2012	0.30	11.1
16/07/2013	0.16	17-24/07/2013	0.18	25/07/2013	0.17	6.3
25/07/2013	0.17	26/07/2013	0.16	27/07/2013	0.18	5.9
28/07/2013	0.16	29/07/2013	0.15	30/07/2013	0.23	43.8
30/07/2013	0.23	31/07/2013	0.19	01/08/2013	0.25	8.7
06/08/2013	0.16	07-09/08/2013	0.16	10/08/2013	0.26	62.5
12/08/2013	0.19	13-15/08/2013	0.19	16/08/2013	0.24	26.3
31/08/2013	0.18	01/09/2013	0.18	02/09/2013	0.24	33.3
26/09/2013	0.16	27/09/2013	0.15	28/09/2013	0.24	50.0

#### 4.2. Debris features and debris coverage rate ( $C_r$ )

The spatial variability of the fine debris cover was highlighted from 2011 data. The sediment analysis performed in the lab indicates significant variability in the total organic carbon (*TOC*, from 0.57% to 5.91%, see Table 2). The highest content of

6. A pilot study to evaluate sparse supraglacial debris and dust and their influence on ice albedo of Alpine glaciers: the case study of the Forni Glacier (Italy)

---

organic matter was found in samples 5, 6 and 8; in particular, sample 5 was wholly cryoconite, where generally the development of algae and bacteria communities is extremely favoured (Takeuchi et al., 2000, 2005). The lowest value of total organic carbon was found in sample 2, which was collected on a glacier area located close to the flank of the nesting rock walls, a site which receives a high amount of debris originating from macrogelivation and weathering processes. Rock debris coverage here is younger (recent deposition) and unstable, and therefore poorly colonized by supra-glacial organisms. Moreover, the grain-size analysis shows that samples collected at these sites are characterized by coarser sediments, in keeping with their origin, mostly due to slope erosion.

6. A pilot study to evaluate sparse supraglacial debris and dust and their influence on ice albedo of Alpine glaciers: the case study of the Forni Glacier (Italy)

*Tab. 2: Properties of sites sampled for sedimentological analyses and results. The grain-size classes are referred to Krumbein's scale (Wentworth, 1922). With the asterisk it is indicated a debris sample not enough to grain size analysis.*

Sample	Sampling Date	Description	Gravel (%)	Sand (%)	Silt (%)	Clay (%)	TOC (g/kg)	Weight (g)
1	30/06/2011	Central tongue	2.06	17.42	58.77	12.26	2.68	/
2	30/06/2011	Eastern tongue, near the flank of the hosting cirque	6.60	69.75	19.58	0.57	0.57	/
3	30/06/2011	Median moraine (5 cm thick debris)	18.95	50.19	24.30	4.46	1.61	/
4	30/06/2011	Central tongue, predominantly bare ice	0.38	29.36	30.97	15.85	3.60	/
5	30/06/2011	Central tongue, cryoconite	5.60	32.99	30.98	15.78	5.15	/
6	30/06/2011	Eastern tongue.	0.05	14.50	35.35	20.49	4.99	/
7	25/08/2011	Eastern tongue, near the flank of the hosting cirque	6.21	72.39	15.75	3.37	1.98	/
8	25/08/2011	Eastern tongue.	0.08	21.37	31.73	22.76	5.91	/
9a	04/07/2012	Central tongue	19.72	66.28	8.91	2.23	1.58	67.67
10a	04/07/2012	Central tongue	8.64	33.61	25.73	12.29	26.25	1559.40
11a	04/07/2012	Eastern tongue	0.12	17.70	35.48	19.68	18.32	432.00
9b	07/08/2012	Central tongue, the same site of sample 9a	13.01	75.03	7.41	2.10	1.28	11.92
10b	07/08/2012	Central tongue, the same site of sample 10a*	/	/	/	/	40.84	4026.90
9c	09/09/2012	Central tongue, the same site of samples 9a and 9b	22.48	66.27	7.92	2.27	5.38	49.41
10c	09/09/2012	Central tongue, the same site of samples 10a and 10b	2.37	23.63	40.95	16.67	38.07	2356.68
11c	09/09/2012	Eastern tongue, the same site of sample 11a	2.59	25.35	35.23	14.86	41.87	462.39
12a	11/07/2013	Central tongue	/	/	/	/	/	29.13
12b	31/07/2013	Central tongue, the same site of sample 12a	/	/	/	/	/	159.50
12c	06/09/2013	Central tongue, the same site of sample 12a and 12b	/	/	/	/	/	308.33
12d	04/10/2013	Central tongue, the same site of sample 12a, 12b and 12c	/	/	/	/	/	59.46

Regarding the debris origin, X-Ray Diffraction analysis indicates that the samples are enriched with quartz, muscovite, chlorite, sericite and albite, thus confirming the geological origin of debris mostly from local rock outcrops (a local formation of micaschist). By SEM analysis we found algae, spore, pollen, microfauna (Fig. 6). Moreover we observed also spherical structures (Fig. 6d) characterized (from EDS analysis) by an abundance of FeO (45.26%) and Al<sub>2</sub>O<sub>3</sub> (19.78%). This composition confirms that these structures are cenospheres (i.e. a residual product of carbon combustion, Kolay and Singh, 2001). These cenospheres can be carried out by a wind

6. A pilot study to evaluate sparse supraglacial debris and dust and their influence on ice albedo of Alpine glaciers: the case study of the Forni Glacier (Italy)

contribution probably from siderurgic district at the northern fringe of the Po Plain (c. more than 150 km southward the Forni Glacier), suggesting a limited allochthonous input and a human impact even at the glacier surface.

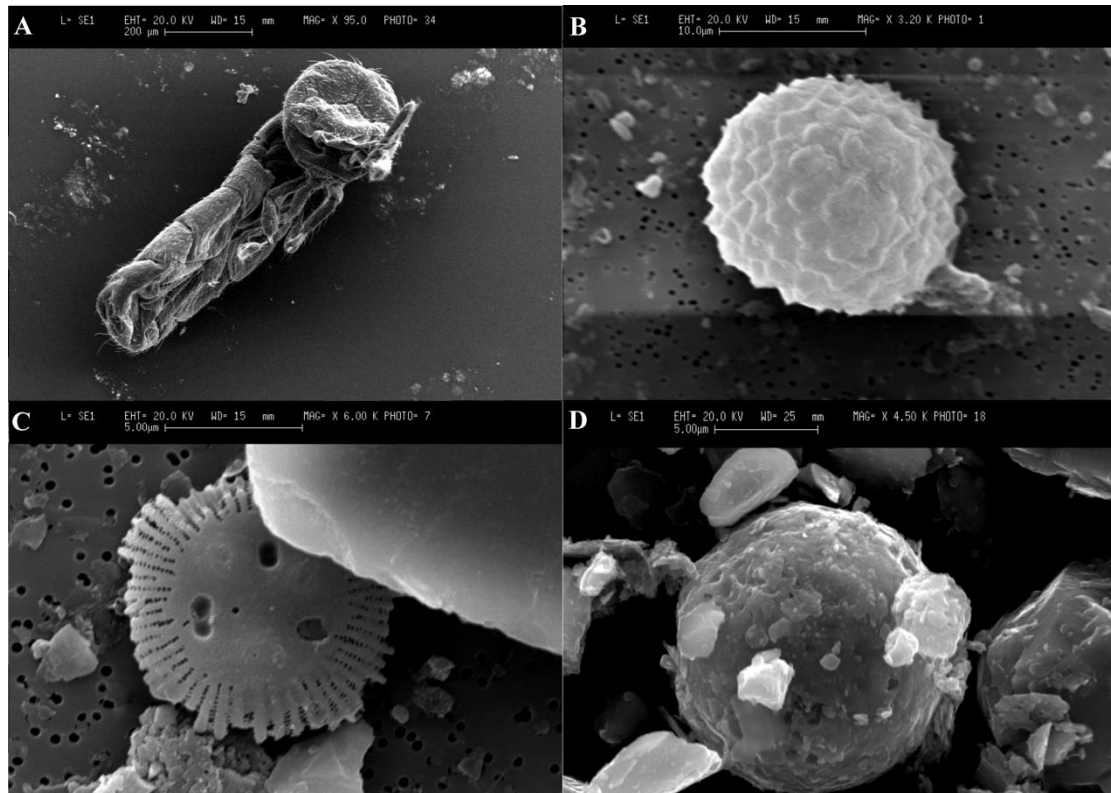


Fig. 6: SEM investigation on bulk samples from Forni Glacier evidenced the presence of A) organism of collembolan order, B) spore, C) diatom and D) cenosphere (a residual product of carbon combustion).

To evaluate the fine debris cover evolution, during ablation seasons 2012 and 2013 the debris coverage rate ( $C_r$ ) was evaluated (see equation 3). From 4<sup>th</sup> July to 9<sup>th</sup> September 2012 we found a higher  $C_r$  on sites characterized by coarser dust (i.e. 96 g/m<sup>2</sup> per day along an entire ablation season) than in the sites featuring finer sediment (i.e. 1 g/m<sup>2</sup> per day). In 2013 measures are more representative of the average debris cover conditions on the ablation tongue of the glacier: a  $C_r$  equal to 6 g/m<sup>2</sup> per day was found.

As at the each field survey the parcels were not distinguishable from glacier areas nearby, the development of debris coverage resulted occurring at a fast rates. This evolution is highlighted also from the sedimentological analyses performed on the 2012 samples. During the ablation season the grain-size remains almost similar with a slight



## 6. A pilot study to evaluate sparse supraglacial debris and dust and their influence on ice albedo of Alpine glaciers: the case study of the Forni Glacier (Italy)

---

increasing of finer sedimentological classes (i.e. silt and clay), on the other hand a more intense growing of the total organic carbon (i.e. *TOC*) is observed. At the beginning of July the *TOC* ranges from 1.58 g/kg (at sample 9a) to 26.25 g/kg (at sample 10a), at the end of the ablation period the organic carbon arises up to 41.87 g/kg. The higher values are in correspondence of finer debris (i.e. samples 9a, 9b, 9c, 11a and 11c, enriched in silt and clay), on the contrary in coarser sample 10a, 10b and 10c the *TOC* results lower. The evolution of the supraglacial debris is also analysed in SEM observations. At the beginning of the melting time frame 2012, the sediment is characterized by sharp and angular clasts; on the other hand, the samples collected in September 2012 feature more rounded shapes, suggesting a supraglacial mass transport.

## 5. Discussion

To investigate the robustness of our method to quantify  $d$  and its sensitivity to changes in the chosen  $T_{GS}$ , we firstly varied the applied  $T_{GS}$  values up to  $\pm 10\%$  of their initial values ( $T_{GS-10\%}$  and  $T_{GS+10\%}$  respectively, Figure 7): for example whenever the applied  $T_{GS}$  value to discriminate debris from bare ice was 100, we recalculated  $d$  with 90 ( $T_{GS-10\%}$  obtaining  $d_{-10\%}$ ) and with 110 ( $T_{GS+10\%}$  obtaining  $d_{+10\%}$ ). We applied this simple test to all the performed measurements (51 field data) thus obtaining 51  $d_{-10\%}$  values and 51  $d_{+10\%}$  values. Then we evaluated the departures of  $d_{-10\%}$  ( $d - d_{-10\%}$ ) from  $d$  which resulted up to -0.07 (with a mean value of -0.02). Moreover we calculated the departures of  $d_{+10\%}$  ( $d - d_{+10\%}$ ) from  $d$  which were found lower than +0.09 (with a mean value of +0.02). We found that whenever  $d$  was higher than 0.25 the  $d - d_{-10\%}$  and  $d - d_{+10\%}$  values reached their maxima. In fact  $d - d_{-10\%}$  was -0.07 when  $d$  value was found 0.28 and  $d - d_{+10\%}$  was +0.09 with a  $d$  value was equal to 0.60. Considering the whole sample it resulted that the slightly more than 70.0% of  $d$  featured  $d - d_{-10\%}$  up to -0.02 and  $d - d_{+10\%}$  lower than +0.03.

6. A pilot study to evaluate sparse supraglacial debris and dust and their influence on ice albedo of Alpine glaciers: the case study of the Forni Glacier (Italy)

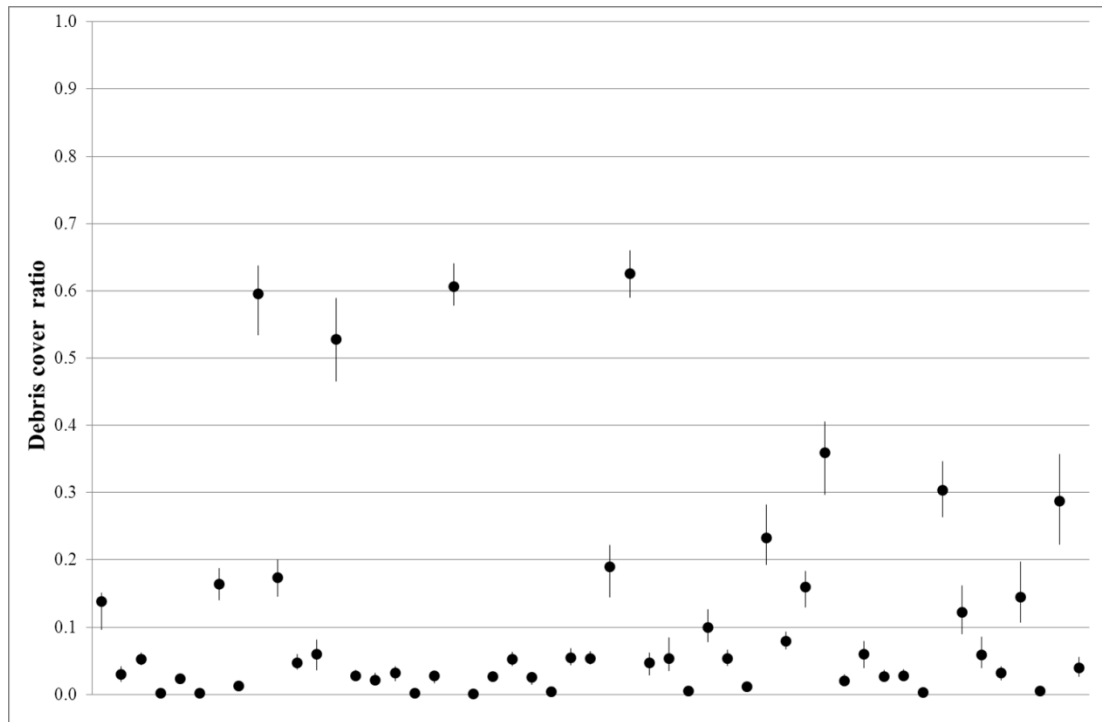


Fig. 7: Values of  $d$  from 51 measurements performed in 2011, 2012 and 2013 ablation seasons (black dots). The vertical bars indicate the  $d_{+10\%}$  and  $d_{-10\%}$  values.

Moreover we applied  $d_{-10\%}$  and  $d_{+10\%}$  values to look for a relation with  $\alpha$  obtaining two new equations (reported in Table 3 together with equation 4). Applying these 3 equations to  $d$  dataset it was possible to model glacier albedo; the modelled albedo values were compared to the albedo data obtained from field radiation measurements and the departures between the two records resulted very small, with a mean value lower than  $\pm 0.011$ .

Tab. 3: Depending on the 3 different ratio datasets (considering  $d_{\pm 10\%}$  and  $d$ ) the differences between measured ( $\alpha_M$ ) and calculated ( $\alpha_C$ ) albedo data are shown.

Relation equation	Min ( $\alpha_M - \alpha_C$ )	Mean ( $\alpha_M - \alpha_C$ )	Max ( $\alpha_M - \alpha_C$ )
$\ln(\alpha) = (-2.20 \pm 0.21) d_{-10\%} + (-1.52 \pm 0.04)$	-0.06	+0.11	+0.13
$\ln(\alpha) = (-2.04 \pm 0.19) d + (-1.50 \pm 0.04)$	-0.07	+0.05	+0.12
$\ln(\alpha) = (-1.89 \pm 0.17) d_{+10\%} + (-1.48 \pm 0.04)$	-0.07	-0.01	+0.12

This suggests that the sensitivity of our method to changes in the applied threshold is not so high to affect the reliability of the results. Moreover we also tested the method using an unique threshold value. For this attempt we applied  $T_{GS-AVE}$  (i.e. 92) obtained

6. A pilot study to evaluate sparse supraglacial debris and dust and their influence on ice albedo of Alpine glaciers: the case study of the Forni Glacier (Italy)

averaging all the 51  $T_{GS}$  values thus obtaining 51  $d_{AVE}$  values. Then we compared these  $d_{AVE}$  values to  $d$  dataset obtained through the supervised classification (51  $T_{GS}$  values). The obtained scatter plot (Fig. 8) indicates a not negligible relation among the two datasets thus suggesting that a unique threshold value could be sufficient to describe debris distribution on different images.

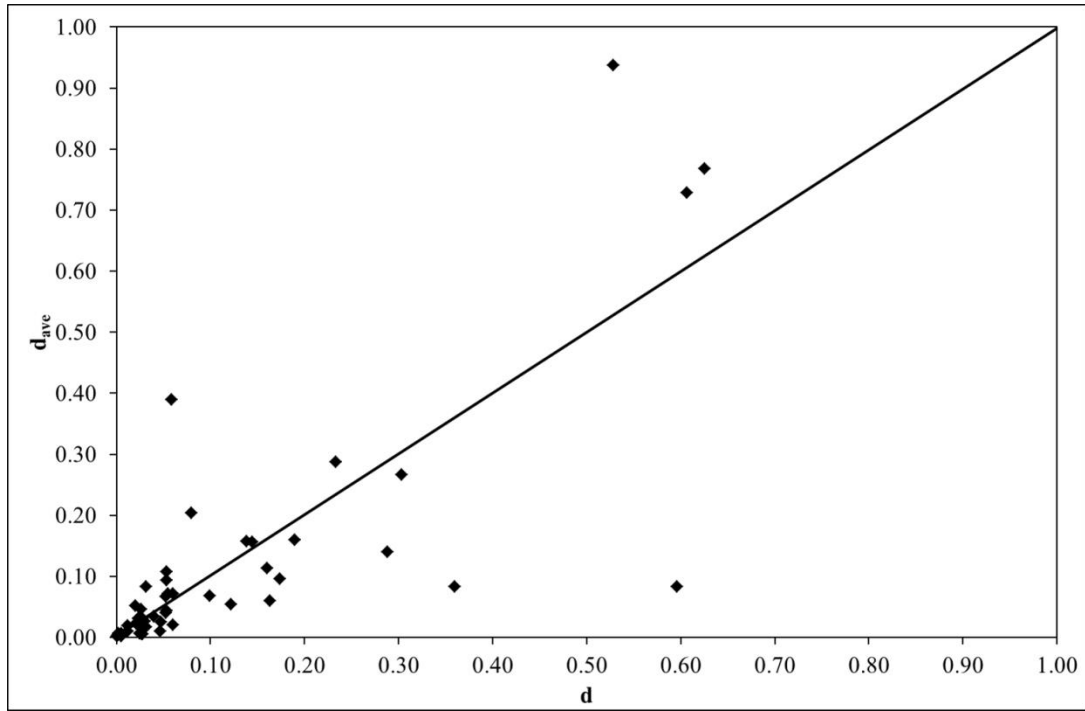


Fig. 8: Scatter plot reporting  $d$  (obtained from  $T_{GS}$ ) vs  $d_{AVE}$  (obtained from  $T_{GS-AVE}$ ) values.

Then we applied the obtained 51  $d_{AVE}$  values to look for a relation with  $\alpha$  data finding the following equation:

$$\ln \alpha = (-1.38 \pm 0.21) \cdot d_{AVE} + (-1.58 \pm 0.05) \quad (5)$$

Equation 5 features a R value of 0.68, meaningful but lower than the one of equation 4 thus suggesting that the different  $T_{GS}$  we found for each image (even if they require to spend more time in the image analysis) permit a better and detailed determination of debris distribution and then a more accurate  $d$  evaluation and  $\alpha$  prediction.

Then summarizing, to look for the most reliable relation between  $d$  and  $\alpha$  the best and suitable solution is to apply as many specific  $T_{GS}$  values as are the images to be analysed

## 6. A pilot study to evaluate sparse supraglacial debris and dust and their influence on ice albedo of Alpine glaciers: the case study of the Forni Glacier (Italy)

---

thus describing with further details the large variability of surface conditions which affect glacier surface during the summer season.

The relation between albedo and debris cover we found underlines a strong influence driven by the glacier surface characteristics. The dust resulted featuring a high spatial (over the glacier tongue) and temporal (during the summer season) variability. In proximity of the nesting rock flanks and of the median moraine sediments are more diffuse and poorly sorted, indicating deposition after mass transport. At the end of the ice melting season a more diffuse fine debris coverage occurs on the glacier surface. Similarly to the dust distribution, the albedo variability is higher at the end of the ice melting time window as well. Another parameters affecting the fine sediment accumulation are represented by supraglacial water streams (i.e.: bedieres), wind contribution, and *in situ* weathering of coarser clasts.

Moreover also the liquid precipitation resulted playing a not negligible effect on ice albedo but their effect was found short lasting (from 1.8 to 1 day long) thus the actual impact on other processes driven by surface albedo (like ice melt rates and magnitude) depends on frequency and duration of summer rainfall.

Regarding the debris origin, X-Ray Diffraction analysis indicates that the largest part of our samples were enriched with minerals which confirm the local geological origin of debris mostly from rock outcrops. Nevertheless the spherical structures characterized (from EDS analysis) by an abundance of FeO and Al<sub>2</sub>O<sub>3</sub> we found through SEM analysis and we identified as cenospheres suggest an impact on glacier from siderurgic factories located at the northern fringe of the Po Plain.

The evolution of sedimentological properties can be evaluated sampling a same site at the beginning and at the end of ablation season. The organic content (*TOC*) resulted increasing during the summer time frame and its distribution resulted controlled by the grain-size of the supraglacial sediment. In fact *TOC* seems to be more abundant in correspondence with finer sediments (Table 2). This can be explained by the stability of the finer debris area: it is likely that this place offers refuge for organic particles transported by wind and the environmental conditions suitable for development of algae, yeasts and bacteria. Yeasts had already been identified at the Forni Glacier surface (see Turchetti et al., 2008). Moreover, Gobbi et al. (2006) reported the presence of arthropod fauna on the surface of the Forni Glacier, which by decaying can supply significant organics.

## 6. Conclusions

This work represents an attempt for improving the research on supraglacial fine debris coverage and contributing to fill a knowledge gap. In fact, several studies are dealing with dust and black carbon occurrence at the snow surface and its effect on snow melt rates and glacier evolution (see Aoki et al., 1998; Qian et al., 2011; Yasunari et al., 2010). On the other hand, no systematic studies have been previously performed at the melting surface of glaciers. Moreover, dust and black carbon occurrence on ice seems to have increased over the last recent years due to the ongoing glacier shrinkage that makes larger and wider rock exposures, rock outcrops and nunataks (Oerlemans et al., 2009, Diolaiuti and Smiraglia, 2010), thus requiring accurate studies to describe debris occurrence, pattern and evolution and their influence on ice albedo. The spatial distribution of ice albedo needs to be better prescribed in distributed energy balance models. For this reason, we proposed a simple methodological approach to standardize the procedures to quantify fine and sparse debris/dust coverage at the glacier melting surface and its influence on ice albedo.

The image analysis permitted to evaluate 51  $d$  values which were found ranging from a minimum equal to 0.01 to a maximum of 0.63. The ice albedo acquired by the net portable radiometer was found varying from 0.06 to 0.32.

The debris quantification method is based on image analysis. The greyscale threshold values ( $T_{GS}$ ) are chosen by a supervised classification in which the threshold is iteratively adjusted until the isolated image pixels best coincide with the debris/dust. We investigated the robustness of this approach with some sensitivity tests: i) varying the selected threshold up to  $\pm 10\%$  for each image (thus obtaining  $T_{GS-10\%}$  and  $T_{GS+10\%}$ ) and ii) applying a unique threshold ( $T_{GS-AVE}$ ) obtained by averaging all the chosen  $T_{GS}$  thus obtaining 51  $d_{-10\%}$  values and 51  $d_{+10\%}$  values and 51  $d_{AVE}$  values. Then we evaluated the departures of  $d_{-10\%}$  from  $d$  which resulted up to -0.07 (with a mean value of -0.02). Moreover we calculated the departures of  $d_{+10\%}$  from  $d$  which were found lower than +0.09 (with a mean value of +0.02). Considering the whole sample it resulted that the 70.59% of  $d$  featured  $d - d_{-10\%}$  up to -0.02 and  $d - d_{+10\%}$  lower than +0.03. These results suggest that the sensitivity of our method to changes in the applied threshold is not so high to affect the reliability of the derived data. Moreover we also tested the method using a unique threshold value ( $T_{GS-AVE}$ : 92). Then we compared the obtained  $d_{AVE}$

## 6. A pilot study to evaluate sparse supraglacial debris and dust and their influence on ice albedo of Alpine glaciers: the case study of the Forni Glacier (Italy)

---

values to the actual  $d$  dataset (from 51  $T_{GS}$  values). The obtained scatter plot indicates a not negligible relation among the two datasets. Nevertheless  $d_{AVE}$  data resulted an input data less accurate than  $d$  to predict ice albedo variability thus suggesting that the different  $T_{GS}$  found for each image (even if they require to spend more time in the image analysis) permit a better and detailed determination of debris distribution and then a more accurate  $d$  evaluation and  $\alpha$  prediction. Then summarizing to look for the most reliable relation between  $d$  and  $\alpha$  the best and suitable solution is to apply as many specific  $T_{GS}$  values as are the images to be analysed thus describing with further details the large variability of surface conditions which affect glacier surface during the summer season.

To evaluate the fine debris cover evolution, during ablation seasons 2012 and 2013 the debris coverage rate ( $C_r$ ) was evaluated (see equation 3). From 4<sup>th</sup> July to 9<sup>th</sup> September 2012 we found a higher  $C_r$  on sites characterized by coarser dust (i.e. 96 g/m<sup>2</sup> per day along an entire ablation season) than in the sites featuring finer sediment (i.e. 1 g/m<sup>2</sup> per day). In 2013  $C_r$  resulted equal to 6 g/m<sup>2</sup> per day representing the average debris coverage over the Forni ablation tongue.

The debris cover could be also evaluated with better time resolution making automatic the digital imagery acquisition by installing an automatic camera on the mast of a permanent AWS. Then several photos could be acquired on the same sample area. Presently, we are developing all these improvements, which surely will give fundamental inputs to the research; nevertheless, this first test gives an important contribution to standardize the field work method for evaluating and sampling fine sparse debris at the melting glacier surface.

The preliminary analyses of the supraglacial debris evolution suggest a variable sediment evolution during the melting season assessed by rapid changes in sedimentological features and in the content of organic carbon. The organic content resulted increased during the summer time frame and its distribution is controlled by the grain-size of the supraglacial sediment. In fact  $TOC$  seems to be more abundant in correspondence with finer sediments.

Moreover, the surface fine debris evolution is resulted forced by the occurrence of liquid precipitation that washes out the dust accumulation on glacier surface. This influence was quantified in an albedo increasing up to 20%, limited to less than 2 days. This is due to rain smoothing effect on the ice surface as well, thus reducing the roughness.

## 6. A pilot study to evaluate sparse supraglacial debris and dust and their influence on ice albedo of Alpine glaciers: the case study of the Forni Glacier (Italy)

---

Regarding the debris origin, X-Ray Diffraction analysis indicates that the samples are enriched with quartz, muscovite, chlorite, sericite and albite, thus confirming the geological origin of debris mostly from local rock outcrops (a local formation of micaschist). By SEM analysis we found algae, spore, pollen, microfauna and spherical structures characterized (from EDS analysis) by an abundance of FeO (45.3%) and Al<sub>2</sub>O<sub>3</sub> (19.8%). This composition confirms that these structures are cenospheres probably carried out by a wind contribution from siderurgic industries of Po Plains, suggesting a limited allochthonous input. This human contribution affects the glacier energy budget: in fact, the black carbon reduces the reflectivity and increases the ablation (Painter, 2013).

Thanks to the reliability of our analytical protocol, further improvements are expected from data collected in other Alpine sites, in Himalaya (Everest region) and Karakoram, where field campaigns are presently ongoing under the umbrella of SHARE projects. Future results are expected to increase our knowledge on the relation between albedo and debris cover and their effects on the energy balance of glaciers at different latitudes. In conclusion, though this methodological approach is applied to a very small scale (parcel of 1 m x 1 m), it could be extended to a larger scale. For instance, the image analysis can be performed on higher resolution imagery such as orthophotos (for Lombardy Alps available with pixel resolution of 0.5 m x 0.5 m) or satellite imagery (featuring a resolution of 3-5 m or better). This improvement and the jump of scale will permit to distribute ice albedo once the debris properties are analysed and the relationship between albedo and debris ratio is known.

6. A pilot study to evaluate sparse supraglacial debris and dust and their influence on ice albedo of Alpine glaciers: the case study of the Forni Glacier (Italy)

---

## References

- Aoki Te., Aoki Ta., Fukabori M., Tachibana Y., Zaizen Y., Nishio F. and Oishi T. (1998): Spectral albedo observation on the snow field at Barrow, Alaska. *Polar Meteor. Glaciol.*, 12, 1-9.
- Aoki Te., Motoyoshi H., Kodama Y., Yasunari T.J., Sugiura K. and Kobayashi H. (2006): Atmospheric aerosol deposition on snow surfaces and its effect on albedo. *Sola* 2, 13-16.
- Brock B.W. (2004): An analysis of short-term albedo variations at Haut Glacier d'Arolla, Switzerland. *Geografiska Annaler*, A86, 53-65
- Brock B.W., Willis I.C. and Sharp M.J. (2000): Measurement and parameterization of albedo variations at Haut Glacier d'Arolla, Switzerland. *Journal of Glaciology*, 46(155), 675-688.
- Citterio M., Diolaiuti G., Smiraglia C., Verza G. and Meraldi E. (2007): Initial results from the automatic weather station (AWS) on the ablation tongue of Forni Glacier (Upper Valtellina, Italy). *Geografia Fisica e Dinamica Quaternaria*, 30, 141-151.
- Conway J., Gades A. and Raymond C.F. (1996); Albedo of dirty snow during conditions of melt. *Water Resources Research*, 32 (6), 1713-1718.
- D'Agata C., Bocchiola D., Maragno D., Smiraglia C. and Diolaiuti G. (2013): Glacier shrinkage driven by climate change during half a century (1954-2007) in the Ortles-Cevedale Group (Stelvio National Park, Lombardy, Italian Alps). *Theor. Appl. Climatol.* Online 10.1007/s00704-013-0938-5
- Diolaiuti G., Smiraglia C., Verza G.P., Chillemi R. and Meraldi E. (2009): La rete micrometeorologica glaciale lombarda: un contributo alla conoscenza dei ghiacciai alpini e delle loro variazioni recenti, in: Smiraglia, C., Morandi, G., Diolaiuti, G. (Eds.), *Clima e Ghiacciai, la crisi delle risorse glaciali in Lombardia. Regione Lombardia*, pp. 69-92. Also available on line at: <http://users.unimi.it/glaciol>
- Diolaiuti G. and Smiraglia C. (2010): Changing glaciers in a changing climate: how vanishing geomorphosites have been driving deep changes in mountain landscapes and environments. *Géomorphologie: relief, processus, environnement*, 2, 131-152.
- Diolaiuti G., Bocchiola D., D'Agata C. and Smiraglia C. (2012): Evidence of climate change impact upon glaciers' recession within the Italian Alps: the case of Lombardy glaciers. *Theoretical and Applied Climatology*, 109 (3-4), 429-445. DOI 10.1007/s00704-012-0589-y.



6. A pilot study to evaluate sparse supraglacial debris and dust and their influence on ice albedo of Alpine glaciers: the case study of the Forni Glacier (Italy)

---

- Flanner M.G., Zender C.S., Hess P.G., Mahowald N.M., Painter T.H., Ramanathan V. and Rasch P.J. (2009): Springtime warming and reduced snow cover from carbonaceous particles. *Atmos. Chem. Phys.*, 9, 2481-2497.
- Fujita K. (2007): Effect of dust event timing on glacier runoff: sensitivity analysis for a Tibetan glacier. *Hydrol. Process.*, 21 (21), 2892-2896.
- Gale S.J. and Hoare P.G. (1991): *Quaternary sediments*. New York, Belhaven Press.
- Garavaglia V., Pelfini M., Diolaiuti G., Pasquale V. and Smiraglia C. (2012): Evaluating tourist perception of environmental changes as a contribution to managing natural resources in glacierized areas. A case study of the Forni Glacier (Stelvio National Park, Italian Alps). *Environmental Management*, ISSN: 1432-1009, doi: 10.1007/s00267-012-9948-9
- Gobbi M., De Bernardi F., Pelfini M., Rossaro B. and Brandmayr P. (2006): Epigeal Arthropod Succession along a 154-year Glacier Foreland Chronosequence in the Forni Valley (Central Italian Alps). *Arctic, Antarctic, and Alpine Research*, 38 (3), 357-362.
- Hartmann D.L. (1994): Global physical climatology. *International geophysics*, 56, 411 pp
- Heiri O., Lotter A.F. and Lemcke G. (2001): Loss on ignition as a method for estimating organic and carbonate content in sediments: Reproducibility and comparability of results. *J. Paleolimn.*, 25, 101-110.
- Irvine-Fynn T., Bridge J. and Hodson A. (2010): Rapid quantification of cryoconite: granule geometry and in situ supraglacial extents, using examples from Svalbard and Greenland. *Journal of Glaciology*, 56(196), 297-308.
- Kolay P.K. and Singh D.N (2001): Physical, chemical, mineralogical, and thermal properties of cenospheres from an ash lagoon. *Cement and Concrete Research*, 31 (4), 539-542.
- Mihalcea C., Mayer C., Diolaiuti G., Lambrecht A. and Smiraglia C. (2006): Ice ablation and meteorological conditions on the debris covered area of Baltoro Glacier, Karakoram (Pakistan), *Annals of Glaciology*, 43, 292-300.
- Ming M., Xiao C., Cachier H., Qin D., Qin X., Li Z. and Pu J. (2009): Black Carbon (BC) in the snow of glaciers in West China and its potential effects on albedos. *Atmos. Res.*, 92, 114-123.
- Montrasio A., Berra F., Cariboni M., Ceriani M., Deichmann N., Ferliga C., Gregnanin A., Guerra S., Guglielmin M., Jadoul F., Longhin M., Mair V., Mazzoccola D.,

6. A pilot study to evaluate sparse supraglacial debris and dust and their influence on ice albedo of Alpine glaciers: the case study of the Forni Glacier (Italy)

---

- Sciesa E. and Zappone A. (2008): Note illustrative della Carta Geologica d'Italia: foglio 024, Bormio. ISPRA, Servizio Geologico d'Italia.
- Motoyoshi H., Aoki Te., Hori M., Abe O. and Mochizuki S. (2005): Possible effect of anthropogenic aerosol deposition on snow albedo reduction at Shinjo, Japan. *J. Meteor. Soc. Japan*, 83A, 137-148.
- Nakawo M. and Young G.J. (1982): Estimate of glacier ablation under a debris layer from surface temperature and meteorological variables. *Journal of Glaciology*, 28(98), 29-34.
- Nakawo M. and Rana B. (1999): Estimation of ablation rate of glacier ice under a supraglacial debris layer. *Geografiska Annaler*, 41, 228-230.
- Oerlemans J., Giesen R.H. and Van Den Broeke M.R. (2009): Retreating alpine glaciers: increased melt rates due to accumulation of dust (Vadret da Morteratsch, Switzerland). *Journal of Glaciology*, 55(192), 729-736.
- Oerlemans J. (2010): *The microclimate of Valley Glaciers*. Igitur, Utrecht Publishing & Archiving Services, Universiteitsbibliotheek Utrecht.
- Painter T.H., Flanner M.G., Kaser G., Marzeion B., Van Curen R.A. and Abdalati W. (2013): End of the Little Ice Age in the Alps forced by industrial black carbon. *PNAS*, 110 (38), 15216-15221.
- Paul F. and Kääb A. (2005): Perspectives on the production of a glacier inventory from multispectral satellite data in the Canadian Arctic: Cumberland Peninsula, Baffin Island. *Annals of Glaciology*, 42, 59-66.
- Paul F., Kääb A. and Haeberli W. (2007): Recent glacier changes in the Alps observed from satellite: Consequences for future monitoring strategies. *Global Planetary Change*, 56(1/2), 111-122.
- Qian Y., Flanner M.G., Leung L.R. and Wang W. (2011): Sensitivity studies on the impacts of Tibetan Plateau snowpack pollution on the Asian hydrological cycle and monsoon climate. *Atmos. Chem. Phys.*, 11, 1929-48.
- Ramanathan V. (2007): *Role of Black Carbon in Global and Regional Climate Change*. Testimonial to the House Committee on Oversight and Government Reform, October 18, 2007.
- Senese A., Diolaiuti G., Mihalcea C. and Smiraglia C. (2010): Meteorological evolution on the ablation zone of Forni Glacier, Ortles-Cevedale Group (Stelvio National Park, Italian Alps) during the period 2006-2008. *Bollettino della Società Geografica Italiana*, Roma, Serie XIII, vol. III, fascicolo 4, 845-864.

6. A pilot study to evaluate sparse supraglacial debris and dust and their influence on ice albedo of Alpine glaciers: the case study of the Forni Glacier (Italy)

---

- Senese A., Diolaiuti G., Mihalcea C. and Smiraglia C. (2012a): Energy and mass balance of Forni Glacier (Stelvio National Park, Italian Alps) from a 4-year meteorological data record. *Arctic, Antarctic, Alpine Research*, 44 (1), 122-134. <http://instaar.metapress.com/content/r34075016632020l/fulltext.pdf>
- Senese A., Diolaiuti G., Verza G.P. and Smiraglia C. (2012b): Surface energy budget and melt amount for the years 2009 and 2010 at the Forni Glacier (Italian Alps, Lombardy). *Geografia Fisica e Dinamica Quaternaria*, 35(1), 69-77.
- Sodermann H., Palmer A.S., Schwierz C., Schwikowski M. and Vernli H. (2006): The transport history of two Saharan dust events archived in an Alpine ice core. *Atmos. Chem. Phys.*, 6, 667-688.
- Takeuchi N., Kohshima S., Yoshimura Y., Seko K. and Fujita K. (2000): Characteristics of cryoconite holes on a Himalayan glacier, Yala Glacier Central Nepal. *Bull. Glaciol. Res.*, 17, 51-59.
- Takeuchi N., Kohshima S. and Seko K. (2001): Structure, formation, darkening process of albedo reducing material (cryoconite) on a Himalayan glacier: a granular algal mat growing on the glacier. *Arctic Antarctic Alpine Research*, 33, 115-122.
- Takeuchi N. (2002): Surface albedo and characteristics of cryoconite on an Alaska glacier (Gulkana Glacier in the Alaska Range). *Bull. Glaciol. Res.*, 19, 63-70.
- Takeuchi N., Matsuda Y., Sakai A. and Fujita K. (2005): A large amount of biogenic surface dust (cryoconite) on a glacier in the Qilian Mountains, China. *Bull. Glaciol. Res.*, 22, 1-8.
- Turchetti B., Buzzini P., Goretti M., Branda E., Vaughan-Martini A., Diolaiuti G., D'Agata C. and Smiraglia C. (2008): Psychrophilic yeasts in glacial environments of Alpine glaciers. *FEMS Microbiology Ecology*, 63, 73–83. DOI:10.1111/j.1574-6941.2007.00409.x.
- Walkley A. and Black I.A. (1934): An examination of Degtjareff method for determining soil organic matter and a proposed modification of the chromic acid titration method. *Journal of Soil Science*, 37, 29-38.
- Wentworth C.K. (1922): A scale of grade and class terms for clastic sediments. *Journal of Geology*, 30, 377-392.
- Wiscombe W.J. and Warren S.G. (1980): A model for spectral albedo of snow. I. Snow Containing Atmospheric Aerosols. *Journal of Atmospheric Science*, 37, 2734-2745.
- Wiscombe W.J. and Warren S.G. (1985): Dirty snow after nuclear war. *Nature*, 313, 469-470.

6. A pilot study to evaluate sparse supraglacial debris and dust and their influence on ice albedo of Alpine glaciers: the case study of the Forni Glacier (Italy)
- 

World Meteorological Organization (2008): Guide to meteorological instruments and method of observation. Seventh edition.

Yasunari T.J., Bonasoni P., Laj P., Fujita K., Vuillermoz E., Marinoni A., Cristofanelli P., Duchi R., Tartari G. and Lau K.M. (2010): Estimated impact of black carbon deposition during pre-monsoon season from Nepal Climate Observatory-Pyramid data and snow albedo changes over Himalayan glaciers *Atmos. Chem. Phys.* 10: 6603-6615.

#### WEB REFERENCES

<http://rsbweb.nih.gov/ij> - Last visited on November, the 19<sup>th</sup>, 2013.

# Chapter 7

## **Computation of turbulent fluxes distributed over the glacier surface. The case study of the Forni Glacier (Italian Alps)**

### **Abstract**

To investigate the spatial distribution of the energy and mass balance fluxes over a glacier surface it is necessary to take into account not only the radiative components, but the turbulent fluxes too. Then several methods were applied to estimate the turbulent fluxes over the Forni Glacier surface: the well-known bulk aerodynamic formulas and another approach depending not directly on wind speed. This latter is indirectly encountered in the back-ground turbulent exchange coefficient. Nevertheless we are looking for more accurate algorithms which allow to distribute the wind speed over the glacier surface.

To assess these fluxes over the whole glacier surface, it was firstly necessary to distribute the air temperature and the vapour pressure. The first one was already investigated in chapter 5 of this PhD Thesis. The computation of the distributed vapor pressure was analyzed in this chapter. Apart from the distribution of these two parameters, the turbulent exchange coefficient was evaluated, found equal for the latent and sensible heat flux.

## 1. Introduction

To investigate the spatial distribution of the energy and mass balance fluxes over a glacier surface it is necessary to take into account not only the radiative components, but the turbulent fluxes too. These latter have lower influence on ablation with respect to the radiative ones. In fact, the sensible heat flux ( $SH$ ) and the latent heat flux ( $LE$ ) represent ca. 16% and ca. 2% of the net energy amount respectively (Senese et al., 2012a). The importance of net radiation relative to the turbulent fluxes tends to increase with altitude, as a result of reduced turbulent fluxes due to the vertical lapse rates of air temperature and vapour pressure (Röthlisberger and Lang, 1987). In any case the turbulent fluxes play an important role in shaping boundary layers (detailed treatments about the atmospheric boundary layer and turbulence are presented for instance in Stull, 1988).

As winds flow along the surface of a glacier, turbulent eddies mix the air vertically. The temperature of the air adjacent to the glacier surface (the skin temperature) equals the temperature of the ice or snow. If the overlying air (the lower boundary layer or surface layer) is warmer than the surface, the mixing transfers sensible heat to the surface, at rate per unit area ( $SH$ ). The air moisture content at the surface is determined by the saturation vapour pressure and hence the skin temperature. In the presence of drier overlying air, mixing transfers moisture away from the surface. The surface must evaporate or sublimate to maintain saturation of the air adjacent to it. This consumes latent heat, at rate per unit area ( $LE$ ). In general, both of these fluxes can be either positive or negative. The energy fluxes  $LE$  and  $SH$  are roughly proportional to the contrasts of moisture and temperature between the surface and the overlying air. Fluxes also increase with the strength of vertical turbulent exchange, depending on the frequency of eddies and their distance of propagation. In bulk, the turbulent exchange of air relates to three factors: i) how fast the air flows (measured by the wind speed  $V$  a few meters above the surface), ii) how rough the surface is, and iii) whether buoyancy stabilizes the air against vertical mixing or not (“stability”). Of these, the wind speed is the most important. Thus, defining two coefficients,  $C_{SH}$  and  $C_{LE}$ , as the bulk exchange parameters for heat and moisture, a first approximation takes the form (Oerlemans, 2001):

$$SH = \rho_a \cdot c_p \cdot C_{SH} \cdot V \cdot (T - T_s) \quad (1)$$

## 7. Computation of turbulent fluxes distributed over the glacier surface. The case study of the Forni Glacier (Italian Alps)

---

$$LE = \rho_a \cdot L_V \cdot C_{LE} \cdot V \cdot (q - q_S) \quad (2)$$

where  $\rho_a$  is air density,  $c_P$  is the specific heat capacity of air at constant pressure,  $L_V$  is the latent heat of vaporisation.  $V$ ,  $T$  and  $q$  are the wind speed, temperature and specific humidity at the reference level.  $T_S$  and  $q_S$  are temperature and humidity at the surface. The turbulent exchange coefficients (denoted by  $C_{SH}$  and  $C_{LE}$ , dimensionless) depend on the height at which the measurements are performed (Oerlemans and Klok, 2002). In fact,  $V$ ,  $T$  and  $q$  are regarded as representative values for the lower boundary layer, assumed to be thoroughly mixed (Garratt, 1992) and then these parameters vary with height. For this reason, the above shown algorithms can be considered as the “bulk aerodynamic approach”.

In more details  $C_{SH}$  and  $C_{LE}$  should be considered as empirical constants that depend on the nature of the turbulence and, consequently, on the general atmospheric conditions and the roughness. Values found from field experiments are in the  $10^{-2}$  to  $10^{-4}$  range (Oerlemans, 2001).

These algorithms are valid for neutral conditions. When the atmosphere is not neutrally stratified but is stably stratified (i.e. potential temperature increases with height) or unstably stratified (i.e. potential temperature decreases with height), the scheme to calculate the fluxes is normally modified by applying Monin-Obukov similarity theory (MO-theory) (Stull, 1988). The major implication is that the turbulent fluxes are suppressed in stable conditions and enlarged in unstable conditions. Since the temperature and wind profiles themselves depend on the fluxes, it is now more complicated to determine the fluxes from measurements (Munro and Davies, 1978). In the first place, measurements are needed from at least two levels. Secondly, some kind of iterative procedure has to be used.

Over melting glacier surfaces, the application of MO-theory turns out to be problematical. Because of the large stability (temperature gradients of the order of  $1 \text{ K m}^{-1}$ ) and the rough surface there is a zero-referencing problem: the fluxes and surface roughnesses determined by MO-theory become very dependent on how the height of the instruments is defined (Munro, 1989). This is an undesirable situation. It appears that the use of bulk equations in combination with a method for determining the surface roughness with a microtopographic method yield satisfactory results.



## 7. Computation of turbulent fluxes distributed over the glacier surface. The case study of the Forni Glacier (Italian Alps)

---

On the Forni Glacier the turbulent fluxes computation were already investigated in Senese et al. (2012a and 2012b). In this case the point energy balance model was applied from meteorological data recorded by a supraglacial automatic weather station (AWS) set up on the Forni Glacier tongue (named AWS1 Forni). Because measurements were available for one level only, no attempt was made to use sophisticated schemes for the calculation of the turbulent heat fluxes. Instead the well-known bulk aerodynamic formulas were used according to the methods introduced by Oerlemans (2000):

$$SH = \rho_a \cdot c_P \cdot C_H \cdot V_{2m} \cdot (T_{2m} - T_S) \quad (3)$$

$$LE = 0.622 \cdot \rho_a \cdot L_V \cdot C_H \cdot V_{2m} \cdot \frac{(e_{2m} - e_S)}{p} \quad (4)$$

where  $\rho_a$  is air density ( $0.87 \text{ kg m}^{-3}$ ),  $c_P$  is the specific heat of dry air ( $1004 \text{ J kg}^{-1} \text{ K}^{-1}$ ),  $C_H$  is the turbulent exchange coefficient ( $0.00127 \pm 0.00030$ ; from Oerlemans, 2000),  $V_{2m}$  is wind speed value at 2 m,  $T_{2m}$  is air temperature value at 2 m,  $T_S$  is the surface temperature,  $L_V$  is the latent heat of vaporization (Harrison, 1963),  $e_{2m}$  is vapor pressure value at 2 m,  $e_S$  is vapor pressure value at the surface (calculated using the Wexler formula; Wexler, 1976) and  $p$  is air pressure value at sensor level. The  $T_S$  was calculated by using the Stephan-Boltzmann law:

$$T_S = \sqrt[4]{\frac{LW_{out}}{\sigma \cdot \varepsilon}} \quad (5)$$

where  $\sigma$  is the Stephan-Boltzmann constant,  $5.67 \cdot 10^{-8} \text{ W m}^{-2} \text{ K}^{-4}$  and  $\varepsilon$  is the emissivity of the snow/ice surface, assumed to be equal to the unity. Wind speed and air temperature and humidity were measured at 5 m and 2.6 m respectively, then they were calculated at 2 m (following the method introduced by Oerlemans, 2000). The  $C_H$  was assumed to be constant, because no information on how the roughness lengths change during the year was available (Oerlemans and Klok, 2002). An overestimation of the turbulent fluxes calculations may occur in spring due to overestimation of air temperature under low wind/high global radiation conditions.

Some issues can be arisen whenever the turbulent fluxes above a glacier surface are calculated from data of synoptic weather station located close the glacier. In fact the

## 7. Computation of turbulent fluxes distributed over the glacier surface. The case study of the Forni Glacier (Italian Alps)

temperatures, vapour pressures and wind speeds measured outside the glacier surface differ from the values recorded in the glacier boundary layer, where the glacier wind affects them. In Figure 1 a typical summer time situation in a glacierized mountain region is sketched. Mountains appears as large roughness elements to the synoptic-scale atmospheric flow and a large-scale boundary layer will be present (Fig. 1, on the left). On the other hand in the valleys the diurnal rhythm of the valley/mountain wind system dominates the flow (Fig. 1, on the right). It interacts with the large-scale boundary layer in a complex way. The glacier wind is a tiny element of this system but regulates the turbulent fluxes to or from the glacier surface. Balloon ascents have made it clear that the glacier wind is rather shallow, normally only some tens of metres. Measurements have also shown that it does not penetrate very far into the valley. At the point where the valley and glacier wind meet, a weak front is present (indicated by F in Figure 1). On really warm summer days the valley wind can become so strong that it erodes the glacier wind on the lower part of the glacier: the front moves upwards.

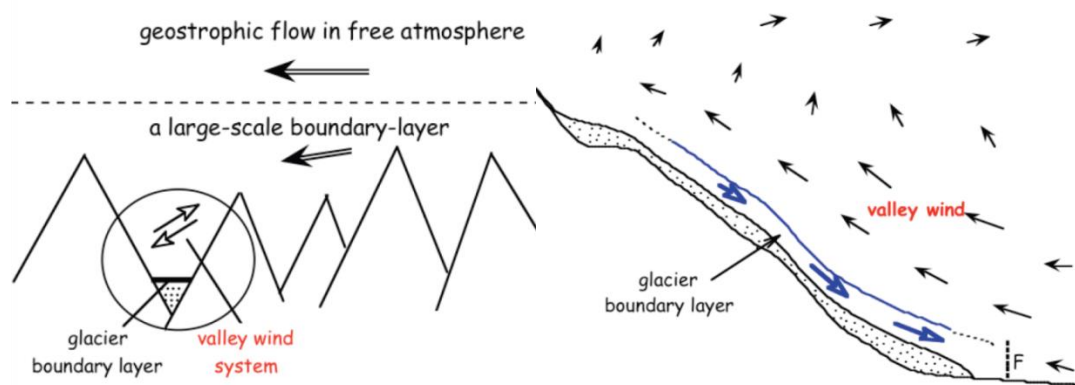


Fig. 1: The basic structure of atmospheric circulation in a glacierized mountain region (from Oerlemans, 2001).

## 2. Methods

As explained in the introduction it is very difficult to assess the wind, temperature and humidity conditions over the glacier surface from data recorded outside the glacier or in the valley. Methods to estimate the turbulent fluxes should therefore relate the atmospheric conditions outside the glacier boundary layer to those inside it. To supply this issue we applied the algorithms proposed by Oerlemans and Grisogono (2002) in

## 7. Computation of turbulent fluxes distributed over the glacier surface. The case study of the Forni Glacier (Italian Alps)

---

order to calculate the turbulent fluxes and the approach suggested by Shea and Moore (2010) for distributing the vapour pressure.

The sensible ( $SH$ ) and latent ( $LE$ ) heat flux are assessed as (Oerlemans and Grisogono, 2002; Oerlemans, 2010):

$$SH = \rho_a \cdot c_p \cdot C^* \cdot (T_{2m} - T_S) \quad (6)$$

$$LE = 0.622 \cdot \rho_a \cdot L_V \cdot C^* \cdot \frac{(e_{2m} - e_S)}{p} \quad (7)$$

where  $\rho_a$  is air density ( $0.87 \text{ kg m}^{-3}$ ),  $c_p$  is the specific heat of dry air ( $1004 \text{ J kg}^{-1} \text{ K}^{-1}$ ),  $T_{2m}$  is air temperature value at 2 m,  $T_S$  is the surface temperature,  $L_V$  is the latent heat of vaporization (Harrison, 1963),  $e_{2m}$  is vapor pressure value at 2 m,  $e_S$  is vapor pressure value at the surface (calculated using the Wexler formula; Wexler, 1976) and  $p$  is air pressure value at sensor level.

There are two contributions to the turbulent exchange coefficient (denoted by  $C^*$ , taken equal for the latent and sensible heat flux).  $C_{kat}$  represents the contribution from the katabatic wind system and  $C_b$  represents a back-ground contribution associated with the turbulence generated by the atmospheric circulation on a synoptic/regional scale.  $C^*$  can be calculated as:

$$C^* = \begin{cases} C_b + C_{kat} = C_b + k \cdot (T_{2m} - T_S) \cdot \sqrt{\frac{g}{T_0 \cdot \lambda_{PT} \cdot Pr}} & \text{for } T_{2m} - T_S > 0 \\ C_b & \text{for } T_{2m} - T_S \leq 0 \end{cases} \quad (8)$$

where  $k$  is an empirical constant,  $g$  is the gravity,  $T_0$  is a reference temperature ( $273.15 \text{ K}$ ),  $\lambda_{PT}$  is the background potential temperature lapse rate, and  $Pr$  is the eddy Prandtl number. Values for  $Pr$  and  $k$  were taken from Oerlemans and Grisogono (2002) estimated from extensive eddy correlation measurements on Pasterze Glacier ( $Pr = 5$  and  $k = 0.0004$ ). We calculated  $\lambda_{PT}$  from the potential air temperature estimated at Bormio (1225 m a.s.l., a village ca. 17 km far from the Forni Glacier terminus) and at the AWS1 Forni site (2631 m a.s.l.). The potential temperature ( $\theta$ ) is the temperature which a parcel of air would have if it were brought adiabatically to the reference pressure ( $p_0$ , usually taken to be 1000 mbar or  $1.01325 \times 10^5 \text{ Pa}$ ):

7. Computation of turbulent fluxes distributed over the glacier surface. The case study of the Forni Glacier (Italian Alps)

---

$$\theta = T \left( \frac{p_0}{p} \right)^{R/c_p} \quad (9)$$

where  $p$  is the actual atmospheric pressure,  $R$  is the gas constant for air ( $8.31 \text{ J K}^{-1} \text{ mol}^{-1}$ ) and  $c_p$  is the specific heat of dry air ( $1004 \text{ J kg}^{-1} \text{ K}^{-1}$ ). The potential temperature is generally useful because it remains constant as a parcel undergoes an adiabatic change pressure (Hartmann, 1994). The vertical gradient of potential temperature determines the dry static stability of the atmosphere. If  $\theta$  increases with height, then parcels raised adiabatically from their initial height will always be colder and thus more dense than their environment and will sink back to their original pressure:

$$\lambda_{TP} = \frac{d\theta}{dz} > 0 \rightarrow \textit{stable} \quad (10)$$

If the potential temperature decreases with height, then parcels raised up will be warmer than their environment when they reach the lower pressure and will accelerated upward by buoyancy (Hartmann, 1994):

$$\lambda_{TP} = \frac{d\theta}{dz} < 0 \rightarrow \textit{unstable} \quad (11)$$

Whenever  $\lambda_{PT}$  assumed negative values (e.g. on very warm days),  $C_{kat}$  cannot be calculated (Klok and Oerlemans, 2002).

$C_b$  was optimized from 2006-2009 hourly turbulent fluxes calculated in Senese et al. (2012a; 2012b).

In order to assess the sensible heat flux ( $SH$ ) the air temperature ( $T_g$ ) was distributed applying a most suitable lapse rate ( $\lambda_T$ ) found processing 4-year data (from 1<sup>st</sup> January 2006 to 31<sup>st</sup> December 2009) from Bormio (1225 m a.s.l.), S. Caterina Valfurva (1730 m a.s.l.) and Forni Diga (2180 m a.s.l.) weather stations (located at villages nearby the Forni Glacier). These two latter stations were not included in the computation of the potential temperature gradient (equations 9, 10 and 11) as the pressure datasets were not available. We calculated hourly series of lapse rates considering the following couples of weather stations: i) Bormio and AWS1 Forni, ii) S. Caterina Valfurva and AWS1 Forni and iii) Forni Diga and AWS1 Forni. In order to avoid thermal inversions affecting too much the data, only the warmest hours per day (from 12 am to 4 pm) have

## 7. Computation of turbulent fluxes distributed over the glacier surface. The case study of the Forni Glacier (Italian Alps)

been considered in the calculation of the daily average lapse rate values. Finally we found a function between lapse rate values ( $\lambda_T$ ) and time (day) following a truncated Fourier series at the second order (Fig. 2):

$$\lambda_T = -7.88 + 1.27 \cos\left(\frac{day \cdot 2\pi}{365}\right) + 0.45 \sin\left(\frac{day \cdot 2\pi}{365}\right) - 0.16 \cos\left(2 \frac{day \cdot 2\pi}{365}\right) - 0.73 \sin\left(2 \frac{day \cdot 2\pi}{365}\right) \quad (12)$$

where *day* corresponds to the Julian date (1 = 1<sup>st</sup> January, 365 = 31<sup>st</sup> December) (for more details in the method for distributing air temperature see Senese et al., submitted and the chapter 5 of this PhD Thesis). Leap years are neglected and the introduced errors are considered unimportant (Hock and Tijm-Reijmer, 2011).

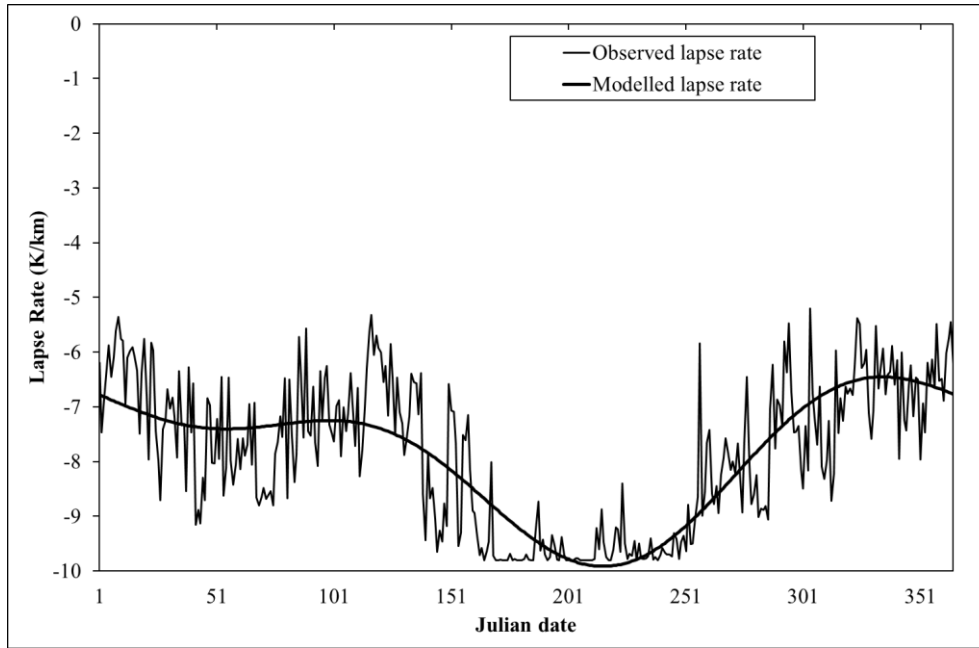


Fig. 2: Daily averaged temperature lapse rate calculated considering only the hottest hours per day (from 12 am to 4 pm, “observed” in the legend) and the smoothed daily values obtained by a truncated Fourier series at the second order (“modelled” in the legend).

To define the latent heat flux (*LE*) we distributed the vapour pressure ( $e_g$ ) over the whole glacier surface following the approach proposed by Shea and Moore (2010). They compared on-glacier observations with the ambient values estimated from a

7. Computation of turbulent fluxes distributed over the glacier surface. The case study of the Forni Glacier (Italian Alps)

---

regional network of off-glacier weather stations. In particular they found variations in near-surface vapour pressure related to processes of condensation or evaporation/sublimation at the glacier surface, which are controlled by the vapour pressure gradient between the surface and the ambient air.

We firstly analysed air temperature ( $T$ ) and relative humidity ( $RH$ ) to estimate the saturation vapour pressure ( $e_s$ ) following Tetten's formulae (Bolton, 1980):

$$e_s = \begin{cases} 6.108 \cdot 10^{(9.5 \cdot T)/(T+265.5)}, & T > 0^\circ\text{C} \\ 6.108 \cdot 10^{(7.5 \cdot T)/(T+237.3)}, & T \leq 0^\circ\text{C} \end{cases} \quad (13)$$

and the vapour pressure ( $e$ ) was then calculated as:

$$e = e_s \cdot \frac{RH}{100} \quad (14)$$

From  $T_a$  and  $RH_a$  hourly data recorded by Bormio (1225 m a.s.l.) and Santa Caterina Valfurva (1730 m a.s.l.) weather stations, the vapour pressure for the ambient was estimated ( $e_a$ ), and then the daily vertical gradient was defined from 1<sup>st</sup> January 2006 to 31<sup>st</sup> December 2009 datasets. Finally to smooth this record, a regression model was used between daily mean lapse rate values ( $\lambda_e$ ) and time ( $day$ ) following a truncated Fourier series at the second order (Fig. 3):

$$\lambda_e = -0.00571 + 0.00382 \cos\left(\frac{day \cdot 2\pi}{365}\right) + 0.00098 \sin\left(\frac{day \cdot 2\pi}{365}\right) - 0.00028 \cos\left(2 \frac{day \cdot 2\pi}{365}\right) - 0.00030 \sin\left(2 \frac{day \cdot 2\pi}{365}\right) \quad (15)$$

where  $day$  corresponds to the Julian date (1 = 1<sup>st</sup> January, 365 = 31<sup>st</sup> December). Leap years are neglected and the introduced errors are considered unimportant (Hock and Tijm-Reijmer, 2011).

In this case the dataset collected at the Forni Diga station was not considered due to the unavailability of relative humidity values.

## 7. Computation of turbulent fluxes distributed over the glacier surface. The case study of the Forni Glacier (Italian Alps)

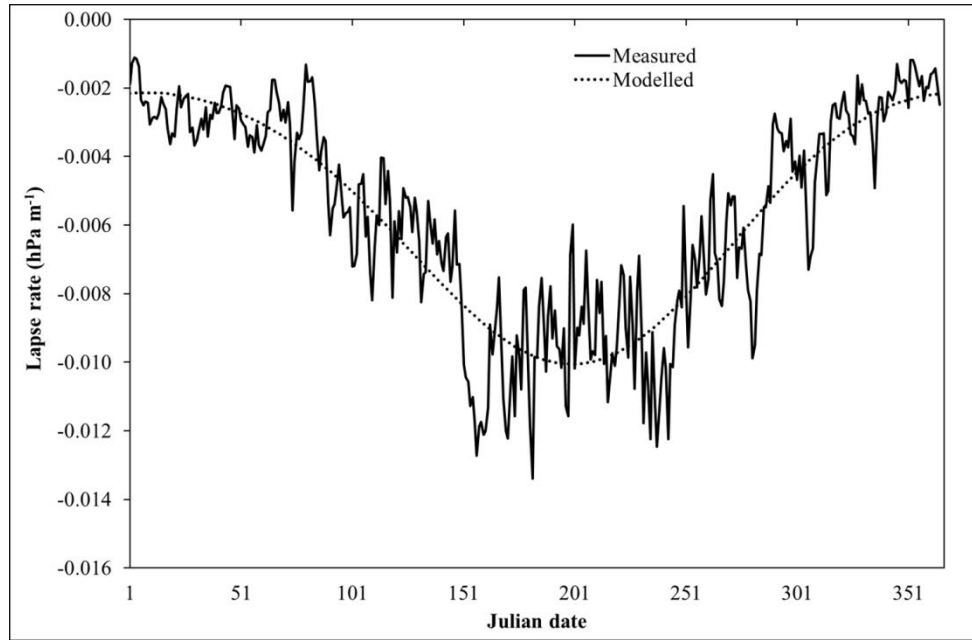


Fig. 3: Daily averaged vapor pressure lapse rate and the smoothed daily values obtained by a truncated Fourier series at the second order (“modelled” in the legend).

Applying this  $\lambda_e$  dataset, the ambient vapour pressure ( $e_{a-AWS}$ ) was calculated from  $e_a$  estimated at Bormio and shifted to the AWS1 Forni elevation.

From data collected by the AWS1 Forni ( $T_{AWS}$  and  $RH_{AWS}$ ), the observed vapour pressure for the glacier near-surface ( $e_{AWS}$ ) was calculated.

Two separate linear functions were determined from the glacier near-surface and ambient values of vapour pressure estimated at the AWS1 Forni site ( $e_{AWS}$  and  $e_{a-AWS}$ , respectively), depending on the measured temperature ( $T_{AWS}$ ):

$$e_{AWS} = \begin{cases} j_1 \cdot e_{a-AWS} + j_2, & T_{AWS} \geq 0^\circ\text{C} \\ j_3 \cdot e_{a-AWS} + j_4, & T_{AWS} < 0^\circ\text{C} \end{cases} \quad (16)$$

where  $j_i$  are fitted coefficients.

### 3. Results and discussions

The village of Bormio is located in an area wetter than Santa Caterina Valfurva (Tab. 1). In fact from 2006 to 2009 daily data, the mean value of vapour pressure estimated at Bormio is higher than the one calculated from Santa Caterina Valfurva dataset (8.87 hPa

7. Computation of turbulent fluxes distributed over the glacier surface. The case study of the Forni Glacier (Italian Alps)

and 6.15 hPa, respectively). Generally Bormio area features more snowfall than Santa Caterina Valfurva even if, due to the lower altitude and consequently the more intense thaw processes, the snow is completely melted out earlier.

*Tab. 1: Minimum, mean, maximum values of vapour pressure estimated at Bormio (1225 m a.s.l.) and Santa Caterina Valfurva (1730 m a.s.l.) (values in hPa).*

	<b>Bormio</b>			<b>Santa Caterina Valfurva</b>		
	<b>Max</b>	<b>Mean</b>	<b>Min</b>	<b>Max</b>	<b>Mean</b>	<b>Min</b>
2006	20.81	9.14	1.98	14.25	6.21	1.28
2007	22.52	9.61	2.52	12.97	6.02	1.41
2008	18.98	8.59	2.08	13.77	6.31	1.39
2009	19.70	8.15	1.14	14.52	6.09	0.70
<b>Mean</b>	<b>22.52</b>	<b>8.87</b>	<b>1.14</b>	<b>14.52</b>	<b>6.15</b>	<b>0.70</b>

The daily vertical gradient of vapour pressure ( $\lambda_e$ ) calculated from Bormio and Santa Caterina Valfurva data resulted ranging from  $-0.002 \text{ hPa m}^{-1}$  to  $-0.010 \text{ hPa m}^{-1}$ . This results quite in agreement with findings for example by Shea and Moore (2010) at the southern Coast Mountains of British Columbia (from  $-0.001 \text{ hPa m}^{-1}$  to  $-0.006 \text{ hPa m}^{-1}$ ).

*Tab. 2: Minimum, mean, maximum values of vapour pressure vertical gradient ( $\text{hPa m}^{-1}$ ) calculated from Bormio (1225 m a.s.l.) and Santa Caterina Valfurva (1730 m a.s.l.) data.*

	<b>Max</b>	<b>Mean</b>	<b>Min</b>
2006	-0.026	-0.008	-0.0002
2007	-0.020	-0.007	-0.001
2008	-0.013	-0.004	-0.0002
2009	-0.016	-0.004	-0.001
<b>Mean</b>	<b>-0.013</b>	<b>-0.005</b>	<b>-0.001</b>
<b>Modelled</b>	<b>-0.010</b>	<b>-0.005</b>	<b>-0.002</b>

From Bormio data we calculated the ambient vapour pressure at the AWS1 Forni elevation ( $e_{a-AWS}$ ) applying the lapse rate (equation 15) and we compared these values with  $e_{AWS}$  dataset from 2006 to 2009 (Fig. 4). A higher annual variability was found with regards to the ambient values respect to the glacier ones which featured lower values especially during summer season. This can be due to the climate conditions occurring at Bormio area which was found wetter for instance than Santa Carterina



## 7. Computation of turbulent fluxes distributed over the glacier surface. The case study of the Forni Glacier (Italian Alps)

Valfurva. Anyway from 2008 to 2009 the differences between vapour pressures measured from AWS1 Forni and estimated from Bormio data resulted less evident.

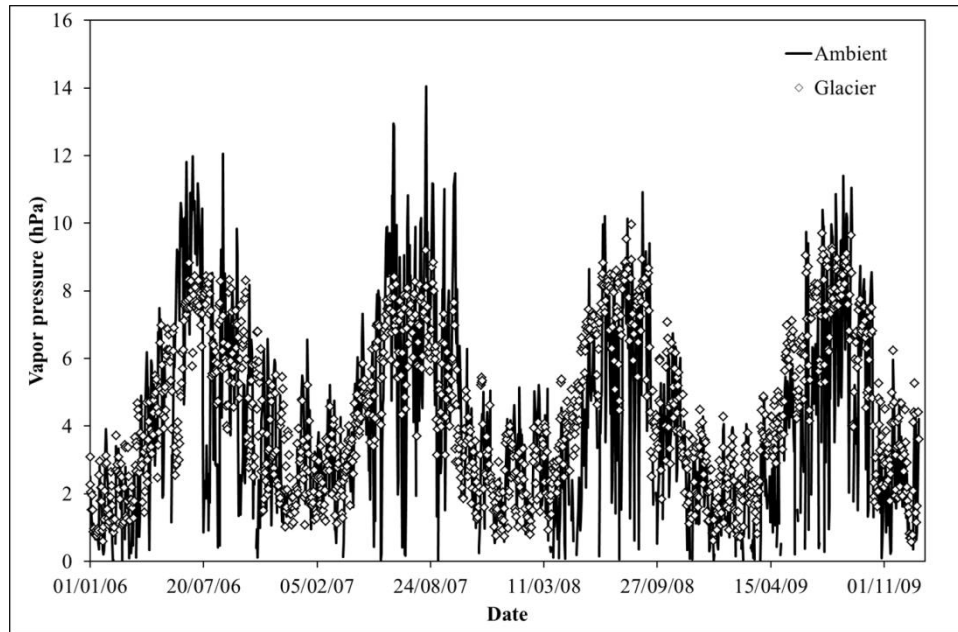


Fig. 4: Ambient and observed vapour pressure at the AWS1 Forni site from 2006 to 2009.

A scatter plot of  $e_{a-AWS}$  and measured  $e_{AWS}$  at AWS1 Forni site illustrates the behaviour of near-surface vapour pressure within the katabatic boundary layer (Fig. 5). Two separate linear functions resulted:

$$e_g = \begin{cases} 0.29 \cdot e_a + 4.79, & T_g \geq 0^\circ\text{C} \\ 0.34 \cdot e_a + 2.01, & T_g < 0^\circ\text{C} \end{cases} \quad (17)$$

The root mean squared error (*RMSE*) resulted 0.99 hPa and 1.33 hPa with regards to negative and positive temperature, respectively. Reduced values of  $e_g$  are observed for  $e_a > 6.11$  hPa and enhanced values of  $e_g$  result for  $e_a < 6.11$  hPa.

The regression lines resulted in agreement with findings by Shea and Moore (2010), in fact they found the  $j_i$  fitted coefficients ranging from 0.43 to 0.79 ( $j_1$ ), from 1.34 to 2.92 ( $j_2$ , in hPa), from 0.63 to 1.21 ( $j_3$ ), from -1.69 to 1.41 ( $j_4$ , in hPa). Moreover the regression line for  $T_g \geq 0^\circ\text{C}$  featured a slope less than the unity ( $j_1 < 1$ ) and cross the 1:1 line near 6.11 hPa as defined also by Shea and Moore (2010). With regard to the linear fit for observations below  $0^\circ\text{C}$ , a slope near the unity ( $j_3 = 1$ ) and an intercept near zero

## 7. Computation of turbulent fluxes distributed over the glacier surface. The case study of the Forni Glacier (Italian Alps)

( $j_4 = 0$  hPa) indicate that moisture exchanges between the surface and the near-surface layers appear to be minimal (Shea and Moore, 2010). These values did not result from our observations thus suggesting a more occurrence of moisture exchanges. This can be due to the climate conditions over the area studied by Shea and Moore (2010): the southern Coast Mountains of British Columbia generally feature a maritime climate and hence wetter than the central Italian Alps (where the Forni Glacier is located).

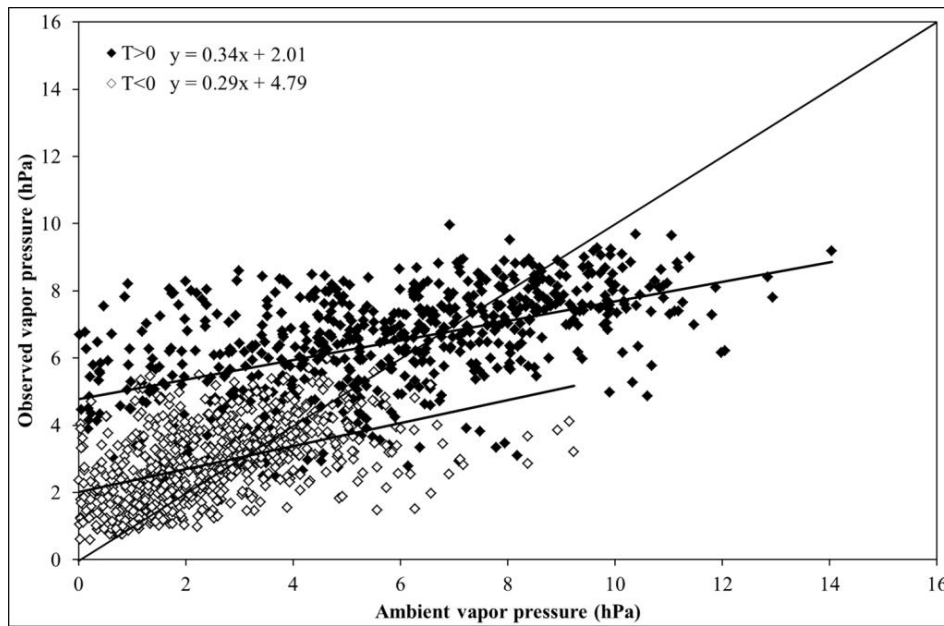


Fig. 5: Scatter plot showing ambient (x-axis) and observed (y-axis) vapour pressure at the AWS1 Forni site from 2006 to 2009.

The background potential temperature lapse rate between Bormio and AWS1 Forni sites ( $\lambda_{PT}$ ) resulted ranging from  $-0.0053 \text{ K m}^{-1}$  to  $0.0140 \text{ K m}^{-1}$  from 2006 to 2009. The largest part of hours featured a positive gradient (90.16%). On the other hand about 1/3<sup>rd</sup> of the negative values are found in the warmer hours (from 1 pm to 3 pm).

From values of air and surface temperature collected by AWS1 Forni ( $T_{2m}$  and  $T_S$ , respectively), reference temperature ( $T_0$ ) and background potential temperature lapse rate between Bormio and AWS1 Forni sites ( $\lambda_{PT}$ ), hourly  $C_{kat}$  values were estimated from 2006 to 2009 with a mean value of 0.0035 (ranging from 0 to 0.3437). This results in agreement with the values found in the literature dealing with this approach: for instance Klok and Oerlemans (2002) found a mean  $C_{kat}$  value of 0.0031 during 2009.

## 7. Computation of turbulent fluxes distributed over the glacier surface. The case study of the Forni Glacier (Italian Alps)

---

Generally  $C_{kat}$  is largest on warm days because the temperature difference between the air and the glacier surface is large and the potential temperature gradient often small (Klok and Oerlemans, 2002). On these days, glacier winds develop and generate turbulence.

The turbulent exchange coefficient ( $C^*$ ) resulted equal for both the latent and sensible heat flux as observed also in Oerlemans (2010). Its mean value was found equal to 0.0055.

Finally from 2006-2009 hourly turbulent fluxes of sensible and latent heat calculated in Senese et al. (2012a; 2012b), a mean value of  $C_b$  was found equal to 0.0027 ranging from -0.3411 to 0.0277. This value was compared with findings by Klok and Oerlemans (2002). They optimized this back-ground turbulent exchange coefficient ( $C_b$ ) in a such a way that calculated melt was in agreement with observed melt for 1999, obtaining a value of 0.0037. In that case the wind values were not available due to a wind speed sensor was not installed at the supraglacial automatic weather station. On the other hand the AWS1 Forni is equipped with an anemometer as well, making possible a more accurate computation of  $C_b$ . In fact we firstly calculated the turbulent fluxes applying the well-known bulk aerodynamic formulas (equations 3 and 4), secondly we estimate  $C^*$  (from equations 6 and 7) and  $C_{kat}$  (from the second term in the first formula of equations 8) and then we estimated  $C_b$  following equation 8. In spite of different approaches in calculating  $C_b$  respect to Klok and Oerlemans (2002) we found similar values of the back-ground turbulent exchange coefficient.

## 4. Conclusions

In this chapter the spatial distribution of the turbulent fluxes was investigated. They feature lower influence on ablation amount with respect to the radiative components: the sensible heat flux affects for 16% of the net energy amount and the latent heat flux for 2% (Senese et al., 2012a). In any case the turbulent fluxes play an important role in shaping boundary layers.

To assess these fluxes over the whole glacier surface, it was necessary to distribute the air temperature and the vapour pressure. The first one was already investigated in Senese et al. (submitted, see chapter 5 of this PhD Thesis). The computation of the distributed vapor pressure was analyzed in this chapter.

## 7. Computation of turbulent fluxes distributed over the glacier surface. The case study of the Forni Glacier (Italian Alps)

---

The input data were the daily vertical gradient of vapour pressure ( $\lambda_e$ ), the ambient vapour pressure estimated at Bormio site ( $e_a$ ) and the measured glacier near-surface vapour pressure ( $e_{AWS}$ ).

The daily vertical gradient ( $\lambda_e$ ) calculated from Bormio and Santa Caterina Valfurva data (equation 15) resulted ranging from  $-0.002 \text{ hPa m}^{-1}$  to  $-0.01 \text{ hPa m}^{-1}$  (in agreement with findings by Shea and Moore, 2010).

From Bormio  $e_a$  data, we calculated the ambient vapour pressure at the AWS1 Forni elevation ( $e_{a-AWS}$ ) applying the lapse rate ( $\lambda_e$ ). By comparing  $e_{a-AWS}$  with  $e_{AWS}$  dataset from 2006 to 2009, a higher annual variability was found with regards to the ambient values respect to the glacier ones which resulted featuring lower values especially during summer season. This can be due to the climate conditions occurring at Bormio area which was found wetter for instance than Santa Carterina Valfurva.

From a scatter plot of  $e_{a-AWS}$  and measured  $e_{AWS}$  at AWS1 Forni site, two separate linear functions resulted depending on  $T_{AWS}$  values (in equation 17  $e_a$  corresponds to  $e_{a-AWS}$ ,  $e_g$  to  $e_{AWS}$ , and  $T_g$  to  $T_{AWS}$ ), with a *RMSE* resulting 0.99 hPa and 1.33 hPa. In particular reduced values of  $e_g$  were observed for  $e_a > 6.11 \text{ hPa}$  and enhanced values of  $e_g$  resulted for  $e_a < 6.11 \text{ hPa}$ . These regression lines resulted in agreement with findings by Shea and Moore (2010): the regression line for  $T_g \geq 0^\circ\text{C}$  featured a slope less than the unity and cross the 1:1 line near 6.11 hPa as defined also by Shea and Moore (2010). With regard to the linear fit for observations below  $0^\circ\text{C}$ , a slope near the unity and an intercept near zero indicate that moisture exchanges between the surface and the near-surface layers appear to be minimal (Shea and Moore, 2010). These values did not resulted by our observations thus suggesting a more occurrence of moisture exchanges. This can be due to the climate conditions about the area studied by Shea and Moore (2010): the southern Coast Mountains of British Columbia feature a maritime climate and then as wetter as than the central Italian Alps (where the Forni Glacier is located). Finally the glacier near-surface vapour pressure at any glacier point ( $e_g$ ) can be estimated applying the algorithms showed in equation 17 to the ambient vapour pressure estimated at Bormio station and shifted to the glacier point elevation ( $e_a$ ) (by equation 15).

Apart from the distribution of both air temperature and vapour pressure parameters, it was necessary to assess the turbulent exchange coefficient ( $C^*$ ), found equal for the latent and sensible heat flux. In particular there are two contributions to the turbulent exchange coefficient: the contribution from the katabatic wind system ( $C_{kat}$ ) and a back-

## 7. Computation of turbulent fluxes distributed over the glacier surface. The case study of the Forni Glacier (Italian Alps)

---

ground contribution associated with the turbulence generated by the atmospheric circulation on a synoptic/regional scale ( $C_b$ ). The first one depends on the background potential temperature lapse rate ( $\lambda_{PT}$ ) estimated between Bormio and AWS1 Forni sites, and the air and surface temperatures collected by AWS1 Forni ( $T_{2m}$  and  $T_s$ , respectively). The latter coefficient was optimized from 2006-2009 hourly turbulent fluxes calculated in Senese et al. (2012a; 2012b). The obtained mean values of  $C^*$ ,  $C_{kat}$  and  $C_b$  (0.0055, 0.0035 and 0.0027, respectively) were found in agreement with findings for instance by Klok and Oerlemans (2002) in spite of different applied approaches. In fact Klok and Oerlemans (2002) optimized  $C_b$  from observed melt values for 1999 because the wind records were not available and then the turbulent fluxes cannot be calculated applying the well-known bulk aerodynamic formulas (which depend on wind speed values).

In this chapter we investigated several methods to estimate the turbulent fluxes over a glacier surface. For this reason we considered the sensible and latent heat fluxes assessed applying the well-known bulk aerodynamic formulas and applying another approach depending not directly on wind speed. In fact this latter is indirectly encountered in the back-ground turbulent exchange coefficient. Nevertheless we are looking for more accurate algorithms which allow to distribute the wind speed over the glacier surface. For this reason the literature dealing with the vertical structure of glacier wind regime was considered (e.g. Oerlemans, 2010). Generally well developed glacier winds occur over ablation regions where the melt rates are typically between 5 and 10 cm of ice per day and the morphology of the surface changes continuously. Moreover a well developed glacier wind is characterized by a distinct wind maximum at a height of 5 to 10 meters but it's influenced by the topography as well. During daytime the valley above the glacier is filled with warm air that is advected by the valley wind (negative downslope winds of up to  $-3 \text{ m s}^{-1}$ ). This leads to higher near surface temperatures, and also to a larger vertical temperature gradient near the surface. The advection of warm air has a two-fold effect on the strength of the glacier wind: i) the temperature deficit increases and implies a larger forcing to the glacier wind, ii) the upslope valley wind tends to retard the downslope glacier wind by friction. On very warm days the valley wind can be so strong that the glacier wind disappears temporarily. The mean daily cycle shows two maxima in the downslope wind component. The maximum in the night can be explained by the fact that katabatic downslope winds from the mountain walls

7. Computation of turbulent fluxes distributed over the glacier surface. The case study of the Forni Glacier (Italian Alps)

---

merge with the glacier wind. The maximum at the end of the afternoon is probably related to the weakening of the valley wind, while the temperature forcing is still large (Van den Broeke, 1997). With regards to future prospective in order to better understand these phenomena on the Forni Glacier, several wind sensors should be installed over the glacier and along the valley. In this way the spatial and temporal wind regime could be assessed.

## References

- Bolton D. (1980): The computation of equivalent potential temperature. *Mon. Weather Rev.*, 108, 1046-1053.
- Garratt J. R.: (1992): *The Atmospheric Boundary Layer*, Cambridge University Press, Cambridge, 316 pp.
- Hartmann D.L. (1994): *Global Physical Climatology*. Academic Press, 411 p.
- Harrison L.P. (1963): Fundamentals concepts and definitions relating to humidity. In Wexler A. (Editor) *Humidity and moisture*. Reinhold Publishing Co., N.Y, 3.
- Hock R. and Tilm-Reijmer C. (2011): A mass-balance, glacier runoff and multi-layer snow model. Program documentation and users manual.
- Klok E.J. and Oerlemans J. (2002): Model study of the spatial distribution of the energy and mass balance of Morteratschgletscher, Switzerland. *Journal of Glaciology*, 48 (163), 505-518.
- Munro D.S. and J.A. Davies (1978): On fitting the log-linear model to wind speed and temperature profiles over a melting glacier. *Boundary-Layer Meteorology*, 15, 423-437.
- Munro D.S. (1989): Surface roughness and bulk heat transfer on a glacier: comparison with eddy correlation. *Journal of Glaciology*, 35 (121), 343-348.
- Oerlemans J. (2000): Analysis of a 3 years meteorological record from the ablation zone of Morteratschgletscher, Switzerland: energy and mass balance. *Journal of Glaciology*, 46 (155), 571-579.
- Oerlemans J (2001): *Glaciers and Climate Change*, Lisse, Balkema, 2001.
- Oerlemans J. and Klok E.J. (2002): Energy balance of a glacier surface: analysis of automatic weather station data from the Morteratschgletscher, Switzerland. *Arctic, Antarctic, and Alpine Research*, 34 (4), 477-485.
- Oerlemans J. and Grisogono B. (2002): Glacier winds and parameterisation of the related surface heat fluxes. *Tellus*, 54A, 440-452.
- Oerlemans J. (2010): *The Microclimate of Valley Glaciers*. Igitur, Utrecht Publishing & Archiving Services, Universiteitsbibliotheek Utrecht, 138 pp.
- Röthlisberger H. and Lang H. (1987): Glacial hydrology. In Gurnell A.M. and Clark M.J. editors, *Glacio-fluvial sediment transfer. An Alpine perspective*. New York, Wiley, 207-284.

7. Computation of turbulent fluxes distributed over the glacier surface. The case study of the Forni Glacier (Italian Alps)

---

- Senese A., Diolaiuti G., Mihalcea C. and Smiraglia C. (2012a): Energy and mass balance of Forni Glacier (Stelvio National Park, Italian Alps) from a 4-year meteorological data record. *Arctic, Antarctic, and Alpine Research*, 44 (1), 122-134.
- Senese A., Diolaiuti G., Verza G.P. and Smiraglia C. (2012b): Surface energy budget and melt amount for the years 2009 and 2010 at the Forni Glacier (Italian Alps, Lombardy). *Geografia Fisica e Dinamica Quaternaria*, 35 (1), 69-77. DOI 10.4461/GFDQ.2012.35.7
- Senese A., Ferrari S., Maugeri M., Confortola G., Bocchiola D., Smiraglia C. and Diolaiuti G. (submitted): An enhanced T-index model including solar and infrared radiation to evaluate distributed ice melt at the Forni Glacier tongue (Italian Alps).
- Shea J.M. and Moore R.D. (2010): Prediction of spatially distributed regional-scale fields on air temperature and vapor pressure over mountain glacier. *Journal of Geophysical Research*, 115 (D23107).
- Stull R.B. (1988): *An Introduction to Boundary Layer Meteorology*. Kluwer (Dordrecht), 666 pp.
- Van den Broeke M.R. (1997): Structure and diurnal variation of the atmospheric boundary layer over a mid-latitude glacier in summer. *Bound.-Lay. Meteorol.*, 83(2), 183-205.
- Wexler A. (1976): Vapor pressure formulation for water in the range 0° to 100°C-A Revision. *Journal of Research of the National Bureau of Standards*, 80A, 775.



# Chapter 8

## **Ablation computation at the debris-covered area of Forni Glacier: an approach based on computation of debris thermal resistivity**

### **Abstract**

This study is aimed at evaluating the applicability of a simple method to quantify the distribute ice melting over the debris covered area of the Forni Glacier. In fact, even if the widest Italian valley glacier is largely debris-free, darkening phenomena are ongoing and the confluence of three ice streams originating from rock outcrops generates two distinct ice-cored medial moraines. Then to evaluate the melt amount of the whole glacier it is necessary to assess also the ablation derived from buried ice melt and this requires to model the heat conduction along the debris layer and the processes at the debris-ice contact.

The applied approach is based on the assumption that the debris layer is in thermal equilibrium, i.e. the heat stored in the layer is constant over time, and accepting it means that the conductive heat flux at the debris surface is the same as at the ice interface. This latter was estimated through a simple empirical calculation depending on the temperature gradient from surface debris to ice. This approach resulted a valid tool for estimating the ice losses over the medial moraines.

## 1. Introduction

This study is aimed at evaluating the applicability of a simple method to quantify the distribute ice melting over the debris covered area of the Forni Glacier (Italy). In fact, even if the widest Italian valley glacier is largely debris-free, darkening phenomena are ongoing (Diolaiuti and Smiraglia 2010; Diolaiuti et al. 2012) and the confluence of three ice streams originating from rock outcrops generates two distinct ice-cored medial moraines (Fig. 1) (Smiraglia, 1989). Then to evaluate the melt amount of the whole glacier it is necessary to assess also the ablation derived from buried ice melt and this requires to model the heat conduction along the debris layer and the processes at the debris-ice contact (Mihalcea et al., 2008; Nicholson and Benn, 2006). Metamorphic rocks, mostly micaschist rich in quartz, muscovite, chlorite and sericite, constitute the dominant lithology (Montrasio et al., 2008).

Moreover there is growing evidence that glacier recession due to global warming leads to a general increase in supra-glacial slopes, enhancing the rate of paraglacially-mobilized debris input from either bedrock or pre-existing sediment storages. Consequently, the supra-glacial debris cover is prone to enlargement (Kellerer-Pirklbauer et al., 2008; Diolaiuti et al., 2009; Pelfini et al., 2012). Generally the origins of the supra-glacial debris are from the erosion of the rocky sides of the glacier basin and from the following weathering processes. Consequently it is very important to study this phenomenon since a debris cover may play a significant role in glacier hydrology. For instance, Mattson (2000) showed that the debris cover on the Dome Glacier acts as a regulator of streamflow producing annual variances of volumetric discharge of only 1% between 1994 and 1995 as compared with 24% for the debris-free Athabasca Glacier. This most likely occurs because of the changes of moisture content within the debris cover between field seasons. When atmospheric conditions are warm and dry, and ample energy is available for melt, the debris cover retards the transfer of energy to the ice because of its low thermal conductivity. When atmospheric conditions are cool and wet, and little energy is available for melt, the debris cover promotes the transfer of energy to the ice because of its increased thermal conductivity. This implies that a debris-covered glacier may not be as sensitive to changes in climate as would be a debris-free glacier.

This particular role of the debris is due to its thickness which affects ice ablation rate and magnitude (e.g. Mihalcea et al., 2006; 2008). Debris cover provides ablation rates

## 8. Ablation computation at the debris-covered area of Forni Glacier: an approach based on computation of debris thermal resistivity

higher than upon bare ice whenever the debris thickness is thinner than a “critical value” (*sensu* Mattson et al., 1993; Kayastha et al., 2000). This is mainly due to rock thermal conductivity and debris albedo, this latter is generally lower than the reflectivity featured by bare ice. Conversely debris layer whenever thicker than the critical value reduces the effective net energy at the debris-ice interface decreasing magnitude and rates of ice melt (Fig. 1, on the right). The critical debris thickness depends on rock lithology, grain size, porosity and water content and then should be locally evaluated through field experiments, see Mattson et al., 1993 and Mihalcea et al., 2006). Then the surface energy flux is mainly used to increase debris temperature and only a residual conductive heat flux reaches the ice-debris interface, thus reducing energy available for melting.

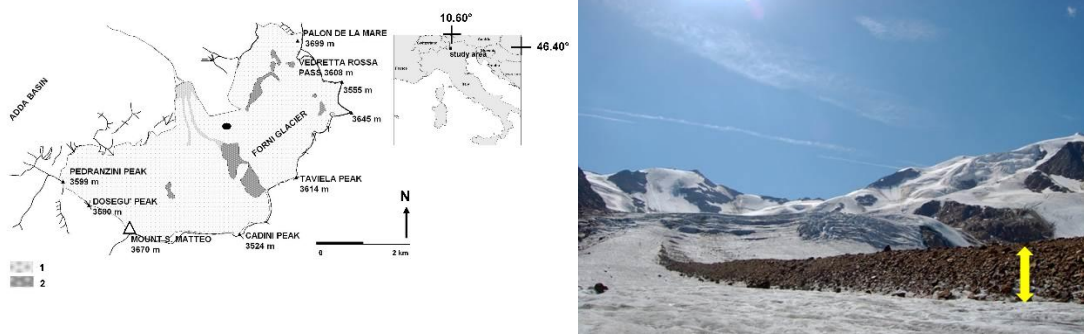


*Fig. 1: The Forni Glacier (Italian Alps). On the left the light grey areas are used to mark supraglacial debris coverage, the dark grey areas are used to indicate rock exposures and nunataks. On the right a detail of the eastern medial moraine (the yellow arrow remarks the elevation difference between bare and buried ice due to differential ablation processes: the buried ice melting slower than bare ice results higher).*

Due to the instable debris layer, it is almost difficult to manage an automatic weather station (AWS) above the glacier debris covered surface for more than one season, making problematic the availability of measured energy fluxes dataset (Fig. 2). The longest data set was acquired at the surface of the Miage debris covered Glacier where an AWS was running on summer 2005, 2006 and 2007 (see Brock et al., 2010). In Lombardy, on Venerocolo Glacier an AWS was set up at the debris-covered ablation area: it was installed on July 27<sup>th</sup> 2007 and removed on October 11<sup>th</sup> 2007 (Diolaiuti et al., 2011). Another example is represented by an experiment performed on summer

8. Ablation computation at the debris-covered area of Forni Glacier: an approach based on computation of debris thermal resistivity

2011 at the eastern medial moraine of the Forni Glacier: personnel from Ev-K2-CNR committee carried out field measurements of atmospheric black carbon concentration through a portable station named nanoSHARE (project developed under the umbrella of the SHARE - *Stations at High Altitude for Research on the Environment* - Program). The test regarding atmospheric sampling was successful but the medial moraine resulted affected by too fast movements thus not permitting to maintain the verticality of the instruments and then neither meteorological measurements nor energy ones were performed.

These experiments suggest to choose a simpler method to estimate the ice melting over the Forni medial moraines without depending on dedicated instruments to be deployed at the debris covered surfaces and maintained along the whole summer season. Then besides of a more accurate energy balance approach, we followed a simple approach, mainly based on the use of debris surface temperature and debris thermal resistance to determine the energy available for ice melting (Nakawo and Young, 1981; Nakawo and Takahashi, 1982; Mihalcea et al., 2008a).

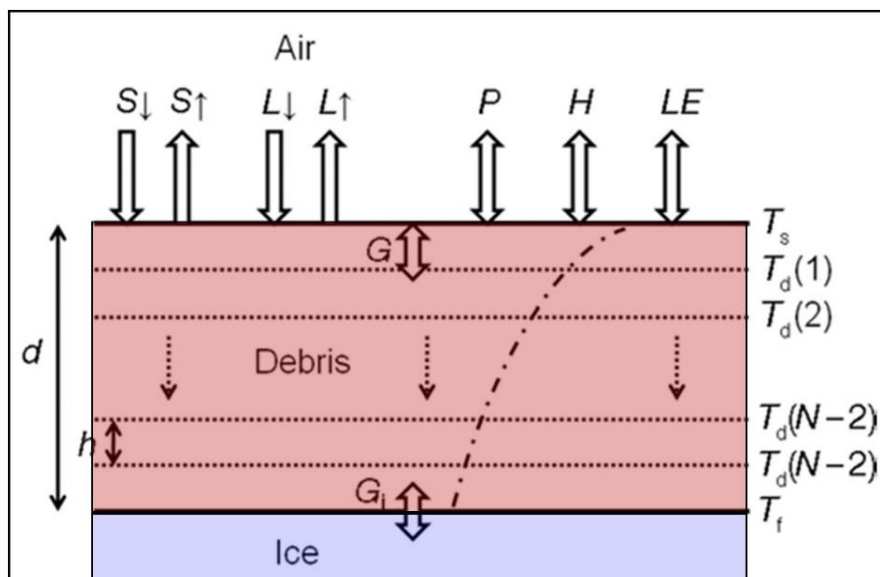


Fig. 2: Schematic of the debris energy balance model showing heat fluxes at the top and the bottom of a debris layer of thickness  $d$ . The dash-dot curve is an example of temperature profile where temperature increases toward the right (modified from Reid and Brock, 2010).

## 2. Methods

The data input of the model we applied to estimate the ice melting over the Forni medial moraines were: the surface debris temperature ( $T_S$ ), the debris thickness ( $d$ ) and the point measured ablation amount ( $M_{meas}$ ), this latter derived from field measurements through ablation stakes.

The point surface debris temperature ( $T_S$ , in °C) was measured during the summer season 2012 and 2013 (every 10 minutes) by thermistors and data loggers (further details of the method can be found in Mihalcea et al., 2008b), close to the ablation stakes. The sensor tips (Tinytag, Fig. 3) were attached to flat rock surface (2 cm thick, 10 cm x 10 cm), at 2 cm below the debris surface. The data recorded at this depth are normally considered the indicative of point surface temperature, and used within several international protocols to study permafrost and frozen ground (see Osterkamp, 2003; Guglielmin, 2006; Guglielmin et al., 2008).



*Fig. 3: The thermistor (Tinytag) installed at the base (bottom face) of a flat (ca. 2 cm deep) rock following the protocol of the permafrost (see Osterkamp, 2003; Guglielmin, 2006; Guglielmin et al., 2008).*

At the same site where we placed the thermistor we also measured the debris thickness ( $d_{meas}$ , in m) and drilled into the buried ice an ablation stake to quantify the melting rate ( $M_{meas}$ , in m w.e. considering an ice density equal to  $917 \text{ kg m}^{-3}$ ). The time frame we

## 8. Ablation computation at the debris-covered area of Forni Glacier: an approach based on computation of debris thermal resistivity

---

analyzed to calculate buried ice melt ranges from 56 to 99 days. The varying time frame is due to the intense surface instability and to the high dynamic featured by the terminal sector of the medial moraines which suggested in some cases an earlier retrieval of the instruments (especially during summer 2013). Moreover also a different time resolution in thermistor data logging affected the record length (especially during summer 2012). As depending on the energy available at the debris-ice interface, the melt amount ( $M$  in m w.e.) can be generally estimated as:

$$M = \frac{G \cdot \Delta t}{\rho_i \cdot L_m} \quad (1)$$

where  $G$  corresponds to the conductive heat flux,  $\Delta t$  the time-step,  $\rho_i$  the ice density ( $917 \text{ kg m}^{-3}$ ) and  $L_m$  is the latent heat of phase change of ice ( $3.34 \times 10^5 \text{ J kg}^{-1}$ ).  $G$  can be deduced from the temperature gradient from the top of the debris layer to the ice glacier surface:

$$G = \frac{(T_S - T_i)}{R} \quad (2)$$

where  $T_S$  is the debris surface temperature ( $^{\circ}\text{C}$ ),  $T_i$  is the ice temperature (set to the melting point during ablation season,  $0^{\circ}\text{C}$ ) and  $R$  is the effective thermal resistance of the debris layer ( $\text{m}^2 \text{ }^{\circ}\text{C W}^{-1}$ ). From equations 1 and 2, the observed thermal resistance ( $R_{obs}$ ) is quantified from the field measurements of melting ( $M_{meas}$ ) and from the measured surface temperature averaged in the considered time window ( $T_{S-ave}$ ):

$$R_{obs} = \frac{\sum T_{S-ave} \cdot \Delta t}{M_{meas} \cdot \rho_i \cdot L_m} \quad (3)$$

A linear relation from regression model between the measured debris thickness data ( $d_{meas}$ ) and the debris effective thermal resistance values from field measurements ( $R_{obs}$ ) was found ( $r = 0.997$ ). In this way since the debris thickness map of the Forni Glacier moraines will be calculated, the debris thermal resistance ( $R_{mod}$ ) can be estimated applying the obtained relation as well:

$$R_{mod} = 0.04457 \cdot d_{meas} \quad (4)$$

## 8. Ablation computation at the debris-covered area of Forni Glacier: an approach based on computation of debris thermal resistivity

---

Finally the ablation amount ( $M_{mod}$ , value in m w.e.) over the whole investigated debris-covered area ( $n$  pixels) in  $k$  days was modelled as:

$$M_{mod} = \sum_{i=1}^n \sum_{i=1}^k \left( \frac{T_S}{R} \frac{1}{L_m \rho_i} \Delta t \right) \quad (5)$$

in this case  $T_S$  is the daily mean surface debris temperature and  $\Delta t$  is number of seconds in a day ( $8.64 \times 10^4$ ).

### 3. Results

The measured surface temperature featured a typical daily cycle and resulted depending on the meteorological conditions (see an example in Fig. 4). In fact the most affecting parameter is the incoming shortwave radiation. For this reason whenever a snow layer covers the debris surface, this latter results isolated from the atmospheric conditions and is characterized by a constant temperature value. During summer 2012 two snowfalls occurred in the time frame July-October (see the blue circles in Fig. 4): in correspondence of these two events  $T_S$  remained continuously about at 0°C.



8. Ablation computation at the debris-covered area of Forni Glacier: an approach based on computation of debris thermal resistivity

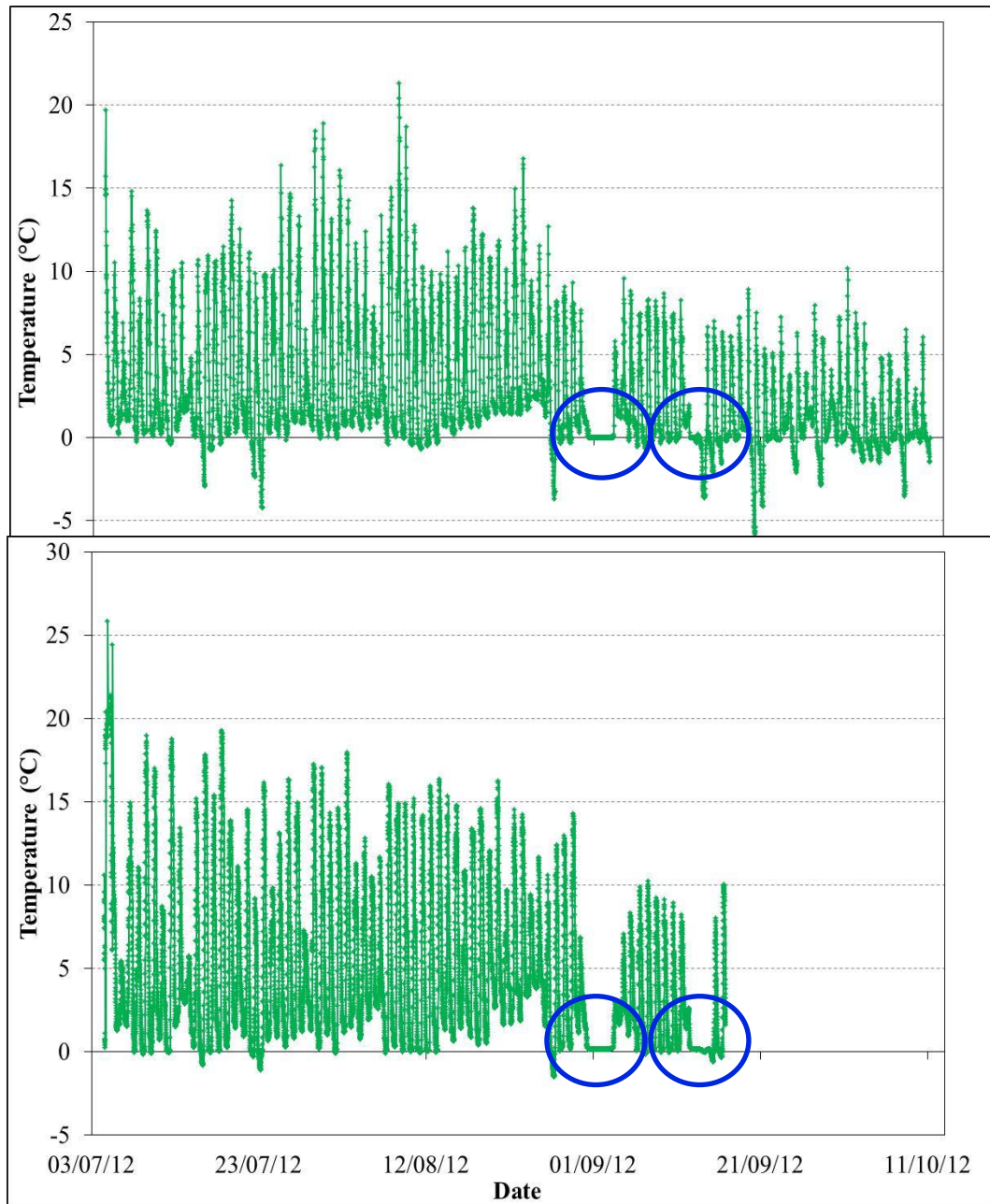


Fig. 4: The measured surface temperature during summer 2012 at 2491 m a.s.l. (above) and at 2635 m a.s.l. (at the bottom).

As expected the measured melt rate decreases with the elevation: from -0.029 m w.e. at 2491 m a.s.l. to -0.015 m w.e. at 2739 m a.s.l. (Tab. 1, column 5<sup>th</sup>).

The observed debris effective thermal resistance results ranging from  $0.0267 \text{ m}^2 \text{ }^\circ\text{C W}^{-1}$  to  $0.0758 \text{ m}^2 \text{ }^\circ\text{C W}^{-1}$  (with a debris thickness of 0.06 m and 0.17 m, respectively) (Tab. 1, column 8<sup>th</sup>). From the obtained relation between  $d_{meas}$  and  $R_{obs}$  (equation 4), the

8. Ablation computation at the debris-covered area of Forni Glacier: an approach based on computation of debris thermal resistivity

debris effective thermal resistance was estimated and the modelled values differ from the observed ones up to  $0.004 \text{ m}^2 \text{ }^\circ\text{C W}^{-1}$  (Tab. 1, column 9<sup>th</sup>).

The modelled cumulative melt amount resulted slightly underestimated up to -7.0% (Tab. 1, column 11<sup>th</sup>). This comparison of modelled and measured ablation data suggests to consider reliable our computations.

*Table 1: For each measurement site, the elevation (m a.s.l.), the considered time-frame (days), the measured debris thickness ( $d_{meas}$ , m), the measured ablation value ( $M_{meas}$ , m w.e.) and rate ( $M_{meas}$  rate,  $\text{m d}^{-1}$ ), the measured mean surface temperature ( $T_{S-ave}$ ,  $^\circ\text{C}$ ), the observed and modelled thermal debris resistance ( $R_{obs}$  and  $R_{mod}$  respectively,  $\text{m}^2 \text{ }^\circ\text{C W}^{-1}$ ), and finally the modelled ablation value ( $M_{mod}$ , m w.e.).*

Stake	Elevation (m a.s.l.)	Time frame (days)	$d_{meas}$ (m)	$M_{meas}$ (m)	$M_{meas}$ rate ( $\text{m d}^{-1}$ )	$T_{S-ave}$ ( $^\circ\text{C}$ )	$R_{obs}$ ( $\text{m}^2 \text{ }^\circ\text{C W}^{-1}$ )	$R_{mod}$ ( $\text{m}^2 \text{ }^\circ\text{C W}^{-1}$ )	$M_{mod}$ (m)	$\Delta M$ (%)
1	2491	99	0.06	-2.87	-0.029	2.71	0.0267	0.0284	-2.71	-5.5
2	2545	56	0.08	-1.48	-0.026	3.32	0.0354	0.0378	-1.39	-6.3
3	2635	74	0.17	-1.28	-0.017	4.63	0.0758	0.0804	-1.19	-7.0
4	2739	84	0.14	-1.28	-0.015	3.47	0.0642	0.0686	-1.20	-6.3

## 8. Ablation computation at the debris-covered area of Forni Glacier: an approach based on computation of debris thermal resistivity

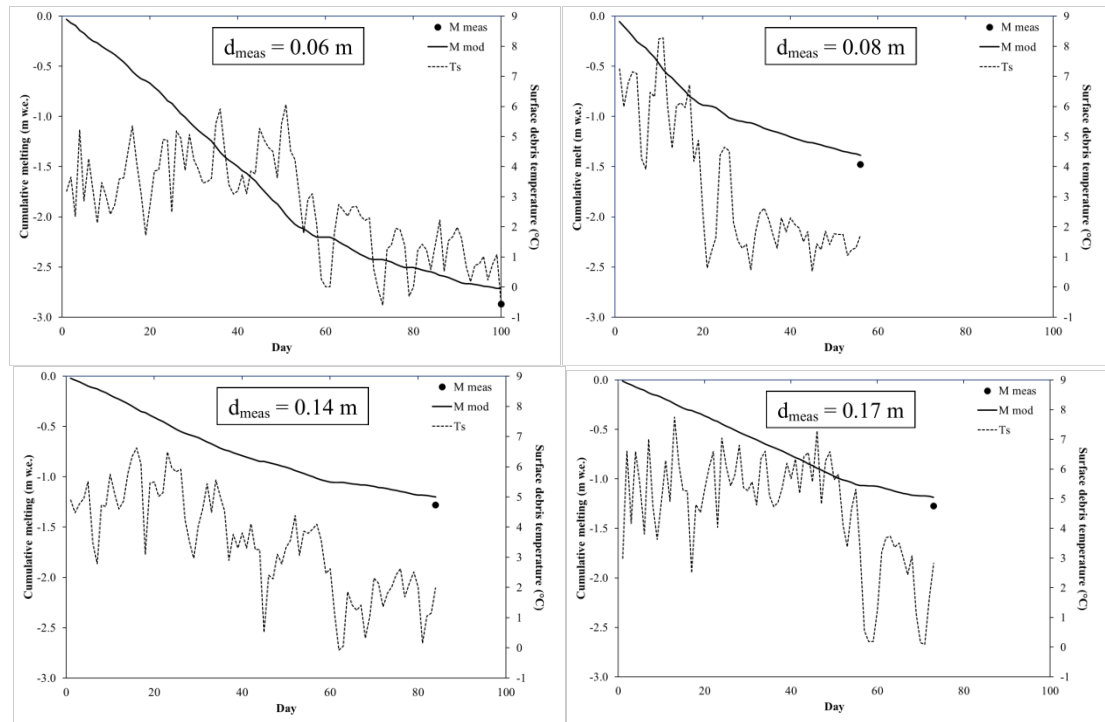


Fig. 5: The measured and modelled melting and the daily mean surface debris temperature during summer 2012 and 2013.

## 4. Discussion and conclusion

The applied approach is based on the assumption that the debris layer is in thermal equilibrium, i.e. the heat stored in the layer is constant over time, and accepting it means that  $G$  at the debris surface is the same as at the ice interface. However, surface temperatures of supraglacial debris vary on a variety of timescales in response to changing meteorological conditions, and this drives ongoing changes in the thermal regime of the debris layer. Nakawo and Young (1981) calculated day-time and night-time ablation from meteorological data, assuming steady state was attained over these timescales, but data from vertical temperature profiles through supraglacial debris demonstrate that this assumption is not valid (Nicholson, 2004).

Under stable weather conditions the thermal regime of the debris is dominated by the diurnal cycle (Conway and Rasmussen, 2000; Nicholson, 2004; Humlum, 1997), so in debris cover of more than a few centimeters in thickness, equilibrium within the debris layer cannot be expected over time intervals of anything less than 24 hours. Consequently, the assumption of a linear temperature gradient will not be met on sub-

## 8. Ablation computation at the debris-covered area of Forni Glacier: an approach based on computation of debris thermal resistivity

---

diurnal timescales, but is much more likely to apply on a 24 hour timescale (Conway and Rasmussen, 2000). For this reason the melt calculation is performed from daily temperatures although the availability of dataset with a higher time resolution.

The measured surface temperature resulted featuring a typical daily cycle and resulted depending on the meteorological conditions. In fact whenever a snow layer covers the debris surface, this latter results isolated from the atmospheric conditions and is characterized by a constant temperature value (about at 0°C). Consequently in these time frames the melt cannot occur.

The obtained relation between  $d_{meas}$  and  $R_{obs}$  allowed to estimate the debris effective thermal resistance with a slightly overestimation up to  $0.004 \text{ m}^2 \text{ }^\circ\text{C W}^{-1}$ . Consequently the modelled cumulative melt amount resulted slightly underestimated (i.e. up to -7.0%). In spite of this, the estimated ablation feature (like the measured one) an inverse trend with the elevation.

Finally we can conclude that our results demonstrate that a simple empirical calculation of the conductive heat flux depending on the temperature gradient from surface debris to ice can be considered a valid tool for estimating the ice losses over the medial moraines.

## References

- Brock B.W., Mihalcea C., Kirkbride M.P., Diolaiuti G., Cutler M.E.J. and Smiraglia C. (2010): Meteorology and surface energy fluxes in the 2005–2007 ablation seasons at the Miage debris-covered glacier, Mont Blanc Massif, Italian Alps.
- Conway H. and Rasmussen L.A. (2000): Summer temperature profiles within supraglacial debris on Khumbu Glacier Nepal. IAHS Publ. 264 (Symposium at Seattle 2000 – Debris-Covered Glaciers), 89-97.
- Diolaiuti G., D’Agata C., Meazza A., Zanutta A. and Smiraglia C. (2009): Recent (1975-2003) changes in the Miage debris-covered glacier tongue (Mont Blanc, Italy) from analysis of aerial photos and maps. *Geografia Fisica e Dinamica Quaternaria*, 32, 117-127.
- Diolaiuti G. and Smiraglia C. (2010): Changing glaciers in a changing climate: how vanishing geomorphosites have been driving deep changes in mountain landscapes and environments. *Géomorphologie: relief, processus, environnement*, 2, 131-152.
- Diolaiuti G., Senese A., Mihalcea C., Verza G.P., Mosconi B. and Smiraglia C. (2011): AWS measurements on glaciers in the Italian Alps. In “Workshop on the use of automatic measuring systems on glaciers. Extended abstracts and recommendations.” IASC Workshop, 23-26 March 2011, Pontesina (Switzerland). Organized by C.H. Tijm-Reijmer and J. Oerlemans.
- Diolaiuti G., Bocchiola D., D’Agata C. and Smiraglia C. (2012): Evidence of climate change impact upon glaciers' recession within the Italian Alps: the case of Lombardy glaciers. *Theoretical and Applied Climatology*, 109 (3-4), 429-445. DOI 10.1007/s00704-012-0589-y.
- Guglielmin M. (2006): Ground surface temperature (GST), active layer, and permafrost monitoring in continental Antarctica. *Permafrost and Periglacial Processes*, 17, 133-143.
- Guglielmin M., Ellis Evans J.C. and Cannone N. (2008): Ground thermal regime under different vegetation conditions in permafrost areas and sensitivity to climate change: a case study at Signy Island (maritime Antarctica). *Geoderma*, 144, 73-85.
- Humlum O. (1997): Active layer thermal regime at three rock glaciers in Greenland. *Permafrost Periglacial Process*, 8 (4), 383-408.
- Kayastha R.B., Takeuchi Y., Nakawo M. and Ageta Y. (2000): Practical prediction of ice melting beneath various thickness of debris cover Khumbu Glacier, Nepal, using

8. Ablation computation at the debris-covered area of Forni Glacier: an approach based on computation of debris thermal resistivity

---

- a positive degree-day factor. Debris-Covered Glacier (Proceedings of the Seattle workshop, September 2000). IAHS Publication no. 264, 71-81.
- Kellerer-Pirklbauer A., Karl Lieb G., Avian M. and Gspurning J. (2008): The response of partially debris-covered valley glaciers to climate change: the example of the Pasterze Glacier (Austria) in the period 1964 to 2006. *Geografiska Annaler*, 90 A (4), 269-285.
- Mattson L.E., Gardner J.S. and Young G.J. (1993): Ablation on debris covered glaciers: an example from the Rakhiot Glacier, Punjab, Himalaya. In: *Snow and Glacier Hydrology* (ed. by G.J. Young) (Proc. Kathmandu Symp., November 1992), 289-296. IAHS Publ. no. 218.
- Mattson L.E. (2000): The influence of a debris cover on the midsummer discharge of Dome Glacier, Canadian Rocky Mountains. Debris-Covered Glaciers (Proceedings of a workshop held at Seattle, Washington, USA, September 2000). IAHS Publ. no. 264.
- Mihalcea C., Mayer C., Diolaiuti G., Lambrecht A., Smiraglia C. and Tartari G. (2006): Ice ablation and meteorological conditions on the debris covered area of Baltoro Glacier (Karakoram, Pakistan). *Annals of Glaciology*, 43, 292-300.
- Mihalcea C., Brock B.W., Diolaiuti G., D'Agata C., Citterio M., Kirkbride M.P., Cutler M.E.J., C. (2008a): Using ASTER satellite and ground-based surface temperature measurements to derive supraglacial debris cover and thickness patterns on Miage Glacier (Mont Blanc Massif, Italy). *Cold Regions Science and Technology*, 52 (3), 341-354.
- Mihalcea C., Mayer C., Diolaiuti G., D'Agata C., Smiraglia C., Lambrecht A., Vuillermoz E. and Tartari G. (2008b): Spatial distribution of debris thickness and melting from remote-sensing and meteorological data, at debris-covered Baltoro Glacier, Karakoram, Pakistan. *Annals of Glaciology*, 48, 49-57.
- Montrasio A., Berra F., Cariboni M., Ceriani M., Deichmann N., Ferliga C., Gregnanin A., Guerra S., Guglielmin M., Jadoul F., Longhin M., Mair V., Mazzoccola D., Sciesa E. and Zappone A. (2008): Note illustrative della Carta Geologica d'Italia: foglio 024, Bormio. ISPRA, Servizio Geologico d'Italia.
- Nakawo M. and Young G.J. (1981): Field experiments to determine the effect of a debris layer on ablation of glacier ice. *Annals of Glaciology*, 2, 85-91.

8. Ablation computation at the debris-covered area of Forni Glacier: an approach based on computation of debris thermal resistivity

---

- Nakawo M. and Takahashi S. (1982): A simplified model for estimating glacier ablation under a debris layer. IAHS Publ. 138 (Symposium at Exeter 1982 – Hydrological Aspects of Alpine and High Mountain Areas), 137-145.
- Nicholson L. (2004): Modelling melt beneath supraglacial debris: implications for the climatic response of debris-covered glaciers. (PhD thesis, University of St Andrews.)
- Nicholson L. and Benn D.I. (2006): Calculating ice melt beneath a debris layer using meteorological data. *Journal of Glaciology*, 52 (178), 463-470.
- Osterkamp T.E. (2003): Establishing long-term permafrost observatories for active-layer and permafrost investigations in Alaska:1997-2002. *Permafrost and Periglacial Processes*.
- Pelfini M., Diolaiuti G., Leonelli G., Bozzoni M., Bressan N., Brioschi D. and Riccardi A. (2012): The influence of glacier surface processes on the short-term evolution of supraglacial tree vegetation: A case study of the Miage Glacier, Italian Alps. *The Holocene*, . doi:10.1177/0959683611434222
- Reid T.D. and Brock B.W. (2010): An energy-balance model for debris-covered glaciers including heat conduction through the debris layer. *Journal of Glaciology*, 56 (199), 903-916.
- Smiraglia C. (1989): The medial moraines of Ghiacciaio dei Forni, Valtellina, Italy: morphology and sedimentology. *Journal of Glaciology*, 358(119), 81-84.

# Chapter 9



### **Conclusions**

In this PhD thesis the distributed snow and ice melt at the glacier surface was quantified by applying different approaches: from the easiest method (i.e.: degree-day model) which depends only on the air temperature data (Braithwaite, 1985) to the most exhaustive models based on the energy budget computation (e.g. Brun et al., 1989; Bloschl et al., 1991; Arnold et al., 1996; Klok and Oerlemans, 2002). In particular some models to estimate and distribute the meteorological parameters and the energy fluxes were applied and tested. In this way i) all the factors driving the short-term energy balance variations were computed and distributed to the whole glacierized area; ii) the spatial and temporal variations of the energy balance components were investigated; iii) the air temperature and vapour pressure conditions were evaluated; iv) the spatial distribution of topographic shading and of potential and global solar radiation for selected time intervals was predicted; v) the incoming infrared radiation was modelled; vi) the turbulent fluxes were assessed; and vii) the melt amount also over the debris-covered areas was quantified.

Following in details the results obtained.

---

## Chapters 2: Energy and mass balance of Forni Glacier (Stelvio National Park, Italian Alps) from a 4-year meteorological data record

The automatic weather station set up on the Forni Glacier tongue (AWS1 Forni) has been delivered a unique dataset of meteorological conditions on a glacier melting tongue in the Italian Alps. The dataset (4 mass balance years) allows the study of the seasonal variation of surface energy fluxes. In particular, the complete point surface energy balance was calculated at the AWS location, where radiative fluxes are known and non-radiative contributing factors (sensible and latent heat,  $SH$  and  $LE$ , respectively) can be calculated. At this site snow accumulation is known as well thanks to the snow pits annually performed at the end of the spring by personnel from ARPA Lombardia (they follow AINEVA protocol). Also the hourly-scale analysis allows the calculation of surface ablation.

The complete energy balance analysis confirms that the parameter most influencing the surface net energy available for melting ice/snow ( $R_S$ ) is the net shortwave radiation ( $SW_{net}$ ), during melting ( $T_S = 0^\circ\text{C}$  and  $R_S > 0 \text{ W m}^{-2}$ ) and condensation ( $T_S = 0^\circ\text{C}$  and  $LE > 0 \text{ W m}^{-2}$ ) conditions. For a mean  $R_S$  value of  $185 \text{ W m}^{-2}$  (during melting) and  $146 \text{ W m}^{-2}$  (during condensation), mean  $SW_{net}$  is  $176 \text{ W m}^{-2}$  and  $123 \text{ W m}^{-2}$ , respectively; instead  $SH$  is ca.  $30 \text{ W m}^{-2}$  for both conditions, and  $LE$  was  $4 \text{ W m}^{-2}$  and  $12 \text{ W m}^{-2}$ , respectively. Therefore, non-radiative fluxes have less influence on ablation (during melting  $SH$  is ca. 16% and  $LE$  is ca. 2% of the  $R_S$  amount, and during condensation  $SH$  is ca. 21% and  $LE$  is ca. 8% ).

These results are also supported by the comparison between field-measured and calculated ablation values during summer 2009, which shows only small differences mainly due to the ice surface ablation variability. Moreover our results demonstrate that the simple empirical calculation of the turbulent fluxes is valid and the heat conduction into snow/ice has little effect on total available melt energy.

During the 4-year analysis (from 2005 to 2009), the total ice ablation calculated from the complete energy balance is  $-21.7 \text{ kg m}^{-2}$  or  $\text{m w.e.}$ , and the snow accumulation is  $+2.8 \text{ m w.e.}$ , thus giving a mass balance of  $-18.8 \text{ m w.e.}$  The maximum melt is registered during 2005/2006 and 2008/2009 with an amount of  $-5.6 \pm 0.020 \text{ m w.e.}$ , instead the minimum during 2007/2008 ( $-5.0 \pm 0.021 \text{ m w.e.}$ ). 2008/2009 is characterized by the highest accumulation ( $+0.8 \pm 0.007 \text{ m w.e.}$ ) and 2006/2007 by the smallest one ( $+0.6 \pm 0.005 \text{ m w.e.}$ ). The most negative mass balance is observed during

## 9. Conclusions

---

2005/2006 and 2006/2007 ( $-4.9 \pm 0.023$  and  $-4.9 \pm 0.021$ , respectively), whereas the less negative ones occurs during 2007/2008 ( $-4.2 \pm 0.023$  m w.e.).

Our findings suggest that the surface conditions, especially the role played by the solid precipitation during summer and fall seasons, are important in determining the net energy available for ice melting. Particularly important are the permanence of spring snow cover (whenever longer it may postpone the start of ice melting) and the occurrence of earlier solid precipitation during the fall season.

Glacier energy budget is also controlled by surface albedo. Its seasonal changes are driven by snowfalls and dust deposition. On this latter, the current literature (Flanner et al., 2009) suggests to consider the possibility that atmospheric soot (dust and black carbon) is playing a role in driving the spring decrease of snow albedo also on the Alpine glaciers' surfaces.

---

### **Chapters 3: Surface energy budget and melt amount for the years 2009 and 2010 at the Forni Glacier (Italian Alps, Lombardy)**

The data collected by a permanent AWS permit to quantify the complete energy balance and the melt amount with a high time resolution, also including the turbulent fluxes that affect the glacial ablation for the 20%-30% (Senese et al., 2012a), and to describe the surface albedo variability. Moreover sky and surface conditions can be deduced from measured meteorological parameters.

During 2009 and 2010 the results obtained from AWS1 Forni prove to be consistent with results from other 4 years of data acquisition (i.e. Citterio et al., 2007; Senese et al., 2010; 2012a).

The wind blows steadily down the glacier from SE that is along the fall line. The wind regime is characterized by a provenance from ca. 120° and a speed of a few meters per second, generally featured katabatic-type flows. Moreover higher wind speeds are found not directly correlated with a particular range of temperature.

Analysing albedo data, the ice ablation periods result long of 104 days (2009) and 88 days (2010). During 2009 ablation season 2 snowfalls are observed (totally covering 5 days featuring snow albedo values) and during 2010 ablation season 5 snow fall events are detected (the snow persisted at the glacier surface for 16 days in total). Moreover the snow albedo (with a mean value of 0.77 between the 2 years) tends to decrease for larger values of the incoming radiation. The characteristic albedo for ice is found equal to 0.24 (in 2009) and 0.23 (in 2010).

Regarding energy balance, the net solar radiation, the turbulent fluxes and the net energy are characterized by similar trends with maximum during summer and minimum during winter. Instead the net longwave radiation results varying between slightly positive values and values up to  $-100 \text{ W m}^{-2}$ .

During 2009-2010 the total calculated mass loss results  $-11.32 \text{ kg m}^{-2}$  (or m w.e.). The comparison of the measured and modelled ice ablation shows differences of less than 0.06 m w.e. and therefore indicates that the model applied is correct.

Consequently the AWSs installed on glaciers are essential for calibrating and validating the glacier energy balance models, to characterize quantitatively the glacier boundary layer conditions, and to describe wind regime.

---

### **Chapters 4: Air temperature thresholds to evaluate snow melting at the surface of Alpine glaciers by degree-day models: the case study of Forni Glacier (Italy)**

By applying a point energy balance model (following Senese et al., 2012a) at the AWS1 Forni site on the glacier ablation tongue we found that a not negligible annual snow melt occurs. In the 7-year period 2005-2012 it ranges from 17.6% to 29.2% of the total (ice and snow) annual ablation (-37.5 m w.e.), which was estimated through energy budget computations by considering both positive energy budget and surface temperature above 273.15 K. During April-June at the AWS1 Forni site all the snow coverage disappears due to melting processes; in fact, from 2006 to 2012 the snow ablation over the April-June time frame is found -8.47 m w.e. corresponding to the 66.59% of the total April-June melting amount (i.e. considering snow and ice). Moreover we also computed the April-June mass loss without considering the glacier surface temperature and conditions, obtaining a melt amount equal to -13.43 m w.e. thus underlining an overestimation (+5.6% with respect to the actual melting over the same period). Then the knowledge of glacier surface temperature results really important to assess with a good accuracy the melt amount. On the other hand these information are available only on a small number of glaciers where supraglacial AWS have been running thus suggesting to look for different strategies to assess the snow melt amount. The most diffuse and simple method is the T-index approach (also named degree-day model) based on data acquired outside the studied glacier.

The major uncertainty in computing the degree days amount at the glacier surface and then in assessing snow melt is given by the choice of an appropriate air temperature threshold: a not negligible variability of the cumulative degree days resulted applying different thresholds. In fact ablation does not occur only with daily average air temperature higher than 273.15 K since it is determined by the surface energy balance and this latter is only indirectly affected by air temperature (Kuhn 1987). Then, to assess the most suitable temperature threshold, hourly melt values were firstly analysed (obtained from AWS1 Forni data and applying the energy balance model) in the April-June period to detect if ablation occurs and how long this phenomenon takes (number of hours per day). The largest part of the melting (97.7% of the whole ablation) resulted occurring on days featuring at least 6 melting hours thus suggesting to consider the minimum average daily temperature value calculated for this temporal length class as a

## 9. Conclusions

---

suitable temperature threshold (268.6 K and 268.1 K considering the temperature data from AWS1 Forni and from Bormio, respectively). These data were applied to detect the actual melting days. The first threshold was applied to air temperature data from AWS1 Forni and permitted to select 586 melting days describing the 99.4% (-12.64 m w.e.) of the total ablation. Considering the temperature data estimated from Bormio, the threshold of 268.1 K permitted to detect 601 melting days giving a cumulative melting of -12.66 m w.e. equal to 99.5% of the total.

Then a simple T-index model was run varying the temperature threshold (273.15 K, 268.1 K and 274.7 K). The resulting ablation curves show a similar trend but the total amount of snow melting over the 7 year long period results quite different. The cumulative melting assessed by energy balance in the same period results -8.23 m w.e. and this values is also obtained applying as threshold 268.11 K. These results suggest to use as threshold the minimum of daily average temperature calculated for days featuring at least 6 melting hours. This value permits to better explain magnitude and variability of snow melting. As regards the threshold 273.15 K, which has been largely used in the literature dealing with degree-day model (e.g. Braithwaite, 1985; Hock, 2003), it drives an underestimation of snow melt (-11.5% with respect to the melting value). Moreover in the case the main purpose should be only the detection of the melting days and not the assessing of the melt amount, the application of the 273.15 K threshold drives an underestimation as well. With this threshold 481 melting days are detected against 601 melting days selected by applying the 268.1 K threshold.

Summarizing it results that applying a different temperature threshold used to assess the cumulative degree days amount considerably affect the magnitude of the estimated melt amount. In fact a 5.0 K lower threshold value (with respect to the largely applied 273.15 K) avoids most of the sampling problem in the application of the positive T-index models and permits the most reliable reconstruction of snow melt. Moreover our air temperature threshold analysis on an Alpine glacier results in agreement with findings by van den Broeke et al. (2010) in Greenland ice sheet. They found an about 5 K lower threshold value by observing the cumulative distribution of daily average temperature for days with melt at three AWSs. From their study this value resulted to allow also an appropriate calculation of snow and ice degree-day factors. In fact applying the common 273.15 K threshold they obtained non-sense factors values. Then probably the choice of a 268 K value as air temperature threshold for computing degree days amount

## 9. Conclusions

---

could be generalized and applied not only on Greenland glaciers but also on Mid latitude and Alpine ones like the Forni Glacier.

---

**Chapters 5: An enhanced T-index model including solar and infrared radiation to evaluate distributed ice melt at the Forni Glacier tongue (Italian Alps)**

Melt models of different complexity were applied to predict ice melting upon the Forni Glacier. Further, an attempted was performed to improve ice melt prediction by including the net longwave radiation as an input. To apply these algorithms, the solar and infrared fluxes and the air temperature were distributed to the whole glacier surface. The solar radiation distribution was benchmarked against radiation data measured during field campaigns in summer 2011 and 2012. The two datasets were in agreement within -29.2% to +25.9%, with a mean absolute percentage error of 13.4%, thus suggesting to consider suitable the proposed radiation model. A good agreement was further found between the measured (by the AWS1 Forni) and modelled infrared values from 2006 to 2012. In fact, only 14.5% of the samples featured underestimation larger than  $50 \text{ W m}^{-2}$ , and the underestimation was always within  $90 \text{ W m}^{-2}$ , which translates in a maximum underestimated daily mass loss of 6 mm w.e. Hence, the infrared model can be considered appropriate and the obtained underestimation possibly negligible. Finally, ice ablation was modelled applying 4 different methods during June-August 2011, from simple degree-day to enhanced models including incoming shortwave and longwave fluxes. The radiative approaches here are more suitable than the classical T-index model (Braithwaite, 1985), which features the highest mean divergence (i.e. 8.91%) from the measured mass loss.

The T-index model, driven by temperature, solar and infrared radiation, quantifies with some more accuracy ice melt (6.72% of mean disagreement), slightly improving the approach introduced by Pellicciotti et al. (2005). In summary, our model and the one by Pellicciotti et al. (2005) are the most suitable to predict ice melt and describe ablation variability over time upon the Forni Glacier. Thus, it is suggested that upon the Forni Glacier radiation flux may explain part of ice melt variability, and thus one needs to consider all the radiative components to improve the degree-day approach for ice melt assessment. Eventually, the present study provides some information concerning errors in modelling solar and infrared radiation, useful for quantifying glacier melt rate, and our melt approach displays that use of both the radiative components may provide some gain in accuracy when estimating ice melting.



---

## **Chapters 6: A pilot study to evaluate sparse supraglacial debris and dust and their influence on ice albedo of Alpine glaciers: the case study of the Forni Glacier (Italy)**

An attempt was performed for improving the research on dust and black carbon occurrence at the melting surface of glaciers and contributing to fill a knowledge gap. In fact, several studies are dealing with dust and black carbon occurrence only at the snow surface and its effect only on snow melt rates and glacier evolution (see Aoki et al., 1998; Qian et al., 2011; Yasunari et al., 2010). Moreover, dust and black carbon occurrence on ice seems to have increased over the last recent years due to the ongoing glacier shrinkage that makes larger and wider rock exposures, rock outcrops and nunataks (Oerlemans et al., 2009; Diolaiuti and Smiraglia, 2010), thus requiring accurate studies to describe debris occurrence, pattern and evolution and their influence on ice albedo. For these reasons, a simple methodological approach was proposed in order to standardize the procedures to quantify fine and sparse debris/dust coverage ( $d$ , it is the ratio of surface covered by dust and fine debris with respect to the whole analysed surface area) at the glacier melting surface and its influence on ice albedo.

As the debris quantification method is based on image analysis, the greyscale threshold values ( $T_{GS}$ ) are chosen by a supervised classification in which the threshold is iteratively adjusted until the isolated image pixels best coincide with the debris/dust. The robustness of this approach was investigated with some sensitivity tests: i) varying the selected threshold up to  $\pm 10\%$  for each image (thus obtaining  $T_{GS-10\%}$  and  $T_{GS+10\%}$ ) and ii) applying an unique threshold ( $T_{GS-AVE}$ ) obtained by averaging all the chosen  $T_{GS}$  thus obtaining 51  $d_{-10\%}$  values and 51  $d_{+10\%}$  values and 51  $d_{AVE}$  values. Since the departures of  $d$  from  $d_{-10\%}$  and of  $d$  from  $d_{+10\%}$  were found restricted, these results suggest that the sensitivity of our method to changes in the applied threshold is not so high to affect the reliability of the derived data. Moreover we also tested the method using an unique threshold value ( $T_{GS-AVE}$ : 92). Even if a scatter plot allows to observe a not negligible relation among the obtained  $d_{AVE}$  values and the actual  $d$  dataset (from 51  $T_{GS}$  values),  $d_{AVE}$  data resulted an input data less accurate than  $d$  to predict ice albedo variability. This suggests that the different  $T_{GS}$  found for each image (even if they require to spend more time in the image analysis) permit a better and detailed determination of debris distribution and then a more accurate  $d$  evaluation and  $\alpha$

## 9. Conclusions

---

prediction. Then summarizing to look for the most reliable relation between  $d$  and  $\alpha$  the best and suitable solution is to apply as many specific  $T_{GS}$  values as are the images to be analysed thus describing with further details the large variability of surface conditions which affect glacier surface during the summer season.

To evaluate the fine debris cover evolution, during ablation seasons 2012 and 2013 the debris coverage rate ( $C_r$ ) was evaluated. From 4<sup>th</sup> July to 9<sup>th</sup> September 2012 a higher  $C_r$  was found on sites characterized by coarser dust (i.e. 96 g/m<sup>2</sup> per day along an entire ablation season) than in the sites featuring finer sediment (i.e. 1 g/m<sup>2</sup> per day). Presently, we are developing several improvements to the method, which surely will give fundamental inputs to the research; nevertheless, this first test gives an important contribution to standardize the field work method for evaluating and sampling fine sparse debris at the melting glacier surface.

Moreover, the surface fine debris evolution is resulted forced by the occurrence of liquid precipitation that washes out the dust accumulation on glacier surface. This influence was quantified in an albedo increasing of 21.6%, limited to 1.8 days. This is due to rain smoothing effect on the ice surface as well, thus reducing the roughness.

Regarding the debris origin, X-Ray Diffraction analysis confirms the geological origin of debris mostly from local rock outcrops (a local formation of micaschist). By SEM (Scanning Electron Microscope) analysis we found algae, spore, pollen, microfauna and cenospheres (probably carried out by a wind contribution from siderurgic industries of Po Plains), suggesting a limited allochthonous input. This latter human contribution affects the glacier energy budget: in fact, the black carbon reduces the reflectivity and increases the ablation (Painter, 2013).

In conclusion, though this methodological approach is applied to a very small scale (parcel of 1 m x 1 m), it could be extended to a larger scale. For instance, the image analysis can be performed on higher resolution imagery such as orthophotos (for Lombardy Alps available with pixel resolution of 0.5 m x 0.5 m) or satellite imagery (featuring a resolution of 3-5 m or better). This improvement and the jump of scale will permit to distribute ice albedo once the debris properties are analysed and the relationship between albedo and debris ratio is known.

---

## Chapter 7: Computation of turbulent fluxes distributed over the glacier surface. The case study of the Forni Glacier (Italian Alps)

Several methods were investigated to estimate the turbulent fluxes over a glacier surface. The turbulent fluxes generally feature lower influence on ablation amount with respect to the radiative components: the sensible heat flux affects for 16% of the net energy amount and the latent heat flux for 2% (Senese et al., 2012a). In any case the turbulent fluxes play an important role in shaping boundary layers.

To assess these fluxes over the whole glacier surface, the well-known bulk aerodynamic formulas and another approach depending not directly on wind speed were applied. Then it was necessary to distribute the air temperature and the vapour pressure. The first one was already investigated in Senese et al. (submitted, see also chapter 5 of this PhD Thesis). The computation of the distributed vapor pressure was analyzed in this section. The input data were the daily vertical gradient of vapour pressure ( $\lambda_e$ ), the ambient vapour pressure estimated at Bormio site ( $e_a$ ) and the measured glacier near-surface vapour pressure ( $e_{AWS}$ ).

The daily vertical gradient ( $\lambda_e$ ) calculated from Bormio and Santa Caterina Valfurva data resulted ranging from  $-0.002 \text{ hPa m}^{-1}$  to  $-0.01 \text{ hPa m}^{-1}$  (in agreement with findings by Shea and Moore, 2010).

From Bormio  $e_a$  data, we calculated the ambient vapour pressure at the AWS1 Forni elevation ( $e_{a-AWS}$ ) applying the lapse rate ( $\lambda_e$ ). By comparing  $e_{a-AWS}$  with  $e_{AWS}$  dataset from 2006 to 2009, a higher annual variability was found with regards to the ambient values respect to the glacier ones which resulted featuring lower values especially during summer season. This can be due to the climate conditions occurring at Bormio area which was found wetter for instance than Santa Carterina Valfurva.

From a scatter plot of  $e_{a-AWS}$  and measured  $e_{AWS}$  at AWS1 Forni site, two separate linear functions resulted depending on  $T_{AWS}$  values, with a RMSE resulting 0.99 hPa and 1.33 hPa. In particular reduced values of  $e_g$  were observed for  $e_a > 6.11 \text{ hPa}$  and enhanced values of  $e_g$  resulted for  $e_a < 6.11 \text{ hPa}$ . These regression lines resulted in agreement with findings by Shea and Moore (2010): the regression line for  $T_g \geq 0^\circ\text{C}$  featured a slope less than the unity and cross the 1:1 line near 6.11 hPa as defined also by Shea and Moore (2010). With regard to the linear fit for observations below  $0^\circ\text{C}$ , a slope near the unity and an intercept near zero indicate that moisture exchanges between the surface and the near-surface layers appear to be minimal (Shea and Moore, 2010). These values

## 9. Conclusions

---

did not resulted by our observations thus suggesting a more occurrence of moisture exchanges. This can be due to the climate conditions about the area studied by Shea and Moore (2010): the southern Coast Mountains of British Columbia feature a maritime climate and then as wetter as than the central Italian Alps (where the Forni Glacier is located).

Apart from the distribution of both air temperature and vapour pressure parameters, it was necessary to assess the turbulent exchange coefficient ( $C^*$ ), found equal for the latent and sensible heat flux. In particular there are two contributions to the turbulent exchange coefficient: the contribution from the katabatic wind system ( $C_{kat}$ ) and a background contribution associated with the turbulence generated by the atmospheric circulation on a synoptic/regional scale ( $C_b$ ). The first one depends on the background potential temperature lapse rate ( $\lambda_{PT}$ ) estimated between Bormio and AWS1 Forni sites, and the air and surface temperatures collected by AWS1 Forni ( $T_{2m}$  and  $T_s$ , respectively). The latter coefficient was optimized from 2006-2009 hourly turbulent fluxes calculated in Senese et al. (2012a; 2012b). The obtained mean values of  $C^*$ ,  $C_{kat}$  and  $C_b$  (0.0055, 0.0035 and 0.0027, respectively) were found in agreement with findings for instance by Klok and Oerlemans (2002) in spite of different applied approaches. In fact Klok and Oerlemans (2002) optimized  $C_b$  from observed melt values for 1999 because the wind records were not available and then the turbulent fluxes cannot be calculated applying the well-known bulk aerodynamic formulas (which depend on wind speed values).

---

**Chapters 8: Assessment of ice ablation at the debris-covered area of Forni Glacier: an approach based on computation of debris thermal resistivity**

This part of the study was aimed at evaluating the applicability of a simple method to quantify the distribute ice melting over the debris covered area of the Forni Glacier (Italy). In fact, even if the widest Italian valley glacier is largely debris-free, darkening phenomena are ongoing (Diolaiuti and Smiraglia 2010; Diolaiuti et al. 2012) and the confluence of three ice streams originating from rock outcrops generates two distinct ice-cored medial moraines (Smiraglia, 1989). Then to evaluate the melt amount of the whole glacier it is necessary to assess also the ablation derived from buried ice melt and this requires to model the heat conduction along the debris layer and the processes at the debris-ice contact (Mihalcea et al., 2008a; Nicholson and Benn, 2006). Previous tests performed on actual alpine debris covered glaciers indicated that debris covered areas due to the occurrence of differential ablation processes are characterized by faster changes thus making more complicate the maintenance of supraglacial AWS. These latter are needed to describe with full details the buried ice energy budget and to compute the complete mass losses thus suggesting to choose a simpler method to estimate the ice melting over the Forni medial moraines without depending on dedicated instruments to be deployed at the debris covered surfaces and maintained along the whole summer season. Then besides of a more accurate energy balance approach, we followed a simple approach, mainly based on the use of debris surface temperature and debris thermal resistance to determine the energy available for ice melting (Nakawo and Young, 1981; Nakawo and Takahashi, 1982; Mihalcea et al., 2008a).

The data input of the model we applied to estimate the ice melting over the Forni medial moraines were: the surface debris temperature ( $T_s$ ), the debris thickness ( $d$ ) and the point measured ablation amount ( $M_{meas}$ ), this latter derived from field measurements through ablation stakes.

Our approach was based on the assumption that the debris layer is in thermal equilibrium, i.e. the heat stored in the layer is constant over time, and accepting it means that conductive heat flux at the debris surface is the same as at the ice interface.

Under stable weather conditions the thermal regime of the debris is dominated by the diurnal cycle (Conway and Rasmussen, 2000; Nicholson, 2004; Humlum, 1997), so in debris cover of more than a few centimeters in thickness, equilibrium within the debris

## 9. Conclusions

---

layer cannot be expected over time intervals of anything less than 24 hours. Consequently, the assumption of a linear temperature gradient will not be met on sub-diurnal timescales, but is much more likely to apply on a 24 hour timescale (Conway and Rasmussen, 2000). For this reason the melt calculation is performed from daily temperatures although the availability of dataset with a higher time resolution.

The measured surface temperature resulted featuring the typical daily cycle and resulted depending on the meteorological conditions. In fact whenever a snow layer covers the debris surface, this latter results isolated from the atmospheric conditions and is characterized by a constant temperature value (about at 0°C). Consequently in these time frames the melt cannot occur.

As expected the measured melt rate decreases with the elevation: from -0.029 m w.e. at 2491 m a.s.l. to -0.015 m w.e. at 2739 m a.s.l. The observed debris effective thermal resistance ( $R_{obs}$ ) results ranging from 0.0267 m<sup>2</sup> °C W<sup>-1</sup> to 0.0758 m<sup>2</sup> °C W<sup>-1</sup> (with a debris thickness  $d_{meas}$  of 0.06 m and 0.17 m, respectively).

The obtained relation between  $d_{meas}$  and  $R_{obs}$  allowed to estimate the debris effective thermal resistance with a slightly overestimation up to 0.004 m<sup>2</sup> °C W<sup>-1</sup>. Consequently the modelled cumulative melt amount resulted slightly underestimated (i.e. up to -7.0%). In spite of this, the estimated ablation feature (like the measured one) an inverse trend with the elevation.

Finally we can conclude that our results demonstrate that a simple empirical calculation of the conductive heat flux depending on the temperature gradient from surface debris to ice can be considered a valid tool for estimating the ice losses over the medial moraines.

---

### References

- Aoki Te, Aoki Ta, Fukabori M, Tachibana Y, Zaizen Y, Nishio F and Oishi T (1998) Spectral albedo observation on the snow field at Barrow, Alaska. *Polar Meteor. Glaciol.* 12: 1-9.
- Arnold, N.S., I.C. Willis, M.J. Sharp, K.S. Richards and W.J. Lawson. 1996. A distributed surface energy-balance model for a small valley glacier. I. Development and testing for Haut Glacier d'Arolla, Valais, Switzerland. *J. Glaciol.*, 42(140), 77–89.
- Blöschl, G., Kirnbauer, B. and Gutknecht, D. 1991: Distributed snowmelt simulations in an Alpine catchment. 1. Model evaluation on the basis of snow cover patterns. *Water Resources Research* 27, 3171–79.
- Braithwaite R.J. (1985) Calculation of degree-days for glacier-climate research. *Zeitschrift fue Gletscherkunde und Glazialgeologie*, 20/1984, 1-8.
- Brun, E., Martin, E., Simon, V., Gendre, C. and Coleou, C. 1989: An energy and mass model of snow cover suitable for operational avalanche forecasting. *Journal of Glaciology* 35, 333–42.
- Citterio M., Diolaiuti G., Smiraglia C., Verza G. & Meraldi E. (2007) – *Initial results from the Automatic Weather Station (AWS) on the ablation tongue of Forni Glacier (Upper Valtellina, Italy)*. *Geografia Fisica e Dinamica Quaternaria*, 30, 141-151.
- Conway H. and Rasmussen L.A. (2000): Summer temperature profiles within supraglacial debris on Khumbu Glacier Nepal. *IAHS Publ.* 264 (Symposium at Seattle 2000 – Debris-Covered Glaciers), 89–97.
- Diolaiuti G and Smiraglia C (2010) Changing glaciers in a changing climate: how vanishing geomorphosites have been driving deep changes in mountain landscapes and environments. *Géomorphologie: relief, processus, environnement* 2: 131-152.
- Diolaiuti G., Bocchiola D., D'Agata C. and Smiraglia C. (2012): Evidence of climate change impact upon glaciers' recession within the Italian Alps: the case of Lombardy glaciers. *Theoretical and Applied Climatology*, 109 (3-4), 429-445. DOI 10.1007/s00704-012-0589-y.
- Flanner M.G., Zender C.S., Hess P.G., Mahowald N.M., Painter T.H. Ramanathan V. & Rasch P.J., 2009: Springtime warming and reduced snow cover from carbonaceous particles. *Atmospheric Chemistry and Physics*, 9: 2481-2497.

## 9. Conclusions

---

- Hock R. (2003) Temperature index melt modelling in mountain areas. *Journal of Hydrology* 282(1-4), 104–115.
- Humlum O. (1997): Active layer thermal regime at three rock glaciers in Greenland. *Permafrost Periglacial Process*, 8(4), 383–408.
- Klok E.J. and Oerlemans J., 2002: Model study of the spatial distribution of the energy and mass balance of Morteratschgletscher, Switzerland. *Journal of Glaciology*, 48 (163): 505-518.
- Kuhn M. (1987) Micro-meteorological conditions for snow melt. *J. Glaciol.* 33 (113), 263–272.
- Mihalcea C., Brock B.W., Diolaiuti G., D'Agata C., Citterio M., Kirkbride M.P., Cutler M.E.J., C. (2008a): Using ASTER satellite and ground-based surface temperature measurements to derive supraglacial debris cover and thickness patterns on Miage Glacier (Mont Blanc Massif, Italy). *Cold Regions Science and Technology*, 52 (3), 341-354.
- Nakawo M. and Young G.J. (1981): Field experiments to determine the effect of a debris layer on ablation of glacier ice. *Annals of Glaciology*, 2, 85-91.
- Nakawo M. and Takahashi S. (1982): A simplified model for estimating glacier ablation under a debris layer. *IAHS Publ.* 138 (Symposium at Exeter 1982 – Hydrological Aspects of Alpine and High Mountain Areas), 137-145.
- Nicholson L. and Benn D.I. (2006): Calculating ice melt beneath a debris layer using meteorological data. *Journal of Glaciology*, 52 (178), 463-470.
- Nicholson L. (2004): Modelling melt beneath supraglacial debris: implications for the climatic response of debris-covered glaciers. (PhD thesis, University of St Andrews.)
- Oerlemans J, Giesen RH and Van Den Broeke MR (2009) Retreating alpine glaciers: increased melt rates due to accumulation of dust (Vadret da Morteratsch, Switzerland). *Journal of Glaciology* 55(192): 729-736.
- Painter TH, Flanner MG, Kaser G, Marzeion B, Van Curen RA, Abdalati W (2013) - End of the Little Ice Age in the Alps forced by industrial black carbon. *PNAS* 110 (38), 15216-15221.
- Pellicciotti F., Brock B., Strasser, P., Burlando, M., Funk, J., Corripio (2005) An enhanced temperature-index glacier melt model including the shortwave radiation balance: development and testing for Haut Glacier d'Arolla, Switzerland. *Journal of Glaciology*, Vol. 51, No. 175, 573-587.



## 9. Conclusions

---

- Qian Y, Flanner MG, Leung LR and Wang W (2011) Sensitivity studies on the impacts of Tibetan Plateau snowpack pollution on the Asian hydrological cycle and monsoon climate. *Atmos. Chem. Phys.* 11: 1929-48.
- Senese A., Diolaiuti D., Mihalcea C. & Smiraglia C. (2010) – *Evoluzione meteorologica sulla lingua di ablazione del Ghiacciaio dei Forni, gruppo Ortles-Cevedale (Parco Nazionale dello Stelvio, Lombardia) nel periodo 2006-2008*. Bollettino Della Società Geografica Italiana, XIII, 3(4), 845-864.
- Senese A., Diolaiuti G., Mihalcea C. and Smiraglia C. (2012a) – Energy and mass balance of Forni Glacier (Stelvio National Park, Italian Alps) from a 4-year meteorological data record. *Arctic, Antarctic, and Alpine Research*, 44 (1), 122-134.
- Senese A., Diolaiuti G., Verza G.P. & Smiraglia C. (2012b) – Surface energy budget and melt amount for the years 2009 and 2010 at the Forni Glacier (Italian Alps, Lombardy). *Geografia Fisica e Dinamica Quaternaria*, 35 (1), 69-77. DOI 10.4461/GFDQ.2012.35.7
- Senese A., Ferrari S., Maugeri M., Confortola G., Bocchiola D., Smiraglia C. and Diolaiuti G. (submitted) An enhanced T-index model including solar and infrared radiation to evaluate distributed ice melt at the Forni Glacier tongue (Italian Alps).
- Shea J.M. and Moore R.D. (2010): Prediction of spatially distributed regional-scale fields on air temperature and vapor pressure over mountain glacier. *Journal of Geophysical Research*, 115 (D23107).
- Smiraglia C. (1989): The medial moraines of Ghiacciaio dei Forni, Valtellina, Italy: morphology and sedimentology. *Journal of Glaciology*, 35(119), 81-84.
- van den Broeke M., Bus C., Ettema J. and Smeets P. (2010) Temperature thresholds for degree-day modeling of Greenland ice sheet melt rates. *Geophysical Research Letters*, 37, L18501.
- Yasunari TJ, Bonasoni P, Laj P, Fujita K, Vuillermoz E, Marinoni A, Cristofanelli P, Duchi R, Tartari G and Lau KM (2010) Estimated impact of black carbon deposition during pre-monsoon season from Nepal Climate Observatory-Pyramid data and snow albedo changes over Himalayan glaciers *Atmos. Chem. Phys.* 10: 6603-6615.

## Acknowledgements

I would like to thank my supervisors prof. Claudio Smiraglia, PhD Guglielmina Diolaiuti, prof. Maurizio Maugeri and PhD Andrea Zerboni for numerous helpful advices, comments and support.

This work has been performed in the framework of the SHARE-Stelvio project funded by Lombardy Region and managed by FLA (Fondazione Lombardia per l'Ambiente) and Ev-K2-CNR Committee. The AWS1 Forni project is developed under the umbrella of the SHARE Program. SHARE (Stations at High Altitude for Research on the Environment) is an international program developed and managed by the Ev-K2-CNR Committee. Moreover this AWS is included in the CEOP-GEWEX and WMO Solid Precipitation Intercomparison Experiment (SPICE) networks.

I wish also to thank the Lombardy Regional Agency for Environmental Protection (ARPA Lombardia) who kindly provided meteorological data useful for the modelling approach.

I'm grateful to Gian Pietro Verza, Paolo Turcotti, Eraldo Meraldi and Roberto Chillemi for their fundamental technical assistance on the field in managing the AWS, in performing snow pits and providing accumulation data. I thank all the thesis students (bachelor and master degree) for their kind help on the field.

## Ringraziamenti

Ringrazio con sentito affetto Willy e il prof. Smiraglia per aver creduto in me e nelle mie capacità sin dalla laurea triennale. È dal 2007 che mi supportate e incentivate a fare sempre meglio. Ho imparato tanto da voi: non siete solo tutor a livello scientifico ma anche confidenti e saggi consiglieri, figure importanti nel mio percorso di crescita.

Grazie al prof. Maugeri e ad Andrea Zerboni per i loro consigli soprattutto in campo fisico, statistico e geologico.

Grazie a tutti coloro che hanno contribuito a questo progetto di ricerca: Claudia M., tutti i miei tesisti (Alessandro C., Alice M., Annalisa T., Elena D., Roberta G., Sara G., Stefano F., Veronica M. ed in particolare Roberto A.) e a tutto il gruppo di glaciologia.

Trilly abbraccia con un super sorriso i suoi “vicini di piano”: come avrei fatto senza la vostra solare e ilare compagnia a superare i periodi più stressanti? Grazie a (in ordine alfabetico) Agostino, Claudio, Franco, Gabriele, Giovanni e William. E anche a tutte le meravigliose e sempre disponibili “segretarie amministrative”.

E ora dal mondo dell’università all’universo personale...

Grazie alla mia famiglia, ai miei splendidi genitori che mi hanno seguito, supportato e incoraggiato in tutto questo mio percorso, sempre presenti ma mai invadenti, da “dottoressa bis” a “dottoressa ter”! Sempre fiduciosi e orgogliosi delle mie capacità, insegnandomi i veri valori attraverso la vita quotidiana.

Grazie al “mio” Davide. È entrato nella mia vita all’improvviso, inaspettatamente proprio all’inizio di quest’ultimo ciclo di studi, poco prima dell’esame di ammissione. Hai vissuto con me ogni esperienza del mio dottorato, sia i sorrisi dovuti per esempio agli articoli accettati sia i deliri di fine progetto (soprattutto quello cileno).

Grazie alla mia “best” Stefania. Riusciremo a realizzare il nostro sogno “dalla maternità alla maturità”? Comunque anche se sotto cieli diversi la luna rimane sempre la stessa, quindi anche se saremo in città diverse la nostra amicizia rimarrà sempre vera! E poi nel caso c’è Skype!

Grazie a tutti i miei amici (milanesi e torinesi) per i bei momenti passati insieme.

... E quindi eccomi alla fine del terzo ciclo di studi universitari. E pensare che quando mi sono iscritta a Scienze Naturali nel 2004 non ne ero per nulla convinta e una volta

## Ringraziamenti

---

laureata alla magistrale non volevo assolutamente provare il dottorato. E invece ora sono contenta di tutte le scelte che ho preso in questi 9 anni e della persona che sono diventata.

Grazie a tutti coloro che nel bene o nel male mi hanno portata a essere l'Antonella che sono oggi.

*Grazie!*

## Curriculum vitae

Antonella Senese was born on the 27<sup>th</sup> of November, 1985 in Milan (Italy). In October 2007 she graduated in “Natural Sciences” (Grade: 109/110), a three-year bachelor degree (1<sup>st</sup> level degree program or BSc), at the University of Milan, Italy. In October 2009 she graduated Cum Laude in “Analysis and Management of Natural Environments”, a two-year Master degree (2<sup>nd</sup> level degree program or MSc), at the University of Milan, Italy. Her first graduation project dealt with a study on the micrometeorology of an alpine glacier (Forni Glacier, Italy). As a second graduation project, she investigated the surface energy balance from energy and meteorological data collected by a supraglacial automatic weather station set up on the Forni Glacier. Immediately after the master degree, she awarded a scholarship at the Earth Sciences Department of the University of Milan (Italy). In 2011 she started her PhD-research at the University of Milan. Prof. C. Smiraglia and Prof. M. Maugeri with the collaboration of PhD G. Diolaiuti and PhD A. Zerboni supervised her research on the distribution of the surface energy balance over the whole Forni Glacier surface. Fortunately, her research not only contained computer work, but also field investigations on some glaciers in Italy (Forni, Dosdè, Giant, Platigliole, Sforzellina, Cevedale and Presena Glaciers), with the aims to collect glaciological data and to maintain the automatic weather stations. She enjoyed some foreign trips for study courses (Karthus), conferences (Pontresina, Zurich, Lecco and Palermo) and activities as guest scientist (Santiago in Chile). As regards to this latter, she carried out the task of expert of glacier energy and mass balance, at the *Dirección de Aguas del Ministerio de Obras Públicas* in Santiago in Chile, under the umbrella of *Plan de Acción para la conservación de glaciares ante el cambio climático* managed by Ev-K2-CNR Committee.



## List of publications

1. Minora U., Bocchiola D., D'Agata C., Maragno D., Mayer C., Lambrecht A., Mosconi B., Vuillermoz E., **Senese A.**, Compostella C., Smiraglia C., Diolaiuti G. (2013): 2001–2010 glacier changes in the Central Karakoram National Park: a contribution to evaluate the magnitude and rate of the "Karakoram anomaly". *The Cryosphere Discussions*, 7, 2891-2941, ISSN: 1994-0440, doi: 10.5194/tcd-7-2891-2013
2. **Senese A.**, Diolaiuti G., Mihalcea C. & Smiraglia C. (2012): Energy and mass balance of Forni Glacier (Stelvio National Park, Italian Alps) from a 4-year meteorological data record. *Arctic, Antarctic, and Alpine Research*.
3. **Senese A.**, Diolaiuti G., Verza G.P. & Smiraglia C. (2012): Surface energy budget and melt amount for the years 2009 and 2010 at the Forni Glacier (Italian Alps, Lombardy). *Geografia Fisica e Dinamica Quaternaria*, 35 (1), 69-77. DOI 10.4461/GFDQ.2012.35.7
4. **Senese A.**, Diolaiuti G., Mihalcea C. & Smiraglia C. (2010): Evoluzione meteorologica sulla lingua di ablazione del Ghiacciaio dei Forni (Lombardia, gruppo Ortles-Cevedale) nel periodo 2006-2008. *Bollettino della Società Geografica Italiana (BSGI)*, Roma, Serie XIII, vol. III, fascicolo 4, pp. 845-864.

### **Popular papers (not peer reviewed):**

1. **Senese A.**, Azzoni R., Mosconi B., Maragno D., Smiraglia C., Diolaiuti G. and Trenti A. (in press): Sperimentazione di nuovi geotessili per la riduzione della fusione nivoglaciale risultati dal Ghiacciaio del Presena nell'estate 2012. *Neve & Valanghe*.
2. Diolaiuti G., **Senese A.**, Chillemi R., Smiraglia C. (2012): Il futuro delle Alpi senza ghiacciai? *Montagne 360. La rivista del Club Alpino Italiano*. Dicembre 2012, 16-19.
3. Diolaiuti G., **Senese A.**, Mosconi B., D'Agata C., Mihalcea C., Smiraglia C. and Trenti A. (2011): Effetti delle misure di protezione glaciale attiva sul bilancio energetico puntuale del Ghiacciaio Presena in provincia di Trento. *Neve & Valanghe*, 74, 54-63.

**Proceedings:**

1. Vuillermoz E., **Senese A.**, Diolaiuti G., Smiraglia C., Cristofanelli P., Marinoni A., Bocchiola D., Verza G.P., Bonasoni P. (2013): Studying Himalayan Glaciers to understand atmospheric dynamics and ongoing cryosphere variations. Data and findings from the Changri Nup Glacier (Nepal, Himalaya). Geophysical Research Abstracts, Vol. 15, EGU2013-7444, 2013, EGU General Assembly 2013
2. Minora U., Bocchiola D., D'Agata C., Maragno D., Mayer C., Lambrecht A., Mosconi B., Vuillermoz E., **Senese A.**, Compostella C., Smiraglia C., Diolaiuti G. (2013): 2001-2010 glacier changes in the Central Karakoram National Park: a contribution to evaluate the magnitude and rate of the "Karakoram anomaly". Geophysical Research Abstracts, Vol. 15, EGU2013-7444, 2013, EGU General Assembly 2013
3. Diolaiuti G., **Senese A.**, Mihalcea C., Verza G.P., Mosconi B. and Smiraglia C. (2011): AWS measurements on glaciers in the Italian Alps. In "Workshop on the use of automatic measuring systems on glaciers. Extended abstracts and recommendations." IASC Workshop, 23-26 March 2011, Pontresina (Switzerland). Organized by C.H. Tijm-Reijmer and J. Oerlemans.
4. **Senese A.**, Diolaiuti G., Mihalcea C., Smiraglia C., Vuillermoz E. & Bocchiola D. (2010): Analysis of a 4-year record of meteorological data and energy and mass balance of Forni Glacier, Ortles-Cevedale Group (Stelvio National Park, Italian Alps). Geophysical Research Abstracts 12, EGU2010-PREVIEW, EGU General Assembly 2010.
5. Vuillermoz E., **Senese A.**, Diolaiuti G., Verza GP., Marinoni A., Bonasoni P. (2010): Contribution to the comprehension of climate change towards cryosphere and atmospheric analysis: the cases study of Changri Nup Glacier, Nepal Himalayas and of Forni Glacier, Italian Alps. Atti Conclusivi della Conferenza Internazionale Global Change and the World's Mountains tenutasi a Perth (UK) tra il 26 ed il 30 Settembre 2010.

**Submitted papers:**

1. **Senese A.**, Maugeri M., Vuillermoz E., Smiraglia C. and Diolaiuti G. (submitted): Air temperature thresholds to evaluate snow melting at the surface of Alpine glaciers by degree-day models: the study case of Forni Glacier (Italy).

## List of publications

---

2. **Senese A.**, Ferrari S., Maugeri M., Confortola G., Bocchiola D., Smiraglia C., and Diolaiuti G. (submitted): An enhanced T-index model including solar and infrared radiation to evaluate distributed ice melt at the Forni Glacier tongue (Italian Alps).
3. Azzoni R.S., **Senese A.**, Zerboni A., Maugeri M., Smiraglia C. and Diolaiuti G. (submitted): A pilot study to evaluate sparse supraglacial debris and dust and their influence on ice albedo of Alpine glaciers: the case study of the Forni Glacier (Italy).
4. Gambelli S., **Senese A.**, D'Agata C., Smiraglia C. and Diolaiuti G. (under revision): Preliminary analysis for distribution of the surface energy budget of the Forni Glacier, Valtellina (Ortles-Cevedale Group, Italy). *Geografia Fisica e Dinamica Quaternaria*.
5. Urbini S., Zirizzotti A., Baskaradas J., Tabacco I.E., Cafarella L., **Senese A.**, Smiraglia C. and Diolaiuti G. (submitted): A new RES system to evaluate ice thickness and volume: preliminary results from pilot tests performed on Alpine glaciers.
6. **Senese A.**, Vuillermoz ., Azzoni R.S., Verza G.P., Smiraglia C. and Diolaiuti G. (submitted): Air temperature thresholds to assess snow melt at the Forni Glacier surface (Italian Alps) in the April-June period: a contribution to the application of Temperature index models. *IAEG Proceeding*
7. Vuillermoz E., **Senese A.**, Diolaiuti G., Smiraglia C., Cristofanelli P., Marinoni A., Verza G. P. and Bonasoni P. (submitted): The case study of the Changri Nup glacier (Nepal, Himalaya) to understand atmospheric dynamics and ongoing cryosphere variations. *IAEG Proceeding*